Targeting NF-κB subunits p50 and p65 in chronic lymphocytic leukaemia with cell penetrating peptides

Rosária Alexandre

July 2014

Dr Paul Brennan

Prof Chris Pepper

Dr Arwyn Jones

A Thesis submitted in requirement of Cardiff University

for the degree of Doctor of Philosophy

Table of Contents

List of Figures

List of Tables

Oral and poster presentations

Oral presentations

"Chronic Lymphocytic Leukaemia & Cell Penetrating Peptides"
Cancer IRG Seminar Series, Cardiff, UK (October, 2011)

"Therapeutic targeting of CLL cells with peptides directed to NF-κB subunits p50 and p65"
NF-κB subunit workshop, Rauischholzhausen, Germany (October, 2012)

"Chronic Lymphocytic Leukaemia & Cell Penetrating Peptides"
7th Annual Normal and Malignant Lymphocyte Meeting, Cardiff, UK (January, 2013)

Poster presentations

"Targeting Chronic Lymphocytic Leukaemia Survival with Bioactive Cell Penetrating Peptides"
BSH Annual Scientific Meeting, Glasgow, UK (April, 2012)

"Developing novel CPPs for targeting NF-κB in chronic lymphocytic leukaemia cells"
Protein-Protein Interactions Network Annual Meeting, London, UK (January, 2013)

Abbreviations

ABIN-3 – A20-binding protein 3

ACN – Acetronitrile

AID – Activation-induced deaminase

Akt – Protein kinase B

ANK – Ankyrin repeats

AntP – Antennapedia

AP – Alkaline phosphatase

APC – Allophycocyanin

APRIL – A proliferation-inducing ligand

APS – Ammonium persulfate

ARF – ATP rybosilation factor

ATM – Ataxia telangiectasia mutated

ATP – Adenosine triphosphate

Bac7 – Bactenicin 7

BAFF – B-cell activating factor

Bax – Bcl-2-associated X protein

Bcl-2 – B-cell lymphoma 2-encoded protein

Bcl-3 – B-cell lymphoma 3-encoded protein

Bcl-xL – B-cell lymphoma extra large protein

BCR – B-cell receptor

BH3 – Bcl-2 homology domain

BIRC5 – Baculoviral inhibitor of apoptosis repeat-containing 5

BLNK – B-cell linker

BSA – Bovine serum albumin

BTK – Burton's tyrosine kinase

cAMP – Cyclic adenosine monophosphate

CC2 – second coiled-coil

CCL – C-C chemokine ligand

CCR – C-C chemokine receptor

CD40L – CD40 ligand

Cdk6 – Cell division protein kinase 6

CFLAR - CASP8 and FADD-like apoptosis regulator

c-FLIP – Cellular FLICE inhibitory protein

CHCA - α-Cyano-4-hydroxycinnamic acid

c-IAP – Cellular inhibitor of apoptosis

CLL – Chronic lymphocytic leukaemia

CO_2 – Carbon dioxide

COX2 – Cytocrome c oxidase subunit 2

CPP – Cell penetrating peptide

CREB – cAMP response element-binding protein

CYLD – Cylindromatosis gene

Cyt c – Cytochrome c

CXCL – C-X-C chemokine ligand

CXCR – C-X-C chemokine receptor

DD – Death domain

dH_2O – deionised water

DHMEQ - Dehydroxymethylepoxyquinomicin

DMATP – dimethylamino-parthenolide

DMEM – Dulbeccos's modified Eagle's medium

DNA – Deoxyribonucleic acid

DTT – Dithiothreitol

EDTA – Ethylenediaminetetraacetic acid

EMSA – Electrophoretic mobility shift assay

ERK – Extracellular-signal regulated kinase

FADD - Fas-Associated protein with death domain

FCR – Fludarabine Cyclophosphamide Rituximab

FISH – Fluorescence in situ hybridisation

FITC – Fluorescein isothiocyanate

FLICE - FADD-like IL-1β-converting enzyme

FR – Fludarabine Rituximab

GFP – Green fluorescent protein

GRR – Glycine rich region

GST – Glutathione S-transferase

GTP – Guanosine triphosphate

HIV - Human immunodeficiency virus

HPLC – High-performance liquid chromatography

HSP90 – Heat shock protein 90

IAP – Inhibitor of apoptosis

Ig – Immunoglobulin

IκB – Inhibitor of κB

IKK – IκB kinase

IL – Interleukin

iNKT – Invariant natural killer cells

IRAK4 – Interleukin-1 receptor associated kinase 4

JNK - c-Jun N-terminal kinase

KCl – Potassium chloride

LC_{50} – Lethal dose 50

LDL - Low-density lipoprotein

LDS – Lithium dodecyl sulphate

LPS - Lypopolysaccharide

LZ – Leucine zipper

MALDI-TOF - Matrix-assisted laser desorption/ionization – Time of flight

MALT – Mucosa-associated lymphoid tissue

MAP – Model amphipathic peptide

Mcl-1 – myeloid cell leukaemia sequence 1

M-CLL – mutated CLL

MFI – Mean fluorescence intensity

miRNA – micro RNA

$MgCl_2$ – Magnesium chloride

MMP-9 – Matrix metallopeptidase 9

mRNA – messenger RNA

MyD88 – Myealoid differentiation primary response (88)

MW – Molecular weight

NaCl – Sodium chloride

NBD – NEMO binding domain

NEMO – NF-κB essential modulator

NES – Nuclear export signal

NFAT – Nuclear factor of activated T-cells

NF-κB – Nuclear factor kappa B

NIK - NF-κB inducing kinase

NK – Natural killer

NLC – Nurse-like cells

NLF-1 – NCA localisation factor 1

NLS – Nuclear localisation sequence

NOXA - Phorbol-12-myristate-13-acetate-induced protein 1

NP40 – Nonyl phenoxypolyethoxylethanol 40

NSIAD – Nonsteroidal anti-inflammatory drugs

NTL – Non-transfected fibroblasts

OS – Overall survival

PAD – Pro-apoptotic domain

PAGE – Polyacrylamide gel electrophoresis

PARP – Poly (ADP-ribose) polymerase

PBMC – Peripheral blood mononuclear cells

PBS - Phosphate buffered saline

PEST – Proline (P), glutamic acid (E), serine (S), threonine (T) domain

PI – Propidium iodide

PI3K – Phosphatidylinositol-4,5-bisphosphate 3-kinase

PIK3CA – PI3K catalytic subunit alpha

PKC – Protein kinase C

PLC-γ2 – Phospholipase C γ2

PMO - phosphorodiamidate morpholino oligomers

PMSF – phenylmethanesulfonylfluoride

PNA – Peptide nucleic acid

Poly dI-dC - Poly(deoxyinosinic-deoxycytidylic) acid

PS – Phosphatidylserine

PTD – Protein transduction domain

PTM – Post-translation modification

Q-LL – Lower left quadrant

Q-LR – Lower right quadrant

qPCR – Quantitative polymerase chain reaction

Q-UL – Upper left quadrant

Q-UR – Upper right quadrant

RDX – Radixin

RHD – Rel homology domain

RIP – Receptor-interacting protein

RNA – Ribonucleic acid

RPMI – Roswell Park Memorial Institute medium

SD – Standard deviation

SDS – Sodium dodecyl sulfate

smIg – surface membrane Immunoglobulin

Syk – Spleen tyrosine kinase

TAD – Transactivation domain

TBE – Tris-Borate-EDTA

TE – Tris-EDTA

TEMED – Tetramethylethylenediamine

TFA – Trifluoroacetic acid

TIRAP – Toll-interleukin-1 receptor adaptor protein

TLR – Toll-like receptor

TNFα – Tumour necrosis factor alpha

TNFR – Tumour necrosis factor receptor

TRAF6 – TNF receptor associated factor 6

TTFT – Time to first treatment

TTST – Time to subsequent treatment

U-CLL – Unmutated CLL

UK – United Kingdom

Und. – Undetermined

UTC – 5-(4-fluorophenyl)-2-ureido-thiophene-3 carboxylic acid amide

VCAM-1 – Vascular cell adhesion protein 1

VEGF – Vascular endothelial growth factor

VLA-4 – Very late antigen 4 or

XIAP – X-linked inhibitor of apoptosis protein

Zap-70 – zeta-chain associated protein kinase 70

Abstract

Cell penetrating peptides (CPP) are short amino acid sequences with the potential to be used as vectors for delivering macromolecular therapeutics into cells. Five CPPs [R_8, FFR_8, $(RXR)_4$, TP10 and PFV] were studied in primary human chronic lymphocytic leukaemia (CLL) cells using fluorescence-labelled CPPs. Uptake, sub-cellular localisation and toxicity were studied by confocal microscopy and flow cytometry. Two of the CPPs were selected, based on their cellular uptake and intracellular distribution characteristics, and used as delivery vectors for peptide-based NF-κB inhibitors.

Four novel NF-κB inhibitory CPPs directed against p50 and p65 subunits were tested in primary CLL cells. Apoptosis was measured using AnnexinV/PI labelling and a caspase-3 activity assay by flow cytometry. Apoptosis was evident after one hour in cells treated with TP10-p50i and TP10-p65i and the LC_{50} of TP10-p50i and TP10-p65i was 6 μM and 10 μM respectively at 24 hours. This represents a ten-fold increase in toxicity when compared to the commercially available CPP NF-κB-inhibitors.

Western blot analysis of NF-κB subunit translocation revealed NF-κB inhibition in some of the samples treated with TP10-p50i. However, the effects of the peptide varied from sample to sample. Studies using EMSA to measure NF-κB DNA binding revealed similar inconsistencies, even when CLL cells were stimulated with CD40L or CpG.

Flow cytometic analysis of cell surface makers in CLL cells demonstrated that TP10-p50i did not alter the expression of CD69, a cell surface molecule regulated by NF-κB, indicating that the variations seen previously by EMSA and western blotting did not result from direct NF- κB inhibition. Although the exact mechanism of action of TP10-p50i was not determined, the cytotoxic effects observed with TP10-p50i are not likely to be related to a modulation of NF-κB activity.

Acknowledgements

I would like to thank my supervisors Dr Paul Brennan and Prof Chris Pepper for giving me the opportunity to carry out this PhD and for their support during the course of my degree. I am also very grateful for the support given by Dr Arwyn Jones.

I would like to thank the members of the Cardiff CLL research group for their support and guidance, and in particular to Sophie Betteridge, who became more than a colleague and who helped me immensely throughout this process. I would also like to thank other members of our lab, in particular Julia Grimstead and Marie Clarke for the friendship and continuous support.

A special thank you to the Leukaemia Reserch Appeal for Wales for funding my PhD and believing in my project. I would also like to acknowledge Prof Chris Fegan, Dr Guy Pratt and Dr Ceri Jones for providing the blood samples, which were essential to my work.

I would like to thank all of my friends for all the support and encouragement, as you all played a crucial role in my life. I would like specially thank Johanne Pentier and Eric Bull for helping me in the final stretch of my PhD. Your support was vital to the success of my degree.

In the most recent months, I have had the pleasure of befriending Johanne Pentier, who quickly became a very important person for me. Thank you Joh for keeping me sane, for making me laugh (bringing me to tears several times) and for making me believe that I am capable of great things.

The biggest thank you goes to my favourite family in the world, the Alexandres. Without them, I would not be here today. So thank you Maria Natividade, Luis, Júlia and Feijóo for supporting me unconditionally from the moment I came into your lives. I hope this thesis serves as an example to my nephew Tiago, who was born this year, that with your family behind you, you can achieve anything you set yourself to.

I have left my home country Portugal, to pursue a dream and I am happy that this thesis is a testament of the realisation of that dream. For that, a last thank you to all the people that have come into my life in the recent years, and that in some big or small way have contributed to my success.

Ó mar salgado, quanto do teu sal
São lágrimas de Portugal!
Por te cruzarmos, quantas mães choraram,
Quantos filhos em vão rezaram!
Quantas noivas ficaram por casar
Para que fosses nosso, ó mar!

Valeu a pena? Tudo vale a pena
Se a alma não é pequena.
Quem quer passar além do Bojador
Tem que passar além da dor.
Deus ao mar o perigo e o abismo deu,
Mas nele é que espelhou o céu.

Oh salty sea, how much of your salt
are tears of Portugal!
For crossing you, how many mothers cried,
how many sons in vain prayed!
How many brides stayed unmarried
to make you ours, oh sea!

Was it worth it? Everything is worth it
if the soul is not small.
Who wants to pass beyond the Bojador
has to pass beyond the pain.
God gave to the sea the peril and abyss,
but in it mirrored the sky.

Fernando Pessoa

Chapter 1- Introduction

1.1. Chronic Lymphocytic Leukaemia

Chronic lymphocytic leukaemia (CLL) is a lymphoid malignancy characterised by the expansion of $CD19^{+}/CD5^{+}$ B lymphocytes (B-cells) in the peripheral blood, bone marrow and lymph nodes (Deaglio et al., 2008; Lobetti-Bodoni et al., 2013). The view of CLL is that there is a dynamic balance between cells circulating in the blood and cells located in niches in lymphoid organs (Zenz et al., 2010). The circulating lymphocytes resemble mature B-cells and are relatively resistant to apoptosis, whereas the lymphocytes in the lymphoid organs either undergo proliferation or apoptosis according to the microenvironment signals (Chiorazzi et al., 2005).

In the United Kingdom, around 3,800 people are diagnosed with CLL every year; this represents 35% of all leukaemia cases and it makes it the most common leukaemia in the Western world (Haematological Malignancy Research Network, 2012). The incidence of CLL in the UK is approximately seven new cases per 100,000 persons, with a male to female ratio of 1.7:1 (Haematological Malignancy Research Network, 2012). The diagnosis often occurs at an early stage of the disease following a routine blood analysis and around 75% of the diagnosed individuals are over the age of 60 (Lobetti-Bodoni et al., 2013).

The diagnosis of CLL is defined by an absolute lymphocyte count of at least $5x10^{9}$ B-cells/L persistent for at least 3 months, expressing the characteristic phenotypic profile of CLL cells (CD5 and CD23 positive B-cells) (Lobetti-Bodoni et al., 2013). Upon confirmation of the diagnosis of CLL the clinical staging is assessed. There are two staging systems in place, the Rai and Binet systems (Binet et al., 1981; Rai et al., 1975). The Rai system is based on the concept that CLL is a gradual disease and it can be categorised according to the symptoms presented (i.e. lymphocytosis, lymphadenopathy, splenomegaly, hepatomegaly, anaemia and thrombocytopenia) (Rai et al., 1975). The Binet system takes into account the number of enlarged lymphoid tissues and the presence of anaemia and/or thrombocytopenia (Binet et al., 1981). Both systems are in wide use, but the International Workshop Group in CLL recommends that in practice, they should be used in one integrated system where each Binet stage is further identified by the Rai stage (i.e. A0, AI, AII, BI, BII, CIII, CIV)

(International Workshop on Chronic Lymphocytic Leukemia, 1989). However, this has not been widely implemented, and the majority of clinicians use either the Rai or Binet systems (International Workshop on Chronic Lymphocytic Leukemia, 1989). The staging systems remain the most useful clinical tools for the assessment of CLL, as they only require a physical examination and standard laboratory tests (Hallek, 2013; Lobetti-Bodoni et al., 2013). Staging is used to determine the clinical management of individual patients; patients with advanced stage disease often require immediate treatment whilst patients with early stage disease are usually monitored by a watchful waiting strategy (Lobetti-Bodoni et al., 2013).

The evaluation of additional prognostic factors, such as serum markers (i.e. lactate dehydrogenase and β2-microglobulin), cytogenetic analysis by fluorescence *in situ* hybridisation (FISH; del11q, del13q, trisomy 12 and del17) and cellular markers (i.e. *IGHV* mutational status, ZAP-70 and CD38) contributes to determine the tumour burden and to more accurately determine the prognosis of the disease (Lobetti-Bodoni et al., 2013).

Table 1.1 - CLL Staging Systems. Adapted from **(Binet et al., 1981; Rai et al., 1975)**.

Staging System	Stage	Clinical manifestations	Disease Stage
Rai	0	Lymphocytosis only	Early
	I	Lymphocytosis and lymphadenopathy	Intermediate
	II	Lymphocytosis, splenomegaly and/or hepatomegaly, with/without lymphadenopathy	
	III	Lymphocytosis and anaemia, with/without organomegaly	Advanced
	IV	Lymphocytosis and thrombocytopenia, with/without anaemia and organomegaly	
Binet	A	Fewer than 3 areas of enlarged lymphoid tissue	Early
	B	More than 3 areas of enlarged lymphoid tissue	Intermediate
	C	Anaemia and thrombocytopenia	Advanced

1.1.1. Cytogenetic markers

A set of specific genetic abnormalities has been identified as having predictive value for CLL outcome: deletion at 13q14, trisomy 12, deletion at 11q22-23 and 17p deletion (Döhner et al., 2000).

The most common genetic abnormality in CLL is the deletion at 13q14 (Döhner et al., 2000). Calin et al. (2002) identified a locus in the gene *DLEU2* that codes for two microRNAs (also known as miRNA or miR), *miR15a* and *miR16-1* that was lost in the majority of CLL cases. MicroRNAs are small RNA molecules that regulate protein expression by degrading mRNA or by inhibiting translation to protein (Calin et al., 2002). miRNAs usually have a large number of targets, but miR15a and miR16-1 have been shown to induce apoptosis by regulating *BCL2* (Cimmino et al., 2005). The deletion of this cluster could affect survival of CLL cells. Mice with a knockout in the *miR15a/16-1* cluster of *DLEU2* have been shown to develop $CD5^+$ leukaemias similar to CLL (Klein et al., 2010; Lia et al., 2012).

Approximately 15% of CLL patients present with trisomy 12, and they have a shorter survival time than patients with a normal FISH panel analysis (Chiorazzi, 2012). An association between trisomy 12 and the presence of mutations in the *NOTCH1* gene has been postulated (Chiorazzi, 2012). Patients with *NOTCH1* mutations have shorter time to first treatment (TTFT) and overall survival (OS) (Fabbri et al., 2011; Lopez-Guerra et al., 2012), but when combined with trisomy 12 both TTFT and OS are even shorter (Balatti et al., 2012).

Another cytogenetic marker is the 11q22-23 deletion, found in approximately 15% of CLL patients. These patients often present with bulky lymphadenopathy, an unusual feature in CLL, and have a more aggressive disease with shorter survival (Döhner et al., 2000). This deletion occurs more frequently in unmutated CLL (U-CLL) patients, which could explain the adverse clinical outcome (Damle et al., 1999; Hamblin et al., 2002). The 11q22-23 deletion often involves the *Radixin (RDX)* and *Ataxia telangiectasia mutated (ATM)* genes (Stilgenbauer et al., 2002). The *ATM* gene is involved in DNA repair, therefore the deletion of this gene can lead to enhanced clonal aggressiveness and evolution due to the acquisition of novel genomic variants (Braggio et al., 2012; Gunnarsson et al., 2011; Knight et al., 2012).

Approximately 7% of CLL patients have a 17p deletion, with an adverse clinical course possibly caused by TP53 loss (Döhner et al., 2000). This deletion facilitates the expansion of a more aggressive clone and it is often associated with a poor response to therapy or relapse (Lozanski et al., 2004). Abnormalities with TP53 seem to be related to low levels of miR34a (Zenz et al., 2009), which reinforces that miRNA levels play an important role in CLL (Chiorazzi, 2012).

1.1.2. Therapy

CLL is predominantly a leukaemia of the elderly, due to the majority of patients being diagnosed over the age of 60. Although the majority of patients do not require initial treatment and a “watch and wait” approach is put in place, when treatment is required it needs to be tailored individually according to disease staging and ability of the patient to tolerate toxic agents (Hallek, 2013). The initial therapy of newly diagnosed fit and relatively healthy patients is usually a combination of fludarabine with cyclophosphamide and rituximab (FCR) or fludarabine and rituximab (FR), which have shown high response rates (Wu et al., 2013). With an overall response rate of approximately 90% and a complete remission between 30 and 75%, it has been shown to be the ideal therapy for young patients (<65 years). Therapy for elderly and unfit patients is the use of single agent chlorambucil (Hallek, 2013). Its low toxicity, low cost and convenience of being an oral drug are the main advantages (Hallek, 2013). The disadvantages of this agent are the low to non-existent complete remission rate and side effects that occur from prolonged use, such as cytopenia, myelodysplasia and secondary acute leukaemia (Hallek, 2013).

The introduction of monoclonal antibodies into CLL therapy has improved the treatment of this disease. CD20 is expressed by mature B-cells and the majority of B-cell malignancies, therefore it became a very attractive target (Hallek, 2013). Rituximab is an anti-CD20 antibody less effective as a single agent, but highly effective when used in combination with other agents (Hallek, 2013). Nevertheless, fludarabine- and pentostatin-based therapies induce grade 3 and 4 neutropenia, as well as suppression of T-cell mediated immunity (Danilov, 2013). To overcome this, other anti-CD20 antibodies have been designed that challenge the efficiency of Rituximab, such as Ofatumumab and Obinutuzumab (GA101) (Hallek, 2013). Another monoclonal antibody used for CLL therapy is Alemtuzumab, an anti-CD52 agent (Hallek, 2013). This antibody showed response rates of 33 to 53% in patients with advanced CLL (Hallek, 2013). It also showed improved efficiency in patients with high-risk genetic markers such as del11q, del17p and TP53 mutations (Hallek, 2013).

New agents have been introduced to CLL therapy in the past few years, such as lenalidomide. Lenalidomide is classed as an immunomodulatory drug and is derived from thalidomide but its mechanism of action is currently unknown (Ferrajoli et al., 2008). However, it is known to inhibit tumour necrosis factor alpha (TNF-α) and stimulate T-cell proliferation and activation of natural killer (NK) cells (Ferrajoli et al., 2008). Lenolidomide has shown promising results in patients with relapsed/refractory

CLL (Wu et al., 2013). Bendamustine is a unique alkylating agent, with several mechanisms of actions, that has been shown to induce and overall response rate of 59% in previously untreated CLL patients (Wu et al., 2013). Ibrutinib is a BTK inhibitor, targeting the B-cell recptor (BCR) signalling in CLL, and it has been shown to be well tolerated in CLL patients, producing a response rate of 60% and being particularly active in relapsed/refractory CLL patients (Advani et al., 2013). Idelalisib, also known as GS-1101 and CAL-101 is a specific inhibitor of PI3K that produces potent responses in CLL (Wu et al., 2013). It has been shown to be a good agent for relapsed/refractory CLL patients and recent studies showed overall response rates higher than 70% for combination therapies with Rituximab and/or Bendamustine (Wu et al., 2013). Navitoclax, also known as ABT-263, is an inhibitor of the pro-survival Bcl-2 protein family. It mimics the BH3 domain found in this family of proteins (Wu et al., 2013). Although it produces favourable responses in relapsed/refractory CLL patients and also treatment-naive patients it has recently been replaced by ABT-199 that overcomes the platelet inhibition problems encountered with ABT-263 (Wu et al., 2013)

1.1.3. The biology of CLL

1.1.3.1. *IGHV* mutational status

Normal B-cells and CLL cells express a BCR on their membrane, which is composed of a surface membrane immunoglobulin (smIg) homodimer and a non-covalently bound heterodimer Igα/Igβ (CD79a/CD79b; Figure 1.1). However, CLL cells have low expression of immunoglobulins (Ig), which is a hallmark of the disease (Vuillier et al., 2005). The majority of CLL cells express CD5 and IgM/IgD, which is the phenotype of mantle zone naive cells, which under normal conditions express unmutated *IGHV* genes (Dighiero & Hamblin, 2008). Each normal and malignant B-cell displays a distinct BCR that results from the recombination of the V (variable), D (diverse) and J (joining) segments for the Ig heavy chain and V and J for the Ig light chain (Zenz et al., 2010). To increase the BCR repertoire, B-cells undergo a process called somatic hypermutation (Klein & Dalla-Favera, 2008). Naive B-cells are recruited to the T-cell rich area of peripheral lymphoid tissue were they become activated by $CD4^+$ T-cells (Klein & Dalla-Favera, 2008). Activated B-cells differentiate into centroblasts that undergo clonal expansion in the germinal centre (B-cell rich area in lymphoid tissue) and during proliferation the process of somatic hypermutation introduces base-pair changes into the variable region of the rearranged *IGHV* genes that results in the

production of a wide range of BCRs (Klein & Dalla-Favera, 2008). Centroblasts become centrocytes and move to the light zone were helper T-cells and follicular dendritic cells select the centrocytes with improved binding capability to the antigen that initiated the immune response (Klein & Dalla-Favera, 2008). B-cells with reduced binding capacity undergo apoptosis and B-cells with increased binding capacity either become memory B-cells or undergo class switching and become plasma cells (Klein & Dalla-Favera, 2008).

Research into the *IGHV* mutational status of CLL patients helped divide the disease into two subgroups, the mutated (M-CLL) and U-CLL. The two groups follow different clinical courses, with U-CLL being the more aggressive form with a shorter survival time (Damle et al., 1999; Hamblin et al., 1999). These differences led to the theory that CLL arises from two distinct cellular origins and therefore represents two different diseases (Chiorazzi & Ferrarini, 2011). However, gene expression profiling of U-CLL and M-CLL showed that the profiles were very similar to each other whilst being highly different from normal B-cells (Klein et al., 2001; Rosenwald et al., 2001). This indicated that probably both U-CLL and M-CLL have the same cellular origin (Chiorazzi & Ferrarini, 2011). Recently, Seifert et al. (2012) showed that both U-CLL and M-CLL originate from mature $CD5^+$ B-cells. U-CLL is derived from unmutated $CD5^+CD27^-$ B-cells whereas M-CLL is derived from mutated $CD5^+CD27^+$ B-cells (Seifert et al., 2012). Furthermore, both normal mutated $CD5^+CD27^+$ B-cells and M-CLL cells show mutations in the *BCL6* gene, a trait of germinal centre somatic hypermutation (Seifert et al., 2012). It is also important to know that although U-CLL cells derive from CD27 negative cells, during the course of the disease, CLL cells can upregulate CD27 expression following T-cell independent activation (Seifert et al., 2012).

Differences in the clinical course of U-CLL and M-CLL are likely to be due to external signals and subsequent responsiveness, such as BCR signalling (Chiorazzi & Burger, 2013). M-CLL cells respond to a specific subset of antigens that occur infrequently and consequently the clone either remains stable or expands at a slower rate. U-CLL cells express polyreactive and low-affinity BCRs that react to a wider range of antigens (Chiorazzi & Burger, 2013). Consequently, U-CLL react more frequently, which can lead to increased BCR signalling and increased expression of molecules such as zeta-associated-70 (ZAP-70) and CD38 (Chiorazzi & Burger, 2013; Dighiero & Hamblin, 2008; Zenz et al., 2010).

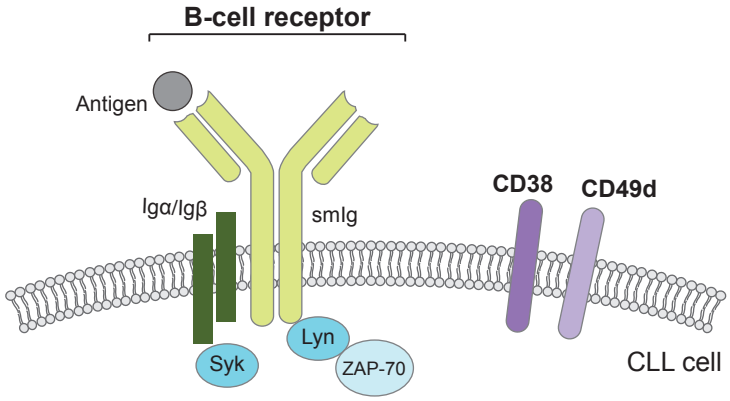

Figure 1.1 – The B-cell receptor and other CLL prognostic markers.
The BCR is composed of two Ig heavy and light chains (variable and constant regions), and Igα/Igβ (CD79a and CD79b), which contain an intracellular activation motif that transmits signals to intracellular tyrosine kinases, such as Syk and Lyn. Adapted from (Chiorazzi & Burger, 2013; Dighiero & Hamblin, 2008; Zenz et al., 2010).

1.1.3.2. ZAP-70

ZAP-70 is a cytoplasmic tyrosine kinase, initially identified in T-cells and subsequently identified in B-cells at various differentiation stages (Chen et al., 2002; Elder et al., 1994; Iwashima et al., 1994). It has a central role in T-cell biology and it is involved in cell migration, apoptosis, T-cell receptor signalling and cell activation (Iwashima et al., 1994). Both normal and malignant B-cells express this molecule, where it plays a role in BCR signalling, upon antigen activation (Figure 1.1) (Chen et al., 2002).

Conflicting results regarding the independent prognostic value of ZAP-70 in CLL have been published. The CLL Research Consortium performed a large study involving 307 CLL patients, where ZAP-70 values were measured alongside the mutational status of *IGHV* (Rassenti et al., 2004). This study showed that in patients with levels of ZAP-70 above a certain threshold, the TTFT was not significantly different between M-CLL and U-CLL. However, for patients considered to be ZAP-70 negative the TTFT was significantly longer (Rassenti et al., 2004). The group concluded then that “ZAP-70 is a stronger predictor of the need for treatment in B-cell CLL” (Rassenti et al., 2004). In 2012, Pepper et al. published a study of prognostic markers in Binet stage A CLL patients, which included 1154 patients. In this study it was demonstrated that ZAP-70 had no independent value as a prognostic marker for stage A CLL patients (Pepper et al., 2012). The most obvious difference between the two studies was that Rassenti et al. (2004) did not take into account the disease stage of the patients when comparing ZAP-70 levels but their cohort contained a significant number of advanced stage

patients. It has been shown previously that ZAP-70 can change over the course of the disease (Smolej et al., 2008; Vroblova et al., 2010), so it is possible that ZAP-70 has limited clinical relevance at early stages of the disease but its expression increases as the disease progresses.

The association of an increase in ZAP-70 with a more adverse clinical course is thought to be related to increased BCR signalling and is not associated with the kinase activity of this molecule (Gobessi et al., 2007). ZAP-70 has been shown to delay the internalisation of IgM and CD79b from the cellular membrane and this, in turn, allows for prolonged BCR signalling (Chen et al., 2008). ZAP-70 positive CLL cells are also more likely to express molecules such as CD49d and chemokine receptors such as CCR7, promoting migration and apoptosis inhibition (Calpe et al., 2011). This indicates that ZAP-70 might induce cell migration to solid tissues where further BCR and chemokine signalling are stimulated, resulting in prolonged survival and proliferation of CLL cells (Chiorazzi, 2012).

1.1.3.3. CD38

CD38 is a transmembrane glycoprotein expressed on a variety of lymphoid and non-lymphoid cells (Deaglio et al., 2008; Malavasi et al., 2011; Rosenquist et al., 2013). The level of expression on lymphoid cells varies according to their differentiation status. It is initially expressed in immature haematopoietic cells, but it is down regulated on mature cells. Upon activation of B- and T-cells the levels increase greatly (Funaro et al., 1990). CD38 can act both as a receptor and as an enzyme (Malavasi et al., 1994). The extracellular domain of CD38 has an enzymatic site used to regulate intracellular levels of calcium (Howard et al., 1993). Upon CD38 ligation with its non-substrate ligand CD31, a signalling cascade is induced that involves tyrosine phosphorylation of a series of targets and an increase in intracellular calcium (Deaglio et al., 2000). Both the enzymatic and receptor capabilities of this molecule result in profound changes in the cell prompting activation, proliferation, differentiation and migration, depending on the cell lineage (Deaglio et al., 2008).

In CLL, CD38 is used as an independent prognosis marker and much like *IGHV* mutational status, it is used to divide the disease into two subgroups with distinct clinical outcomes (Chiorazzi, 2012; Deaglio et al., 2010; Malavasi et al., 2011; Pepper et al., 2012). CD38 is measured by flow cytometry and the optimal cut-off value for the

expression of this molecule varies from study to study, ranging from 5 to 30% (Rosenquist et al., 2013). CD38 expression above the cut-off point is associated with shorter survival, shorter TTFT and higher absolute lymphocyte count (Damle et al., 1999). CD38 positivity, however has a few downsides when used as a prognostic marker: the expression of this molecule can vary during the course of the disease, there is heterogeneity regarding CD38 expression in a blood sample and the lack of a clearly defined cut-off value creates difficulty when comparing studies (Ghia et al., 2003; Hamblin et al., 2002). However, it is an easily assessed prognostic marker and its link to CLL pathogenesis and disease evolution is still being studied (Deaglio et al., 2008). The disease aggressiveness linked to CD38 positivity seems to be due to its ability to induce migration and take advantage of the signals from the microenvironment (Chiorazzi, 2012).

1.1.3.4. CD49d

CD49d has been determined to be a good indicator of CLL outcome in several occasions (Bulian et al., 2014; Gattei et al., 2008; Nückel et al., 2009; Shanafelt et al., 2008). This molecule is an α-integrin subunit (α4) that can pair with CD29 (the β1 subunit) to form a complete integrin (α4β1) (Rose et al., 2002). CD49d functions as an adhesion molecule that mediates cell-to-cell and cell-to-extracellular matrix interactions through binding with vascular cell adhesion molecule-1 (VCAM-1) and fibronectin respectively (Gattei et al., 2008; Rossi et al., 2008). The adhesion of cells to tissues can induce survival, migration and activation signals (Rose et al., 2002). The simultaneous high expression of CD49d and CD38 has been linked to a group of patients with poorer outcome (Pittner et al., 2005; Zucchetto et al., 2009). A large macromolecular complex involving CD49d, CD38, CD44v and MMP-9 has been identified in U-CLL clones (Buggins et al., 2011) and another study has shown CD49d and CD38 to be physically and functionally linked in CLL (Del Poeta et al., 2012b). A recent study showed the independent prognostic value of CD49d in CLL, with CD49d high patients having a shorter TTFT and lower OS (Majid et al., 2011). When combined with other prognostic markers such as *IGHV* status and CD38, CD49d improves the ability to determine TTFT and OS (Majid et al., 2011). The authors suggest that this marker should be routinely used as part of the immunophenotyping panels for CLL (Bulian et al., 2014; Majid et al., 2011).

1.1.4. The CLL Microenvironment

The importance of the microenvironment for the survival of CLL cells is clear. When primary CLL cells are cultured *in vitro* they undergo spontaneous apoptosis unless they are cultured with cytokines or in a co-culture system with adherent cell types such as stromal cells (Lagneaux et al., 1998). *In vivo*, the microenvironment consists of T-cells, monocyte-derived nurse-like cells (NLCs), stromal cells, follicular dendritic cells and soluble factors (Caligaris-Cappio, 2003).

Stromal cells in the bone marrow provide attachment sites and growth factors to haematopoietic cells. In CLL, stromal cells have similar functions and they are capable of protecting CLL cells from cytotoxic agents (Burger, 2011). *In vitro* co-culture with stromal cells induces a rapid migration of CLL cells that is dependent on the expression of CXCR4 and VLA-4 on leukaemic cells (Burger et al., 1999). Stromal cells in other lymphatic tissues have similar protective effects on CLL cells and it is thought that the CXCR4-CXCL12 axis plays an important role by attracting the cell to environments that confer cytoprotection (Burger, 2011). NLCs differentiate from monocytes into large adherent cells and also exert a protective effect on CLL cells, and they are found in the spleen and secondary lymphoid tissues (Bürkle et al., 2007; Tsukada et al., 2002). Cells co-cultured with NLCs manifest increased signaling capacity through the BCR and higher expression of NF-κB and BCR target genes such as CCL3 and CCL4 (Burger et al., 2009; Herishanu et al., 2011). The role of T-cells in the lymph nodes of CLL patients generates controversy. In untreated CLL patients the numbers of T-cells are increased, but it is not known if this results from interactions with CLL cells, with microbial agents that are more prevalent in CLL patients or other reasons (Ramsay et al., 2008). T-cells are also able to supress or stimulate proliferation of CLL cells. In the lymph node, anti-apoptotic and proliferative stimuli are delivered to CLL cells and this results in the formation of proliferation centres, called pseudofollicles, of CLL cells (Bagnara et al., 2011). In these areas $CD4^+$ T-cells co-localise with $CD38^+$ CLL cells, suggesting that these interactions contribute to the expansion of the CLL clone (Buggins et al., 2008).

Several chemokines and receptors contribute to the migration of CLL cells into environments that contribute to the extended survival and proliferation of the cells (Deaglio & Malavasi, 2009). NLCs constitutively secrete CXCL12, which is the ligand for CXCR4 expressed on the majority of circulating CLL cells. This is thought to contribute to the recruitment of CLL cells into the bone marrow and other growth-favourable environments (Burger & Kipps, 2006). However, the responses following

CXCR4 ligation are highly variable in CLL patients and appear dependent on CD38 and ZAP-70 expression (Richardson et al., 2006). A similar situation occurs with CXCR5, which is expressed by CLL cells, and CXCL13 expressed by NLCs (Bürkle et al., 2007). CLL cells also express CXCR3 at variable levels and CCR7 at high levels (Till et al., 2002). They also have increased sensitivity to CCL19 and CCL21, expressed be high endothelial venules in the lymph node, which effectively recruit cells from blood into lymph nodes (Till et al., 2002).

The presence of antigens and other stimuli found in the spleen, bone marrow and lymph nodes, make these the appropriate niches for CLL cells to proliferate (Deaglio & Malavasi, 2009). The best known example is CD40 ligand (CD40L), expressed by T-cells in pseudofollicles, which contributes to the proliferation of $CD40^+$ CLL cells (Bergwelt-Baildon et al., 2004). This stimulus synergises with the BCR signalling and several anti-apoptotic pathways are induced, including the caspase inhibitor survivin (also known as BIRC5), highly expressed at the proliferative centres (Ramsay & Rodriguez-Justo, 2013; Zenz et al., 2010). CLL cells are also known to induce phenotypic changes in T-cells, such as a defective formation of the immunological synapse (Ramsay et al., 2008). NLCs express CD31, a known ligand of CD38 (Deaglio & Malavasi, 2009). These interaction are capable of sustaining CLL viability *in vitro* (Deaglio & Malavasi, 2009).

1.1.5. BCR signalling in CLL

CLL cells are characterised by low levels of IgM expression, variable response to antigen activation and non-antigen dependent activation of anti-apoptotic signalling pathways (Woyach et al., 2012). As mentioned previously, CLL cells present the gene profiles of activated B-cells, and around 50% of the CLL cases present somatic mutations of the *IGHV* genes, indicating that BCR signalling (and response to antigen) has an important role in disease pathogenesis (Chiorazzi & Burger, 2013; Woyach et al., 2012). Deregulation of BCR signalling in CLL is characterised by constitutive phosphorylation of certain kinases, such as Lyn and Syk and the activity of these two kinases has been shown to be higher in CLL when compared to normal B-cells (Woyach et al., 2012). Pharmacological inhibition of Syk induced apoptosis of CLL cells and reduced the downstream signalling of the BCR (Baudot et al., 2009; Quiroga et al., 2009). Inhibition of Lyn also promoted apoptosis in CLL cells (Contri et al., 2005). PI3K has also been shown to be constitutively active in CLL and its inhibition led to

apoptosis of the cells, inhibition of Akt activation, decreased Mcl-1 and XIAP expression, two anti-apoptotic proteins (Herman et al., 2011; Ringshausen et al., 2002). The BTK pathway is also up regulated in CLL, at the protein and gene levels. Its inhibition induced apoptosis in a caspase-dependent manner and inhibited the phosphorylation of Akt, ERK and NF-κB (Herman et al., 2011). CLL cells often manifest constitutive activation of NF-κB and have exaggerated NF-κB responses to CD40L stimulation, including prolonged cell survival (Furman et al., 2000).

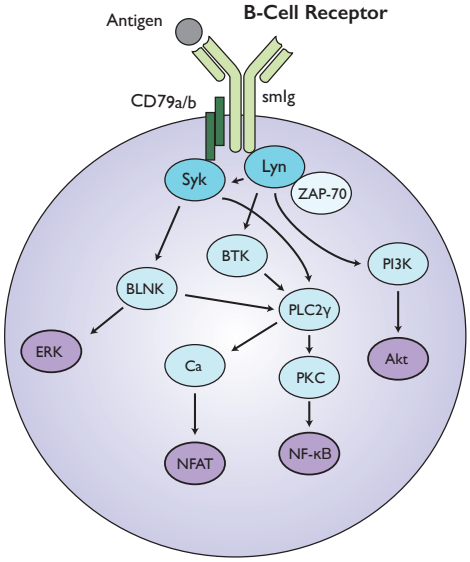

Figure 1.2 – BCR Signalling.
BCR activation by an antigen leads to sustained downstream signalling that is controlled by the signalosome. The downstream signalling pathways lead to changes in proliferation, activation, differentiation and cell death of B-cells. Adapted from (Ramsay & Rodriguez-Justo, 2013; Zenz et al., 2010).
BLNK – B-cell linker; BTK – Burton's tyrosine kinase; ERK – Extracellular signal-regulated kinase; NFAT – Nuclear factor of activated T-cells; PI3K - Phosphatidyl 3-kinase; PKC – Protein kinase C; PLCγ2 - Phospholipase-Cγ2; ZAP-70 – Zeta-chain associated protein 70.

1.2. The transcription factor Nuclear Factor kappa B (NF-κB)

NF-κB is a family of transcription factors, normally found in the cytoplasm in the form of homo- or heterodimers. It was first identified by Sen & Baltimore in 1986, as an enhancer of transcription of the kappa light chain gene in B-cells (Sen & Baltimore, 1986a). Further research showed that NF-κB played an important role in adaptive immunity and inflammation responses (Bonizzi & Karin, 2004; Ruland & Mak, 2003) and since then it has been shown to regulate gene expression that impacts on cell differentiation, proliferation and survival (Hayden & Ghosh, 2008). NF-κB has been found to be persistently active in a variety of diseases, such as cancer, ageing, arthritis, neurodegenerative diseases and heart disease (Balistreri et al., 2013; Karin & Ben-Neriah, 2011; Mogi et al., 2007; Roman-Blas & Jimenez, 2006; Valen et al., 2001).

1.2.1. The NF-κB family

The NF-κB transcription factors bind to DNA as dimers. This family consists of five members, p50, p52, p65 (RelA), RelB and c-Rel. p50 and p52 are short versions of their precursor proteins p105 and p100, also known as NF-κB1 and NF-κB2 respectively (Hayden & Ghosh, 2012). There are 15 possible combinations of dimers using the 5 members of the NF-κB family. However, not all combinations have been proved to exist physiologically (Table 1.3 lists all the combinations found). The p50-p65 dimer is the most commonly found, having been identified in almost all cell types (Oeckinghaus & Ghosh, 2009). Interestingly, RelB is the only subunit that complexes with p50 and p52 (Dobrzanski et al., 1994; Ryseck et al., 1992). The diversity generated by the combination of NF-κB subunits, allows the different homo- and heterodimers to bind to a variety of κB sites and regulate a great number of genes (Hayden & Ghosh, 2008).

Table 1.2 – Possible homo- and heterodimers of NF-κB found physiologically.

p65 – p65	p65 – p52	p52 – c-Rel	p50 – p50	RelB – p52
p65 – c-Rel	c-Rel – c-Rel	p50 – c-Rel	RelB – p50	

All of the members are characterised by the presence of a 300 amino acid long N-terminal Rel homology domain (RHD), highly conserved, it is involved in sequence-specific DNA binding and homo- and heterodimerisation (Figure 1.4) (Baltimore & Beg, 1995; Müller et al., 1996)). Crystal structures of p50-p50 and p50-p65, showed that the N-terminal of the RHD is responsible for binding to κB sites that possess a consensus sequence (5' GGGPuNWPyPyCC 3'; Pu – purine; N – any base; W – adenine or thymine; Py - pyrimidine), while the C-terminal is mostly responsible for dimerisation and IκB interactions (Chen et al., 1998; Ghosh et al., 1995; Müller et al., 1995).

p65, RelB and c-Rel all contain a transactivation domain (TAD) at the C-terminal, which is responsible for an increase in gene expression (Huxford & Ghosh, 2009). p50 and p52 lack this domain, however they can positively regulate transcription by dimerization with NF-κB subunits that possess this domain (Hayden & Ghosh, 2012). Due to the lack of TAD, p50 and p52 homodimers have been associated with transcriptional repression (Plaksin et al., 1993; Schmitz et al., 1991; Udalova et al., 2000). However, association of p50 homodimers with non-Rel proteins that possess transactivation capabilities such as Bcl-3 or CREB-binding protein, has been reported to have a positive transcription effect (Cao et al., 2006; Franzoso et al., 1993; Fujita et al., 1993).

RelB possesses a leucine zipper region in addition to its TAD, which is required for the subunit to be fully active (Dobrzanski et al., 1993). p50 and p52 are generated by the processing of their precursor proteins p105 and p100, respectively, which have a glycine-rich region following the RHD and multiple ankyrin repeats that are characteristic for the IκB family (discussed in more detail later) (Huxford & Ghosh, 2009).

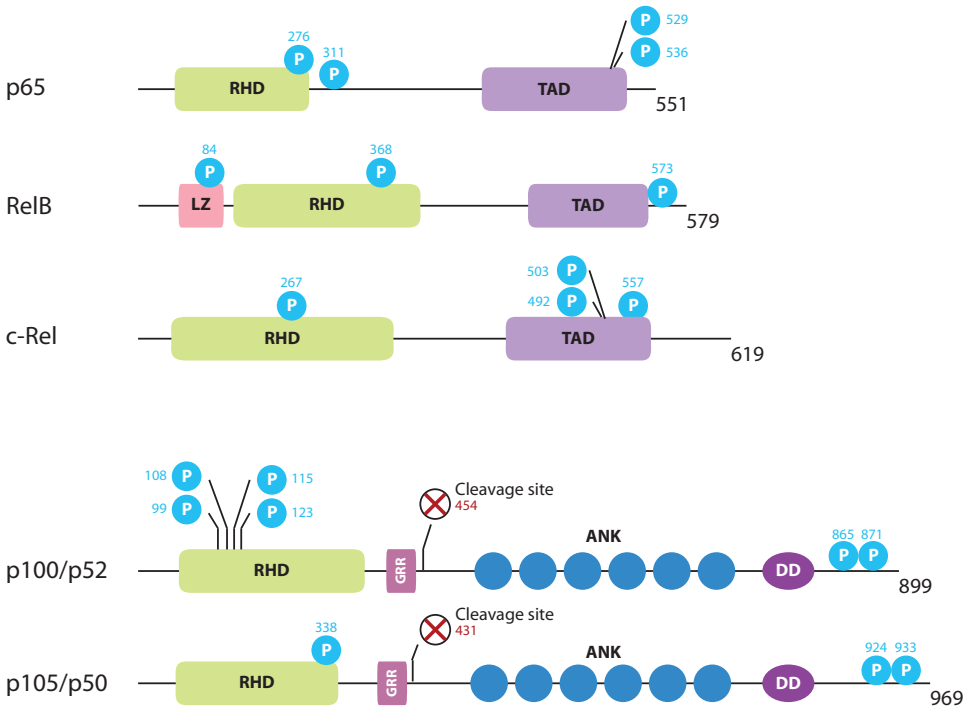

Figure 1.3 - NF-κB family members.
Representation of the different domains of the NF-κB family members. RHD – Rel homology domain; TAD- transactivation domain; LZ – leucine zipper domain; GRR – glycine-rich region; ANK – Ankyrin repeats; DD – death domain; P – phosphorylation sites. Adapted from {Hayden:2008fh, Vallabhapurapu:2009ib, Betts:1996th}.

1.2.2. NF-κB pathway

1.2.2.1. NF-κB inhibition

In their inactive form, NF-κB dimers are found in the cytoplasm bound to an inhibiting protein. The classic inhibiting proteins are IκBα, IκBβ and IκBε, belonging to the IκB family, or the precursor proteins p100 and p105 (Baeuerle & Baltimore, 1988; Huxford & Ghosh, 2009; Li & Nabel, 1997; Thompson et al., 1995). Two other atypical proteins have been found to regulate the activity of NF-κB dimers in the nucleus, Bcl-3 and IκBζ, and an alternative transcript of the p105 gene named IκBγ, only expressed in murine lymphoid cells, but its function still remains undetermined (Inoue et al., 1992; Oeckinghaus & Ghosh, 2009).

The main function of IκB proteins is to inhibit NF-κB by blocking its translocation into the nucleus (Hayden & Ghosh, 2008). All IκB proteins share a common ankyrin repeat domain that mediates their interaction with the RHD and interferes with the nuclear localisation signal (NLS) found on NF-κB dimers (Figure 1.5). Although IκB proteins

have similar structures they usually bind to specific NF-κB dimers and are subjected to different transcriptional regulation (Whiteside & Israël, 1997). The p65-p50 dimer is mostly inhibited by IκBα (Vallabhapurapu & Karin, 2009), while IκBβ has been found to bind to this dimer when it is bound to κB sites for nuclear regulation (Rao et al., 2010; Suyang et al., 1996; Thompson et al., 1995). The crystal structure of IκBα bound to the p65-p50 dimers, reveals that this protein masks only the NLS of p65 leaving p50's NLS uncovered (Ghosh et al., 2001). This exposure coupled with the nuclear export signal (NES) found on IκBα, means that there is a constant shuttling of this complex in and out of the nucleus (Arenzana-Seisdedos et al., 1995; Rodriguez et al., 1999). However, the default location for this complex is the cytoplasm probably due to the additional NES found on p65 (Harhaj & Sun, 1999).

The ankyrin repeats found on p105 allow this protein to function as an IκB (Dobrzanski et al., 1995; Liou et al., 1992) and selectively bind to p50, p65 and c-Rel maintaining them in the cytoplasm (Capobianco et al., 1992; Mercurio et al., 1993). Proteasomal processing of p105 into p50 is constitutively active in unstimulated cells (Beinke & Ley, 2004; Palombella et al., 1994). Upon stimulation, p105 is rapidly degraded without generation of p50, which results in the release of the p105-bound NF-κB dimers (Heissmeyer et al., 2001; Lang et al., 2003). p100, the precursor of p52, binds favourably to RelB to retain it in the cytoplasm, but in the absence of all other IκB proteins most NF-κB subunits stay in the cytoplasm, suggesting p100 can also regulate other subunits (Tergaonkar et al., 2005; Vallabhapurapu & Karin, 2009).

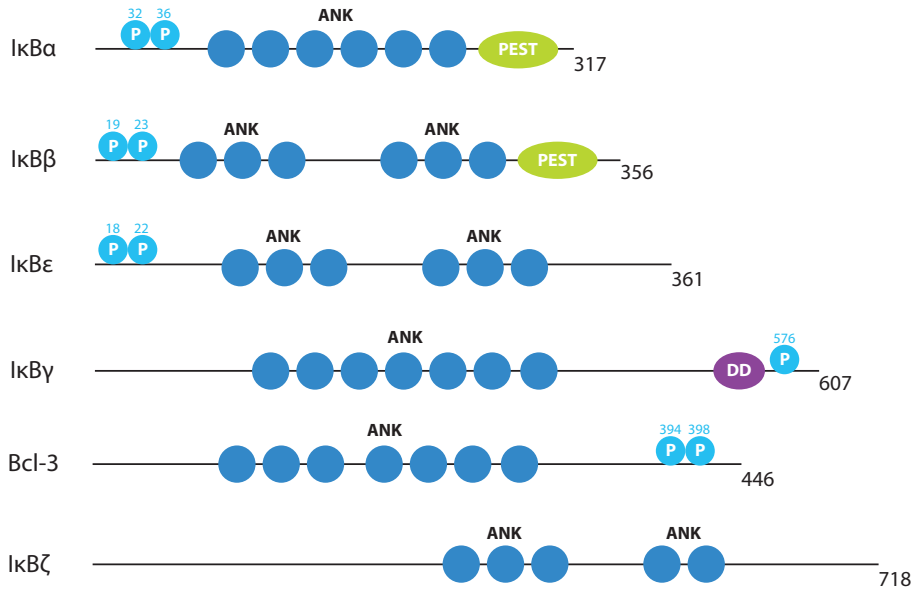

Figure 1.4 – IκB family members.
Representation of the different domains of the IκB family members. ANK – Ankyrin repeats; PEST – Proline (P), glutamic acid (E), serine (S), threonine (T) domains; DD – death domain; P – phosphorylation sites. Adapted from (Hayden & Ghosh, 2008; Vallabhapurapu & Karin, 2009).

1.2.2.2. Activation of NF-κB

Activation of NF-κB can be induced via two pathways, the canonical and the non-canonical (or alternative) pathways (Vallabhapurapu & Karin, 2009). The majority of stimuli activate the canonical pathway, which regulates mainly p65-p50 and c-Rel-p50 heterodimers, while the non-canonical pathway regulates p52-RelB heterodimers (Vallabhapurapu & Karin, 2009). These stimuli include inflammatory cytokines such as TNF-α and interleukin-1 (IL-1) (Osborn et al., 1989), pathogen-associated molecules such as CpG and lypopolysaccharide (LPS) (Krieg, 2000; Sen & Baltimore, 1986b), and other ligands such as CD40L or BAFF (Berberich et al., 1994; Claudio et al., 2002). Both pathways are closely linked since the majority of the stimuli that induce the non-canonical pathway also induce the canonical pathway and consequently the production of p100 and RelB (Scheidereit, 2006).

In the canonical pathway, receptor engagement leads to activation of the IκB kinase (IKK) complex, composed by subunits IKKα, IKKβ and IKKγ (also named NF-κB essential modulator – NEMO), where IKKα and IKKβ are the catalytic subunits and IKKγ is a regulatory subunit that serves as a sensing scaffold and integrator of upstream signals for activation of the catalytic subunits (Karin & Ben-Neriah, 2000). The IKK is responsible for the phosphorylation of IκBα, which targets it for ubiquitination and proteasomal degradation and consequently releases the NF-κB

dimers (Karin & Ben-Neriah, 2000). This exposes the NLS found on p65 and leads to nuclear import of the dimer. The IKK complex also leads to the release of dimers bound to IκBβ and IκBε, as both are also targets of this complex (Scheidereit, 2006). The canonical pathway regulates survival, proliferation, inflammation and immune regulation (Vallabhapurapu & Karin, 2009). In the non-canonical pathway, the NF-κB inducing kinase (NIK) plays an important role by phosphorylating IKKα homodimer, lacking IKKβ and IKKγ. This leads to ubiquitination and proteasomal processing of the complex p100-RelB into p52-RelB (Scheidereit, 2006). The non-canonical pathway is involved in lymphogenesis and B-cell maturation (Vallabhapurapu & Karin, 2009).

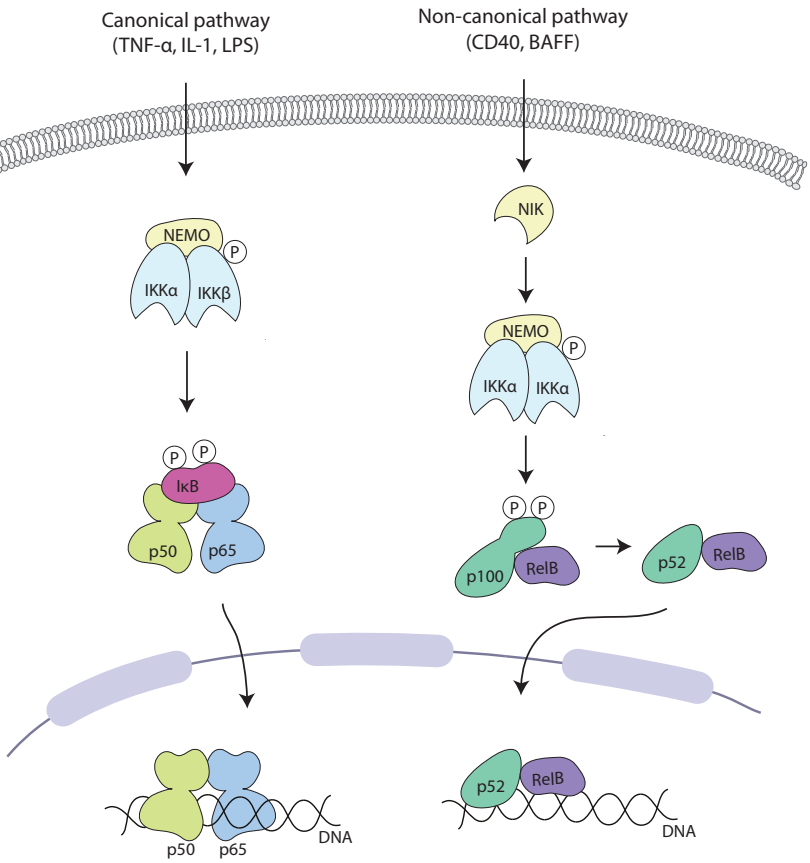

Figure 1.5 – The canonical and non-canonical NF-κB pathways.
Induction of the canonical pathway by stimuli such as TNFα, IL-1 or LPS, results in IKK activity and consequent phosphorylation of IκB. This releases the NF-κB dimer (e.g. p50-p65), which then translocates into the nucleus and induces transcription of target genes. Induction of the non-canonical pathway depends on NIK, which is responsible for activation of IKKα. IKKα consequently phosphorylates p100, leading to proteosomal processing of p100 to p52. This results in nuclear translocation of p52-RelB and transcription of target genes. Adapted from (Oeckinghaus & Ghosh, 2009)).

1.2.2.3. Gene transcription induced by NF-κB

Following nuclear translocation of NF-κB dimers through the classical nuclear import pathway, the homo- and heterodimers bind to the respective κB sites that possess the previously described consensus sequence. These κB sites are widely dispersed through the genome, but NF-κB activation under specific conditions leads to the transcription of a small number of genes. This indicates that other mechanisms might contribute to the regulation of gene transcription by NF-κB (Hoffmann et al., 2006).

The first factor contributing to the wide range of NF-κB target genes is NF-κB dimerization. The combination of NF-κB subunits into homo- and heterodimers confers them different DNA-binding specificity. Therefore, in a certain cell type certain types of dimers can have an increased expression when compared to others and therefore induce transcription of a specific subset of genes (Smale, 2011).

Certain NF-κB-inducing stimuli may also induce activation of other pathways that culminate in the induction of post-translation modifications (PTMs). Events such as phosphorylation, ubiquitinylation, acetylation and other PTMs can alter the capability of NF-κB to bind to DNA or co-regulator proteins and therefore affect which genes get transcribed (Smale, 2011).

Another factor that may contribute to the gene expression variability is the recruitment of heterologous transcription factors. It has long been shown that NF-κB transcriptional activation requires interactions with transcriptional co-activators. The CREB-binding protein and p300, are some of the best described co-activators of NF-κB (Smale, 2011).

The list of NF-κB target genes is long and it affects, as described before, a wide variety of cell functions. Table 1.3 shows some of the target genes.

Table 1.3 – A selection of NF-κB target genes. Source: Gilmore (2008).

NF-κB target genes		**Reference**
Cytokines/chemokines and their modulators	BAFF	(Moon & Park, 2007)
	IL-10	(Xu & Shu, 2002)
	β-interferon	(Hiscott et al., 1989)
	TNF-α	(Shakhov et al., 1990)
Immunoreceptors	CCR5	(Liu et al., 1998)
	CD154	(Srahna et al., 2001)
	CD38	(Kang et al., 2006)
	IL-2 receptor α-chain	(Ballard et al., 1988)
	MHC Class I	(Israel et al., 1989; Johnson & Pober, 1994)
	TLR2	(Wang et al., 2001)
Proteins involved in antigen presentation	Complement factor B	(Huang et al., 2002)
	Complement receptor 2	(Tolnay et al., 2002)
Cell adhesion molecules	CD44	(Hinz et al., 2002)
	Fibronectin	(Lee et al., 2002)
	VCAM-1	(Iademarco et al., 1992)
Acute phase proteins	C-reactive protein	(Zhang et al., 1995)
	Hepcidin	(Liao et al., 2006)
Stress response genes	COX-2	(Yamamoto et al., 1995)
	12-Lipoxygenase	(Arakawa et al., 1995)
Cell surface receptors	CD69	(Lopez-Cabrera et al., 1995)
	Oxytocin receptor	(Terzidou et al., 2006)
Regulators of apoptosis	Bax	(Grimm et al., 2005)
	Bcl-2	(Catz & Johnson, 2001)
	IAPs	(You et al., 1997)
Growth factors, ligands and their modulators	BLINK	(Gupta et al., 2008)
	Prolactin	(Friedrichsen et al., 2006)
	Stem cell factor	(Da Silva et al., 2003)
Transcription factors and their modulators	ABIN-3	(Verstrepen et al., 2008)
	Bcl-3	(Brocke-Heidrich et al., 2006)
	c-myc	(Duyao et al., 1990)
Enzymes	AID	(Gourzi et al., 2007)
	Cdk6	(Iwanaga et al., 2008)
	PIK3CA	(Yang et al., 2008)
Others	Apolipoprotein D	(Do Carmo et al., 2007)
	BRCA2	(Wu et al., 2000)
	Cyclin D1	(Guttridge et al., 1999)
	NLF1	(Warton et al., 2004)
	Prodynorphin	(Bakalkin et al., 1994)

1.2.2.4. Downregulation of NF-κB activity

Once the activity of NF-κB is no longer required, the cell needs to be able to shutdown this pathway to avoid uncontrolled tissue damage or induction of disease (Staudt, 2010). Upon activation of the NF-κB pathway, IκBs are degraded by the proteasome so they no longer can inhibit NF-κB dimers in the cytosol (Karin & Ben-Neriah, 2000). However, IκBα and IκBε genes are regulated by NF-κB and this leads to *de novo* synthesis of these inhibitors, creating a negative feedback loop (Kearns et al., 2006; Le Bail et al., 1993; Sun et al., 1993). IκBα has a nuclear localisation signal, so following synthesis it is translocated into the nucleus where it binds to NF-κB dimers and transports them to the cytoplasm due to its NES (Arenzana-Seisdedos et al., 1995; 1997). However, IκBα can be prevented from binding to NF-κB dimers containing p65 and c-Rel in the nucleus by IκBβ (Rao et al., 2010). IκBβ does not contain a NES, so it prolongs the expression of certain genes such as TNFα and IL-1β (Rao et al., 2010; Scheibel et al., 2010). Complexes containing the CREB-binding protein can acetylate p65 and also prevent binding of IκBα (Lf et al., 2001). Although IκBε expression is considerably delayed compared to IκBα, it can also translocate to the nucleus, bind to NF-κB dimers and translocate them to cytoplasm (Kearns et al., 2006).

The IκBs negative feedback loop is one of the best described methods of NF-κB dowregulation, but other mechanisms are also important for this regulation.For example, deubiquitinases upstream of IKK such as A20, which gene expression is also regulated by NF-κB, provides an alternate negative feedback loop for NF-κB regulation (Hymowitz & Wertz, 2010). The deubiquitinase activity of A20 targets IKK activators such as RIP1, TRAF6, IKKγ, RIP2 and MALT1 (Hymowitz & Wertz, 2010). Other deubiquitinases known to down regulate NF-κB are the A20 family member Cezanne (Enesa et al., 2008) and cylindromatosis (CYLD) (Kovalenko et al., 2003).

Another mechanism reported to stop the NF-κB signalling pathway involves dissociation of signalling complexes, such as the MyD88 interference in LPS-induced TLR activation (Burns et al., 2003). MyD88 interacts with IRAK4 to activate IKK, which leads to NF-κB activation and consequent *de novo* synthesis of a shorter version of MyD88 (Burns et al., 2003). This version is capable of interfering with the MyD88-IRAK4 complex and arrest NF-κB activation (Burns et al., 2003).

1.2.3. NF-κB in CLL

1.2.3.1. NF-κB pathway in CLL

In CLL, constitutive activation of NF-κB has been shown (Cuní et al., 2004; Furman et al., 2000; Hewamana et al., 2008a). Three subunits have been shown to be over expressed compared to normal B-cells, these were p50, p65 and c-Rel (Cuní et al., 2004; Furman et al., 2000; Hewamana et al., 2008a). However, there is heterogeneity in NF-κB expression between patients (Hewamana et al., 2008a). Since CLL cell survival is so dependent on the microenvironment (Ramsay & Rodriguez-Justo, 2013) it is likely that heterogeneity in NF-κB expression is due to different exposures to these stimuli (Pepper et al., 2009).

Several cytokines and cells present in the *in vivo* microenvironment increase CLL cell survival *in vitro* in a NF-κB dependent manner. Romano and colleagues, showed that the use of a stimulating CD40 monoclonal antibody increased the levels of NF-κB expression and that it was capable of reversing the apoptotic effects of the drug fludarabine (Romano et al., 1998). Later, Bernal and colleagues showed that NF-κB was reduced following 4 hours in culture without any additional stimuli, revealing the importance of the microenvironment in NF-κB activation (Bernal et al., 2001). In the same study, Bernal showed that BCR and CD40 engagement were capable of activating NF-κB (Bernal et al., 2001). However, Hewamana et al. showed that BCR engagement could either lead to activation of NF-κB or its inhibition (Hewamana et al., 2008a).

Another molecule shown to be important for sustained NF-κB activation in CLL is the vascular endothelial growth factor (VEGF) (Farahani et al., 2005). CLL cells produce high levels of VEGF, and its levels have been shown to be high in the serum of CLL patients (Chen et al., 2000). This production is dependent on CD40 ligation and NF-κB activation (Farahani et al., 2005). The same study also showed that VEGF had an autocrine effect, by inducing indirect translocation of NF-κB into the nucleus through ligation to the two VEGF receptors (Farahani et al., 2005). BAFF and a proliferation-inducing ligand (APRIL), produced by nurse-like cells and CLL cells, have also been shown to induce NF-κB activation (Endo et al., 2007; Kern et al., 2004).

Given the high levels of NF-κB expression in CLL and the heterogeneity found in patients, Hewamana and colleagues set out to determine if p65 had any prognostic value (Hewamana et al., 2009). p65 DNA-binding activity was strongly associated with

advanced Binet stage, but not CD38 expression, *IGHV* mutational status or ZAP-70 expression (Hewamana et al., 2009). p65 was also predictive of TTFT and time to subsequent treatment (TTST) (Hewamana et al., 2009). This identified p65 as an independent prognostic factor, and one with the ability to predict the duration of response to treatment (Hewamana et al., 2009). NF-κB is therefore, a very appealing target for the treatment of CLL, as its inhibition should improve the apoptotic capabilities of existing drugs.

1.2.3.2. Modulation of NF-κB signalling cascade in CLL

There are currently a number of NF-κB inhibitors available that have proven to be efficient within the field of CLL research. They can be grouped according to their target in the NF-κB pathway: IKK inhibitors, proteasome inhibitors that block IκB degradation, inhibitors of nuclear translocation and suppressors of NF-κB DNA binding.

Several IKK inhibitors have been developed to target IKKβ, which were later proven to also target IKKα (Nakanishi & Toi, 2005). Bay 11-7082 was one of the first IKKβ inhibitors developed, and it acts by inhibiting phosphorylation of IκBα which stops proteasomal degradation and consequent NF-κB translocation into the nucleus (Pierce et al., 1997). In CLL cells, this compound induced caspase-3 and caspase-9-dependent apoptosis in 70% of the cases (Pickering et al., 2007). The efficiency of this inhibitor was not correlated with any CLL prognostic markers and normal B-cells were not susceptible to its effects (Pickering et al., 2007). Another IKKβ inhibitor is the 5-(4-fluorophenyl)-2-ureido-thiophene-3 carboxylic acid amide (UTC) (Endo et al., 2007). UTC acts only on the canonical pathway and was capable of reducing cell viability of CLL cells, but not the viability of normal B-cells (Endo et al., 2007).

BMS-345541 is an inhibitor of the IKK catalytic subunits IKKα and IKKβ, through binding to an allosteric site (Burke et al., 2003). BMS-345541 induces apoptosis in CLL cells, where $CD38^{hi}$ and $ZAP\text{-}70^{hi}$ cells showed more sensitivity to the compound than $CD38^{lo}$ and $ZAP\text{-}70^{lo}$ cells (Lopez-Guerra et al., 2009). Apoptosis in CLL cells was accompanied with the down regulation of NF-κB target genes such as *BCL2* (Lopez-Guerra et al., 2009).

Curcumin is an active ingredient in the spice turmeric, that has been shown to suppress proliferation, angiogenesis and metastasis, by inhibiting IKK and Akt (Aggarwal et al., 2006). In CLL cells, curcumin was able to induce apoptosis at doses

in the low micromolar range and was able to suppress anti-apoptotic proteins such as Mcl-1 (Everett et al., 2007; Ghosh et al., 2009).

Sesquiterpene lactone parthenolide, is normally used in traditional medicine for the treatment of inflammation (Kwok et al., 2001). This compound acts by inhibiting the catalytic subunit IKKβ (Kwok et al., 2001) and it has been shown to be able to induce caspase-dependent apoptosis in CLL cells (Steele et al., 2006). LC-1, also called dimethylamino-parthenolide (DMATP) is an analogue of parthenolide that has also proved to be highly effective in CLL cells (Hewamana et al., 2008b). LC-1 is capable of overcoming the cytoprotective effects of co-culture with CD40L-expressing fibroblasts and IL-4, and its efficiency is correlated with NF-κB levels (Hewamana et al., 2008b). A clinical trial of this drug was initiated in 2009 for CLL patients, however no results have been published yet.

Deguelin, is a plant derivative shown to inhibit IKK activation (Nair et al., 2006). In CLL, deguelin is capable of inducing higher degrees of apoptosis than in normal B-cells (Geeraerts et al., 2007). This apoptosis is dependent on caspase-3 and caspase-9 and (Geeraerts et al., 2007). Parallel to apoptosis, deguelin was capable of inducing the down regulation of Mcl-1 (Geeraerts et al., 2007).

Another approach to target NF-κB is the use of proteasome inhibitors, such as bortezomib, that stop IκB degradation and lead to NF-κB inhibition. Bortezomib is capable of inducing apoptosis in CLL cells *in vitro* (Perez-Galan et al., 2008), however in a phase II clinical trial it was shown to induce a poor response in patients (Faderl et al., 2006). Moreover, it is still unclear if apoptosis induced by bortezomib is due to NF-κB inhibition or activation of the pro-apoptotic protein NOXA (Pérez-Galán et al., 2006).

DHMEQ, is a compound derived from epoxyquinomicin C, an anti-inflammatory agent (Matsumoto et al., 2000). In CLL, DHMEQ was capable of inhibiting translocation of NF-κB into the nucleus and induce apoptosis of the cells *in vitro* (Horie et al., 2006). Apoptosis was accompanied by the down regulation of anti-apoptotic genes such as Bcl-xl, c-IAP, c-FLIP and Bfl-1 (Horie et al., 2006).

The previously mentioned NF-κB inhibitors demonstrate the importance of this pathway for the survival of CLL. More importantly, some of these inhibitors are more cytotoxic to CLL cells than normal B-cells, reinforcing the importance of NF-κB in maintaining cell viability.

1.3. Cell Penetrating Peptides

Cell penetrating peptides (CPP) are a class of peptides, typically comprising 5 to 30 amino acids that are capable of penetrating the cellular membrane. Frankel and Pablo first discovered these capabilities in 1988, while studying the transcription trans-activating (Tat) protein of the human immunodeficiency virus 1 (HIV-1). They found the protein was capable of entering cells and penetrating the nucleus (Frankel & Pabo, 1988). Later, Joliot et al. (1991) found that the *Drosophila* Antennapedia homeodomain peptide (AntP) was also capable of penetrating the cellular membrane of cultured neurons, entering the nucleus and inducing further cellular morphological differentiation (Joliot et al., 1991). The first CPP discovered was based on Joliot and colleagues' work on the 60 amino acid long AntP peptide. Derossi and colleagues found that the third helix of the AntP peptide (see Table 1.5 for sequence), was responsible for the translocation into the cells (Derossi et al., 1996). They named the peptide penetratin, and it is still used today as a delivery vector for a variety of cargoes (Derossi et al., 1996). Vives et al. discovered the amino acid sequence responsible for the penentrating capabilities of Tat in 1997 (see Table 1.4 for sequence) (Vives et al., 1997).

CPPs presented a new and exciting possibility: the delivery of macromolecules into cells and the possibility of using CPPs to deliver different types of cargo *in vivo* (Heitz et al., 2009; Sebbage, 2009). According to Heitz et al. (2009), the minimum requirements to be satisfied by newly developed CPPs should be the following: delivery efficiency in different and challenging cell lines, rapid endosomal release, ability to reach the target, activity at low doses, lack of toxicity and facility of therapeutic application (Heitz et al., 2009).

Schwarze and colleagues demonstrated in 1997 the first *in vivo* application of the penetrating abilities of this type of peptide. The β-galactosidase protein was fused with the protein transduction domain of Tat and was successfully delivered into all tissues of mice, including the brain (Schwarze et al., 1999). At the same time, Pooga and colleagues linked peptide nucleic acids (PNA) complementary to the human galanin receptor type 1 to transportan and penetratin peptides. These were successfully taken up by Bowes cells and were capable of blocking the expression of galanin receptors (Pooga et al., 1998b). Suppression of the expression of these receptors was also demonstrated in rats (Pooga et al., 1998b). Since then, a variety of other CPPs have

been discovered and synthetically developed to deliver a wide variety of cargoes (Copolovici et al., 2014).

1.3.1. Classes of CPPs

There is a great sequence variety in CPPs and they can be classified using different criteria. One of the most common criteria is the classification based on their physico-chemical properties and this identifies three classes: cationic, amphipathic and hydrophobic (Milletti, 2012; Stalmans et al., 2013). Milleti (2012) provides an overview of the current CPP landscape, looking at around 100 CPPs and determining the category to which they belong. The largest class is the amphipathic CPPs representing 44% of the studied CPPs, then the cationic peptides (41%) and the hydrophobic CPPs with 15% (Milletti, 2012).

Amphipathic CPPs comprise peptides with both hydrophobic and hydrophilic residues that can be positively and/or negatively charged (Milletti, 2012; Shin et al., 2014). They can be sub-divided into primary amphipathic, secondary amphipathic α-helical, β-sheet amphipathic and proline-rich amphipathic (Milletti, 2012; Shin et al., 2014). pVEC is an example of a primary amphipathic CPP (Elmquist et al., 2001). Some CPPs are known to form α-helixes, in which hydrophobic and hydrophilic residues are grouped in different sides of the helix. One side has the hydrophobic residues while the other has cationic, anionic or polar residues (Dunkin et al., 2011; Yang et al., 2014). The model amphipathic peptide (MAP) is an example of a secondary α-helical CPP (Oehlke et al., 1998). Some CPPs, such as VT5 are know to form a β-sheet which is crucial for cellular uptake (Oehlke et al., 1997). Proline-rich amphipathic CPPs contain a high number of proline residues that confers on them a unique helix structure, due to the rigidity of the proline residues. Bactenicin-7 (Bac7) is an example of a proline-rich amphipathic CPP (Sadler et al., 2002).

CPPs are categorised as cationic if they have a section of positive charges considered crucial for their uptake and if their three dimensional structure does not generate an amphipathic α-helix (Fei et al., 2011). Anionic CPPs (mainly negative charges) do not make up a class of their own, instead they are normally analysed on a case-by-case basis and assigned to one of the three categories (Milletti, 2012). Cationic peptides are normally rich in arginine and lysine. The most common cationic CPPs are polyarginines (R8, R9, R10 and R12), Tat and penetratin (Schmidt et al., 2010).

CPPs are considered hydrophobic if they only contain apolar residues, have a low net charge or have a hydrophobic motif that is crucial for their uptake regardless of the rest of the sequence (Stalmans et al., 2013). Some examples of hydrophobic CPPs are the C105Y and the shorter version of this CPP, PFVYLI, and Pep-7 (Gao et al., 2002; Rhee & Davis, 2006).

Other classification systems rely on the origin of CPPs. This classification organises CPPs into three groups: protein-derived, chimeric and synthetic peptides (Lindgren & Langel, 2011; Madani et al., 2011). The protein-derived CPPs are also termed protein transduction domains (PTDs) and are based on naturally occurring peptides with cell penetrating properties. Two examples of these peptides are Tat and penetratin (Derossi et al., 1996; Green et al., 1989). Chimeric CPPs have their sequences derived from one or more CPPs (Madani et al., 2011). Transportan, which derives from the sequences of mastoparan and galanin, and also its shorter analogue TP10, are two examples of chimeric CPPs (Pooga et al., 1998a; Soomets et al., 2000). Synthetic CPPs are specifically designed to have cell penetrating properties, such as the oligoarginine family of CPPs (R8, R9, R10 and R12) (Tünnemann et al., 2008).

Table 1.4 – Examples of CPPs in each of the categories.

Class of CPP	Sequence	Reference
Amphipathic		
Primary amphipathic		
pVEC	LLIILRRRIRKQAHAHSK	(Elmquist et al., 2001)
TP10	AGYLLGKINLKALAALAKKIL	(Soomets et al., 2000)
Secondary amphipathic		
α-helix		
MAP	KLALKLALKALKAALKLA	(Oehlke et al., 1998)
β-sheet		
VT5	DPKGDPKGVTVTVTVTVTG KGDPKPD	(Oehlke et al., 1997)
Proline-rich amphipathic		
Bac7	RRIRPRPPRLPRPRPRPLPF PRPGPRPIPRPLPFP	(Sadler et al., 2002)
Cationic		
Tat	GRKKRRQRRRPPQ	(Vives et al., 1997)
Penetratin	RQIKIWFQNRRMKWKK	(Derossi et al., 1996)
Polyarginines	R_n (n=8,9)	(Futaki et al., 2001)
(RXR)4	RXRRXRRXRRXR	(Rothbard et al., 2002)
Hydrophobic		
Pep-7	SDLWEMMMVSLACQY	(Gao et al., 2002)
C105Y	CSIPPEVKFNKPFVYLI	(Rhee & Davis, 2006)
PFVYLI	PFVYLI	{Rhee:2006ew}

1.3.2. Mechanism of CPP entry

Although CPPs have been categorised according to their physico-chemical properties and origin, the mechanism of entry is not the same within CPP families or classes. In earlier studies it was evident that direct translocation was responsible for the uptake of CPPs, due to peptide entry being possible at 4˚C demonstrating an energy-independent route (Richard et al., 2002). However, a re-evaluation of these mechanisms demonstrated that the use of methanol and formaldehyde to fix the cells for confocal microscopy created artefacts that allow CPP entry into the cells (Lundberg & Johansson, 2002; Richard et al., 2002). The use of live (unfixed) cells in subsequent studies eliminated these artefacts. Now, it is generally accepted that the mechanism is dependent on the amino acid sequence and experimental conditions, as the same CPP has been shown to translocate through the membrane using different mechanisms (Fretz et al., 2007). Figure 1.6 shows an overview of the mechanisms of entry used by CPPs, divided into two main categories: endocytosis and direct translocation.

As mentioned, differences in experimental conditions can determine the mechanism of uptake of CPPs. Taking the CPP Tat as an example, several pinocytic mechanisms have been associated with the uptake of the peptide. Unconjugated Tat has been found to be internalised by clathrin-mediated endocytosis (Richard et al., 2005), while Tat and the fusion peptide Tat-HA2 have been described to use macropinocytosis (Gump et al., 2010; Kaplan et al., 2005; Nakase et al., 2004; Wadia et al., 2004). As for the uptake of GST-Tat-GFP, caveolae-mediated endocytosis has been implicated in its membrane translocation (Ferrari et al., 2003; Fittipaldi et al., 2003). In a study by Duchardt et al. (2007), the AntP peptide, Tat and R9 were studied in parallel to determine the mechanism of entry. The study revealed that all three CPPs used three endocytic pathways to penetrate the cells: macropinocytosis, clathrin-mediated and caveolae-dependent endocytosis (Duchardt et al., 2007). An endocytosis-independent mechanism of entry was also utilised by the AntP peptide above a certain concentration threshold (Duchardt et al., 2007). These studies showed the importance of experimental conditions when comparing the uptake of CPPs and that the mechanism used depends entirely on them (Trabulo et al., 2010).

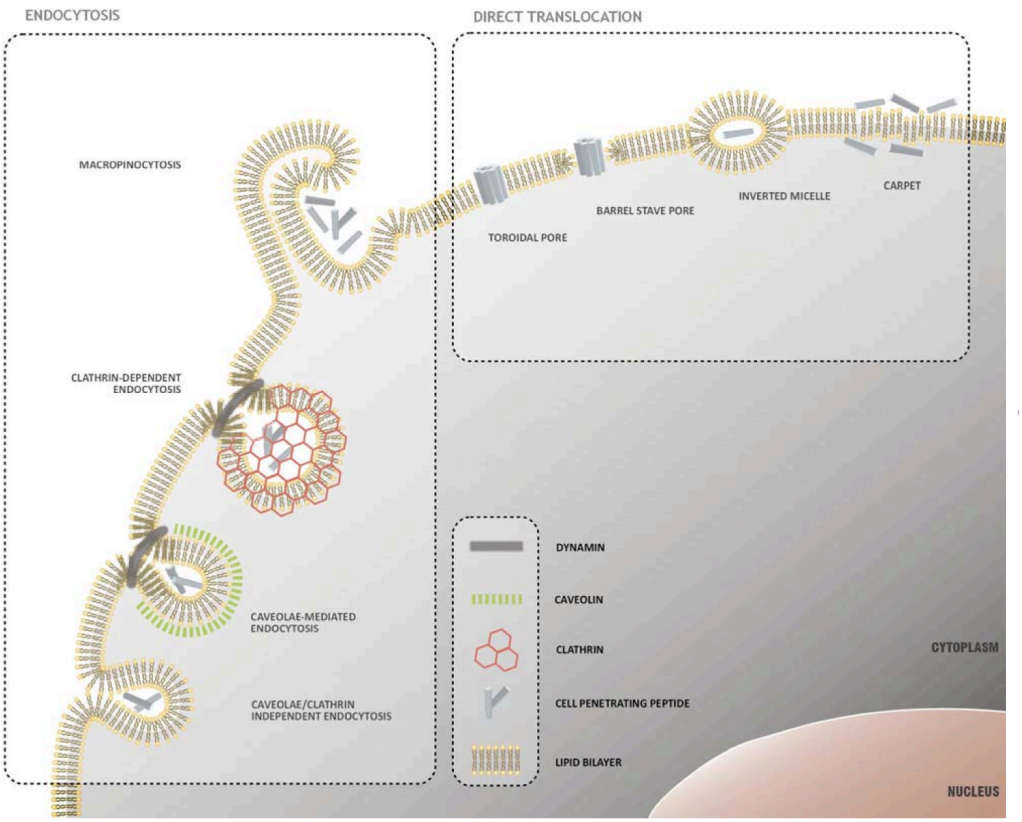

Figure 1.6 – Mechanism of entry of cell penetrating peptides.
The proposed mechanisms of entry of cell penetrating peptides can be devided into two categories: endocytosis and direct translocation. Within endocytosis, several mechanisms have been described, which include macropinocytosis, clathrin-dependent endocytosis, caveolae-mediated endocytosis and clathrin/caveolae independent endocytosis. Within direct translocation, four models have been described: the toroidal pore; barrel stave pore; inverted micelle; and carpet model. Source: Trabulo et al., 2010.

1.3.2.1. Direct translocation

Direct translocation is an energy-independent method that comprises other types of mechanisms such as pore formation, inverted micelle and the carpet model (Trabulo et al., 2010). The first step is common to all of these methods and it is due to the interaction of positively charged residues with the negative charge of phospholipids and/or heparan sulphate present in the cellular membrane. This process involves stable or transient destabilisation of the cellular membrane associated with folding of the peptide in the lipid membrane (Rothbard et al., 2004; Thorén et al., 2003; Wadia et al., 2004). The binding of the peptides to the membrane leads to temporary destabilisation and subsequent mechanisms are highly dependent on peptide concentration, sequence and lipid content of the cellular membrane (Madani et al., 2011).

The inverted micelle model was proposed by Derossi et al. (1996) when studying penetratin (Derossi et al., 1996). The positively charged residues are thought to interact

with the negatively charged phospholipids that would result in the reorganisation of the layer and shuttling of the membrane aided by the hydrophobic residues (Berlose et al., 1996). This interaction would result in the formation of a hexagonal structure (inverted micelle) and the peptides would be trapped in a hydrophilic environment within the structure (Berlose et al., 1996). This structure would then move to the inner part of the lipid bilayer and its contents would be released into the cytosol (Berlose et al., 1996). This mechanism is thought to be dependent on the insertion of tryptophan residues in the hydrophobic region of lipid bilayer, which means that highly cationic CPPs such as Tat and polyarginines are unlikely to use this mechanism of entry (Tsai et al., 2009).

The pore formation model depends on the interaction of the CPP with the membrane and the formation of a transient pore that allows translocation of the peptides and their conjugates through the membrane (Matsuzaki et al., 1996). Within the pore formation model, two types of mechanism have been described: the barrel stave model and toroidal pore model (Matsuzaki et al., 1996). In the barrel stave model, the peptides would form an amphipathic helix, where the hydrophobic face would interact with the lipid chains and the hydrophilic portion of the helix would form the central part of the pore (Matsuzaki et al., 1999; Pouny et al., 1992; Shai, 1999). The toroidal pore model is similar, except that there is a significant lipid rearrangement to allow interaction of the peptide exclusively with the lipid headgroup (polar groups) (Matsuzaki et al., 1996). The pore formation model is linked to concentrations of the peptide above a certain threshold that is dependent on the peptide (Matsuzaki et al., 1996).

In the carpet model, highly cationic peptides interact with the negatively charged components of the cellular membrane. As the concentration passes a certain threshold, interaction of the peptide with the membrane results in transient lipid rearrangement that consequently allows for peptide translocation (Pouny et al., 1992).

1.3.2.2. Endocytosis

Endocytosis is a basic cellular process for the *de novo* production of internal membranes from the plasma membrane lipid bilayer. In doing so, it internalises membrane lipids, integral proteins and extracellular fluid (Doherty & McMahon, 2009). It can be divided into two major categories: phagocytosis and pinocytosis (Trabulo et al., 2010). Phagocytosis is a process used by a cell for the internalisation of a cargo, while pinocytosis is used for fluid phase uptake. Pinocytosis comprises

macropinocytosis, endocytosis dependent on clathrin or caveolin and endocytosis independent of clathrin and/or caveolin (Jones, 2007; Mayor & Pagano, 2007).

Macropinocytosis can be described as the process used by the cell to internalise extracellular fluid and its contents (Jones, 2007). Signalling cascades induce actin polimerisation and originate membrane ruffles (i.e. protrusions in the membrane rich in filamentous actin) (Ridley, 1994). This process is very similar to phagocytosis, but the difference lies on the protrusions formed, that instead of engulfing the ligand-coated molecule, they collapse onto and fuse with the cellular membrane, generating the macropinosomes (large endocytic vesicles) containing extracellular fluid (Hacker et al., 1997).

Caveolae-mediated endocytosis relies on caveolae-coated invaginations of the cellular membrane. They are present in many cells, and tend to concentrate in regions called lipid rafts, rich in cholesterol, sphingolipids, signalling molecules and membrane transporters (Jasmin et al., 2012). The shape and structure of these invaginations is due to caveolin, a dimeric protein. This dimer binds to cholesterol and inserts a loop into the inner leaflet of the membrane, forming a caveolin coat all around the pocket (Li et al., 1996; Monier et al., 1996; Murata et al., 1995).

Clathrin-mediated endocytosis is a process used by the cell for the uptake of essential nutrients such as low density lipoprotein (LDL) that binds to the LDL receptor and transferrin that binds to transferrin receptors (Brodsky et al., 2001; Schmid, 1997). Upon ligand binding onto the respective receptors, clathrin molecules associate with each other and form a hexagon-like mesh that coats the pits on the cytosolic side of the membrane. The pits are then internalised and the receptors are processed by the cell (McMahon & Boucrot, 2011).

As previously mentioned, the number of CPPs that have been described is very large and there is not one consensus sequence that provides the penetrating abilities. For this reason is unlikely that one single mechanism of entry is used by different CPPs.

1.3.3. CPPs as cargo delivery systems

For optimal therapeutic effect, a drug should not only safely reach its target cell but also the appropriate location within the cell (Moghimi & Rajabi-Siahboomi, 2000). As described before, endocytic pathways provide a highly efficient route to introduce

macromolecules across the cellular membrane (Jones et al., 2003). However, it is highly likely that the majority of these will get recycled or end up being degraded in lysosomes. Drug delivery research has provided a number of strategies to overcome this problem, one of them was the application of CPPs to deliver a variety of cargoes ranging from classical molecular drugs to different types of oligonucleotides and proteins (Jones, 2007).

Some CPPs have been found to have intrinsic biological activity (Copolovici et al., 2014). Some examples are: the ARF(1-22) peptide, which mimics the activity of the tumour suppressive protein p14ARF and it is capable of reducing cell proliferation and induce apoptosis (Johansson et al., 2008); a stapled BIM BH3 peptide that targets Bcl-2 proteins, inhibiting their anti-apoptotic activity and inducing cell death (LaBelle et al., 2012); a CPP found within the human cytochrome c amino acids, Cyt $c^{77–101}$, capable of inducing apoptosis (Jones et al., 2010); and a peptide that inhibits MK2, a kinase that is key to regulate inflammation (Brugnano et al., 2011).

In the last two decades, a variety of CPPs have been linked to bioactive cargoes with the intention of being used to cure an array of diseases. Some examples are: D-isomer p53 C-terminal peptide with riHA2, which reduces proliferation and induces apoptosis of bladder cancer cells, and increased survival of tumour-bearing mice to 50% (Araki et al., 2010); a muscle specific/arginine rich chimeric peptide, used to correct dystrophin-deficiency in mice with Duchenne muscular dystrophy (Yin et al., 2010); or the D-JNKI1 peptide, a c-Jun N-terminal kinase (JNK) inhibitor coupled with Tat, used to protect rats from ischemic stroke (Vaslin et al., 2011).

1.3.3.1. CPPs targeting NF-κB

Since NF-κB has been implicated in a variety of diseases, it presents as a very attractive target for CPP therapy. Several CPPs have been designed to target this pathway at different points, these include: receptor signalling, IKK activity, NF-κB activation and nuclear translocation (Orange & May, 2008).

CPPs designed to inhibit receptor signalling adaptor molecules upstream of the NF-κB pathway target either MyD88 or TRAF6. CPPs that target MyD88 include: AntP-TIRAP, a peptide that targets the Toll-interleukin 1 adaptor protein (TIRAP), blocking LPS-induced NF-κB activation (Horng et al., 2001); ST2345 and ST2825, peptides modelled after the structure of MyD88 that are capable of inhibiting IL-1 signalling, including NF-

κB activation (Loiarro et al., 2007; 2005). CPPs that target TRAF6 include L-T6DP-1 and TRAF6BP (Mukundan et al., 2005; Ye et al., 2002). Both of these bind to TRAF6 and inhibit downstream NF-κB signalling (Mukundan et al., 2005; Ye et al., 2002). Sequences can be found in Table 1.5. Targeting proteins that regulate upstream signalling of NF-κB is an unreliable approach, as it also affects other signalling pathways. Nonetheless, all of the described inhibitors were designed to interfere with multiple signalling mechanisms and allowed to determine the importance of the respective target molecules in a variety of signalling pathways (Orange & May, 2008).

CPPs designed to inhibit IKK activity mainly target the IKKγ subunit (also known as NEMO). Yamaoka and colleagues demonstrated that NEMO binds to IKKβ through a six amino acid sequence (LDWSWL) (Yamaoka et al., 1998). This sequence was later identified in IKKα, and it is known as the NEMO binding domain (NBD) (May et al., 2000). Since then several CPPs have been designed using the NBD as a cargo. These include the use of the AntP peptide (May et al., 2000), Tat (Choi et al., 2003) and PTD (Dave et al., 2007; Rehman et al., 2003). Other CPPs targeted NEMO oligomerisation, by interfering with the second coiled-coil (CC2) and leucine zipper (LZ) domain, both critical for oligomerisation (Orange & May, 2008). Two CPP were initially designed to target both of these regions, AntP-NEMO-CC2 and AntP-NEMO-LZ (Agou et al., 2004). Later on, a novel CPP was designed using R7 as the vehicle to deliver the same sequence that targets LZ (Carvalho et al., 2007). See Table 1.5 for amino acid sequence of CPPs.

Another approach used to target NF-κB activity, was to interfere with phosphorylation of subunit p65, or to interfere with the nuclear translocation of subunit p50. Takada and colleagues developed a CPP composed of the PTD sequence fused with an amino acid sequence that mimics the phosphorylation sites required for nuclear translocation of p65 (Takada et al., 2004). SN50 was the first CPP developed to inhibit NF-κB activity, and it composed by the CPP MTS fused with the amino acid sequence corresponding to the NLS found in p50 (Lin et al., 1995). Since then, other CPPs have been developed to target nuclear localisation, such as BMS-205820, BMS-214572 and PN50 (Fujihara et al., 2000; Letoha et al., 2005; Yamaoka et al., 1998). Table 1.5 shows the amino acid sequence of the CPP referred here.

Table 1.5 – CPPs targeting NF-κB.

Target	CPP	Sequence	Reference
Adaptor proteins inhibitors			
MyD88	AntP-TIRAP	RQIKIWFQNRRMKWKKSSSHCRVLLITPGF	(Horng et al., 2001)
	ST2345	RQIKIWFQNRRMKWKKRDVLPGT	(Loiarro et al., 2005)
	ST2825	See Patent No. WO 200606709	(Carminati et al., 2006; Loiarro et al., 2007)
TRAF6	L-T6DP-1	AAVALLPAVLLALLAPRKIPTEDEYTDRPSQPST	(Ye et al., 2002)
	TRAF6BP	AAVALLPAVLLALLAPAPHPKQEPQEIDFPDD	(Mukundan et al., 2005)
IKK inhibitors			
NBD	AntP-NBD	RQIKIWFQNRRMKWKKTALDWSWLQTE	(May et al., 2000)
	Tat-NBD	YGRLLRRQRRRTALDWSWLQTE	(Choi et al., 2003)
	PTD-NBD	RRQRRTSKLMKRGGTALDWSWLQTE	(Rehman et al., 2003)
NEMO oligomerisation	AntP-NEMO-CC2	RQIKIWFQNRRMKWKKSKGMQLEDLRQQLQQA EEALVAKQELIDKLKEEAEQHKIV	(Agou et al., 2004)
	AntP-NEMO-LZ	RQIKIWFQNRRMKWKKYKADFQAERHAREKLV EKKEYLQEQLEQLQREFNKL	(Agou et., 2004)
	R7-NEMO-LZ	RRRRRRRYKADFQAERHAREKLVEKKEYLQEQ LEQLQREFNKL	(Carvalho et al., 2007)
NF-κB activation inhibitors			
p65	AntP-p65-P1	RQIKIWFQNRRMKWKKQLRRPSDRELSE	(Takada et al., 2004)
Nuclear translocation inhibitors			
p50 NLS	SN50	AAVALLPAVLLALLAPVQRKRQKLMP	(Lin et al., 1995)
	BMS-205820	AAVALLPAVLLALLAPPKKKRKV	(Fujihara et al., 2000)
	BMS-214572	AAVALLPAVLLALLAPAKRVKL	(Yamaoka et al., 1998)
	PN50	RQIKIWFQNRRMKWKKVQRKRQKLMPC	(Letoha et al., 2005)

Note: Underlined sequences correspond to the inhibiting cargo. Non-underlined sequences correspond to the CPP.

1.3.4. Cell penetrating peptides used in this project

As previously described, a great variety of sequences have been identified to have cell-penetrating properties. These have been grouped into three classes: cationic, amphipathic and hydrophobic, based on their physico-chemical properties. The amino acid content and its place in a CPP sequence determine most of the cell penetrating properties of the peptide and it is also how its classification is determined. This means that each class of peptides interacts with the cell membrane in different ways, however variability can still be found within classes (Milletti, 2012). For this reason, all three classes of peptides are represented by at least one CPP in this project. The CPP used and the respective amino acid sequences can be found in Table 1.6.

Table 1.6 – Amino acid sequence of CPPs used in this project.

CPP	Sequence	Class
(RXR)4	RXRRXRRXRRXR	Cationic
R8	RRRRRRRR	Cationic
FFR8	FFRRRRRRRR	Cationic
TP10	AGYLLGKINLKALAALAKKIIL	Amphipathic
PFV	PFVYLI	Hydrophobic

Note: X is 6-aminohexanoic acid

1.3.4.1. Cationic peptides: R8, FFR8 and (RXR)4

Cationic peptides have a high number of positive charges and are mainly composed of arginine and/or lysine (Fei et al., 2011). The most commonly used cationic peptides are the Tat peptide, from the HIV transactivator protein Tat, Penetratin, a 16 amino acid domain from the AntP protein of *Drosophila* and oligoarginines (e.g. R8) (Schmidt et al., 2010).

Studies of the Tat 9-mer (RKKRRQRRR or Tat_{49-57}) in Jurkat cells revealed the importance of the positive charge (Wender et al., 2000). Wender and colleagues replaced one amino acid at a time in the Tat 9-mer, which revealed that both lysine and arginine residues were crucial for the uptake of the peptide (Wender et al., 2000). Following these studies a CPP containing nine lysine residues and another CPP containing nine arginine residues were designed and tested in Jurkat cells. Both 9-mers had higher uptake than the Tat 9-mer with the nona-arginine being more effectively taken up than the lysine 9-mer (Wender et al., 2000). Further studies with

oligoarginines helped determine that the optimal length required for an efficient uptake is between seven and nine residues, being eight the one with the highest uptake (Futaki et al., 2001). Furthermore, as the number of arginine residues increases or decreases the ability of the peptides to be taken up becomes compromised (Futaki et al., 2001).

The internalisation mechanisms of cationic peptides is still not entirely understood, but it has been shown to be highly dependent on the incubation conditions (Duchardt et al., 2007; Futaki et al., 2007). Both direct translocation and endocytosis have been implicated in the uptake of these peptides, with the majority of the peptides being internalised by endocytosis at low concentrations and at 37˚C, but being internalised by direct translocation at 4˚C and at high concentrations (Al-Taei et al., 2006; Fretz et al., 2007; Futaki et al., 2007; Nakase et al., 2004; Watkins et al., 2009b).

The guanidinium headgroups of arginine residues are thought to be a critical element for the successful intake of arginine-rich peptides. Studies with polyguanidine contributed to this understanding and also revealed the importance of length and side chain flexibility for the uptake of arginine-rich peptides. To further study how the spacing between arginines impacted the uptake of CPPs, Rothbard et al. (2002) synthesised a range of peptide analogues where non-α amino acids were introduced between arginine residues and their cellular uptake studied in Jurkat cells. The addiction of 6-aminohexanoic acid between arginine residues, also contributed to increase the resistance of the peptides to proteolysis improving the half-life of the peptide (Rothbard et al., 2002). This study led to the discovery of novel CPPs with enhanced capabilities of cellular uptake, the most commonly used of these peptides being (RXR)4 (Rothbard et al., 2002).

(RXR)4 was used in this project and is also known as 6-aminohexanoic oligoarginine. It is composed of 8 arginine residues spaced by a residue of 6-aminohexanoic acid (See Table 1.6 for amino acid sequence). (RXR)4 has been widely used as a vector for the delivery of oligonucleotides *in vitro* in several infectious disease models (Burrer et al., 2007; Lai et al., 2008; Lupfer et al., 2008), Duchenne muscular dystrophy (Fletcher et al., 2007; Jearawiriyapaisarn et al., 2008) and to prevent cardiac ischemia-reperfusion injuries (Boisguerin et al., 2011). (RXR)4 has also been used in the HeLa pLuc705 splice-correction model (Abes et al., 2006) and it has also been tested *in vivo* as a delivery vector of morpholino oligomers that target c-myc (Amantana et al., 2007).

R8 was the polyarginine chosen for this project, due to its previously proven efficacy to deliver pro-apoptotic peptides into leukaemic cell lines and primary human CLL cells (Bánóczi et al., 2010; Looi et al., 2011; Szabó et al., 2010; Watkins et al., 2011). R8 has been used to deliver cargoes targeting a variety of diseases including cancer (Valero et al., 2011; Wang et al., 2013), malaria and tuberculosis (Sparr et al., 2013) and pulmonary arterial hypertension (Yin et al., 2013), to name a few. R8 has also been used to improve the delivery of liposomes packed with anti-tumour drugs (Chen et al., 2013; Nakamura et al., 2013).

The choice to use FFR8 in this project was based on the studies by Kolluri et al. (2008) and Watkins et al. (2011). Kolluri and colleagues used a short peptide sequence (FSRSLHSLL and the D-isomer form fsrslhsll) attached to R8, which proved to have cytotoxic effects on MDA-MB435 (melanoma) cells (Kolluri et al., 2008). A mutant version of these peptides where the N-terminal phenylalanine and the C-terminal leucine were replaced by an alanine residue showed to have no cytotoxic effect on the same cells cultured in the same conditions (Kolluri et al., 2008). This suggested that the phenylalanine residue in the N-terminal and/or the leucine residue in the C-terminal could be determinant for the cytotoxic effects caused by the peptide (Kolluri et al., 2008). The enhanced uptake caused by phenylalanine residues has been observed previously (Mason et al., 2009; Moulton et al., 2004; Takayama et al., 2009). However, it was only when Watkins and colleagues set out to test the D-NuBCP-9-r8 peptide, used by Kolluri and colleagues, that the crucial role of the phenylalanine residue was determined (Watkins et al., 2011). The study combined the use of live confocal microscopy and viability assays, in leukaemia cells lines and primary human CLL cells (Watkins et al., 2011). The study showed that the N-terminal phenylalanine was crucial for the enhanced ability of the peptide to penetrate the cellular membrane and induce cell death (Watkins et al., 2011). For this reason, the incorporation of two phenylalanine residues into the N-terminal of R8 seemed to have the potential to increase the permeability properties of R8.

1.3.4.2. Amphipathic peptide: TP10

Amphipathic CPPs are characterised by possessing both hydrophobic and hydrophilic residues (Milletti, 2012; Shin et al., 2014). They are distinguished from cationic CPPs as they lack (or have very few) arginine residues (Milletti, 2012; Shin et al., 2014). Amphipathicity and lysine residues are thought to play an important role in penetrating

capabilities of these peptides (Milletti, 2012; Shin et al., 2014). A few of the most commonly used amphipathic CPPs are transportan (Pooga et al., 1998a) and its shorter analogue TP10 (Soomets et al., 2000), MPG (Morris et al., 1997), Pep-1 (Morris et al., 2001) and MAP (Oehlke et al., 1998).

Transportan is a 27-residues long chimeric CPP (GWTLNSAGYLLGKINLKALAA-LAKKIL) that contains the first 12 amino acids of the amino-terminal part of the neuropeptide galanin and 14 amino acids from mastoparan (wasp venom peptide), connected by a lysine residue (Pooga et al., 1998a). Transportan contains the N-terminal part of galanin and therefore it is recognised by galanin receptors, and the mastoparan portion of the sequence induces GTPase activity (Soomets et al., 2000). Both of these affect the permeable capabilities of the peptide (Soomets et al., 2000). To minimise these effects and to determine which portion of the sequence is responsible for the membrane translocation properties, Soomets and colleagues synthesised nine truncated versions of transportan (Soomets et al., 2000). One of the analogues proved to have improved membrane translocation, did not induce GTPase activity and was not recognised by galanin receptors (Soomets et al., 2000). This new CPP was named TP10 (Soomets et al., 2000).

TP10 has a 21-amino acid sequence, AGYLLGKINLKALAALAKKIL (Soomets et al., 2000). It forms an α-helical secondary structure and it penetrates the cellular membrane through interactions between the lysine residues and the phospholipids in the bilayer (Dunkin et al., 2011; Song et al., 2011; Yandek et al., 2007). TP10 has been used to target intracellular proteins involved in cell signalling and membrane fusion of basophilic leukaemia (Howl et al., 2003), for the delivery of antisense PNAs in cortical neurons to identify RNA-binding proteins (Zielinski et al., 2006), to target *Plasmodium falciparum* the parasite of malaria (Arrighi et al., 2008), as a delivery system for zinc finger recombinant proteins (Wang et al., 2010), a myc double stranded oligodeoxynucleotide decoy into neuroblastoma and breast cancer cell lines (El-Andaloussi et al., 2005) or a NF-κB PNA decoy in a insulinoma cell line (Fisher et al., 2004).

1.3.4.3. Hydrophobic peptide: PFVLY

Hydrophobic CPPs are considered to have only non-polar residues, have a low net charge or have a hydrophobic motif that is crucial for the uptake of the peptide (Milletti,

2012). A few of the most commonly used hydrophobic peptides are Pep-7 (Gao et al., 2002) and PFVLY or C105Y (Lin et al., 1995; Rhee & Davis, 2006). In this project, PFVLY (from now on named PFV) represents the hydrophobic peptides class. PFV is a shorter analogue of C105Y (CSIPPEVKFNKPFVYLI) and it corresponds to the portion of C105Y responsible for membrane translocation (PFVLY (Rhee & Davis, 2006). C105Y is a synthetic peptide that corresponds to the amino acid sequence between residues 359-374 of α1-antitrypsin (Rhee & Davis, 2006). Watkins et al. (2009a) studied the cellular uptake, distribution and cytotoxicity of PFV coupled with a pro-apoptotic domain (PAD) in adherent and leukaemic cell lines, as well as primary CLL cells. This CPP induced cell toxicity in all cell lines tested within the micromolar concentration range, however this peptide was less effective than R8-PAD (Watkins et al., 2009a).

1.4. Aims and objectives

The previously mentioned NF-κB inhibitors demonstrate the importance of this pathway for the survival of CLL. More importantly, some of these inhibitors are more cytotoxic to CLL cells than normal B-cells, reinforcing the importance of NF-κB in preferentially maintaining CLL cell viability. Although the introduction of drugs such as fludarabine and rituximab have improved greatly the response and survival of CLL patients, CLL still remains an incurable disease. The identification of relevant molecular targets represents an important step forward to tackle the most common form of leukaemia in the Western world. NF-κB is one of those targets.

Since CPPs have been shown to be highly effective at delivering bioactive cargo into cells at doses in the low micromolar range, they are promising candidates to deliver a NF-κB targeting drug. Therefore, this thesis explored the use of CPPs in CLL.

The main hypothesis was that apoptosis can be induced in primary CLL cells, by the use of a novel CPP targeting NF-κB subunits p50 and p65. To achieve this, the project was divided into three parts, representing three main objectives:

1. To determine if five fluorescently-labelled CPPs [(RXR)4, R8, FFR8, TP10 and PFV] can penetrate the membrane of primary human CLL cells and establish their sub-cellular localisation using confocal microscopy.

2. Based on the findings in 1., select a CPP or CPPs to carry a cargo that specifically targets the translocation into the nucleus of either NF-κB subunit p50 or p65 and measure their effects on the viability of primary CLL cells.

3. To determine the LC_{50} values for the novel peptides and establish whether sub-LC_{50} concentrations of the peptides are capable of inhibiting translocation of the NF-κB subunits into the nucleus of primary CLL cells.

Chapter 2- Material and Methods

2.1. Fluorescent Labelling of Cell Penetrating Peptides

The five different peptides were purchased as lyophilised powder with a GC-NH_2 (glycine-cystein-amide) modified end to allow fluorescent tagging (Watkins et al.,

2009a). Lyophilised CPPs (EZBiolab) and Alexa Fluor 488 C_5 maleimide (A-10254, Invitrogen) were diluted with methanol (CH_3OH) to a concentration of 2mg/ml. A 50 μl aliquot of the unlabelled peptide was collected to be used as a control for HPLC peptide purification. The CPPs were then mixed with the Alexa Fluor 488 at a ratio of 1.2 molecules of Alexa Fluor 488 to 1 molecule of CPP. The mixture was prepared and left overnight on a rotator to allow the reaction to reach completion. Two samples of 50 μl of the reaction mixture were collected at 0 and 1 hour to assess the status of the reaction.

2.1.1. CPP Purification and Assessment

To separate labelled peptide from unlabelled in the reaction mixture, reverse-phase HPLC was performed. The purification was performed using a C18 100Å 5 µm semi-preparative column and deionised (dH_2O) and filtered water with 0.1% trifluoroacetic acid (TFA; CF_3COOH) as solvent A and acetonitrile (ACN) with 0.1% TFA as solvent B at a flow rate of 3ml/min and using a 100 µl injection loop. The gradients used to elute the labelled peptides are shown in Table 2.1. Due to the high polarity of the amphipathic and hydrophobic peptides (i.e. TP10 and PFV respectively), the gradient used for the arginine-rich peptides was not appropriate for the separation and discreet elution of these labelled and unlabelled peptides. Therefore, the gradients suggested by EZBiolabs were used to elute these peptides (see Table 2.1).

Table 2.1 – Eluting gradients for the five different peptides.

Peptides	Time (minutes)	H_2O	ACN
(RXR)4 R8 FFR8	0	98%	2%
	5	80%	20%
	25	70%	30%
	30	5%	95%
	35	98%	2%
	35.1	STOP	
TP10	0	75%	25%
	25	50%	50%
	30	0%	100%
	30.1	STOP	
PFV	0	70%	30%
	25	45%	55%
	25.1	0%	100%
	30	STOP	

Before collecting the labelled peptide, test runs were performed to determine the different retention times of the labelled and unlabelled peptide. A sample with 50 μl of pure unlabelled peptide diluted in 50 μl of methanol was analysed first, followed by samples of the reaction mixture diluted with methanol at the same ratio at 0 and 1 hour. Figures 2.1 and 2.2 show two representative chromatographs of the unlabelled and labelled peptide. The fluorescent fractions were collected and a sample of the labelled peptides was saved to determine its mass by matrix-assisted laser desorption/ionisation – time of flight (MALDI-TOF) mass spectrometry (Figure 2.3); the rest was frozen at -20˚C.

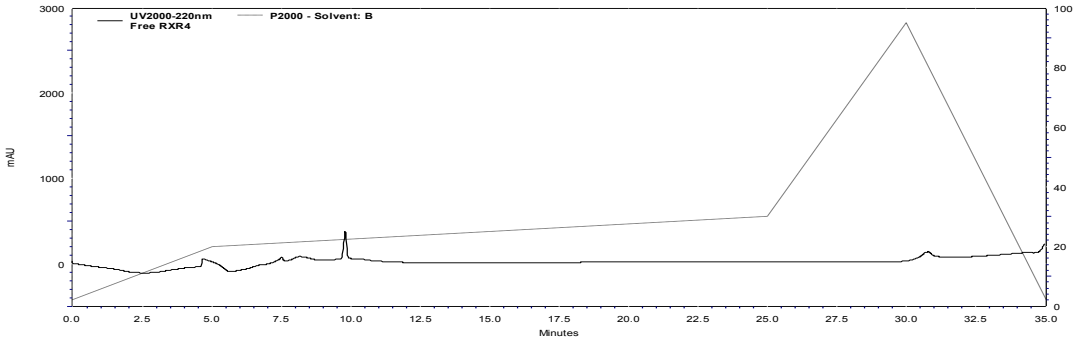

Figure 2.1 – Chromatograph of unlabelled (RXR)4.
Unlabelled (RXR)4 was run through a C18 100Å 5 µm semi-preparative column according to the gradient described in Table 2.1. Free $(RXR)_4$ retention time: ≈ 10min. Light grey line represents the gradient of solvent B (ACN + 0.1% TFA), scaled on the right Y-axis.

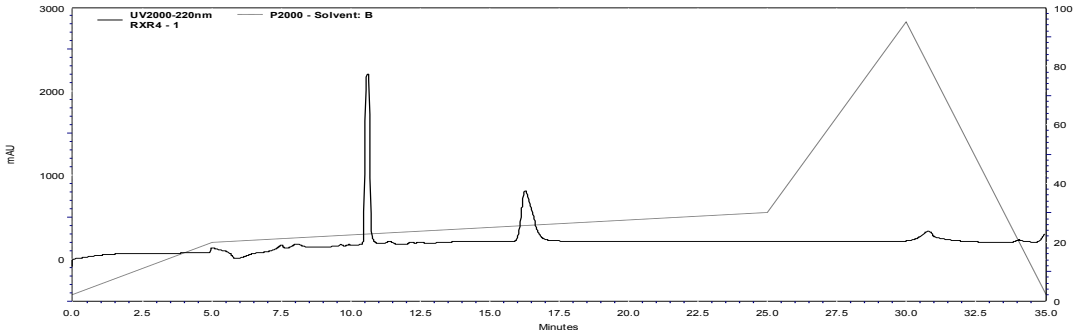

Figure 2.2 - Chromatograph of labelled $(RXR)_4$.
Labelled (RXR)4 was run through a C18 100Å 5 µm semi-preparative column according to the gradient described in Table 2.1. Free $(RXR)_4$ retention time: ≈ 10min.; $(RXR)_4$-Alexa Fluor 488 retention time: ≈ 10.5min.; free Alexa Fluor 488 retention time: ≈ 16.5min. Light grey line represents the gradient of solvent B (ACN + 0.1% TFA), scaled on the right Y-axis.

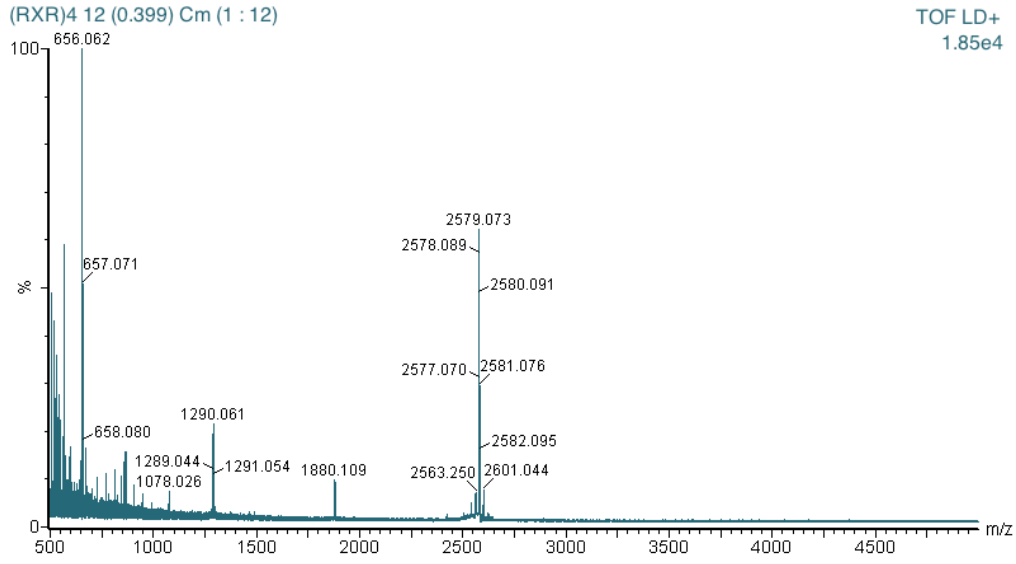

Figure 2.3 - Mass spectrometry trace of labelled $(RXR)_4$.
The labelled peptides were analysed by MALDI-TOF to confirm the presence of labelled peptide within the sample.

$(RXR)_4$ molecular weight (MW): 1880; Alexa Fluor 488 MW: 700; $(RXR)_4$-Alexa Fluor 488 MW: 2580; $[(RXR)_4\text{-Alexa Fluor 488}]^{+2}$ MW: 1290. Each peak represents a fraction of the sample.

Samples were prepared using the ultra thin layer method (Fenyo et al., 2007). Stainless steel MALDI sample plates were rinsed alternately with methanol and distilled H_2O (dH_2O) and wiped with lens tissue to remove any previous sample or debris that could affect the analysis. The thin layer substrate solution was prepared by mixing one part of saturated α-cyano-4-hydroxycinnamic acid (CHCA; 2 parts of ACN plus 1 part of dH_2O and 0.1%TFA) with three parts of isopropanol. Around 30 μl of the thin layer substrate were applied to the plate and with a help of a 200 μl tip the substrate was spread without causing any scratches, and the substrate left to air dry. Ghaith Al-Jayyoussi prepared the matrix solution by mixing 5mg/ml of CHCA with 1 part of dH_2O and 1 part of ACN. The matrix solution was tested by applying 0.5 μl to the plate. If correctly prepared it shouldn't take more than 20 seconds to crystalise. The samples were prepared by diluting them with the matrix solution (1:10) and 0.5 μl of this mixture was spotted onto the plate. After crystallisation of matrix/analyte occurred the excess liquid was removed by vacuum suction. Samples were then analysed by mass spectrometry.

The frozen peptides were then lyophilised and dissolved in dH_2O and using spectrophotometry, a wavelength scan was performed to ensure the highest peak obtain was at Alexa Fluor 488 excitation maximum (519nm). The concentration of each peptide was calculated and the peptides were lyophilised again and dissolved in dH_2O to obtain a concentration of 1mM. The peptides were aliquoted and stored at -80˚C.

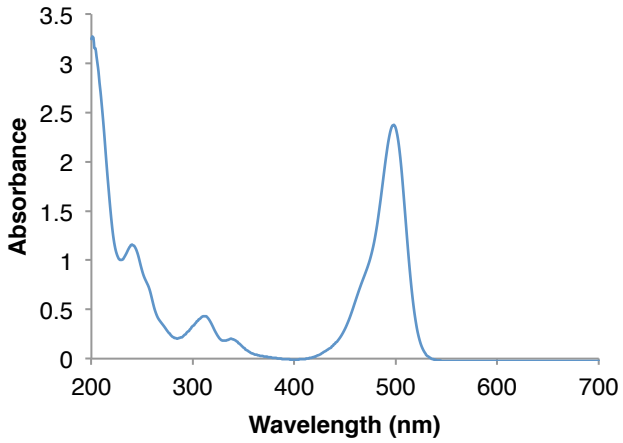

Figure 2.4 – Representative spectrophotometry wavelength scan.
Following elution of the labelled peptides, a spectrophotometry wavelength scan was performed for each of the peptides. Alexa Fluor 488 excitation maximum: 495nm.

2.2. Isolation of mononuclear cells from peripheral blood

Peripheral blood mononuclear cells (PBMC) were isolated by centrifugation using an isosmotic solution, Lymphoprep (Axis-Shield). Peripheral blood was layered on top of Lymphoprep and centrifuged at 300xg for 20 minutes with the centrifuge brake turned off. Following centrifugation, the buffy coat (i.e. layer containing PBMCs) was collected and placed in a new sterile tube, washed with PBS and centrifuged at 300x*g* for 5min. The supernatant was discarded and dH_2O was added to carefully lyse any erythrocytes. The sample was then centrifuged at 300x*g* for 5min. The resulting supernatant was discarded and PBS was added to the pellet. Samples were centrifuged at 300x*g* for 5min. PBS was used to resuspend the cells. Cells were then counted.

2.2.1. Patient samples and ethical approval

Primary CLL cells were collected from CLL patients from the University Hospital of Wales Cardiff and Birmingham Heartlands hospital. The patients' informed consent was obtained in accordance with the ethical approval granted by the South East Wales Research Ethics Committee in accordance with the Declaration of Helsinki.

2.2.2. Cell counting on the Beckman-Coulter Vi-cell XR

Cells were counted using a Vi-cell XR (Beckman-Coulter) cell counter by diluting 50 μl of each sample into 450 μl of PBS (1 in 10 dilution) in a Vi-cell sample cup. Settings could be set for different types of cells (i.e. CLL cells, fibroblasts) and the dilution factor could also be adjusted. The Vi-cell XR uses the trypan blue exclusion method to count the number of viable cells. This method relies on the fact that non-viable cells take up trypan blue, whereas viable cells exclude it.

2.2.3. Cell counting using the Neubauer Haemocytometer

Alternatively, cells were counted using a Neubauer haemocytometer. A small amount of cells (approximately 10 μl depending on the turbidity of the cell suspension) were mixed with 10 μl of trypan blue to stain dead cells. Ten microliters of the mixture was inserted onto a well of a disposable Neubauer haemocytometer and placed under the microscope. The unstained cells in 3 of the small squares were counted, the average of

those counts was calculated and multiplied by 9 (to make up for the 9 squares) and then multiplied by 20,000 to give the number of cells per millilitre.

2.3. Cell culture

2.3.1. Culture media

In all types of culture, Dulbecco's Modified Eagle's Media (DMEM; 11965-092, Invitrogen) was used. In addition to the media 10% foetal calf serum, 2% penicillin/streptomycin and 1% pyruvate were added.

2.3.2. Liquid culture of primary human PBMCs

Liquid cultures of PBMCs derived from CLL patients were typically performed in 48-well plates at a cell density of $1x10^6$ cells in 500 μl of DMEM media. These cultures were routinely supplemented with 5ng/ml of interleukin-4 (IL-4), unless stated otherwise. Incubation was performed at 37˚C in a humidified 5% carbon dioxide (CO_2) atmosphere. If a larger number of cells were required, all volumes were adjusted to ensure the same density was maintained. Liquid culture of PBMCs from healthy donors was performed in 48-well plates at a density of $1x10^6$ cells in 500 μl of DMEM media, with no other supplements.

2.3.3. Culture of transfected and non-transfected mouse fibroblasts L cell lines

The CD40 ligand (CD40L) mouse fibroblast L cells used in this study were a kind gift from Dr Aneela Majid (Leicester University). CD40L cells and non-transfected fibroblasts (NTL) were maintained in T75 flasks with 15ml of DMEM media. These cells have adherent properties, so when they reached confluence the media was discarded and cells left attached to the bottom of the flask. The serum contained in the culture media is known to inhibit the activity of trypsin, so in order to allow trypsin to detach the adherent cells, a washing step with 10ml of PBS was performed. Afterwards, 5ml of trypsin was added to the flask and incubated for 5 minutes at 37˚C and 5% CO_2. To ensure all cells had detached from the plastic, the flask was examined under an inverted light microscope. Once the cells were observed to be floating, 10ml of DMEM

media was added to inactivate trypsin and all the contents of the flask were placed in a 15ml tube and centrifuged at 300x*g* for 5 minutes. The supernatant was then discarded and 10ml of DMEM media was used to resuspend the cells. Between 0.5 and 3ml was placed in a new T75 flask, depending on the amount of cells needed in future experiments, and 15ml of DMEM media was added. The flask was then placed in an incubator at 37˚C with 5% of CO_2 for 2 or 3 days. The rest of the cells were irradiated in readiness for co-culture with CLL cells.

2.3.4. Preparation of transfected and non-transfected mouse fibroblasts L cells for co-culture

Both transfected and non-transfected fibroblasts were used as feeder cells in a co-culture system with CLL cells. These co-culture conditions are designed to mimic the *in vivo* environment experienced by CLL cells in the lymphoid tissues. The transfected mouse fibroblasts were genetically modified to express human CD40 ligand, which is known to activate CLL cells (Pepper et al., 2011; Willimott et al., 2007b). Both transfected and non-transfected fibroblasts were irradiated prior to seeding into the plates. Irradiation inhibits fibroblast growth but does not affect their viability or their biological activities, allowing the CLL cells to be maintained in culture for longer periods.

The fibroblasts were irradiated with 75 Grays (28 minutes in the presence of Caesium-137, γ emission). The cells were then counted and $1x10^6$ feeder cells were plated into each well of a 6-well plate. The cell density was adjusted according to the experimental requirements, with a ratio of 1 CD40L cell to 10 CLL cells being optimal. Cells were left overnight to allow them to adhere to the plate at 37˚C with 5% CO_2. The following day, the old media and any non-adherent cells were removed and replaced with fresh DMEM media and left in the incubator at 37˚C with 5% CO_2, for a maximum of 4 days, until needed.

2.3.5. Co-culture of CLL cells with transfected and non-transfected mouse fibroblasts L cells

Survival of CLL cells is dependent of a variety of signals provided by the *in vivo* microenvironment (Bergwelt-Baildon et al., 2004; Deaglio & Malavasi, 2009; Farahani

et al., 2005). The lymphoid tissues are the main sites for CLL proliferation. Here, CLL cells are stimulated by T-cells and soluble cytokines, which results in their activation and proliferation. The stimulation of CD40, a molecule expressed on normal B-cells and CLL cells, is one of the main mechanisms responsible for B-cell activation. Its ligand, CD154 or CD40L is expressed in a variety of cells including T-cells (Bergwelt-Baildon et al., 2004; Deaglio & Malavasi, 2009; Farahani et al., 2005).

After preparation of the feeder layer of cells as previously described (section 2.3.4), $1x10^7$ CLL cells were added to each well. Cell density was adjusted according to experimental requirements, with an optimal ratio of 1 CD40L cell to 10 CLL cells. In addition, 5ng/ml of IL-4 was added. The co-cultures were then incubated at 37˚C with 5% CO_2 for the required amount of time ranging from 1 hour up to 5 days. Once the full incubation period was reached, CLL cells were carefully collected, trying to avoid removing any fibroblasts that could potentially interfere with downstream analysis. Cells were then washed with PBS and placed in liquid culture or analysed by flow cytometry, depending on the experimental protocol.

2.4. Flow Cytometry

Cell surface expression of a variety of cell or activation markers was monitored by flow cytometry, as well as peptide fluorescence or apoptotic state. For the majority of experiments, a maximum of 3 fluorochromes were used. For these experiments a BD Accuri C6 was used. Phenotyping experiments that employed more than 4 fluorochromes, such as the ones present in Chapter 5, samples were analysed using a BD FACSCanto II or a BD FACSAria. Data from the BD Accuri C6 was analysed using CFlow Plus software and data from the BD FACSCanto II or BD FACSAria was analysed using FlowJo version 10.

2.4.1. CLL cell analysis – CD19 and CD38 expression

As previously described, CLL is characterised by the accumulation of $CD19^+$ $CD5^+$ B lymphocytes. In order to determine the CLL population in a peripheral blood sample, CD19-expressing lymphocytes were quantified by flow cytometry. At the same time, the CD38 status of CLL patients was also assessed, as the expression of this molecule provides prognostic information and is the subject of several on-going research

projects within the lab. To perform this analysis, monoclonal antibodies against CD19 (MHCD1905, Invitrogen) and CD38 (MHCD3804, Invitrogen) were used.

Three hundred thousand ($3x10^5$) PBMCs were aliquoted for CD19 and CD38 staining. One control (no antibody) and one test sample were used for every patient sample. One hundred microliters of PBS was added to the controls and test samples, followed by 4 μl of anti-CD19 and -CD38 antibodies (added to test samples only). All samples were incubated at room temperature and in the dark for 10 minutes. Cells were then washed with 2ml of PBS and centrifuged at 300x*g* for 5 minutes. The supernatant was discarded and cells resuspended in 200 μl of PBS. Cells were analysed using an Accuri C6 flow cytometer. Representative dot plots and histograms are shown in Figure 2.5.

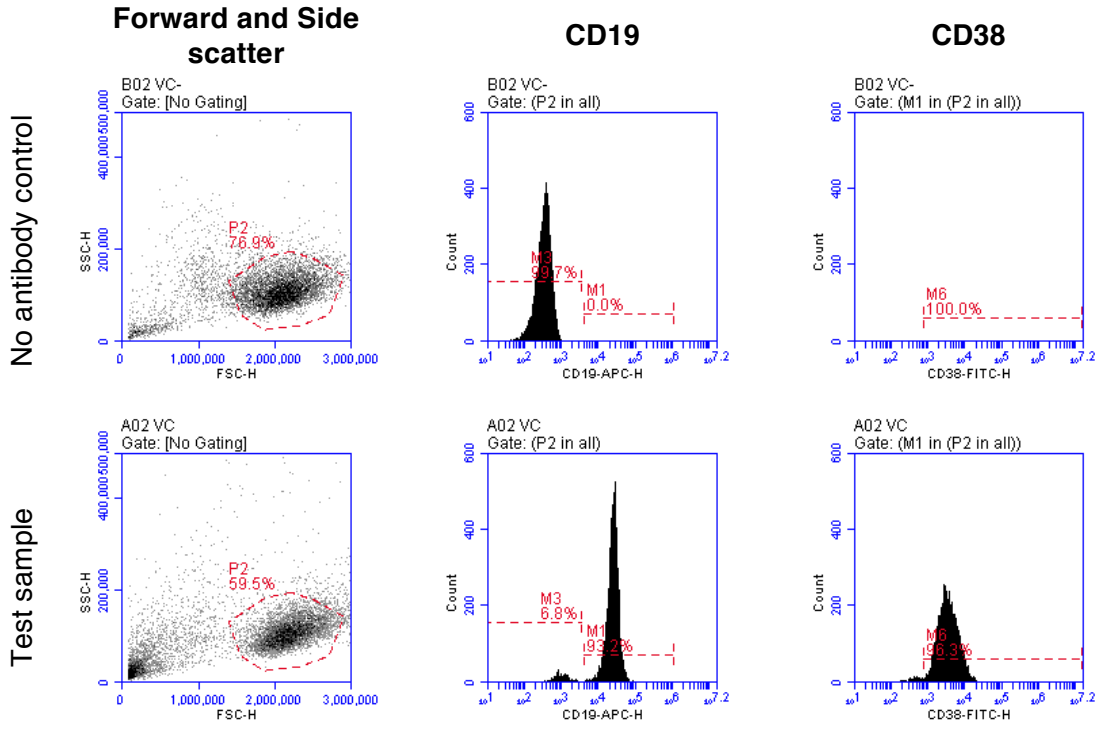

Figure 2.5 –CD19 and CD38 expression of primary CLL cells.

Primary CLL cells were incubated with anti-CD19 and anti-CD38 antibodies for a period of 10 minutes in the dark. Cells were then centrifuged and washed. Analysis was performed using the flow cytometer BD Accuri C6. P2 gates viable lymphocytes. M3 gates $CD19^-$ cells and M1 $CD19^+$. M6 gates $CD38^+$ cells.

2.4.2. Normal B and T cell analysis – CD19 and CD3 expression

CD19 is expressed in B-cells throughout most stages of B-cell development (Otero et al., 2003) and it was used to positively identify B-cells from PBMCs obtained from healthy donors. CD3 is expressed on all T-cells (Guy & Vignali, 2009) and it was used to positively identify T-cells from PBMCs obtained from healthy donors. PBMCs were incubated under conditions dependent on the experimental procedure, and subsequently incubated with 4 μl of anti-CD19 (MHCD1905, Invitrogen) and 2.5 μl of anti-CD3 (12-0036-42, eBiosciences) antibodies for a period of 10 minutes, at room temperature and in the dark. Unbound antibody was washed with PBS and centrifuged at 300x*g* for 5 minutes and the pellet was resuspended in PBS. Antibody fluorescence was measured by flow cytometry.

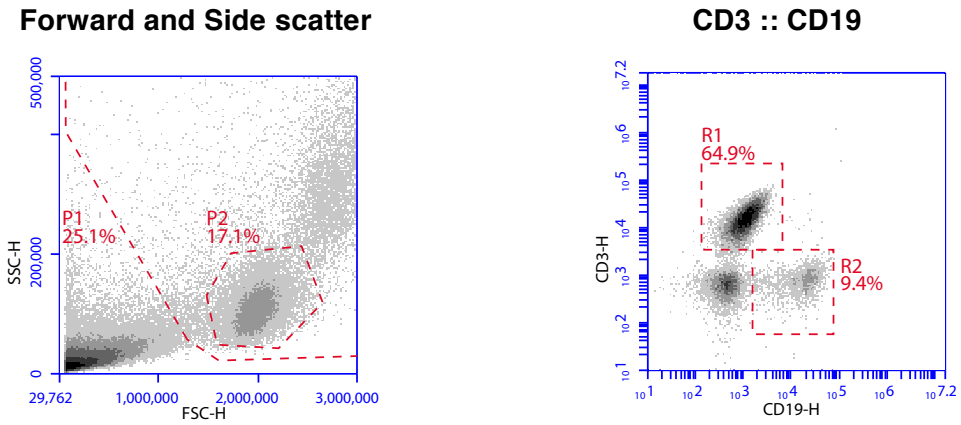

Figure 2.6 – CD3 and CD19 expression in primary CLL cells.

Lymphocytes were gated in P2. Fluorescence of anti-CD3 and -CD19 antibodies was measured within the gate and plotted against each other. R1 gates $CD3^+/CD19^-$ cells (T-cells) and R2 gates $CD3^-/CD19^+$ (B-cells). Monitoring of other markers can be assessed within each of the cell populations.

2.4.3. CPP fluorescence analysis – Alexa 488 fluorescence

As previously described, some of the peptides used in this project were labelled with the fluorochrome Alexa Fluor 488. This allowed their detection within cells using certain techniques, such as flow cytometry. Cells were incubated under the conditions described in section 2.3, depending on the experimental procedure, with or without fluorescently tagged peptides. Cells were harvested and washed with PBS and

analysed by flow cytometry. Figure 2.7 shows the monitoring of peptide fluorescence in an untreated and peptide-treated sample.

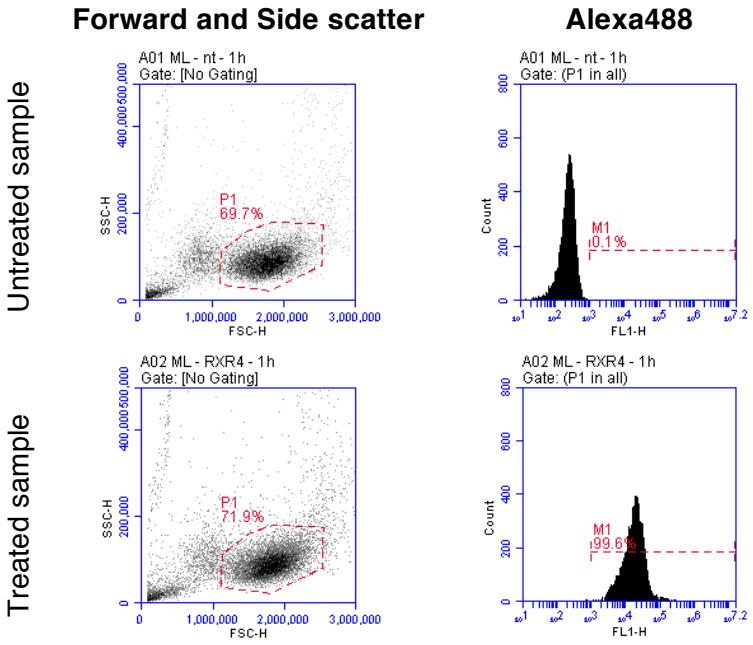

Figure 2.7 – Alexa488 fluorescence in untreated primary CLL cells and cells treated with 2 μM of (RXR)4.

Viable lymphocytes were gated in P1. Alexa488 fluorescence was measured within the viable lymphocyte gate. There's a shift in fluorescence when compared to the untreated sample, which indicates that the cells have taken up the peptide.

2.4.4. Apoptosis detection - Annexin V & propidium iodide staining

Apoptosis is a form of programmed cell death. In viable cells, phosphatidylserine (PS) is located in the inner leaflet of the cellular membrane. When a cell enters the apoptotic process, PS is translocated to the external leaflet of the cell membrane (Boersma et al., 2005). Annexin V is a molecule naturally found in the body that binds to PS; this property has been exploited as a diagnostic tool for the quantification of apoptosis. By attaching a fluorochrome to Annexin V it is possible to detect it using flow cytometry or confocal microscopy. In order to distinguish apoptotic cells from necrotic cells, propidium iodide (PI) was used in conjunction with Annnexin V. In necrotic and late apoptotic cells, the cellular membrane integrity is compromised and therefore PI is able to enter cells and bind to DNA and RNA. The combination of Annexin V and PI enables

the discrimination between viable, early apoptotic and necrotic/late apoptotic cells (Boersma et al., 2005).

Following the appropriate experimental protocols, cells were washed with 500 *μ*l of binding buffer (88-8007-74, eBioscience) and centrifuged at 300x*g* for 5 minutes. The binding buffer contains an optimal concentration of calcium that is crucial for the binding of Annexin V to PS. After centrifugation, the supernatant was discarded and the cells resuspended in 195 *μ*l of binding buffer and 5 *μ*l of APC-conjugated Annexin V (88-8007-74, eBioscience). The cells were incubated for 10 minutes at room temperature in the dark in order to avoid photobleaching of the fluorochrome. Cells were then centrifuged at 300x*g* for 5 minutes and the supernatant was discarded. Cells were resuspended in 200 *μ*l of binding buffer and 5 *μ*l of PI (88-8007-74, eBioscience) was added. Cells were then analysed by flow cytometry. Figure 2.8 shows primary CLL cells untreated and treated with an NF-κB inhibitory peptide.

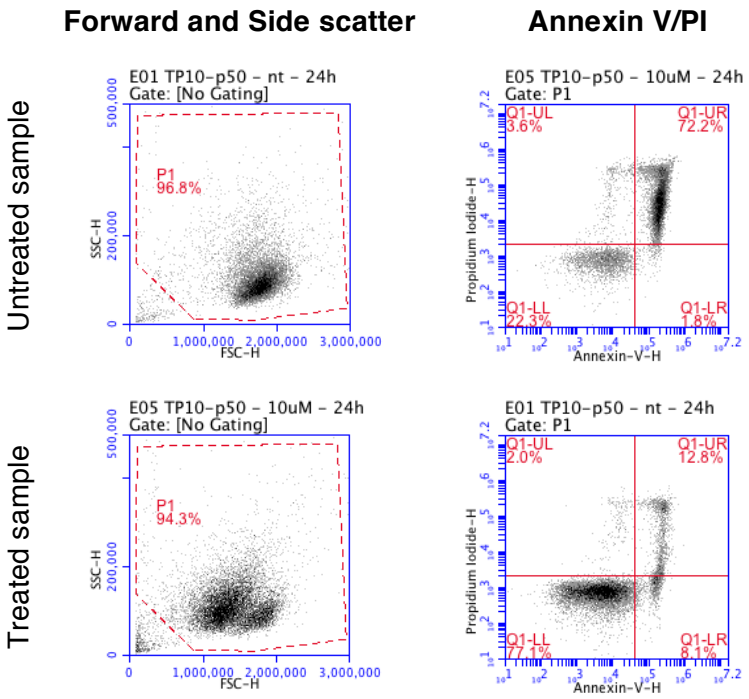

Figure 2.8 – Annexin-V and PI fluorescence of untreated primary CLL cells and TP10-p50i treated cells.
Primary CLL cells were washed with Binding Buffer and posteriorly incubated with Annexin-V for a period of 10 minutes. Cells were then centrifuged and resuspended in binding buffer. Flow cytometry analysis was performed with BD Accuri C6. P1 gates the lymphocyte population. Annexin-V and PI fluorescence is measured within the lymphocyte population. Lower left quadrant, Q1-LL – viable cells ($AnnexinV^-/PI^-$); lower right quandrant, Q1-LR – early apoptotic cells ($AnnexinV^+/PI^-$); upper right quadrant, Q1-UR – late apoptotic cells ($AnnexinV^+/PI^+$).

2.4.5. Apoptosis detection – Caspase-3 assay

Caspases are cysteine-aspartic acid proteases that play an important role in apoptosis. Caspase-3 exists as an inactive proenzyme that is activated as part of a cascade that leads to apoptosis of the cells. Caspase-3 activity can therefore be used to monitor induction of apoptosis. To do this, the cell-permeable substrate PhiPhiLux G_1D_2 (235430, Calbiochem) was used. The substrate contains two fluorochromes, separated by a quenching linking sequence, which upon cleavage by caspase-3 fluoresces green and can be quantified by flow cytometry or fluorescent microscopy.

One million primary CLL cells were treated under the conditions specific for each experimental protocol, harvested and centrifuged at 300x*g* for 5 minutes. Cells were resuspended with the PhiPhiLux G_1D_2 substrate at a concentration of 10 μM. Cells were incubated at 37˚C with 5% CO_2 for 1 hour, with the lid of the tube open. Cells were then washed with 1 ml of ice-cold flow cytometry dilution buffer provided with the assay kit (235430, Calbiochem) and resuspended with 200 μl of fresh ice-cold flow cytometry dilution buffer. Analysis was performed using the BD Accuri C6. Figure 2.9 shows an example of the flow cytometry data obtained.

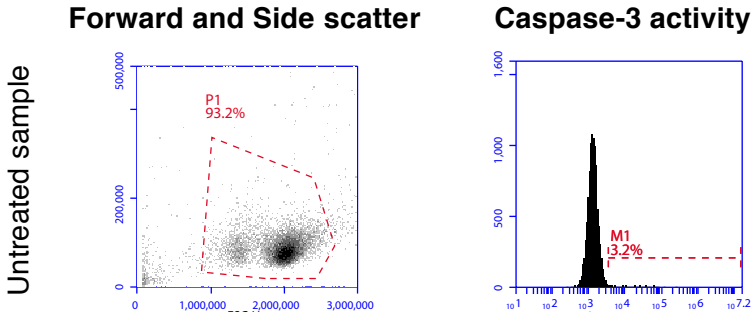

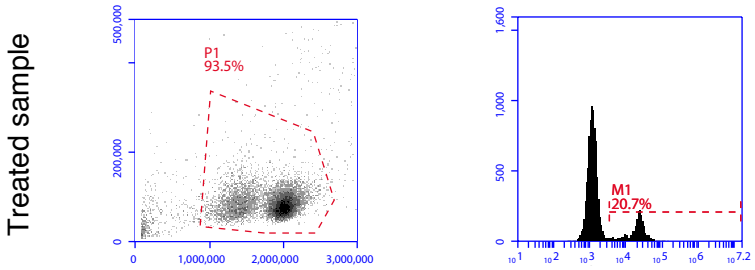

Figure 2.9 – Caspase-3 activity of untreated and treated primary CLL cells.
Primary CLL cells were incubated with PhiPhiLux G_1D_2 substrate for a period of 1 hour. Cells were then centrifuged and resuspended in flow cytometry dilution buffer. Flow cytometry analysis was performed with BD Accuri C6. The lymphocyte population was gated in P1. The substrate fluorescence was measured within the P1 gate. The M1 gate corresponds to caspase-3 activity.

2.5. Confocal microscopy

In order to determine the intracellular localisation of the different peptides, confocal microscopy experiments were performed. One million primary CLL cells were cultured with 4 μM of the fluorescently tagged peptides, in 500 μl of DMEM media, at 37˚C for a determined period of time (1 or 20 hours). Following the incubation period, cells were harvested and washed with PBS. To maintain optimal conditions, cells were resuspended in 30 μl of phenol red-free media (21063-029, Life Technologies) and transferred to a glass-bottomed imaging plate. Five microliters of DRAQ5 (DR50050, Biostatus) were added to cells to allow localisation of the nucleus. Since most nuclear dyes are blue, the colour representing DRAQ5 was artificially altered using the confocal microscopy software from red to blue. Images were taken using a Leica TCS SP5 confocal microscope.

2.6. Molecular Biology

2.6.1. Preparation of cytosolic and nuclear extracts

To assess the translocation inhibition of NF-κB subunits into the nucleus of primary CLL cells, nuclear and cytosolic extracts were generated after incubation with the cell penetrating NF-κB inhibiting peptides, using a protocol based on a previously described method (Brennan & O'Neill, 1995).

In order to generate detectable and comparable bands in western blotting experiments, samples were normalised by cell number. Numbers of cells ranging from $1x10^6$ to $1x10^7$ cells were used to determine the minimum cell number required to generate detectable bands for all of the proteins of interest. $5x10^6$ cells/condition was assessed as the minimum required for these experiments. Therefore the incubation conditions were adjusted in order to maintain the same cell to peptide ratio. Following incubation under conditions specific to the each experimental protocol, cells were harvested into 1.5 ml tubes, washed and resuspended with PBS, or the pellet frozen at -80˚C for later use. Samples were kept on ice for the entire extraction protocol, as well as all buffers used. Samples were centrifuged at 200x*g* for 5 minutes at 4˚C (Heraeus Biofuge Fresco). In the meantime, the low salt buffer was prepared by adding 10 μl of NP40 and 10 μl of phenylmethanesulfonylfluoride (PMSF) to 1 ml of the buffer (full contents of buffer can be found on Table 2.2). Following centrifugation, the supernatant was

discarded and the samples gently resuspended in 25 μl of the low salt buffer and kept on ice for 5 minutes. The volume of buffer used was determined according to the number of cells in the sample; a 25 μl volume was used for $5x10^6$ cells. The supernatant was transferred to a new tube as it contains the cytosolic fraction. The pellet contains the nuclear fraction and it was resuspended in 25 μl of the high salt buffer, supplemented with PMSF (10 μl of PMSF into 1 ml of high salt buffer). Samples were left on ice for 15 minutes. Following incubation, samples were centrifuged at 200x*g* for 5 minutes at 4˚C. The supernatant, containing the nuclear fraction was transferred to a new tube. Samples were stored at -20˚C for short periods of time or -80˚C if they were being stored for longer.

Table 2.2 – Extraction buffers.

Low salt buffer – Buffer A	High salt buffer – Buffer C
10mM Hepes pH 7.9 1.5mM $MgCl_2$ 10mM KCl 1μM PMSF 0.1% NP40	25% Glycerol 20mM Hepes 7.9 420mM NaCl 1.5mM $MgCl_2$ 0.2mM EDTA

2.6.2. Protein quantification

The total protein content of the samples was measured using the Bio-Rad Protein Assay (500-006, Bio-Rad). This assay is based on the Bradford method, which uses Coomasie Brilliant Blue G-250 dye, for which the absorbance shifts from 465 nm to 595 nm when it binds to protein (Bradford, 1976).

The protein standards were prepared using a bovine serum albumin (BSA) solution of 1mg/ml. Standard samples were prepared in duplicates, ranging from 0 to 6 μg of BSA. A sample standard curve is shown in Figure 2.10. The standards were freshly prepared for each protein quantification experiment. For the nuclear and cytosolic extracts, 25 μl of sample were placed on a 96-well plate. Samples were tested as duplicates, whenever possible. The dye reagent was prepared by mixing 1 part of concentrated dye with 4 parts of dH_2O, and 200 μl of the diluted dye was added to test samples and standards. The plate was incubated at room temperature for 5 minutes and the absorbance was read at 595 nm using a 96-well spectrophotometer. The standard curve was plotted using Microsoft Excel software. From the curve a polynomial trend line was drawn as well as the respective equation and R-squared value. The equation was used to calculate the protein concentration of the test samples.

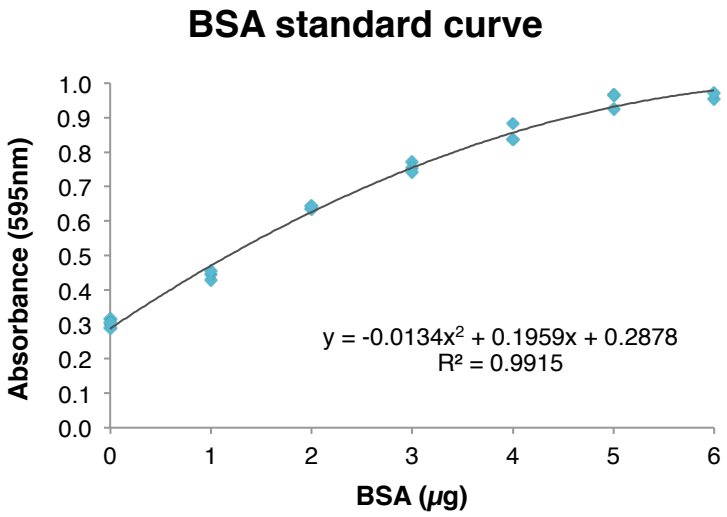

Figure 2.10 – Sample standard curve used to quantify total amount of protein in nuclear and cytosolic extracts.
Duplicates of BSA ranging from 1 to 6 μg of protein were used to create the standard curve. The trendline, respective equation and R^2 were obtained with Microsoft Excel.

2.6.3. Sodium dodecyl sulphate polyacrylamide gel electrophoresis (SDS-PAGE) and western blot analysis

2.6.3.1. Sample preparation

SDS-PAGE is a technique used to separate proteins based on the length of their polypeptide chains or molecular weight. This is based on the use of SDS detergent to remove secondary and tertiary protein structures and maintain the proteins as polypeptide chains. Therefore, the first step in sample preparation is the denaturing of the proteins by reducing the disulphide bonds under slightly alkaline pH conditions. This was achieved by the addition of NuPAGE Sample Reducing Agent (NP0009, Invitrogen), containing dithiothreitol (DTT) and by the addition of NuPAGE lithium dodecyl sulphate (LDS) Sample Buffer (NP0008, Invitrogen) to maintain the pH at an optimal level. The LDS sample buffer also contained Coomasie G250, phenol red and bromophenol blue that allowed the samples to be tracked through the gel. Samples were kept on ice, and 50 μl were transferred to a new 1.5 ml tube. 20 μl of the LDS sample buffer and 8 μl of the sample reducing agent were added to each sample.

Tubes were closed and placed on a heating block, previously heated to 80˚C and left for 10 minutes.

2.6.3.2. SDS-PAGE

Samples were separated using a Novex 4-12% Bis-Tris protein pre-cast polyacrylamide gel (NP321, Invitrogen). Gels were previously removed from package, the insulating tape and well comb were removed and the gel rinsed with dH_2O. Gels were placed in the XCell SureLock Mini-Cell (EI0001, Invitrogen) apparatus. The running buffer was prepared by diluting 25 ml of NuPAGE® MOPS SDS Running Buffer (NP0001, Invitrogen) into 475 ml of dH_2O. The buffer chamber of the apparatus was filled with the diluted running buffer and samples were loaded onto the gel. The first lane was loaded with 7 μl of the molecular marker SeeBlue Plus2 (LC5925, Invitrogen) and the following lanes were loaded with 30 μl of the samples previously prepared. The gel apparatus was closed and plugged to the PowerEase® 500 Power Supply (378723-007, Invitrogen). The power pack was set to run at 200V for 60 minutes. These settings were optimal to allow the gel front to reach the end of the gel and separate proteins.

2.6.3.3. Western blotting

While SDS-PAGE is running, the reagents and material for western blotting were prepared. One litre of transfer buffer was prepared by diluting 50 ml of NuPAGE Transfer Buffer (NP0006-1, Invitrogen) in 750 ml of dH_2O and 200 ml of methanol (Fisher Scientific). The blotting pads were soaked in transfer buffer, as well as the nitrocellulose membrane (BRD-100-540T, Fisher Scientific) and filter paper previously cut to 8.5cm x 7cm.

When the gel front reached the end of the gel, the SDS-PAGE was terminated. The system was dismantled and the XCell II™ Blot Module (EI9051, Invitrogen) was assembled according to the diagram shown in Figure 2.11. The blot module was placed into XCell SureLock Mini-Cell (EI0001, Invitrogen) apparatus, and the buffer chamber was filled with transfer buffer. The module was closed and the assembled system was plugged into the power pack and set to run at 50V, 350 mA for 2 hours.

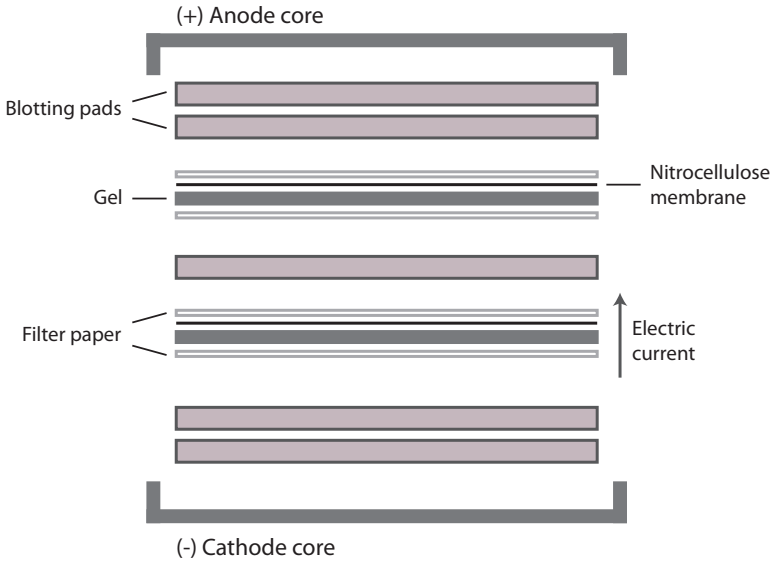

Figure 2.11 – Western blot assembly order.

Two blotting pads are placed in the cathode core, followed by the pre-assembled filter paper/gel/membrane/filter paper sandwich. A blotting pad is placed between the first and second sandwich. Two additional blotting pads are placed between the second sandwich and the anode core, to ensure the system is tightly closed within the cassette, and that the current is able to reach both sandwiches.

2.6.3.4. Immunodetection

To detect the target proteins, specific antibodies are used. The immunodetection can be divided into three stages: blocking, incubation with antibody and detection.

To prevent non-specific binding of primary and/or secondary antibodies to the membrane, a blocking agent is used. Therefore, following blotting, the membrane was placed in 10ml of previously prepared blocking solution for one hour at room temperature. The solution was prepared by placing 10 phosphate buffered saline (PBS) tablets (BPE9739-1, Fisher Scientific), adding dH_2O up to 1L and 1ml of Tween-20 (P7949, Sigma-Aldrich). The PBS-Tween solution was pre-heated to 80˚C, point at which 2g of I-Block™ solution (T2015, Invitrogen) was added and thoroughly mixed. The solution was left to cool down. 4g of sodium azide were added as a preservative and the solution was stored at 4˚C.

Following blocking, the membrane was probed with 10μl of primary antibody diluted in 10ml of blocking solution (1/1000). Depending on the primary antibody, the incubation period could vary from 1 hour at room temperature to overnight at 4˚C. Following

incubation, the membrane was washed three times with 10ml of PBS-Tween (10 PBS tablets, 2ml of Tween-20 in 1L of dH_2O) for periods of 10 minutes on a rocking platform at room temperature. The secondary antibody was diluted in blocking solution at a ratio of 1/10000 (1μl of antibody in 10ml of blocking solution), and the membrane incubated for a minimum of 1 hour at room temperature. The membrane was then washed three times with PBS-Tween for periods of 10 minutes on a rocking platform at room temperature.

Table 2.3 – Primary antibodies used.

Target Protein	Source
PARP (46D11)	9532S, Cell Signaling
NF-κB p65 (D14E12) XP	8242S, Cell Signaling
Phospho-NF-κB p65 (Ser536) (7F1)	3036S, Cell Signaling
NF-κB1 p105/p50	3035S, Cell Signaling
β-Actin (8H10D10)	3700S, Cell Signaling
β-tubulin (9F3)	2128S, Cell Signaling
HSP90 (C45G5)	4877S, Cell Signaling

Table 2.4 – Secondary antibodies used.

Secondary antibody conjugate	Target Species	Detection method	Source
IgG-AP	Mouse	Chemiluminescence	170-6520, Bio-Rad
IgG-AP	Rabbit	Chemiluminescence	170-6518, Bio-Rad
IgG-AlexaFluor680	Mouse	Infrared	A-21057, Life Technologies
IgG-IRDye800	Rabbit	Infrared	611-132-122, Lorne Laboratories Lmt

AP – Alkaline phosphatase

As for the detection step, two methods were used: chemiluminescence and far red detection. For the chemiluminescence detection method, the membrane was incubated with 10ml of alkaline phosphatase buffer (T2187, Applied Biosystems) for 3 minutes. The membrane was then placed in a plastic pouch and 600μl of the substrate Tropix CDP Star (T2146, Applied Biosystems) was added and incubated for 5 minutes. The excess reagent was removed and the membrane in the plastic pouch was placed in a cassette. In a darkroom, a sheet of Kodak X-Omat™ Blue (XB) film (NEF586001EA, Perkin Elmer) was placed on top of the membrane and left to be exposed in the dark for a period of 1 minute up to overnight (depending on the intensity of the bands obtained). The film was developed using an X-ray film developer machine. As for the

infrared detection, following incubation with the secondary antibody and a wash step with PBS-Tween, the membranes were scanned with an Odyssey® Infrared Imaging System (LI-COR).

2.6.4. Electrophoretic mobility shift assay (EMSA)

The EMSA is a method used to detect protein-nucleic acid interactions in a relatively rapid and sensitive manner (Hellman & Fried, 2007). The assay is based on the principle that proteins bound to a nuclei acid have a reduced mobility when compared with a free nucleic acid. Using radioactive labelled nucleic acids it is possible to observe this shift in a native acrylamide gel.

Due to the radioactive component of EMSAs, handling of phosphorus-32 (^{32}P) was carried out in a designated lab room, over plastic spill trays and behind perspex shielding. Other precautions, such as the use of a designated lab coat, two pairs of gloves, including the use of a ring with a radiation dosimeter to monitor exposure to radiation, use of Geiger-Mueller detectors, and disposal of contaminated material into appropriately labelled and shielded containers, were also routinely employed.

2.6.4.1. Labelling NF-κB oligonucleotides with ^{32}P

NF-κB oligonucleotides, with the NF-κB consensus sequence 5'-GGGACTTTCC-3', were labelled with γ-^{32}P. The labelling occurs at the 5' end of the oligonucleotides, as labelling incorporated into DNA would interfere in the DNA-protein complex formation. The first step of the labelling was the preparation of the reaction mix. The mix was prepared according to Table 2.5 and left to incubate for 30 minutes at 37˚C. Following incubation, 1μl of 0.5M EDTA and 20μl of Phenol:Chlorophorm:Isoamyl Alcohol (25:24:1) were added. The mix was vortexed and centrifuged at 13,400x*g* for 2 minutes. The aqueous top layer was removed to a clean tube, and 1μl of 5M NaCl was added followed by 40 μl of ice-cold ethanol. The reaction mix was placed in the freezer, at -20˚C for 30 minutes. Following this period, the mix was centrifuged for 5 minutes at 13,400xg. The ethanol was removed and the tube was left with an open lid at room temperature until all ethanol had evaporated. The pellet was resuspended in 50 μl of Tris-EDTA (TE). The stock solution was frozen at -20˚C.

Table 2.5 – Reaction mix components.

Reaction Mix (total volume: 20μl)		**Source**
10μl	dH_2O	
2μl	10x Kinase Buffer	M4101, Promega
2μl	NF-κB Consensus Oligonucleotide	E3292, Promega
1μl	T4 Polynucleotide Kinase	M4101, Promega
5μl	ATP [γ-^{32}P]	NEG002A250UC, PerkinElmer

2.6.4.2. Electrophoretic mobility shift assay (EMSA)

Initially, 4% native acrylamide gels were prepared following the recipe in Table 2.6. The mix was prepared and poured into the gel cast. The gel was left to polymerise for 2 to 3 hours. To eliminate variability caused by the preparation of gels, 6% native acrylamide gels were purchased (EC6365BOX, Life Technologies).

Table 2.6 – Gel components.

4% Native acrylamide gel (total volume: 40ml)		**Source**
4ml	40% Acrylamide/bis-acrylamide	A7168, Sigma
4ml	10x Tris-Borate-EDTA (TBE)	B52, Thermo Scientific
32ml	dH2O	
	Pour the mix in the cast immediately after adding the last two components	
200μl	10% Ammonium persulfate (APS)	A3678-25G, Sigma
30μl	Tetramethylethylenediamine (TEMED)	T9281, Sigma

The binding reaction mix was prepared by mixing 2μg of sample nuclear extract with 2.5μl of 10x DNA binding buffer, 2μl of 1μg/μl Poly dI-dC (P4929, Sigma) and 1μl of labelled oligonucleotides. The stock solution of 10x DNA binding buffer was prepared according to the mix resented in Table 2.7. This solution was aliquoted and stored at -20˚C. Samples were incubated at room temperature for 30 minutes to allow formation of DNA-protein complexes. Following incubation 2μl of Bromophenol Blue (B3269, Sigma) was added to the binding reaction mix. Samples were loaded onto the gel. The electrophoresis apparatus was assembled and the parameters were set to 75V for 2

hours. Following electrophoresis, gels were removed from the cast and placed onto filter paper, covered with cling film and placed onto a gel drier (165-1746, Bio-Rad) for 30 minutes to one hour. The dried gel was placed onto a cassette, and a phosphor screen placed on top of it. The cassette was closed and left for 1 to 3 days. The screen was then scanned using the Typhoon 9400 laser scanner (Amersham), which is sensitive to radioisotopes.

Table 2.7 – 10x DNA Binding buffer components.

10x DNA Binding buffer (total volume: 870μl)	**Source**
400μl Glycerol	G5516, Sigma
100μl 1mg/ml Nuclease free BSA	B2518, Sigma
20μl 0.5M EDTA	V4231, Promega
50μl 1M DTT	43816, Sigma
200μl 5M NaCl	S3014, Sigma
100μl 1M Tris pH 7.5	93362, Sigma

Chapter 3 - Investigating CPP entry in primary CLL cells

3.1. Introduction

The aim of this chapter was to characterise the entry of five CPPs into primary human CLL cells. A limited number of comparative studies have been performed to assess the cellular uptake of different CPPs (Mueller et al., 2008), and the majority of these employed cell lines. Mueller et al. (2008) performed a large-scale study to compare the cellular uptake of 22 CPPs, using 4 different cell lines (Mueller et al., 2008). One of the conclusions of this study was that, under the same conditions, CPP uptake rate was dependent on the cell line used (Mueller et al., 2008). In this study, they determined that some of the CPPs with the highest uptake rates were penetratin, transportan, R7 and R9; some of the most frequently used CPPs (Mueller et al., 2008). Other studies have employed the use of primary cells, such as Marshall et al. (2007), where R_9F_2, Tat, penetratin, (RXR)4 and His1 were used to deliver PMOs into murine leukocytes. Out of the five tested CPPs, (RXR)4 was able to deliver a functional cargo and was the CPP with the highest uptake rate (Marshall et al., 2007). Although both of these studies used penetratin, the results obtained were divergent. This is likely due to the differences in the experimental conditions in which the peptides were studied. Conditions such as cell type, peptide concentration, type of cargo, type of fluorescent tag, temperature, trypsinisation and others, make it difficult to compare between studies and reach general conclusions (Mueller et al., 2008).

Until now there has been no study comparing the cellular uptake of CPPs in primary human lymphocytes. However, a few studies have employed CPPs to deliver bioactive cargos into human primary CLL cells. Watkins et al. (2009a), used KG1a, HeLa and primary CLL cells to test the uptake of R8 and PFV coupled with a PAD peptide with the following sequence: $(KLAKLAK)_2$. The different cell types used showed different sensitivity to the CPPs (Watkins et al., 2009a). In primary CLL cells, both R8-PAD and PFV-PAD were able to decrease viability, with LC_{50} values lower than 10 μM (Watkins et al., 2009a). Hewamana et al. (2008) used a commercial CPP to induce apoptosis of primary CLL cells. The CPP comprised the penetratin sequence with an aspartic acid residue at the C-terminal (i.e. DRQIKIWFQNRRMKWKK) coupled with a NF-κB p65 subunit inhibiting sequence (Hewamana et al., 2008b; Takada et al., 2004). The NF-κB inhibiting CPP was capable of inducing apoptosis in 70% of the cells at 50 μM (Hewamana et al., 2008b). These studies show that CPPs can effectively penetrate

primary human CLL cells and deliver a cytotoxic cargo. A comparative study, like the one presented in this chapter, provides a better understanding of the uptake of CPPs by primary CLL cells and can lead to the development of novel CPPs with improved therapeutic potential.

In order to characterise the uptake of the five CPPs using flow cytometry and confocal microscopy, the fluorochrome Alexa488 was covalently liked to the N-terminal of the five CPPs (see section 2.1 for detailed protocol). A small number of fluorochromes have been used to label CPPs, such as the Alexa Fluor dyes (i.e. 405, 488, 568, 647), fluorescein (FITC), rhodamine 6G, oregon green, tetramethyl rhodamine and texas red (Jones & Sayers, 2012). Their structures differ greatly, and they probably influence CPP uptake both positively and negatively (Jones & Sayers, 2012). Therefore, the choice of fluorochrome needs to be considered carefully. The most commonly used fluorochromes for the study of cellular uptake of CPPs are Alexa488 and FITC (Palm-Apergi et al., 2012). Previous studies have shown that the fluorescent signal of FITC-labelled CPPs is inhibited by 70% at lysosomal pH, limiting its use as a reporter of CPPs that do not utilise an endosomal mechanism of entry (Jones & Sayers, 2012). However, as some of the CPPs used in this project had not been previously tested in primary CLL cells, it was not possible to know if they utilised an endocytic route to penetrate the cell membrane. To avoid potential loss of fluorescent signal, the fluorochrome Alexa488 was chosen over FITC. The linker between the CPP and Alexa488 used was maleimide, since it provides a longer spacing between the peptide and fluorophore (Jones & Sayers, 2012). The space between the CPP and the reporter is important to ensure that the fluorochrome does not interfere with the penetrating capabilities of the CPP (Jones & Sayers, 2012).

This chapter set out to characterise the uptake of five CPPs, (RXR)4, R8, FFR8, TP10 and PFV, representing all three classes of CPPs, in primary human normal and malignant lymphocytes. The amino acid sequences of the peptides studied are shown in Table 3.1. This study aimed to determine the uptake rate of the five CPPs, their intracellular distribution when taken up by the cells, if the dose administered was proportional to the levels of fluorescence delivered and if the CPPs affect cell viability. This study also aimed to determine if the peptides behave in a similar manner with normal B- and T-cells. This was achieved with the use fluorescently-tagged CPPs in combination with flow cytometry and confocal microscopy.

Table 3.1 – Amino acid sequence of the CPPs used in this project.

CPP	Sequence
(RXR)4	RXRRXRRXRRXR-Alexa488
R8	RRRRRRRR-Alexa488
FFR8	FFRRRRRRRR-Alexa488
TP10	AGYLLGKINLKALAALAKKIL-Alexa488
PFV	PFVYLI-Alexa488

3.2. All CPPs are able to penetrate primary CLL cells and deliver different levels of fluorescence

The first step in this study was to characterise the ability of five different CPPs to deliver a fluorescent cargo into primary CLL cells. Flow cytometry was employed to allow a quantitative comparison of peptide entry, and the simultaneous investigation of cell viability as determined by forward and side scatter. Primary CLL cells were first separated from whole blood and washed with PBS. Cells were placed into liquid culture and Alexa488-conjugated peptides (2 μM) were added to the media. After 1 and 20 hours of incubation, cells were harvested and the fluorescence emitted by Alexa488 was measured by flow cytometry. Figure 3.1 shows flow cytometry data from cells from a single CLL patient cultured with the five CPPs. Viable cells were gated (P1) in the forward and side scatter and the mean fluorescence intensity (MFI) of the cells in channel FL1, within the viable lymphocyte (P1) gate, was measured. The black histogram represents the fluorescence of cells at 1 hour and the red histogram represents the fluorescence of cells at 20 hours. Data from 19 CLL patient samples was collected and a compilation of that data can be found in Figure 3.2 and 3.3. Data from the 19 patients was also plotted in Figure 3.4 with MFI values of 1 hour linked to respective MFI values at 20 hours.

Primary CLL cells were able to take up all the tested CPPs at the 2 μM concentration under one hour, as seen in Figures 3.1 to 3.3. The levels of fluorescence within the cells varied greatly between CPPs; the CPP capable of delivering the highest levels of fluorescence was FFR8, with MFI values at 1 hour of 99,498 (±59,077). The lowest MFI values at 1 hour were associated with PFV-treated cells, with MFI values of 3,666 (±2,510).

Regarding the fluorescence histograms in Figure 3.1, the peptides can be assigned into one of three categories. The first encompassed (RXR)4, R8 and PFV, where two

distinct peaks present different levels of fluorescence after 20 hours. This implies that the peptide was not distributed uniformly within all of the cells but was preferentially taken up (or retained) in a subset of cells. There was a significant increase in MFI following 20 hours for all peptides with the exception of FFR8, suggesting that peptide entry was time dependent. The second category comprised FFR8. Cells incubated with this peptide showed no time-dependent increase in fluorescence. However, the distribution of this peptide within the cell population became more consistent after 20 hours as evidenced by a reduction in the standard deviation of the fluorescence histogram. The third category consisted of TP10. This peptide showed little evidence of differential uptake within the cell population at 1 hour and 20 hours but there was a log increase in fluorescence at 20 hours suggesting that this peptide accumulated in the cells over the timeframe of the assay.

Following one hour of incubation, the order by which the peptides were able to deliver fluorescence into the cells, from the highest to the lowest was as follows: FFR8, (RXR)4, R8, TP10 and PFV. Regarding distribution of fluorescence, FFR8 has the highest standard deviation (SD=59,077), while PFV has the lowest (SD=2,510). After 20 hours of incubation, the order by which the peptides were able to deliver fluorescence into the cells, from the highest to the lowest was the following: FFR8, (RXR)4, TP10, R8 and PFV. Regarding distribution of fluorescence, FFR8 continued to have the highest standard deviation (SD=23,168), and (RXR)4 had the lowest (SD=4,116).

Comparing MFI values at 1 hour with the respective values at 20 hours (Figure 3.4), showed that the only peptides for which the fluorescence values do not significantly change were (RXR)4 ($p=0.50$) and R8 ($p=0.06$). For cells incubated with FFR8, there was a significant decrease in fluorescence ($p<0.001$) between 1 hour and 20 hours. For cells incubated with TP10 and PFV there is a significant increase in fluorescence after 20 hours of incubation (TP10 $p<0.001$ and PFV $p<0.0001$). The peptides can therefore be divided into three categories: the first includes (RXR)4 and R8, where the changes in fluorescence are not significant; the second includes FFR8, where the mean fluorescence values decrease after 20 hours; and the last category that includes TP10 and PFV, for which the mean fluorescence increases.

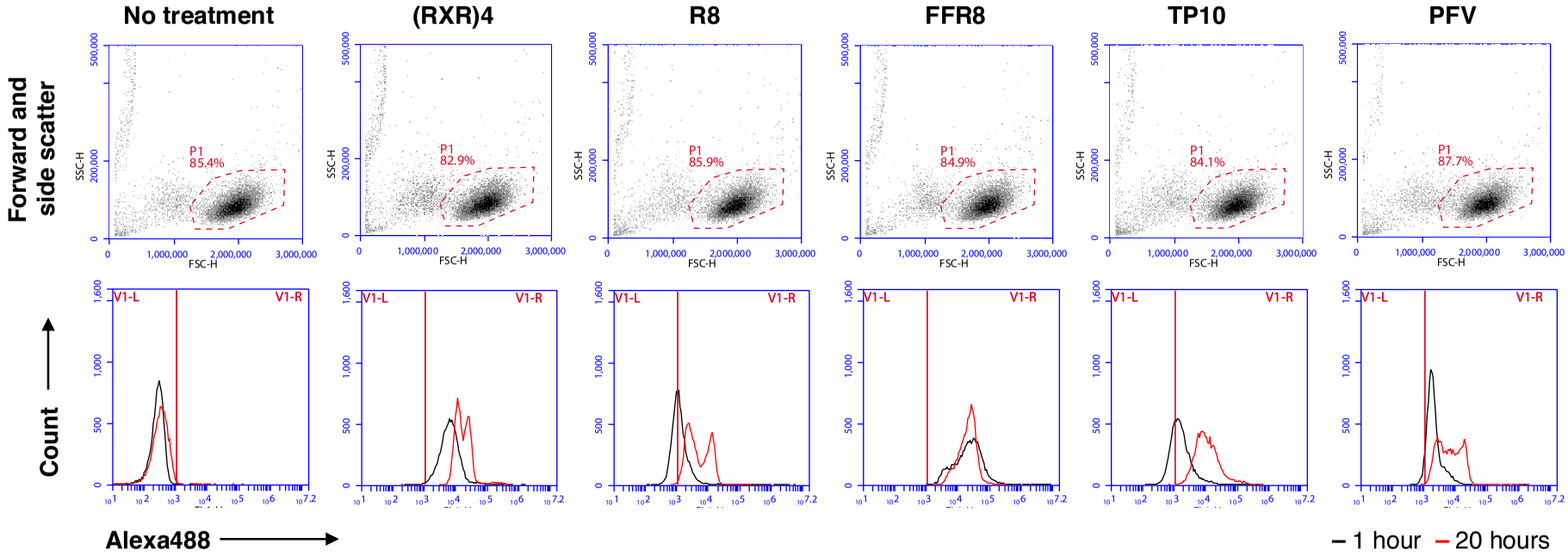

Figure 3.1 – Flow cytometry data of primary CLL cells incubated with (RXR)4, R8, FFR8, TP10, PFV and no peptide for a period of 1 and 20 hours.
Primary CLL cells were incubated with 2 μM of (RXR)4, R8, FFR8, TP10 and PFV for a period of 20 hours. Cells were collected at 1 and 20 hours and washed with PBS. Viable cells were gated in P1 and Alexa488 fluorescence analysed by flow cytometry in FL1. The red vertical line separates basal fluorescence from peptide fluorescence, set using the untreated sample as reference. Black histogram represents cells collected at 1 hour. Red histogram represents cells collected at 20 hours. Data from one patient sample.

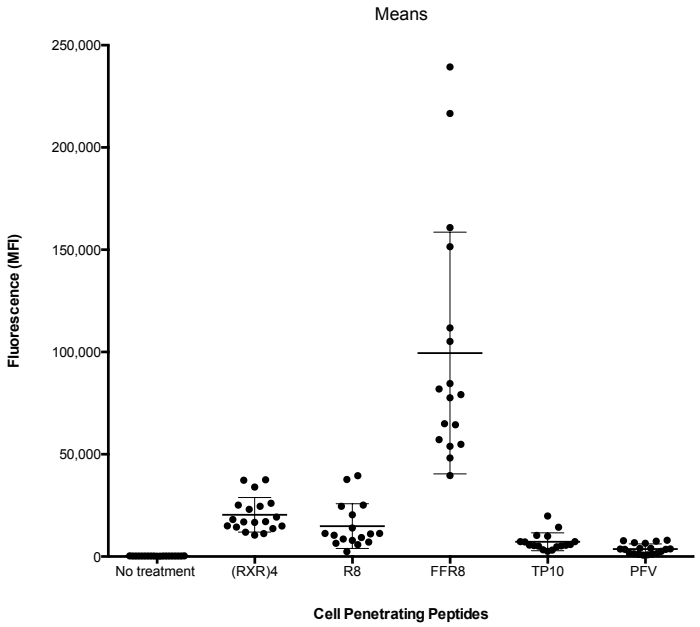

Figure 3.2 - MFI of primary CLL cells after incubation for 1 hour with (RXR)4, R8, FFR8, TP10, PFV and without any treatment.
Primary CLL cells were incubated with 2 μM of (RXR)4, R8, FFR8, TP10, PFV or no peptide for a period of 20 hours. Cells were collect at 1 and 20 hours, washed and analysed by flow cytometry. MFI levels (measured in FL1) correspond to the fluorescence emitted by the fluorochrome Alexa488. Data from 19 CLL patient samples.

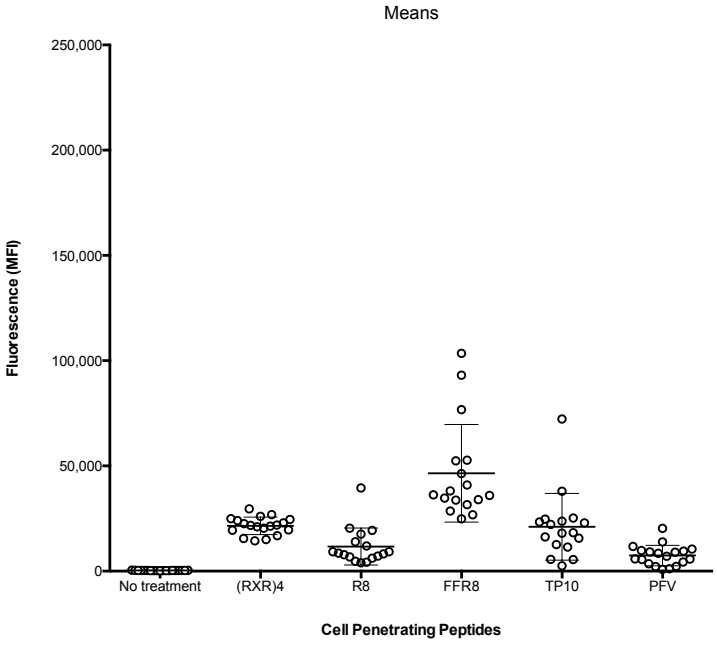

Figure 3.3 - MFI of primary CLL cells after incubation for 20 hours with (RXR)4, R8, FFR8, TP10, PFV and without any treatment.
Primary CLL cells were incubated with 2 μM of (RXR)4, R8, FFR8, TP10, PFV or no peptide for a period of 20 hours. Cells were collect at 1 and 20 hours, washed and analysed by flow cytometry. MFI levels (measured in FL1) correspond to the fluorescence emitted by the fluorochrome Alexa488 inside the CLL cells. Data from 19 CLL patient samples.

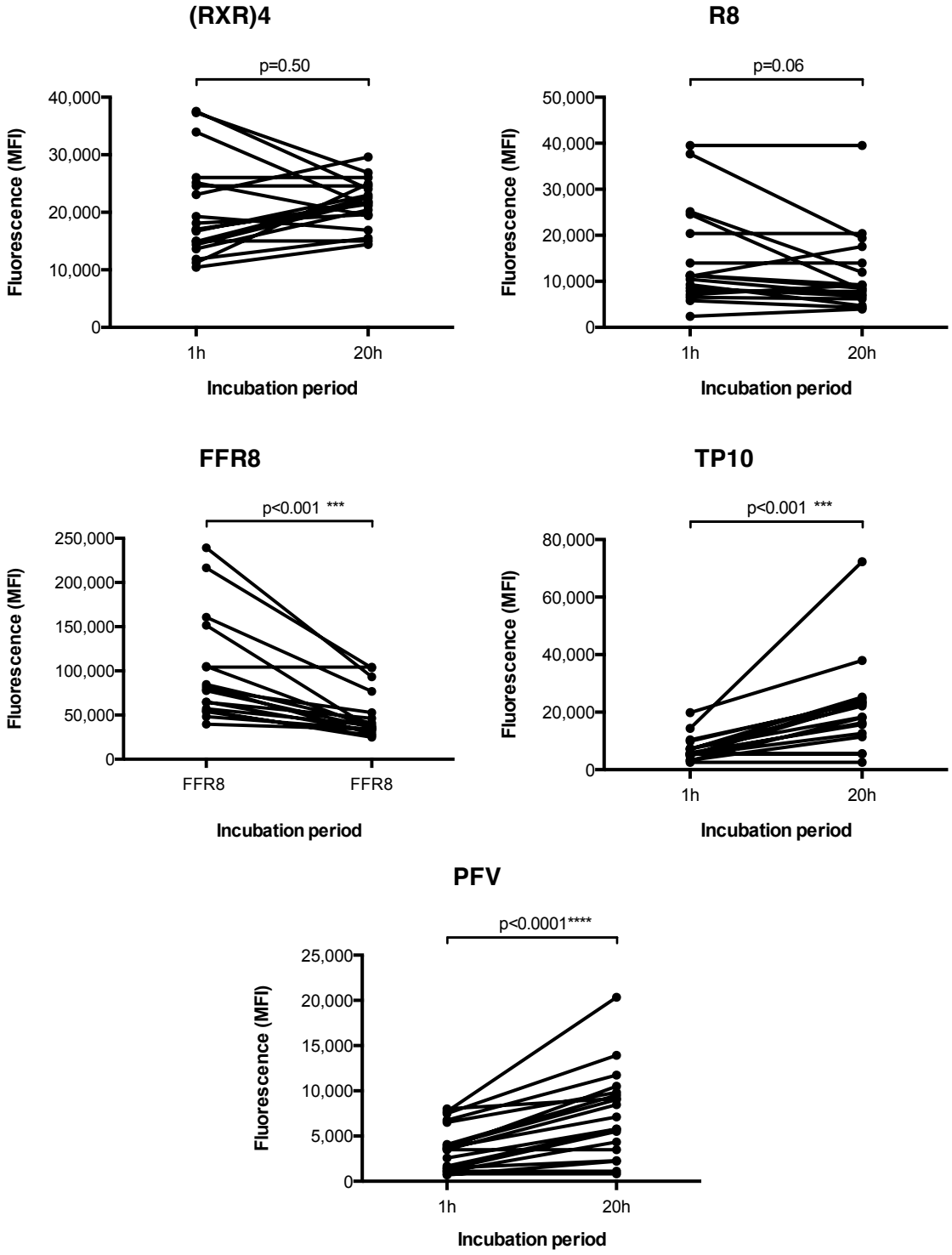

Figure 3.4 – Correlation between MFI levels of 1 and 20 hours of primary CLL samples incubated with the five CPPs.

MFI values of primary CLL cells at one hour were linked to levels at 20 hours. A t test was performed using the Graphpad Prism 6 software to obtain the statistical significance value between 1 and 20 hours. Paired t-test applied using the software Graphpad Prism 6. ** - Statistically significant data. Data from 19 patient samples.

3.3. Fluorescence was proportional to the concentration of peptide

The concentration of CPP used has been reported to affect the way peptides penetrate cells (Jones & Sayers, 2012). To determine if the dose administrated was proportional to the fluorescence measured in the cells, primary CLL cells were cultured with a range of concentrations of the three peptides that delivered the highest levels of fluorescence (RXR)4, R8 and FFR8.

Primary CLL cells were cultured with a range of concentrations (0.25, 0.5, 1, 2 and 4 μM) of (RXR)4, R8 and FFR8. Cells were cultured in DMEM media for up to 20 hours, and were collected after 1 and 20 hours of incubation. They were washed with PBS and Alexa488 fluorescence was measured by flow cytometry. Figure 3.5 shows flow cytometry data of primary CLL cells from one patient cultured with 5 concentrations of (RXR)4 and FFR8 and without any treatment. Figure 3.6 shows a compilation of data from 3 patients. Primary CLL cells showed a concentration-dependent increase in fluorescence when incubated with Alex488-labelled (RXR)4 and R8 (Figure 3.5). FFR8 behaved in the same way with a proportional increase in fluorescence at concentrations ranging from 0 to 2 μM. However, the highest concentration of peptide (4 μM) caused an almost 20-fold increase in fluorescence (Figure 3.6).

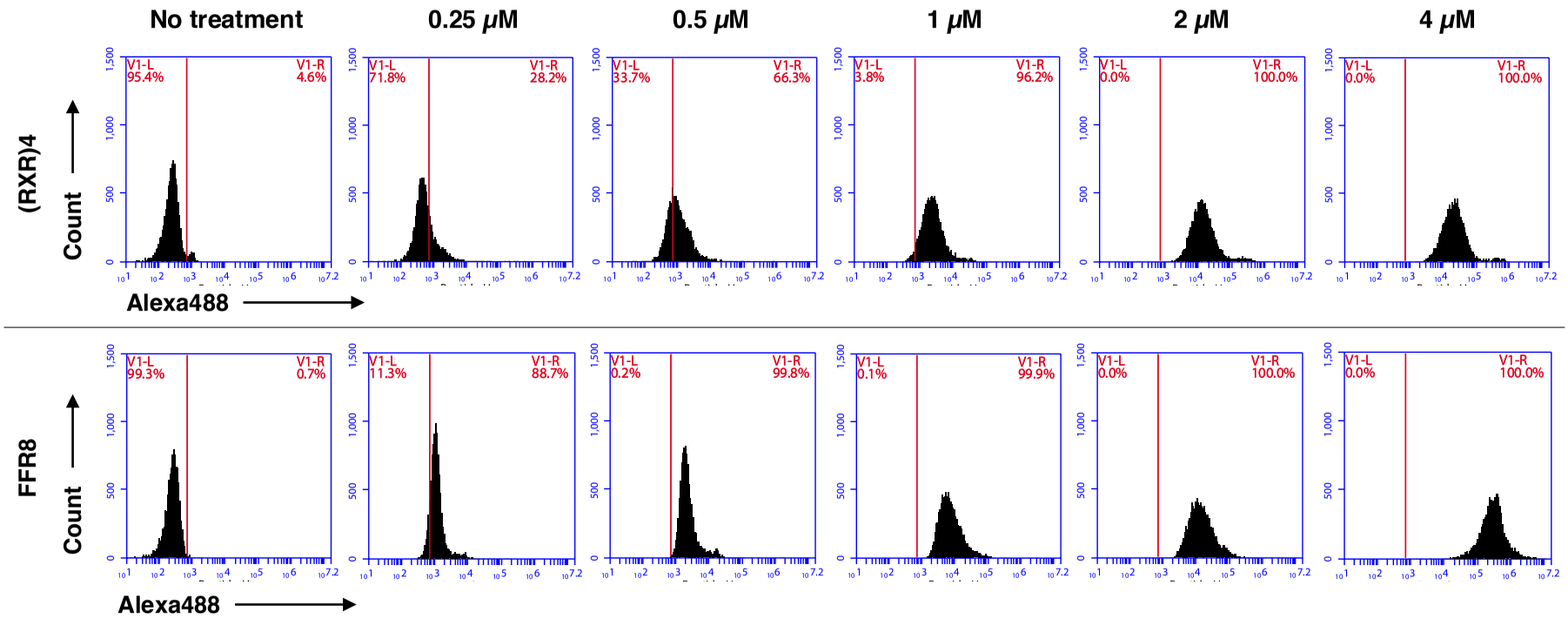

Figure 3.5 – Flow cytometry data of primary CLL cells incubated wit 0, 0.25, 0.5, 1, 2, 4 μM of (RXR)4 and FFR8 for 1 hour.
Primary CLL cells were cultured with 0, 0.25, 0.5, 1, 2 and 4 μM of (RXR)4 and FFR8 for a period of 1 hour. Viable cells were previously gated (data not shown) and Alexa488 fluorescence was measure in FL1. The red vertical line separates basal fluorescence from peptide fluorescence, set using the untreated sample as reference. Data from one patient sample

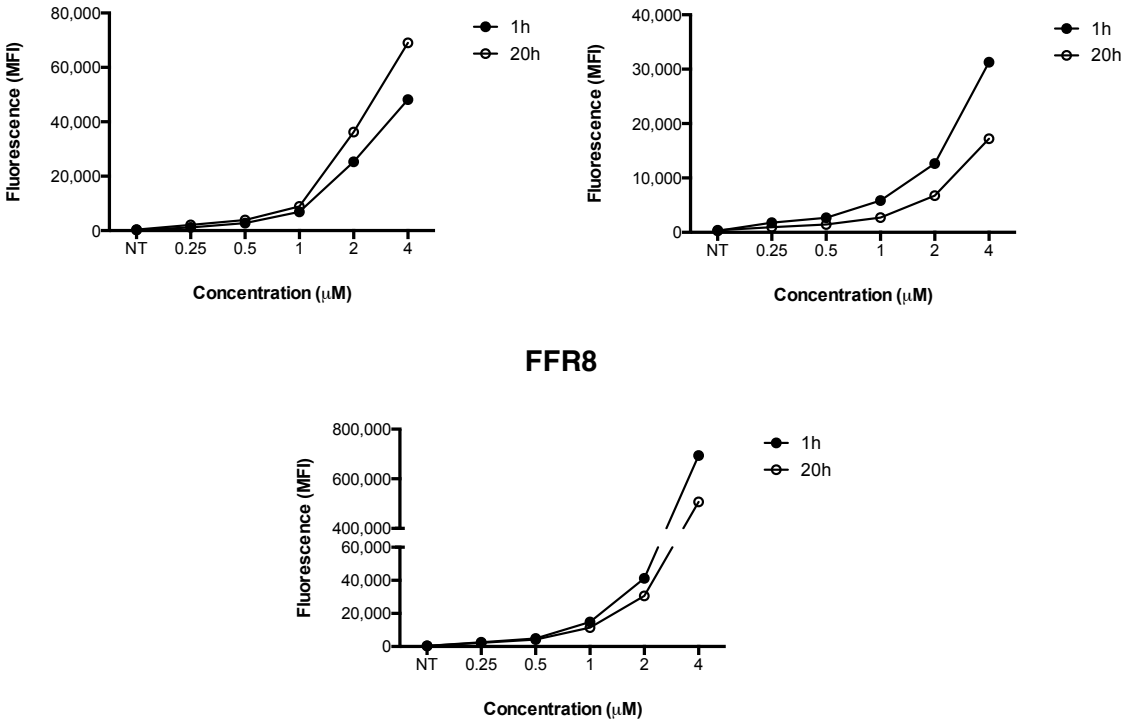

Figure 3.6 – MFI of primary CLL cells after incubation for 1 and 20 hours with different concentrations (0.25, 0.5, 1, 2 and 4 μM) of (RXR)4, R8, FFR8 and without any treatment.
Primary CLL cells were cultured with a range of concentrations (0.25, 0.5, 1, 2 and 4 μM) of (RXR)4, R8 and FFR8 for a period of 20 hours. Cells were collected at 1 and 20 hours, washed and Alexa488 fluorescence analysed by flow cytometry. The Y-axis for FFR8 has been divided into two segments, with a break from 60,000 to 400,000 MFI. Data from 3 patient samples.

3.4. CPPs do not affect CLL viability

In order to investigate if the CPPs caused cytotoxic effects in CLL cells, cell viability was measured after incubation with the peptides. To do so, viability tests using Annexin V and propidium iodide were performed as described previously. Primary CLL cells were incubated with a range of doses (0.25, 0.5, 1, 2 and 4 μM) of the three peptides able to deliver the highest levels of fluorescence, (RXR)4, R8 and FFR8 for a period of 20 hours. Cells were collected at 1 and 20 hours and the viability tests were performed alongside the peptide fluorescence measurements by flow cytometry. Figures 3.6 and 3.7 show the flow cytometry data derived from one patient sample incubated with (RXR)4 and FFR8 for 1 hour. Cells in Q1-LL are Annexin-V and PI negative, consistent with them being viable. Cells in Q1-LR are Annexin-V positive and PI negative, indicative of cells in early apoptosis. Cells in Q1-UR are Annexin-V and PI positive, signifying cells in late apoptosis. An unusual feature of these experiments was the appearance of cells in Q1-UL following incubation with CPPs. These cells were not classically apoptotic as they were Annexin-V negative but they failed to exclude PI. Given that these cells were only evident in CPP-treated cultures it is possible that the CPP causes perturbations in the cytoplasmic membrane resulting in them becoming permeable to PI. Figure 3.9 shows the percentage of cells in apoptosis (early and late apoptosis: Q1-LR + Q1-UR).

Cells incubated with (RXR)4 and R8 showed no increase in apoptosis at 1 and 20 hours, when compared to untreated cells. Cells incubated with FFR8 showed no increase in apoptosis from doses of 0.25 up to 2 μM. At 4 μM, the percentage of cells positive for both Annexin-V and PI or positive solely for Annexin-V increases to 40%. At 20 hours the levels of apoptosis of cells incubated with FFR8 show no increase when compared to untreated cells.

In Figure 3.9, the effect that both (RXR)4 and FFR8 have on the cellular membrane is visible as the cell population shifts upwards on the PI fluorescence scale. This indicates that both peptides interact with the cellular membrane in a way that allows PI to enter the cell, without inducing apoptosis, as there is no expression of PS (cells are Annexin-V negative).

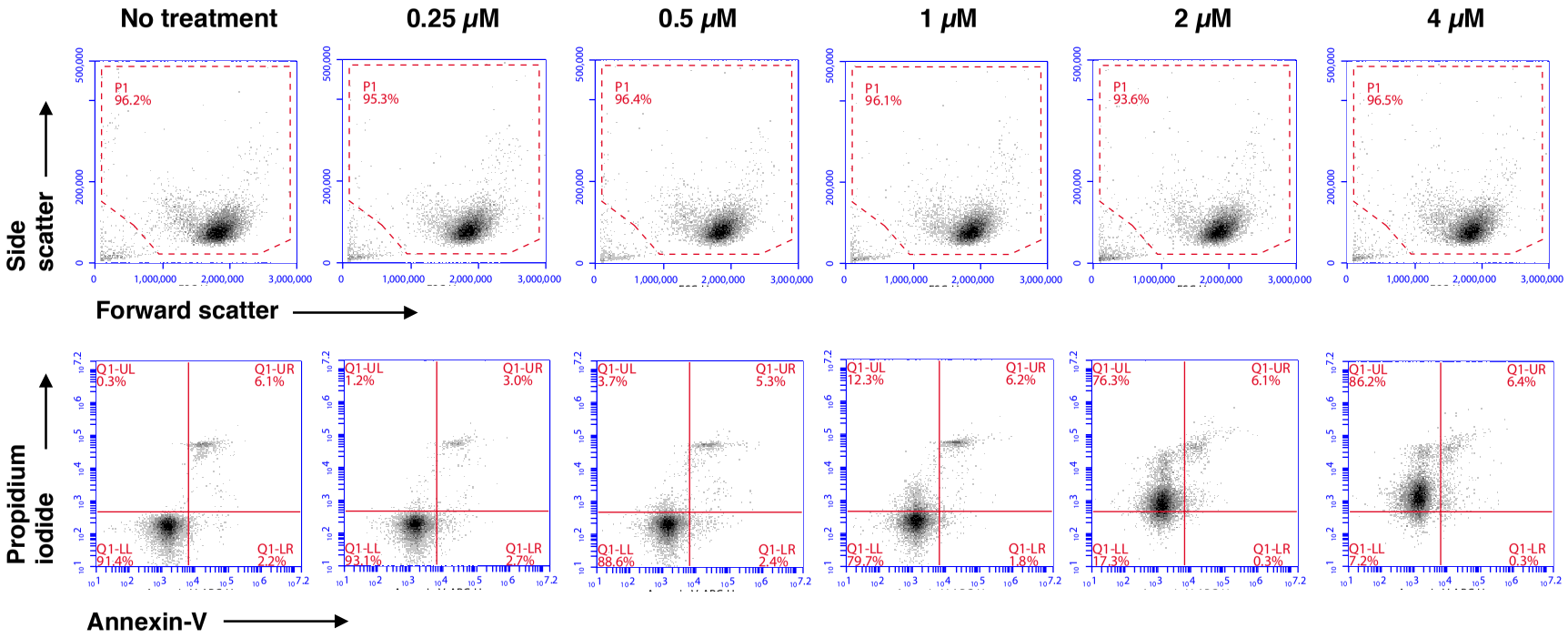

Figure 3.7 – Flow cytometry data of primary CLL cells incubated wit 0, 0.25, 0.5, 1, 2, 4 μM of (RXR)4 for 1 hour.

Primary CLL cells were incubated with 0, 0.25, 0.5, 1, 2 and 4 μM of (RXR)4 for 1 hour. Cells were washed and stained with Propidium Iodide (PI) and Annexin-V and analysed by flow cytomerty. PI fluorescence was measured in FL2 and Annevin-V fluorescence was measured in FL4. Cells in Q1-LL are Annexin-V and PI negative, therefore are viable. Cells in Q1-LR are Annexin-V positive and PI negative, therefore they are in early apoptosis. Cells in Q1-UR are Annexin-V and PI positive, therefore in late apoptosis. Cells in Q1-UL are Annexin-V negative and PI positive, therefore viable but the cellular membrane has been somehow disturbed and allowed penetration of PI into the cells.

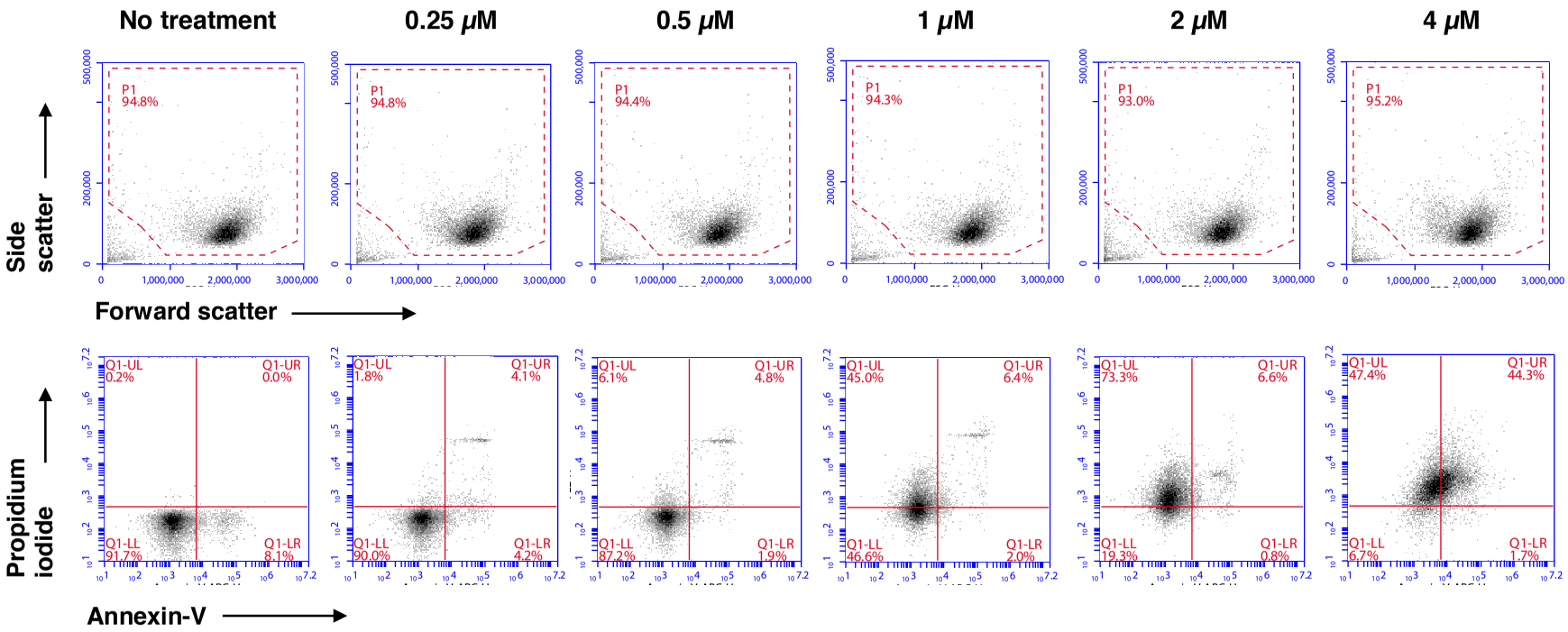

Figure 3.8 – Flow cytometry data of primary CLL cells incubated wit 0, 0.25, 0.5, 1, 2, 4 μM of FFR8 for 1 hour.
Primary CLL cells were incubated with 0, 0.25, 0.5, 1, 2 and 4 μM of FFR8 for 1 hour. Cells were washed and stained with Propidium Iodide (PI) and Annexin-V and analysed by flow cytomerty. PI fluorescence was measured in FL2 and Annevin-V fluorescence was measured in FL4. Cells in Q1-LL are Annexin-V and PI negative, therefore are viable. Cells in Q1-LR are Annexin-V positive and PI negative, therefore they are in early apoptosis. Cells in Q1-UR are Annexin-V and PI positive, therefore in late apoptosis. Cells in Q1-UL are Annexin-V negative and PI positive, therefore viable but the cellular membrane has been somehow disturbed and allowed penetration of PI into the cells. The Annexin-V and PI plot for 4 μM of FFR8 was compensated by removing 5% of the fluorescence of FL1 (Alexa488) from FL2 (PI).

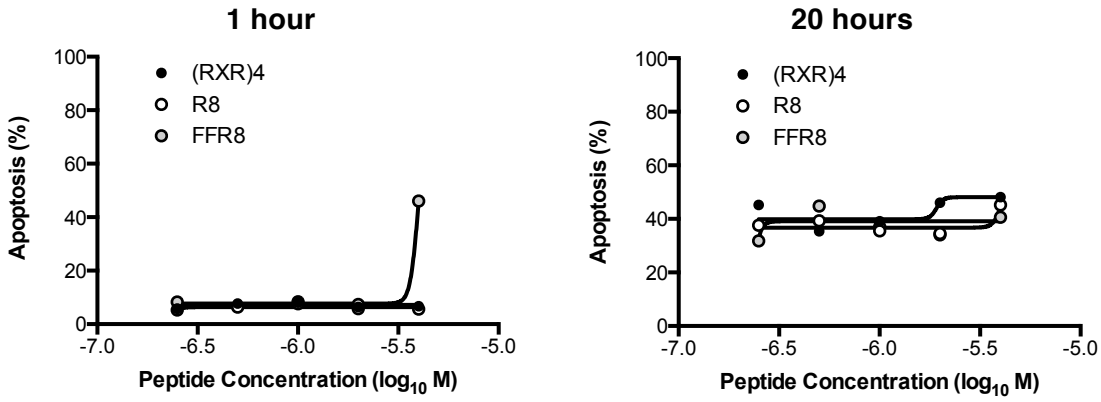

Figure 3.9 - Viability of primary CLL cells incubated with different concentrations (0.25, 0.5, 1, 2 and 4 μM) of (RXR)4, R8 and FFR8.
Primary CLL cells were cultured with a range of concentrations (0.25, 0.5, 1, 2 and 4 μM) of (RXR)4, R8 and FFR8 for a period of 20 hours. Cells were collected at 1 and 20 hours, washed and stained with propidium iodide and Annexin-V and analysed by flow cytometry. Percentage of apoptosis refers to cells double positive for Annexin-V and PI (Q1-UR of Figure 3.7 and 3.8) and cells positive for Annexin-V but negative for PI (Q1-LR of Figure 3.7 and 3.8).

3.5. Differential intracellular localisation of CPPs in primary CLL cells

The next step was to determine the intracellular distribution of the Alexa488-tagged CPPs using confocal microscopy. Primary CLL cells were cultured with 4 μM of Alexa488 labelled CPPs for a period of 20 hours. Cells were collected at 1 and 20 hours and stained with DRAQ5, a far-red emitting fluorescent DNA dye, which binds stoichiometrically into DNA. Cells were washed and incubated with RPMI with no phenol red, to allow visualisation by confocal microscopy. Cells were imaged while still alive; no fixation method was employed.

Figures 3.10 to 3.14 show primary CLL cells incubated with the five CPPs for 1 and 20 hours. Low power and high power fields are shown, with DRAQ5 and Alexa488 fluorescence overlaid (achieved using the software Photoshop CS6). A zoomed field of only the green channel (Alexa488 fluorescence) is also shown. To be consistent with other commonly used DNA dyes, the DRAQ5 labelling employed here was falsely coloured blue. All the confocal pictures were taken using live and unfixed cells to eliminate the potential for fixation artefacts. Figure 3.15 shows images of single CLL cells incubated for 1 hour with the five CPPs. Single cells were cut from Figures 3.10 to 3.14 and assembled in a black background using Photoshop CS6. The images presented in this chapter were not colour enhanced during the assembly process.

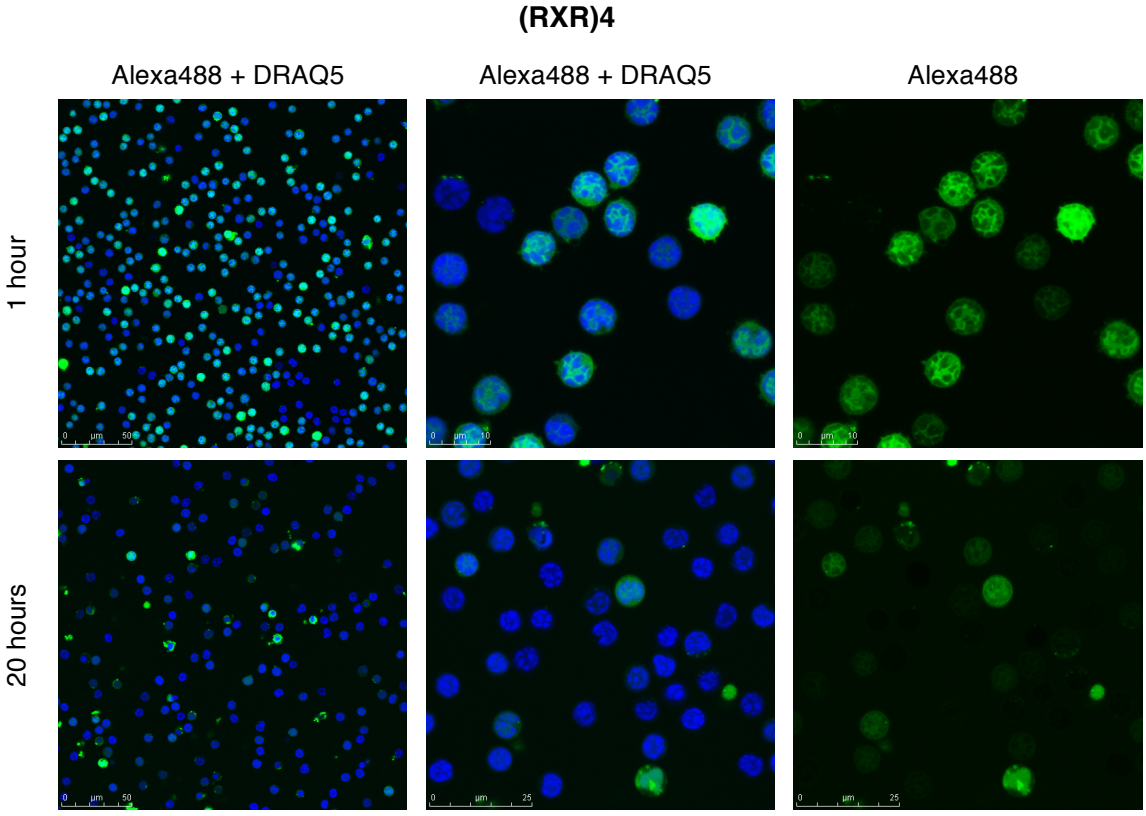

Figure 3.10 – Confocal microscopy images of the uptake of (RXR)4-Alexa488 incubated for 1 and 20 hours with primary CLL cells.
Primary CLL cells were incubated with 4 μM of (RXR)4 for a period of 1 and 20 hours. Cells were stained with DRAQ5 and observed by confocal microscopy. Representative data from 1 patient sample.

The majority of the cells incubated with (RXR)4-Alexa488 showed evidence of CPP loading i.e. they manifested green fluorescence (Figure 3.10). The fluorescence was homogenously distributed in the cytosol and the peptide was able to penetrate the nuclear membrane where it accumulated mainly in the inter-chromosomal space. The homogenous distribution of fluorescence in the cytosol indicated that the most probable mechanism of entry was not via endocytosis. At 20 hours the number of fluorescent cells had decreased and the intensity of the fluorescence within the cells had also diminished. This could be the result of fluorochrome degradation after being internalised or possibly equilibrative mechanisms that result in efflux of the CPP. However, it was not possible to determine if the peptide was degraded using this experimental approach.

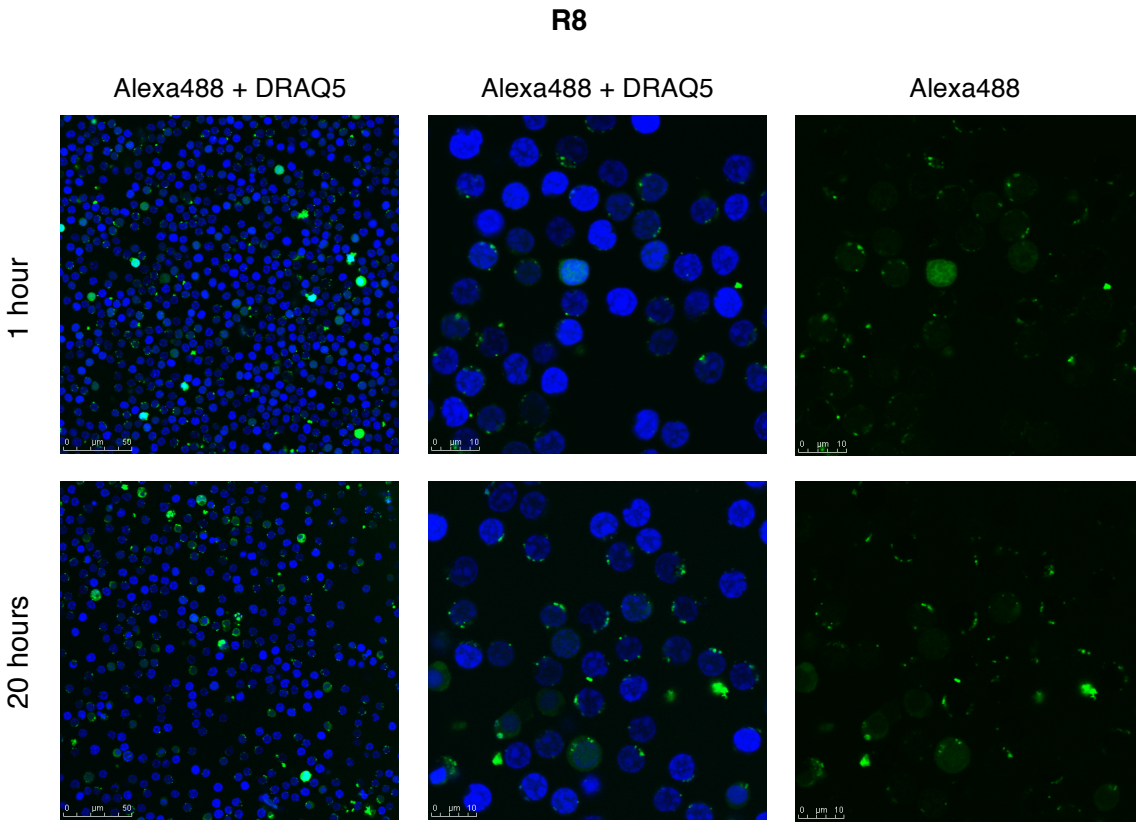

Figure 3.11 – Confocal microscopy images of the uptake of R8-Alexa488 incubated for 1 and 20 hours with primary CLL cells.
Primary CLL cells were incubated with 4 μM of R8 for a period of 1 and 20 hours. Cells were stained with DRAQ5 and observed by confocal microscopy. Data from 1 patient sample.

Figure 3.11 shows cells incubated with R8-Alexa488. The fluorescence distribution of R8 differed from that previously observed with (RXR)4. The cells presented with a punctate distribution of the fluorescent CPP, which is characteristic of an endocytic uptake of the peptide, with a small number of cells showing distribution in the cytosol. At 20 hours, some cells showed signs of the peptide being released into the cytosol, but the majority was still sequestered in vesicles.

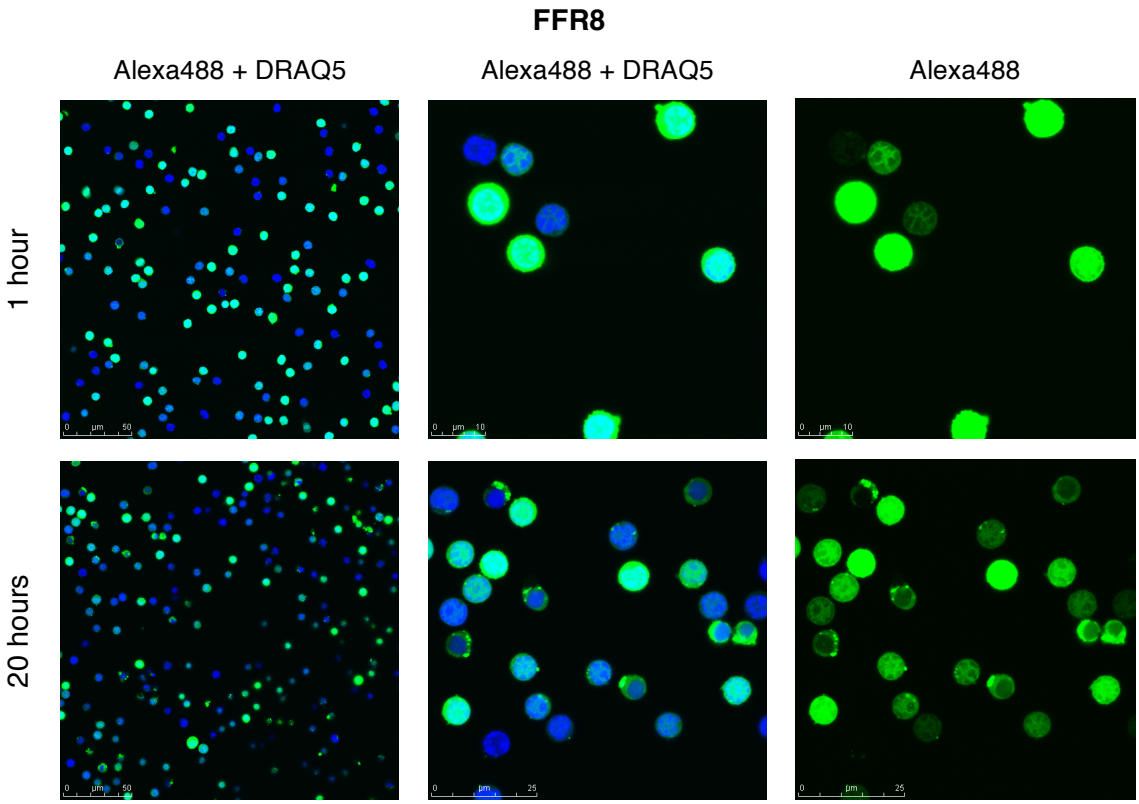

Figure 3.12 – Confocal microscopy images of the uptake of FFR8-Alexa488 incubated for 1 and 20 hours with primary CLL cells.
Primary CLL cells were incubated with 4 μM of FFR8 for a period of 1 and 20 hours. Cells were stained with DRAQ5 and observed by confocal microscopy. Data from 1 patient sample.

Figure 3.12 shows confocal microscopy images of primary CLL cells incubated for 1 and 20 hours with 4 μM of FFR8-Alexa488. These cells presented with levels of fluorescence that exceeded any of the other CPPs used in this project, a finding that is consistent with the flow cytometry data. The intensity of fluorescence varied between cells, with some manifesting very high levels of fluorescence and others very low. The fluorescence was diffused in the cytosol and this pattern indicates direct translocation of the peptide through the cellular membrane. Subsequently, there was nuclear entry where the peptide accumulated in the inter-chromosomal space. At 20 hours, the high levels of fluorescence were maintained, but there was an increase in the number of dead cells.

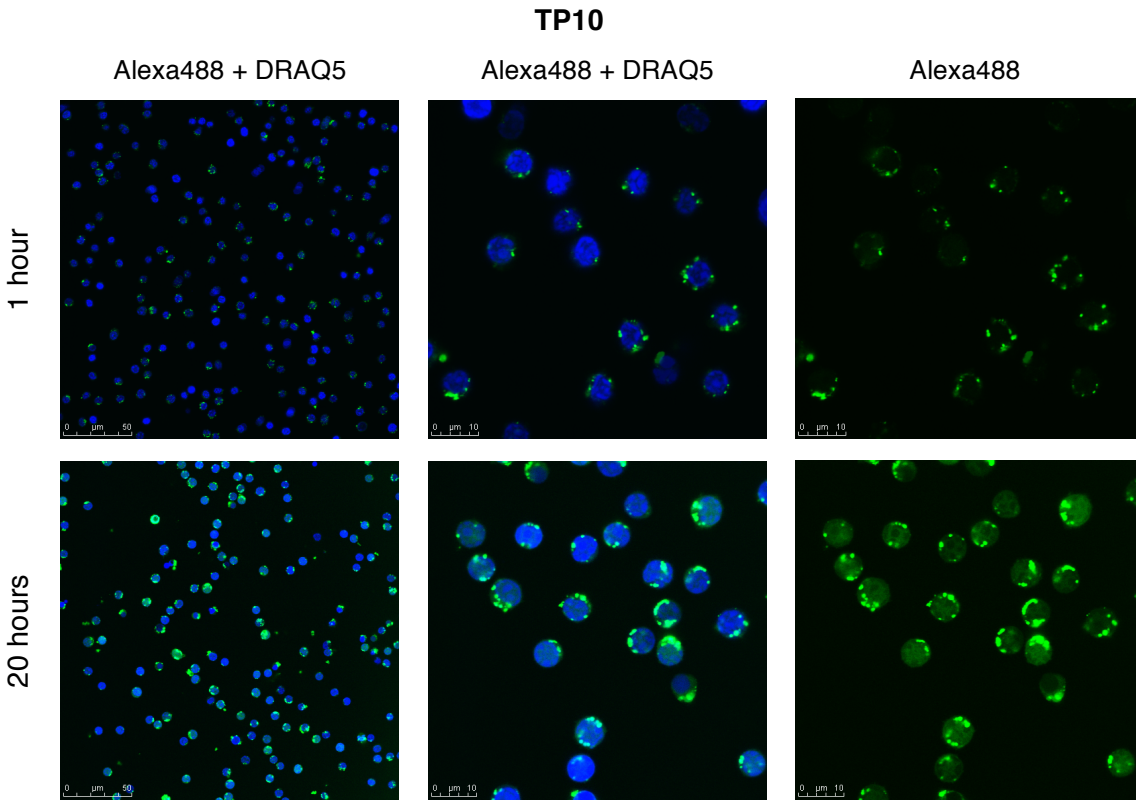

Figure 3.13 – Confocal microscopy images of the uptake of TP10-Alexa488 incubated for 1 and 20 hours with primary CLL cells.
Primary CLL cells were incubated with 4 μM of TP10 for a period of 1 and 20 hours. Cells were stained with DRAQ5 and observed by confocal microscopy. Data from 1 patient sample.

The confocal images taken of primary CLL cells incubated for one hour with 4 μM of TP10-Alexa488 (Figure 3.13) showed the fluorescence was enclosed in vesicles with a very low amount diffused in the cytosol. The number of vesicles varied between cells but there appeared to be more vesicles than when R8-Alexa488 peptides were loaded into primary CLL cells. At 20 hours the intracellular fluorescence was maintained and there was an increase in cytosolic distribution of fluorescence indicating its release from vesicles.

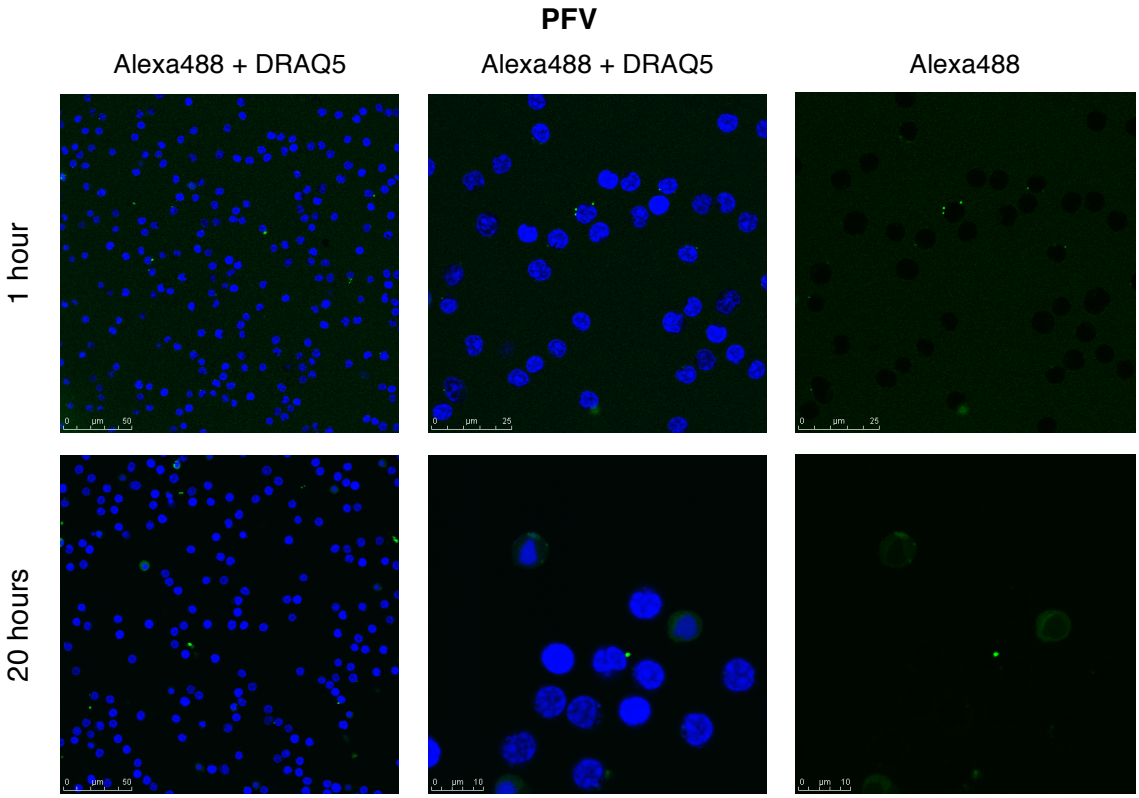

Figure 3.14 – Confocal microscopy images of the uptake of PFV-Alexa488 incubated for 1 and 20 hours with primary CLL cells.
Primary CLL cells were incubated with 4 μM of PFV for a period of 1 and 20 hours. Cells were stained with DRAQ5 and observed by confocal microscopy. Data from 1 patient sample.

Figure 3.14 shows confocal images of cells incubated with 4 μM of PFV-Alexa488 for a period of 1 hour. The levels of Alexa-488 fluorescence within the cells were very low when compared to cells incubated with any of the other CPPs. The few cells that showed evidence of fluorescence contained three or less fluorescent vesicles after 1 hour of incubation. After 20 hours, there was no increase in the fluorescence presented by the cells.

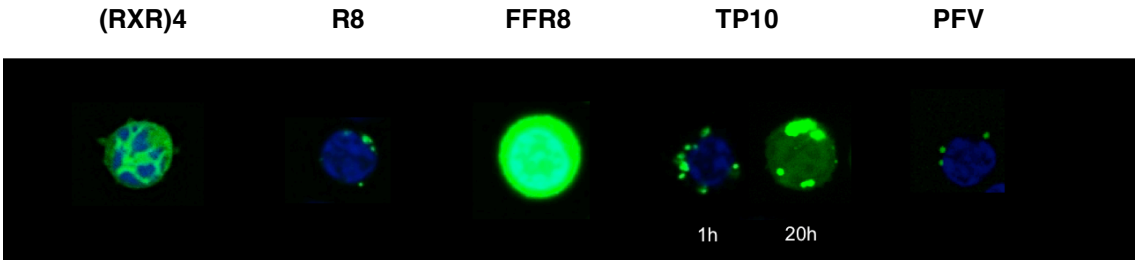

Figure 3.15 – Confocal microscopy image of a single CLL cell incubated with (RXR)4, R8, FFR8, TP10 and PFV for one hour.

To aid the comparison between the 5 CPPs, single representative CLL cells were cut out of the previous images using Photoshop CS6 and placed side by side in Figure 3.15. The CPPs can be grouped by their subcellular localisation: (RXR)4 and FFR8 present a diffused labelling of the cytosol, characteristic of direct translocation through the membrane, with nuclear labelling particularly high in the inter chromosomal space; R8, TP10 and PFV showed distinct endosomal entrapment, with TP10 presenting the highest number of vesicles and with a subsequent release of the peptide into the cytosol after 20 hours.

3.6. The five CPPs behave similarly with B and T-cells, with the exception of FFR8

In order to investigate if the five peptides were able to enter normal B- and T-lymphocytes, peripheral blood of healthy donors was collected and processed following the same protocol for CLL samples to obtain mononuclear cells (section 2.2). These experiments were also designed to determine if the fluorescence and intracellular distribution profiles resembled those observed in primary CLL cells. Peripheral blood mononuclear cells were incubated with 2 μM of the five CPPs for a period of 20 hours. Cells were collected at 1 and 20 hours, washed and then stained with anti-CD19 (B-cell marker; Invitrogen) and anti-CD3 (T-cell marker; EBioscience) antibodies to positively identify B-cells and T-cells. Fluorescence of B-cells and T-cells was measured by flow cytometry. Figure 3.16 shows representative flow cytometry data of one sample. Figure 3.17 shows a summary of the MFI values derived for 3 samples. The uptake of the five CPPs in normal B-cells and T-cells was very similar to the uptake by CLL cells. The main difference was in the uptake of (RXR)4 and FFR8 by T-cells that seemed to be more susceptible to the uptake/retention of these two CPPs, as cells incubated with these peptides present increased fluorescence when compared to CLL cells and normal B-cells.

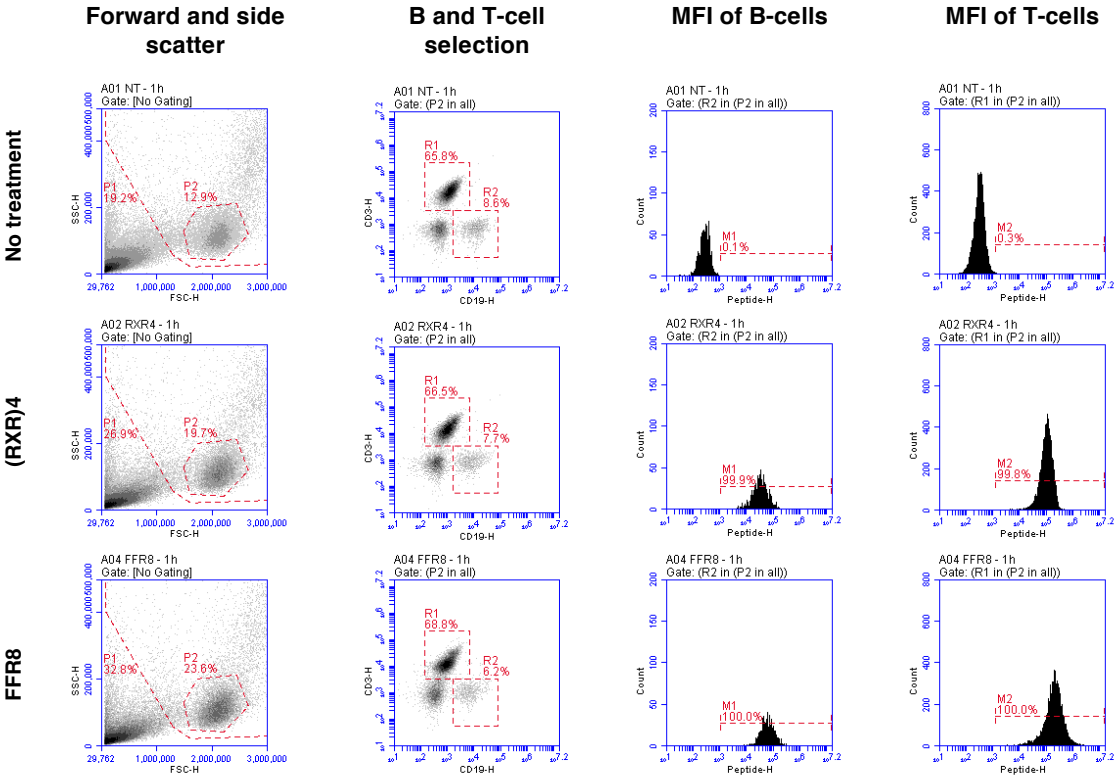

Figure 3.16 – Representative flow cytometry data of primary normal B and T lymphocytes incubated for 1 hour with (RXR)4, FFR8 and no treatment.

Primary PBMCs were incubated with 2 μM of the five peptides for 20 hours. Cells were collected at 1 and 20 hours, washed and stained with anti-CD3 (T cell marker) and anti-CD19 (B cell marker). Viable PBMCs were gated in P2 in the forward and side scatter plot. Anti-CD3 was measured in FL3 and anti-CD19 was measured in FL4. R1 gates CD3 positive and CD19 negative cells, T cells. R2 gates CD3 negative and CD19 positive cells, B cells. Alexa488 fluorescence of cells gated in R1 and R2 was then plotted separately (MFI of B-cells and MFI of T-cells).

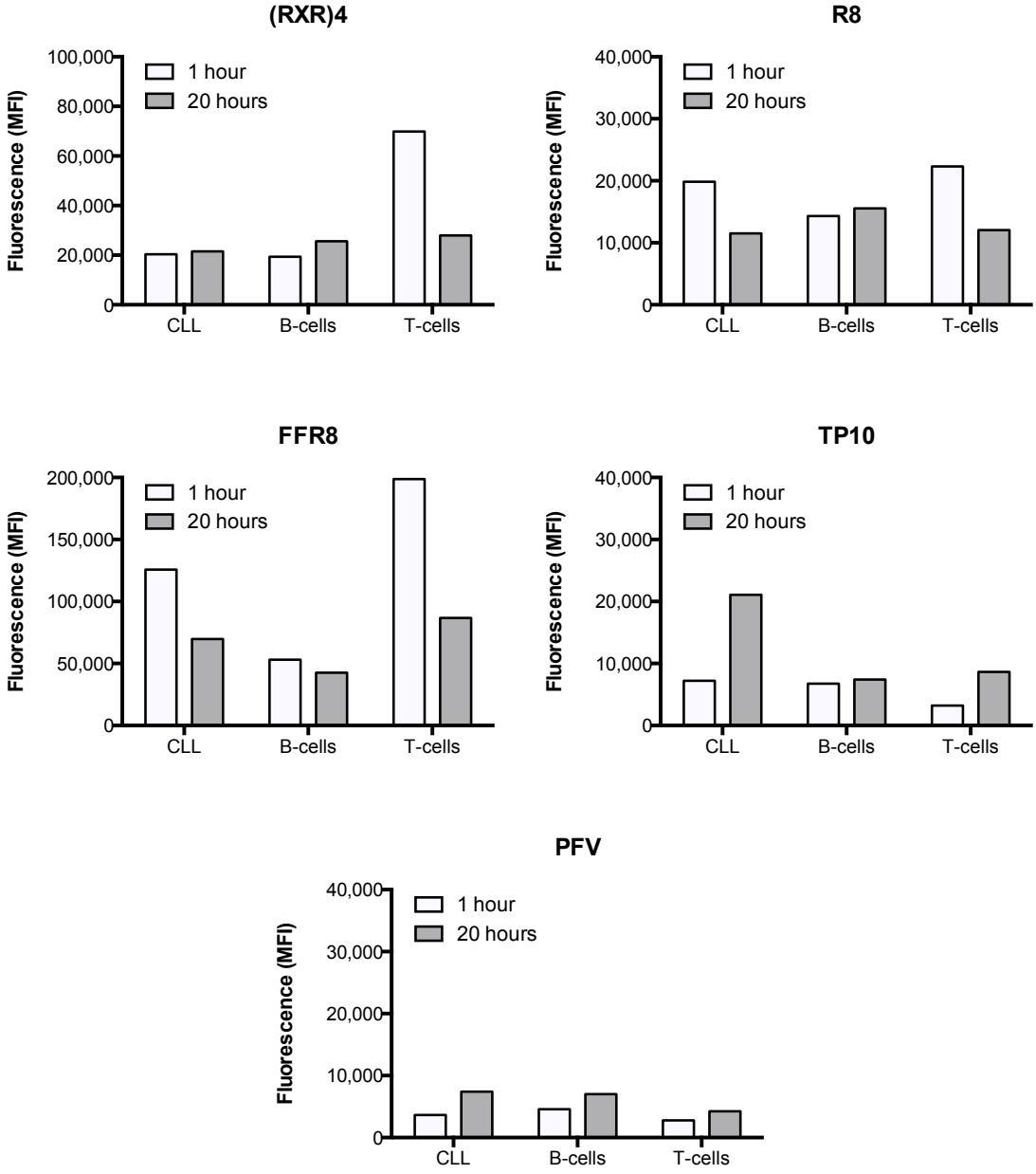

Figure 3.17 – Alexa488 MFI of primary CLL cells and primary B and T lymphocytes cultured with 5 CPPs for 1 and 20 hours.

PBMCs were cultured with 2 μM of (RXR)4, R8, FFR8, TP10 and PFV for 20 hours. Cells were collected at 1 and 20 hours, washed and stained with anti-CD3 and ant-CD19. Fluorescence was measured by flow cytometry (see gating strategy in Figure 3.16). Data from 3 patient samples.

3.7. Discussion & Conclusion

The key aim of this chapter was to compare the uptake of five CPPs in primary CLL cells. With this information, two of the five peptides were selected to be delivery vectors of a bioactive cargo described in the next chapter. The two CPPs selected were FFR8 and TP10. Overall, FFR8 was the most effective peptide. It produced the highest levels of fluorescence in CLL cells, was distributed homogenously in the cytosol but was also able to penetrate the nucleus. Although the MFI values registered were high, uptake of this peptide did not induce cell toxicity at doses lower than 4 μM. For this reason, FFR8 was the first peptide to be selected.

The choice for the second peptide was not as straight forward as with FFR8. In terms of fluorescence, the two next best candidates were (RXR)4 and R8. However, both of these are cationic peptides and therefore very similar to FFR8. Furthermore, side-by-side comparison of single CLL cells showed that the intracellular distribution of (RXR)4 was very similar to FFR8 suggesting that the two peptides were likely to behave in a very similar fashion. (RXR)4 was therefore eliminated as a contender. The three remaining peptides all showed endosomal entrapment, but the low level of fluorescence and the low numbers of vesicles observed in PFV-treated cells resulted in the rejection of this CPP as a potential vehicle for the bioactive cargo. As a result, the choice was then left between R8 and TP10. TP10 was the only peptide that showed initial sequestration within vesicles that that was subsequent released into the cytosol. Although the fluorescence levels achieved with R8 were much higher at one hour than TP10, the apparent retention of the CPP within endosomes led to concerns over the ability of the CPP to deliver the bioactive cargo. For this reason, TP10 was the second choice for a delivery vector of a bioactive cargo. The slower uptake and release of the TP10 CPP was considered to be an interesting comparison to the quick and intense uptake of FFR8 in the next phase of this project.

This chapter also provided new insight into the way (RXR)4, R8, FFR8, TP10 and PFV are taken up by malignant primary B-cells. All five CPPs were able to penetrate primary human CLL cells and deliver a fluorescent tag. However, the level of delivery varied between the five peptides. The CPPs were ranked by order of decreasing MFI as follows: FFR8, (RXR), R8, TP10 and finally PFV (ranking based on MFI values at 1 hour). The top three peptides are all cationic peptides, the most commonly used (Nakase et al., 2013). Arginine-rich peptides like (RXR)4, R8 and Tat are the most commonly used CPPs because of their higher aptitude for being internalised by the

cells (Nakase et al., 2013). This superiority seems to be due to the potential of the guanidinium functional groups, in arginine residues, to form hydrogen bonds with cell surface groups with a complementary charge such as phospholipids, fatty acid salts and sulphates (Nakase et al., 2008; Rothbard et al., 2004).

One of the striking conclusions of this study was the importance of the amino acid content of the CPP on cellular uptake. The effective uptake of CPPs has been shown to be dependent on delivery conditions, and one of those conditions is the CPP sequence (Jones & Sayers, 2012). The first evidence of these effects in this study was the striking superiority of FFR8 over R8. The addition of two phenylalanine residues at the C-terminal of R8 resulted in a 100-fold increase in MFI after 1 hour of incubation (Figure 3.2); a recent study by Watkins, et al. (2009b) showed a similar effect. The phenylalanine residue at the N-terminal of the commercially available D-NuBCP-9-R8 CPP, acted in synergy with R8 to enhance cell membrane penetration (Watkins et al., 2011). Although the delivery effectiveness of R8 can be improved with the addition of one or two phenylalanine residues, the mechanisms by which this happens are still unknown.

The differences between (RXR)4 and R8 were not as remarkable, and considering MFI values, both CPPs showed a not significant difference (p=0.567). The distribution of MFI values of (RXR)4 (SD=8,441) and R8 (SD=18,450) at one hour indicates that, although they deliver very similar levels of fluorescence, the variation between patient samples was far greater for R8 than (RXR)4. Studies comparing (RXR)4 and polyarginines in Jurkats cells, such as the one performed by Rothbard et al. (2002), showed that (RXR)4 was highly superior to R7 but not R10. This is consistent with the observation that as the number of arginines increases, so does the cell penetrating ability of these CPPs (Futaki et al., 2001). And while (RXR)4 was superior to some of the polyarginines, it did not outperform CPPs such as R8 and R10 (Rothbard et al., 2002).

Regarding cytotoxicity, (RXR)4 and R8 did not induced apoptosis at concentrations lower than 4 μM. FFR8, also does not induce cell apoptosis at doses lower than 2 μM. However, at 4 μM the number of cells staining positively for Annexin-V and PI increases (Figure 3.8 and 3.9). Considering the distribution of fluorescence of cells incubated with 4 μM of FFR8 (Figure 3.8), 44.3% were positive for Annexin-V and PI and 47.4% for PI only, which meant that 91.7% of cells were positive for an apoptosis marker. The forward and side scatter plot, however, contradicted this finding as the characteristic decrease in forward scatter and increase in side scatter (Dive et al.,

1992) were not present. There are a few possible explanations for this finding. The first possibility is that the single PI staining is real and that the cells were in a necrotic/late apoptotic state that happen too quickly to allow the translocation of PS to the outside of the membrane (i.e. Annexin-V negative), and this event did not alter the forward and side scatter profile of the cells. The second explanation is that FFR8 at 4 μM disturbed the membrane greatly and allowed for PI leakage into the cell in a manner that did not induce apoptosis. The third explanation is that the fluorescence generated by the Alexa488-tagged-FFR8 was so intense that it overlapped with the PI fluorescence in FL2. The first option is highly unlikely as no such event as ever been described in the literature and at 20 hours the number of viable cells is the same as any other concentration used and the same as untreated cells. The more likely explanations are therefore the second and third, or a combination of both.

All CPPs showed a proportional response to the dose of peptide administrated. FFR8, however has a proportional increase in fluorescence up to 2 μM, point at which the fluorescence increases 20-fold. As observed by Fretz et al. (2007), up to a certain concentration, endocytosis is the used mechanism of entry. However, at higher concentrations the fluorescence appears diffused in the cytosol with a small number of vesicles (Fretz et al., 2007). Due to the short period of incubations (10 minutes) it is highly unlikely that the cause of the diffused staining was the release from endosomal vesicles (Fretz et al., 2007). It seems more plausible that the presence of fluorescence in the cytosol was due to a different mechanism of entry, such as direct translocation (Fretz et al., 2007; Nakase et al., 2008). With this mechanism and membrane damage, cytotoxicity would be expected, but as shown by Fretz et al. (2007) and the results presented on Figure 3.7, cell viability was maintained.

The number of studies that have utilised primary cells to study CPPs is very low. Out of these, none used primary human lymphoid cells. In this study, in addition to using primary CLL cells, B-cells and T-cells from healthy individuals were obtained and incubated with the five CPPs. Normal B-cells were shown to take up the peptides in a similar fashion to malignant B-cells, with the exception of FFR8 and TP10. Levels of FFR8 taken up by normal B-cells were still the highest of all the peptides, with an MFI of approximately 50,000. As for normal B-cells incubated with TP10, MFI levels at 1 hour were similar to CLL cells, but after 20 hours of incubation these did not increase, possibly indicating a different mechanism of action. As for normal T-cells, they behaved similarly to CLL cells, with the exception of (RXR)4, FFR8 and in part TP10. Levels of (RXR)4 were much higher in T-cells than in CLL cells. The same pattern was found

with FFR8. As for TP10, the MFI levels at 1 hour are lower than in CLL cells, but unlike in B-cells, there was an increase in fluorescence at 20 hours.

The differences in CPP uptake between CLL cells, normal B-cells and T-cells is likely to be due to the different collection of membrane lipids, proteins and carbohydrates (Fretz et al., 2007). A study by Marshall et al. (2007), using murine T-cells showed the activation status of T-cells has an effect on how well the peptides were taken up. In this study, the uptake of Tat, penetratin, (RXR)4 and R_9F_2 (nona-arginine with two phenylalanine residues on the C-terminal) was studied in resting and anti-CD3 activated murine primary T-cells (Marshall et al., 2007). Activation enhanced the uptake of all CPPs tested. In most cases it doubled the MFI levels, but for (RXR)4 the increase was 22-fold in $CD4^+$ cells (Marshall et al., 2007). For this project, the activation status of B-cells and T-cells was not measured. In retrospect, the activation status could have been measured simply using activation markers such as CD69 (Caruso et al., 1997) or a separate experiment could have been set up to activate B-cells and T-cells. Unfortunately, the current data does not provide mechanistic insights for the differential uptake by T-cells.

This chapter has shown that primary human CLL cells are able to take up (RXR)4, R8, FFR8, TP10 and PFV, and that the uptake varied between peptides. A dose-response study combined with viability assays showed that the fluorescence within the cells is proportional to the increase in dose, up to 4 μM, and that these doses do not induce cell toxicity in primary CLL cells. Live cell imaging was crucial to determine the intracellular localisation of the peptides and it also provided an insight into the way the CLL cells internalised the peptides. The five CPPs were also incubated with primary B-cells and T-cells from healthy donors and the only significant difference when compared with CLL cells was the uptake of (RXR)4 and FFR8 by T-cells, which proved to be higher than any other peptide. This study enable the choice of two CPPs, FFR8 and TP10, to be used as delivery vectors of a bioactive cargo into primary CLL cells.

Chapter 4 - Characterising cellular toxicity of four novel NF-κB inhibiting CPPs in primary CLL cells

4.1. Introduction

The aim of this chapter was to assess the cytotoxic effects of the novel NF-κB inhibiting CPPs in primary human CLL cells. The NF-κB pathway is an attractive therapeutic target as it is a key regulator of apoptosis resistance due to its transcriptional activation of a number of BCL2 family genes, IAPs and CFLAR (Banno et al., 2005; Chu et al., 1997; Grossmann et al., 2000; Karin & Lin, 2002; Wang et al., 1998). NF-κB has been shown to be constitutively active in several lymphoid malignancies, including CLL (Cuní et al., 2004; Furman et al., 2000; Guzman et al., 2001; Hewamana et al., 2008a; Kirchner et al., 2003; Ni et al., 2001). The constitutive activation of NF-κB in haematological malignancies has important implications, as NF-κB regulates around 300 genes that encode cell cycle regulators, survival factors, cytokines, inflammatory, immuneregulatory and cell adhesion molecules, signalling molecules, transcription factors, enzymes and others (Fuchs, 2010). In CLL, constitutive activation of NF-κB has been shown to up regulate anti-apoptotic genes and promote CLL survival (Horie et al., 2006). Due to its crucial role in cell physiology, NF-κB represents a very attractive target in CLL and other lymphoid malignancies, hence several inhibitors have been used to target the NF-κB pathway in CLL research (Lopez-Guerra & Colomer, 2010). Table 4.1 shows some of the published inhibitors.

The four novel NF-κB inhibitors used in this chapter are composed of a CPP, either TP10 or FFR8, linked to an NF-κB inhibiting sequence (See Table 4.1). The choice of CPPs was based on results discussed in Chapter 3. A number of CPPs that target the NF-κB pathway have already been developed, however none of these employ an amphipathic CPP such as TP10 or a polyarginine such as FFR8 (Orange & May, 2008). The choice of inhibiting sequences was based on previous literature (Hewamana et al., 2008b; Lin et al., 1995; Takada et al., 2004) and commercially available inhibitors (IMG-2001 and IMG-2004, Imgenex). Both NF-κB inhibiting sequences function as competitors for nuclear translocation of subunits p50 and p65.

Post-translation modifications of the p65 NF-κB subnunit are required to induce nuclear translocation. Takada et al. (2004) devised two p65 inhibiting CPPs designed to mimic three phosphorylation sites of the p65 subunit. The CPP used to deliver the inhibiting sequence into the cells was penetratin and the phosphorylation sites mimicked were Ser276, and a combination of Ser529 and Ser536 (Takada et al., 2004). Both peptides were able to penetrate the KBM-5 cells (myelogenous leukaemia cell line) and inhibit translocation of p65 into the nucleus (Takada et al., 2004). However, the effects of the peptide mimicking the Ser276 phosphorylation site were far greater than the peptide mimicking the Ser529 and Ser536 phosphorylation sites (Takada et al., 2004). Therefore, the p65 inhibiting sequence used in this chapter corresponded to the Ser276 phosphorylation site-directed peptide used by Takada et al. (2004)(see Table 4.1). The inhibitory effects of the penetratin-linked peptide were first reported in primary human CLL cells by Hewamana et al. (2008). This peptide set, which included the NF-κB p65 (Ser276) inhibitory peptide (i.e. penetratin plus the p65 inhibitory sequence) and the control peptide (i.e. penetratin), were purchased from Imgenex and incubated at a 50 μM dose for a period of 24 hours with primary human CLL cells (Hewamana et al., 2008b).

The NF-κB p50 subunit has a NLS located at the end of the RHD (Schmitz et al., 1991). Lin et al. (1995) showed that the amino acid sequence VQRKRQKLM, when coupled with a cell penetrating peptide (i.e. AAVALLPAVLLALLAP), inhibited translocation of NF-κB into the nucleus in a concentration-dependent manner (Lin et al., 1995). The p50 inhibiting sequence used in this chapter was the same as the one used by Lin et al. (1995).

Table 4.1 NF-κB inhibitors used in CLL.

Target	Inhibitor	Reference
IKK	BAY-110782	(Pickering et al., 2007; Pierce et al., 1997)
	UTC	(Endo et al., 2007)
	BMS-345541	(Burke et al., 2003)
	NSAIDs	(Lindhagen et al., 2007)
	Curcumin	(Everett et al., 2007)
	Parthenolide	(Steele et al., 2006)
	LC-1	(Hewamana et al., 2008b)
	Deguelin	(Geeraerts et al., 2007; Nair et al., 2006)
Nuclear Translocation	DHMEQ	(Horie et al., 2006)
	NF-κB p65 (Ser276)	(Hewamana et al., 2008b; Takada et al., 2004)

Table 4.2 – Amino acid sequences of the NF-κB inhibiting CPPs.

Name	Sequence
FFR8	FFRRRRRRRR
TP10	AGYLLGKINLKALAALAKKIL
p50 inhibiting sequence	^{359}VQ**RKR**Q**K**LM^{366}
p65 inhibiting sequence	^{270}QLRRP**S**DRELSE^{282}

Note: highlighted residues correspond to NLS for p50 and phosphorylation site for p65.

FFR8-**p50i**	FFRRRRRRRR**VQRKRQKLM**
FFR8-**p65i**	FFRRRRRRRR**QLRRPSDRELSE**
TP10-**p50i**	AGYLLGKINLKALAALAKKIL**VQRKRQKLM**
TP10-**p65i**	AGYLLGKINLKALAALAKKIL**QLRRPSDRELSE**

Note: The highlighted amino acids correspond to the p50/p65 inhibiting sequences.

4.2. Study of the effect of peptide concentration in cell viability

The novel NF-κB inhibiting CPPs were designed with the intention of targeting the translocation of p50 and p65 subunits of NF-κB, with the supposition that this would induce apoptosis in primary CLL cells. To assess the effects of the peptides on cell viability, $1x10^6$ primary CLL cells were incubated with different concentrations (0, 2, 4, 8, 12, 40 and 200 μM) of FFR8-p50i, FFR8-p65i, TP10-p50i and TP10-p65i for a period of 48 hours in 500μl of DMEM supplemented media. Cells were harvested at 24 and 48 hours, resuspended in calcium containing buffer and dual-labelled with Annexin V-APC and propidium iodide. Fluorescence was subsequently measured by flow cytometry (Figure 4.1). Figure 4.2 shows the percentage of viable cells (Annexin V and PI negative) for each concentration.

The choice of plotting viability opposed to apoptosis arose when it was evident that some cells where often found in the upper left quadrant (PI positive). Cells in this quadrant are not normally accounted as apoptotic cells, as the membrane permeabilisation to PI in the apoptotic process does not occur without PS externalization (i.e. Annexin-V positivity). To avoid these cells being counted as viable, a choice was made to plot viability instead of apoptosis. The percentages presented in the figures that follow were retrieved from the lower left quadrant of the Annexin-V/PI plots. The viability curves, or concentration-response curves were generated using the Graphpad Prism 6 software. The program transformed the concentrations used into logarithms and plotted them on the x-axis while the response (i.e. viability) was plotted on the y-axis. To generate the curves presented and to be able to interpolate values

(i.e. LC_{50}) from the data, a non-linear regression was applied. In this situation the software tries to create a sigmoidal curve that best fits the data using the least-squares approach. This approach finds the curve that minimizes the sum of the squares of the vertical distances of the points from the curve, ensuring that the interpolated data is as closest to the real values as possible. The LC_{50} presented in this chapter were all interpolated using the Graphpad Prism 6 software. By transforming the concentrations used into logarithms, the untreated samples were excluded from the viability curves. However, for every sample tested, there was no change in viability in samples cultured with 1 μM of the peptides. The reason why all viability curves start with less than 90% of viable cells is due to the nature of primary CLL cells that are highly dependent on the *in vivo* microenvironment, and when deprived of those stimuli undergo apoptosis (Ramsay & Rodriguez-Justo, 2013; Willimott et al., 2007a).

From both Figure 4.1 and 4.2, it was evident that both TP10 peptides reduced CLL cell viability at doses lower than 40 μM. In contrast, the FFR8 peptides did not induce apoptosis at those concentrations. For this reason, concentrations used were adjusted to ensure an even coverage below 40 μM. Since one of the aims in this chapter is to compare the four novel NF-κB inhibiting CPPs with commercially available NF-κB inhibitors that work at ranges higher than 50 μM, the doses were adjusted to include this concentration. Therefore, cells were cultured with 0, 1, 2.5, 5, 10, 25 and 50 μM of FFR8-p50i, FFR8-p65i, TP10-p50i and TP10-p65i. Figures 4.3 to 4.5 show the forward and side scatter plots, and the Annexin V/PI fluorescence for cells incubated with FFR8-p50i, TP10-p50i and TP10-p65i for some of the concentrations administrated. Figure 4.6 shows the percentage of viable cells (Annexin V and PI negative) for each concentration. Table 4.3 shows the LC_{50} values of the 4 CPPs, which corresponds to the concentration required to kill 50% of the cells in culture.

Of the four CPPs tested, only two affected CLL viability. Those peptides were TP10-p50i and TP10-p65i, presenting an LC_{50} of 5.28 (4.03 - 6.50 μM) and 9.95 μM (7.44 - 13.45 μM) respectively. Both FFR8 peptides induced a decrease in the percentage of viable cells at 25 μM, but this did not decrease further at 50 μM. In all four CPPs, the effects were observed after 24 hours of incubation, and similar viability was maintained after 48 hours.

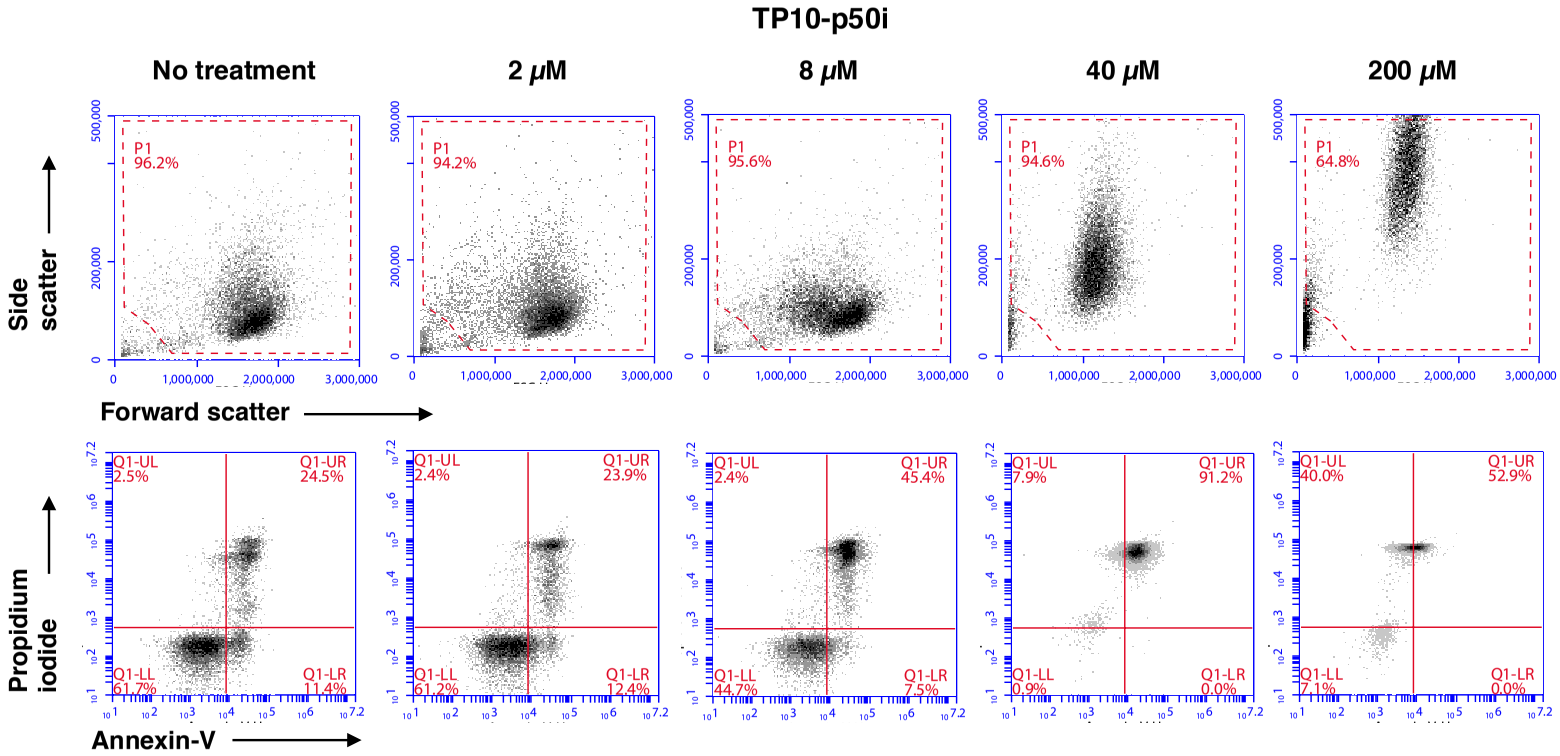

Figure 4.1 – Flow cytometry data of primary CLL cells incubated with TP10-p50i for a period of 24 hours.
Primary CLL cells were incubated with 0, 2, 4, 8, 12, 40 and 200 μM of TP10-p50i for a period of 24 hours. Cells were collected and washed with PBS. Cells were stained for Annexin-V and PI. Viable lymphocytes were gated in the forward and side scatter plot within P1. Cells gated in P1 were plotted according to their fluorescence in FL2 (propidium iodide) and FL4 (Annexin-V). Cells in the lower left quadrant (Q1-LL) are viable cells. Cells in the lower right quadrant (Q1-LR) are in an early apoptosis state. Cells in the upper right quadrant (Q1-UR) are in a late apoptosis state.

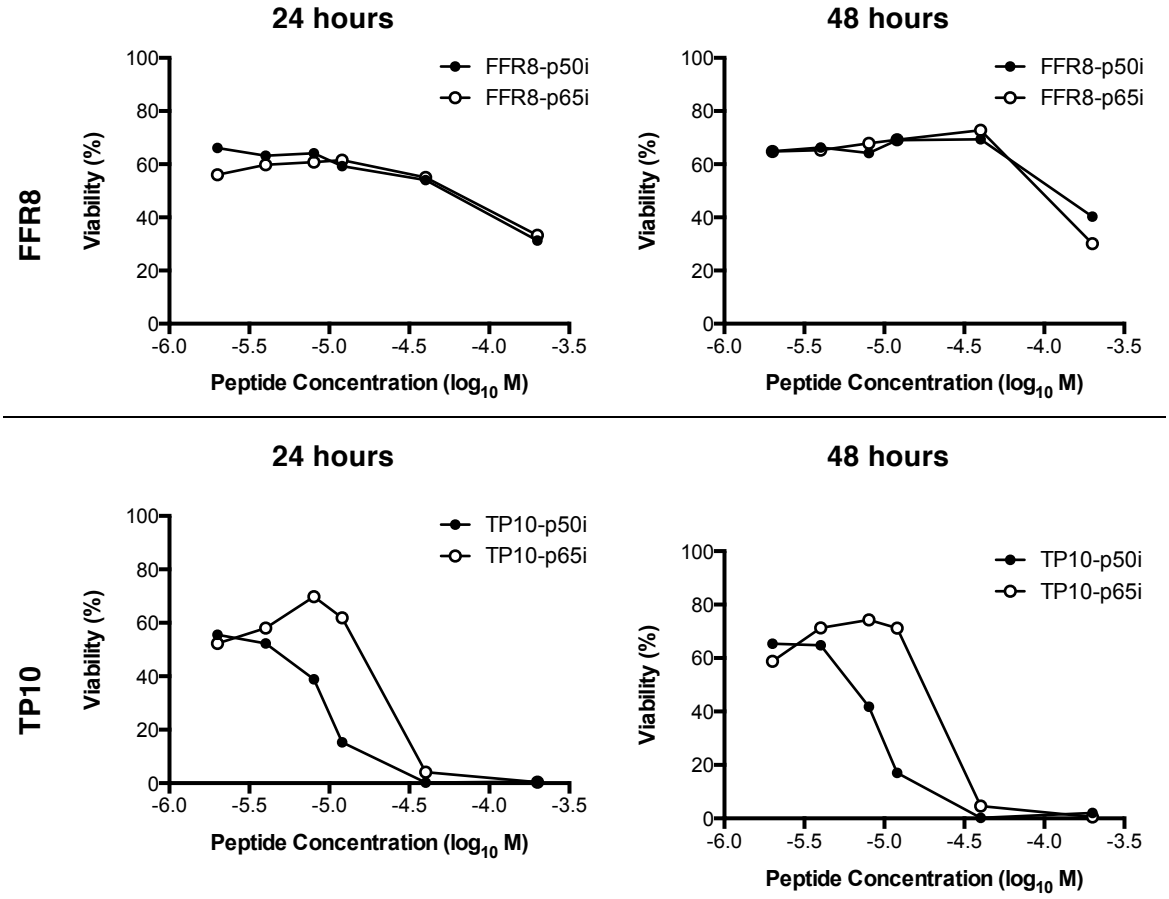

Figure 4.2 - Viability of primary CLL cells incubated with FFR8-p50i, FFR8-p65i, TP10-p50i and TP10- p65i for a period of 24 and 48 hours.

Primary CLL cells were incubated with 0, 2, 4, 8, 12, 40 and 200 μM of FFR8-p50i, FFR8-p65i, TP10-p50i and TP10-p65i for a period of 24 and 48 hours. Viability measured by Annexin-V and PI. Percentage of viable cells corresponds to cells Annexin-V and PI negative. The viability curves were generated using Prism 6 software. Data shown for one patient.

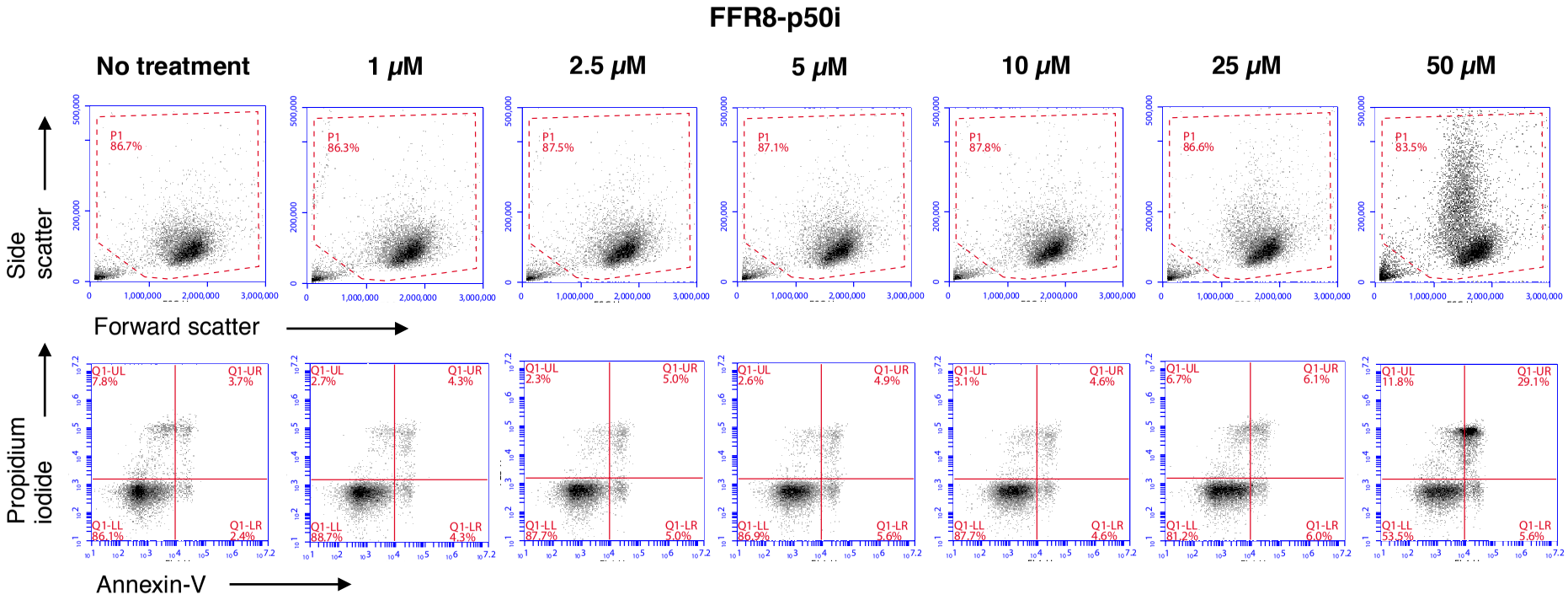

Figure 4.3 – Flow cytometry data of primary CLL cells incubated with FFR8-p50i for a period of 24 hours.
Primary CLL cells were incubated with 0, 1, 2,5, 5, 10, 25 and 50 μM of FFR8-p50i for a period of 24 hours. Cells were collected and washed with PBS. Cells were stained for Annexin-V and PI. Viable lymphocytes were gated in the forward and side scatter plot within P1. Cells gated in P1 were plotted according to their fluorescence in FL2 (propidium iodide) and FL4 (Annexin-V). Cells in the lower left quadrant (Q1-LL) are viable cells. Cells in the lower right quadrant (Q1-LR) are in an early apoptosis state. Cells in the upper right quadrant (Q1-UR) are in a late apoptosis state.

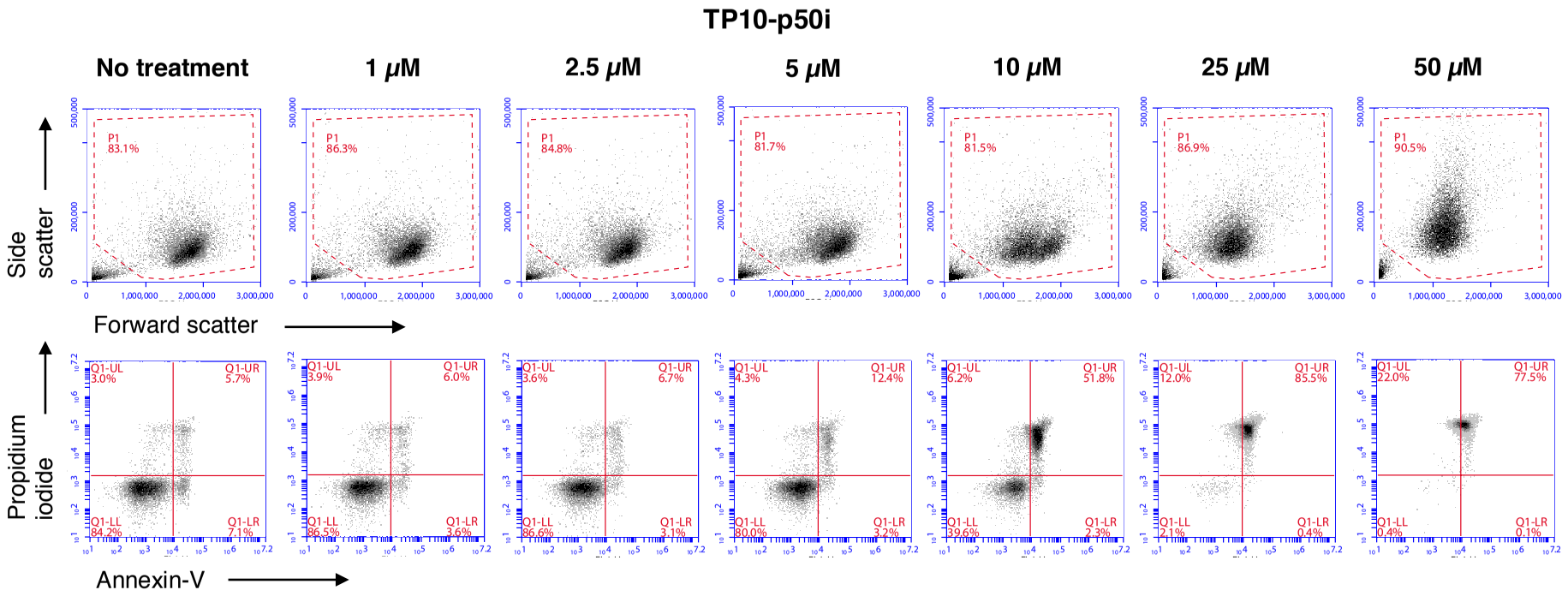

Figure 4.4 – Flow cytometry data of primary CLL cells incubated with TP10-p50i for a period of 24 hours.
Primary CLL cells were incubated with 0, 1, 2,5, 5, 10, 25 and 50 μM of TP10-p50i for a period of 24 hours. Cells were collected and washed with PBS. Cells were stained for Annexin-V and PI. Viable lymphocytes were gated in the forward and side scatter plot within P1. Cells gated in P1 were plotted according to their fluorescence in FL2 (propidium iodide) and FL4 (Annexin-V). Cells in the lower left quadrant (Q1-LL) are viable cells. Cells in the lower right quadrant (Q1-LR) are in an early apoptosis state. Cells in the upper right quadrant (Q1-UR) are in a late apoptosis state.

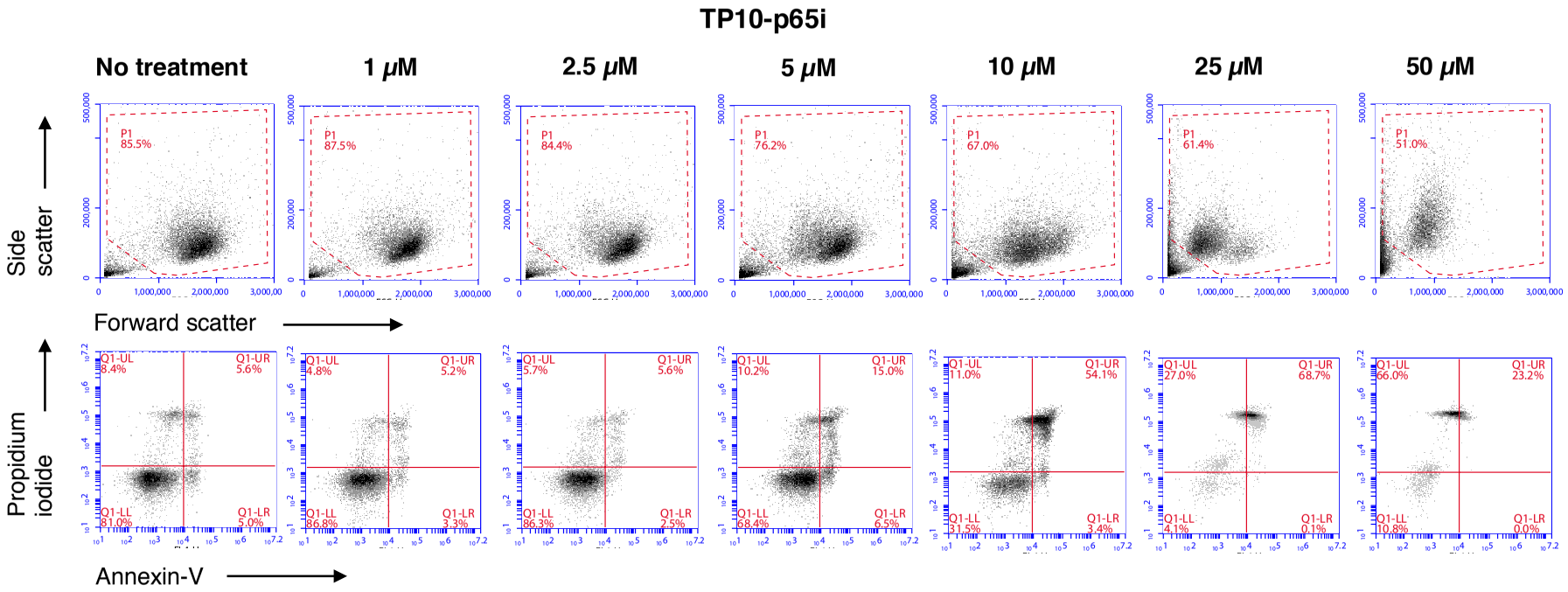

Figure 4.5 – Flow cytometry data of primary CLL cells incubated with TP10—p65i for a period of 24 hours.
Primary CLL cells were incubated with 0, 1, 2,5, 5, 10, 25 and 50 μM of TP10-p65i for a period of 24 hours. Cells were collected and washed with PBS. Cells were stained for Annexin-V and PI. Viable lymphocytes were gated in the forward and side scatter plot within P1. Cells gated in P1 were plotted according to their fluorescence in FL2 (propidium iodide) and FL4 (Annexin-V). Cells in the lower left quadrant (Q1-LL) are viable cells. Cells in the lower right quadrant (Q1-LR) are in an early apoptosis state. Cells in the upper right quadrant (Q1-UR) are in a late apoptosis state.

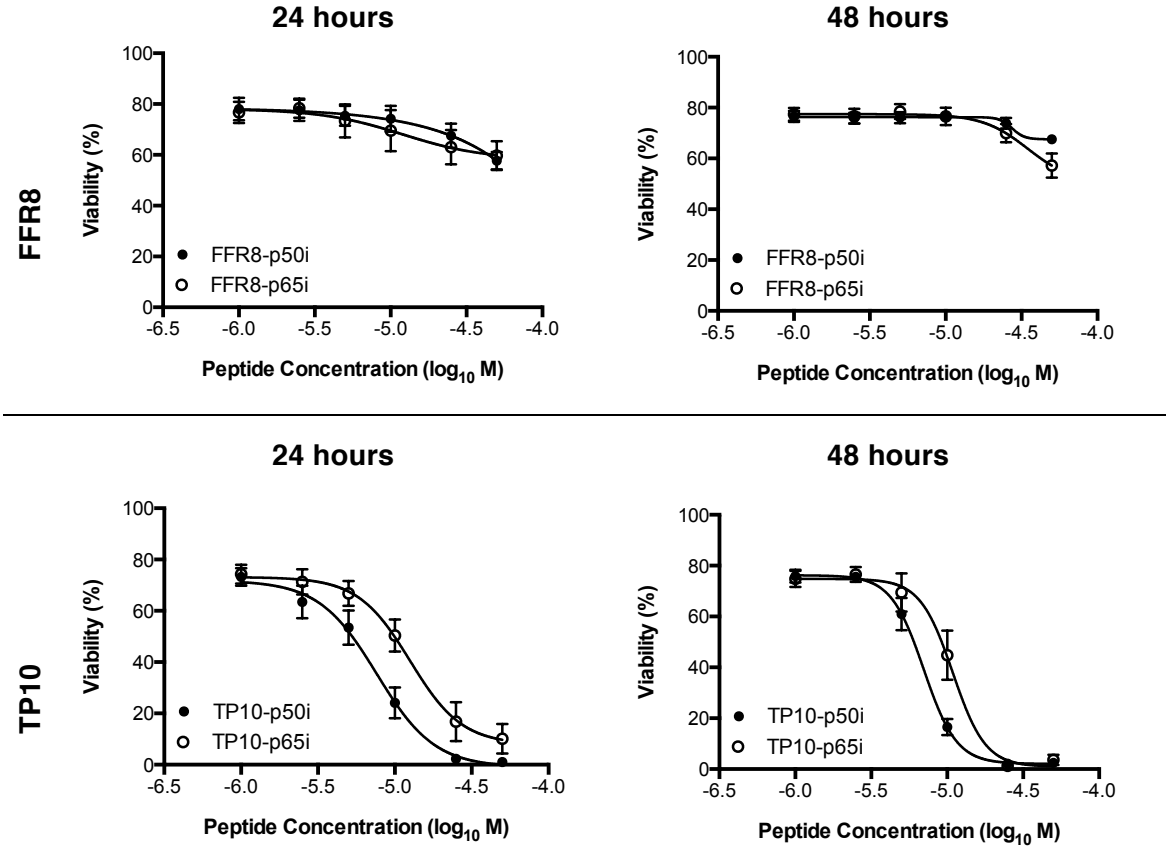

Figure 4.6 - Viability of primary CLL cells incubated with FFR8-p50i, FFR8-p65i, TP10-p50i and TP10- p65i for a period of 24 and 48 hours.
Primary CLL cells were incubated with 0, 1, 2.5, 5, 10, 25 and 50 µM of FFR8-p50i, FFR8-p65i, TP10-p50i and TP10-p65i for a period of 24 and 48 hours. Viability measured by Annexin-V and PI. Percentage of viable cells corresponds to cells Annexin-V and PI negative. The viability curves were generated using Prism 6 software. Data is present as mean (+/- SD) for 8 individual patient samples.

Table 4.3 - NF-κB inhibiting CPPs LC_{50} at 24 hours.

NF-κB inhibiting CPP	LC_{50}	95% Confidence Interval
FFR8-p50i	> 50 μM	Und.
FFR8-p65i	> 50 μM	Und.
TP10-p50i	5.28 μM	4.03 – 6.50
TP10-p65i	9.95 μM	7.44 – 13.45

Note: The LC_{50} values were interpolated using Prism 6 software from the viability curves shown in Figure 4.6.

Table 4.4 - NF-κB inhibiting CPPs LC_{50} at 24 hours for each of the samples tested.

Patient Sample	TP10-p50i		TP10-p65i	
	LC_{50}	95% Confidence interval	LC_{50}	95% Confidence interval
1	3.90	2.71 - 4.98	9.95	Und.
2	7.69	5.42 - 9.26	10.96	Und.
3	8.81	8.64 - 8.97	7.16	5.09 - 9.86
4	3.57	Und. - 5.84	7.92	5.92 - 10.18
5	3.35	Und. - 7.55	4.34	Und.
6	5.47	4.33 - 6.62	7.27	5.49 - 9.20
7	6.19	4.32 - 8.10	9.05	4.97 - 15.63
8	10.09	4.76 - 22.18	49.20	Und.
Mean	5.28	4.03 - 6.50	9.95	7.44 - 13.45

Note: All values were calculated using Prism 6 software.
Und. – The software could not calculate the values.

4.3. The fluorescent tag Alexa488 caused cell toxicity at high concentrations

As mentioned previously, the addition of cargo, whether it be an inhibitor, fluorochrome or other, can alter dramatically the cell penetrating abilities of CPPs (Jones & Sayers, 2012). Choosing an appropriate control therefore can be challenging. Possible options would be the use of the CPP in the absence of cargo (i.e. TP10), the CPP with a scrambled version of the inhibiting sequence, the inhibiting sequence in the absence of the CPP or labelled CPP/ NF-κB inhibiting peptide. Due to the availability of labelled CPP, this was used as control in the following experiments.

Primary CLL cells were incubated with a range of concentrations (0, 1, 2.5, 5, 10, 25 and 50 μM) of FFR8-Alexa488, FFR8-p50i, FFR8-p65i, TP10-Alexa488, TP10-p50i and TP10-p65i. Cells were cultured for a period of 48 hours, and collected at 24 and 48 hours. The previously described viability tests with Annexin V and PI were performed. Figure 4.7 and 4.8 show the forward and side scatter, and the Annexin V and PI distribution of one patient sample. Figure 4.9 shows a compilation of data from 3 patient samples.

The addition of FFR8-Alexa488 and TP10-Alexa488 to culture induced a shift upwards of the CLL cell population along the PI fluorescence scale. This shift was not accompanied by the characteristic apoptotic features (i.e. decrease in the forward scatter and increase in side scatter) until cells were exposed to higher concentrations of the peptides (eg. 50 μM). The shift of the CLL population meant that those cells would no longer be counted as viable and lead to the misinterpretation of cells being apoptotic. As mentioned in chapter 4.2, PI positivity is always preceded by Annexin-V positivity, which is the reason why cells in the top left quadrant are not counted as apoptotic. The single PI positivity observed in Figures 4.7 and 4.8 is an artifact caused by the fluorescently-tagged peptides. For this reason, for the experiments with Alexa488-tagged peptides, a choice was made to plot apoptotic cells (i.e. upper right and lower right quadrants) instead of viable cells.

Twenty-four hours of incubation with FFR8-Alexa488 primary CLL cells showed reduced viability when cultured with concentrations greater than 10 μM (Figure 4.9). FFR8-Alexa488 had a LC_{50} of 27.2 μM (24.1 – 30.83) and both FFR8-p50i and FFR8-p65i had an LC_{50} higher than 50 μM at 24 hours. After 48 hours the LC_{50} values for FFR8-p65i were lower but remained higher than 30 μM.

In contrast to the FFR8-Alexa488 peptide, cells incubated with TP10-Alexa488 did not show signs of apoptosis after 24 and 48 hours. The LC_{50} for the fluorescence-tagged TP10 peptide was greater than 50 μM. Although, the mean apoptosis values of the three samples tested did not show an increase with concentrations up to 50 μM, the sample shown in Figure 4.8 exhibited the characteristic apoptotic profile (i.e. decrease in forward scatter and increase in side scatter) when incubated with 50 μM of the TP10-Alexa488, indicating that doses this high can sometimes have an effect on cell viability. In contrast, the TP10-p50i and TP10-p65i peptides manifested LC_{50} values <10 μM. Out of the two NF-κB inhibiting CPPs, TP10-p50i had the lowest LC_{50} 8.70 μM (8.43 – 8.95).

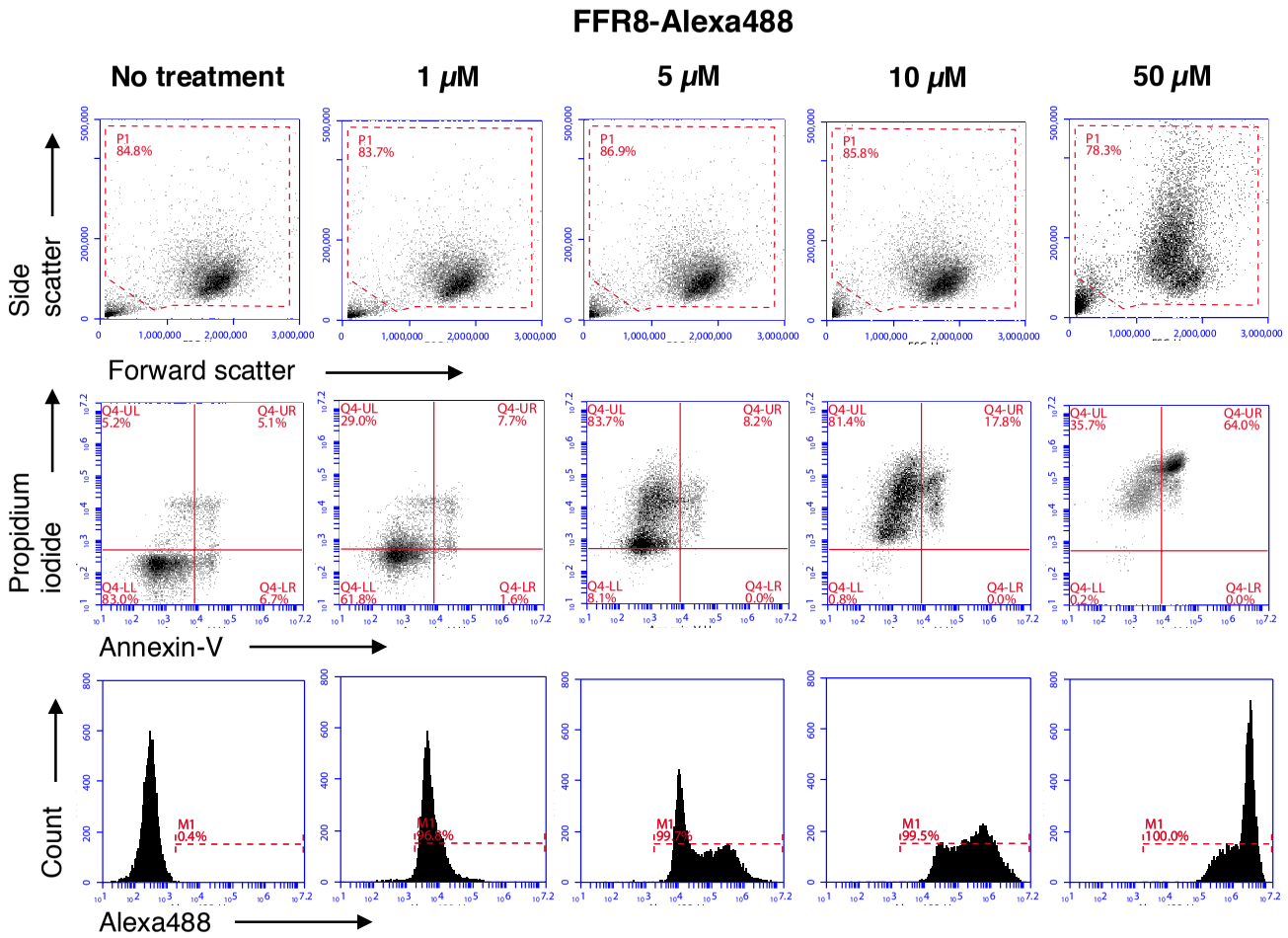

Figure 4.7 – Flow cytometry data of primary CLL cells incubated with FFR8-Alexa488 for a period of 24 hours.
Primary CLL cells were incubated with 0, 1, 2.5, 5, 10, 25 and 50 μM of FFR8-Alexa488 for a period of 24 hours. Cells were collected and washed with PBS. Cells were stained for Annexin-V and PI. Viable lymphocytes were gated in the forward and side scatter plot within P1. Cells gated in P1 were plotted according to their fluorescence in FL2 (propidium iodide) and FL4 (Annexin-V). Cells in the lower left quadrant (Q1-LL) are viable cells. Cells in the lower right quadrant (Q1-LR) are in an early apoptosis state. Cells in the upper right quadrant (Q1-UR) are in a late apoptosis state.

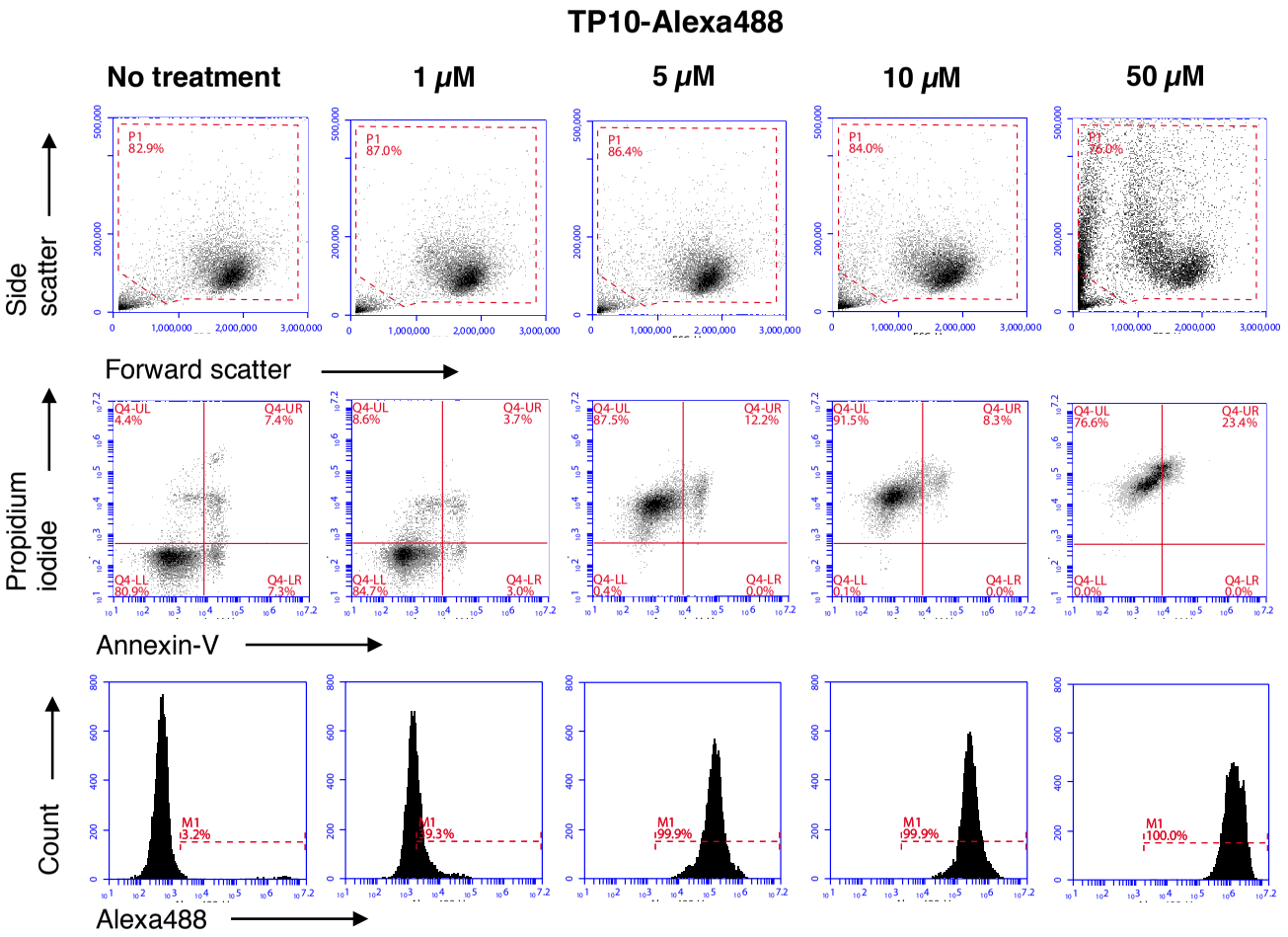

Figure 4.8 – Flow cytometry data of primary CLL cells incubated with TP10-Alexa488 for a period of 24 hours.
Primary CLL cells were incubated with 0, 1, 2.5, 5, 10, 25 and 50 μM of TP10-Alexa488 for a period of 24 hours. Cells were collected and washed with PBS. Cells were stained for Annexin-V and PI. Viable lymphocytes were gated in the forward and side scatter plot within P1. Cells gated in P1 were plotted according to their fluorescence in FL2 (propidium iodide) and FL4 (Annexin-V). Cells in the lower left quadrant (Q1-LL) are viable cells. Cells in the lower right quadrant (Q1-LR) are in an early apoptosis state. Cells in the upper right quadrant (Q1-UR) are in a late apoptosis state.

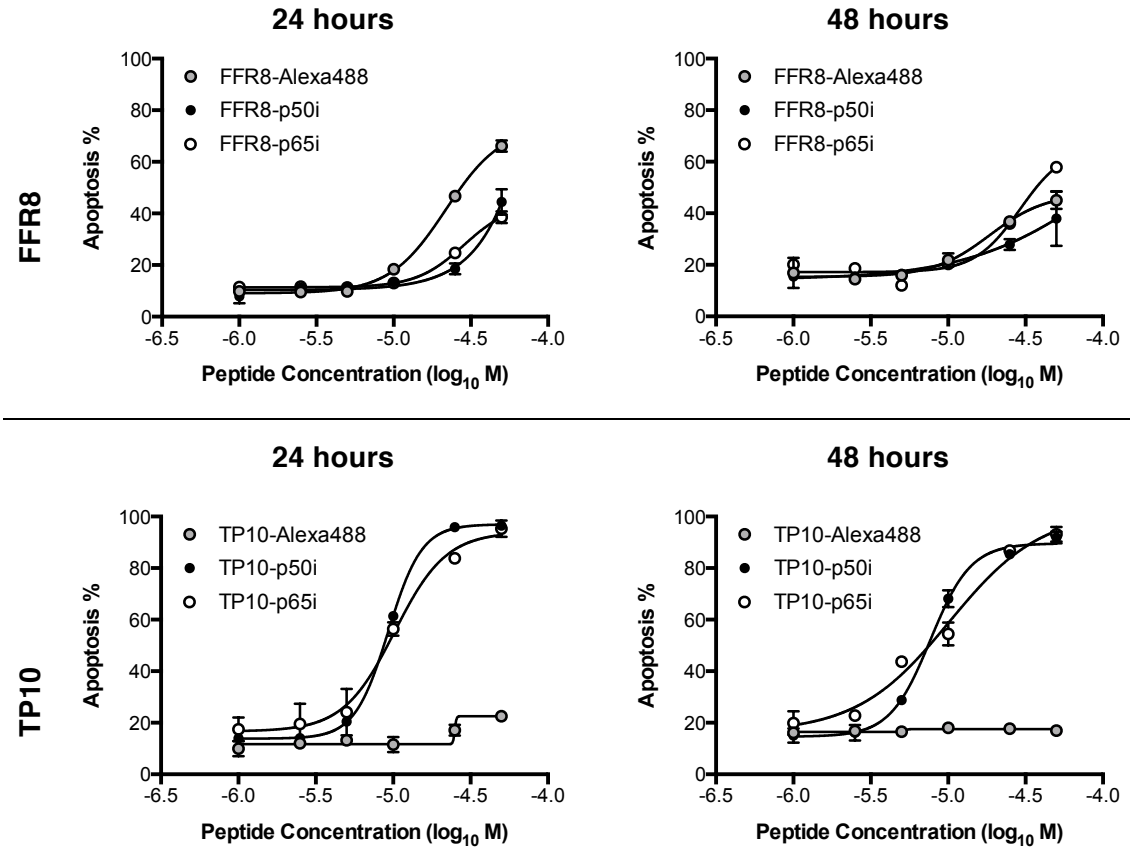

Figure 4.9 - Apoptosis of primary CLL cells incubated with FFR8-Alexa488, FFR8-p50i, FFR8-p65i, TP10-Alexa488, TP10-p50i and TP10- p65i for a period of 24 and 48 hours.
Primary CLL cells were incubated with 0, 1, 2.5, 5, 10, 25 and 50 µM of FFR8-p50i, FFR8-p65i, TP10-p50i and TP10-p65i for a period of 24 and 48 hours. Viability was measured by Annexin-V and PI labelling. The percentage of viable cells was calculated from the Annexin-V and PI negative cell population. The apoptosis curves were generated using Prism 6 software. Data presented are the mean (+/- SD) for the three patient samples analysed.

Table 4.5 – Alexa-labIled and NF-κB inhibiting CPPs LC_{50}.

NF-κB inhibiting CPP	24 hours		48 hours	
	LC_{50}	95% Confidence Interval	LC_{50}	95% Confidence Interval
FFR8-Alexa488	27.2 μM	24.1 – 30.83	> 50 μM	Und.
FFR8-p50i	> 50 μM	Und.	> 50 μM	Und.
FFR8-p65i	> 50 μM	Und.	37.0 μM	13.2 – Und.
TP10-Alexa488	> 50 μM	Und.	> 50 μM	Und.
TP10-p50i	8.70 μM	8.43 – 8.95	7.41 μM	6.03 – 8.93
TP10-p65i	9.18 μM	6.32 – 13.83	7.55 μM	3.68 – 15.66

Note: The LC_{50} values were interpolated using Prism 6 software from the apoptosis curves shown in Figure 4.9.

4.4. IL-4 did not affect the cytotoxic effects of the TP10 NF-κB inhibiting CPPs

The cytokine IL-4 is known to confer cytoprotection to CLL cells (Willimott et al., 2007a). Stimulation of B-cells with IL-4 has been shown to increase NF-κB binding activity (Thieu et al., 2007), and pharmacological inhibition of NF-κB has been shown to abrogate the cytoprotective effects of IL-4 (Zamorano et al., 2001). To determine if stimulation with IL-4 would alter the NF-κB cytotoxic effects of TP10-p50i and TP10-p65i, CLL cells were incubated with 0, 1, 2.5, 5, 10, 25 and 50 μM of TP10-p50i and TP10-p65i with and without 5ng/ml of IL-4 for a period of 24 and 48 hours. Following incubation, cells were labelled with Annexin-V and PI, and analysed by flow cytometry. Figure 4.10 shows the flow cytometry profile of primary CLL cells from one patient sample incubated with TP10-p50i and Figure 4.11 shows the flow cytometry profile of primary CLL cells from the same patient incubated with TP10-p50i in the presence of 5ng/ml of IL-4. Figure 4.12 shows the compilation of the viability of primary CLL cells from four patients following incubation with TP10-p50i and TP10-p65i with and without 5ng/ml of IL-4 for a period of 24 and 48 hours.

Addition of 5ng/ml of IL-4 to primary CLL cells did not alter the cytotoxic effects of these peptides, as LC_{50} values showed no significant difference at 24 hours (TP10-p50i p=0.46 and TP10-p65i p=0.42) and 48 hours (TP10-p50i p=0.55 and TP10-p65i p=0.99). However, in untreated cells the percentage of viable cells (Figure 4.11) increased showing that IL-4 has the capacity to improve cell viability. Regarding the forward and side scatter profile of cells treated with IL-4 and the TP10-p50i peptide (Figures 4.10 and 4.11) differences were apparent. Cells incubated with TP10-p50i without IL-4 showed a decrease in forward scatter and increase in side scatter at 10 μM and 50 μM. The addition of IL-4 to cells incubated with 50 μM of TP10-p50i, although not altering the absolute values of viable cells plotted in Figure 4.12, had an effect on the flow cytometry profile of the cells. At 10 μM 20.7% of the cells incubated with TP10-p50i and IL-4 show positivity for PI only, rivaled to 3.6% of cells positive for PI only when incubated with TP10-p50i. At 50 μM these values are maintained (i.e. 26.1% for TP10-p50i + IL-4 and 1.5% for TP10-p50i only). The increase in PI positivity in cells incubated with IL-4 was accompanied with a decrease in forward scatter a small increase in side scatter. However, the increase in side scatter was not as high as the increase in cells incubated with TP10-p50i only.

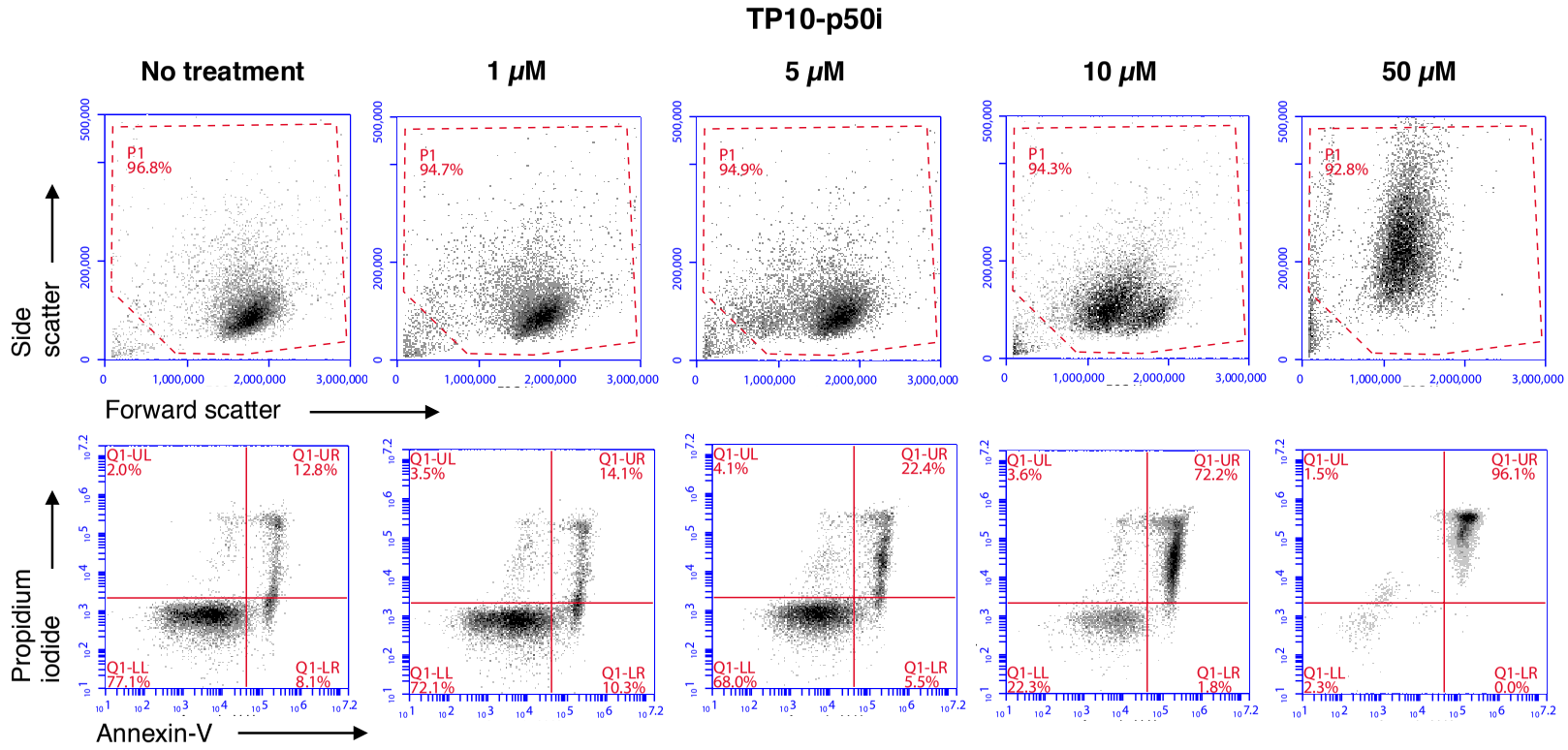

Figure 4.10 – Flow cytometry data of primary CLL cells incubated for 24 hours with TP10-p50i without IL-4.
Primary CLL cells were incubated with 0, 1, 2.5, 5, 10, 25 and 50 μM of TP10-p50i without IL-4 for a period of 24 hours. Cells were collected and washed with PBS. Cells were stained for Annexin-V and PI. Viable lymphocytes were gated in the forward and side scatter plot within P1. Cells gated in P1 were plotted according to their fluorescence in FL2 (propidium iodide) and FL4 (Annexin-V). Cells in the lower left quadrant (Q1-LL) are viable cells. Cells in the lower right quadrant (Q1-LR) are in an early apoptosis state. Cells in the upper right quadrant (Q1-UR) are in a late apoptosis state

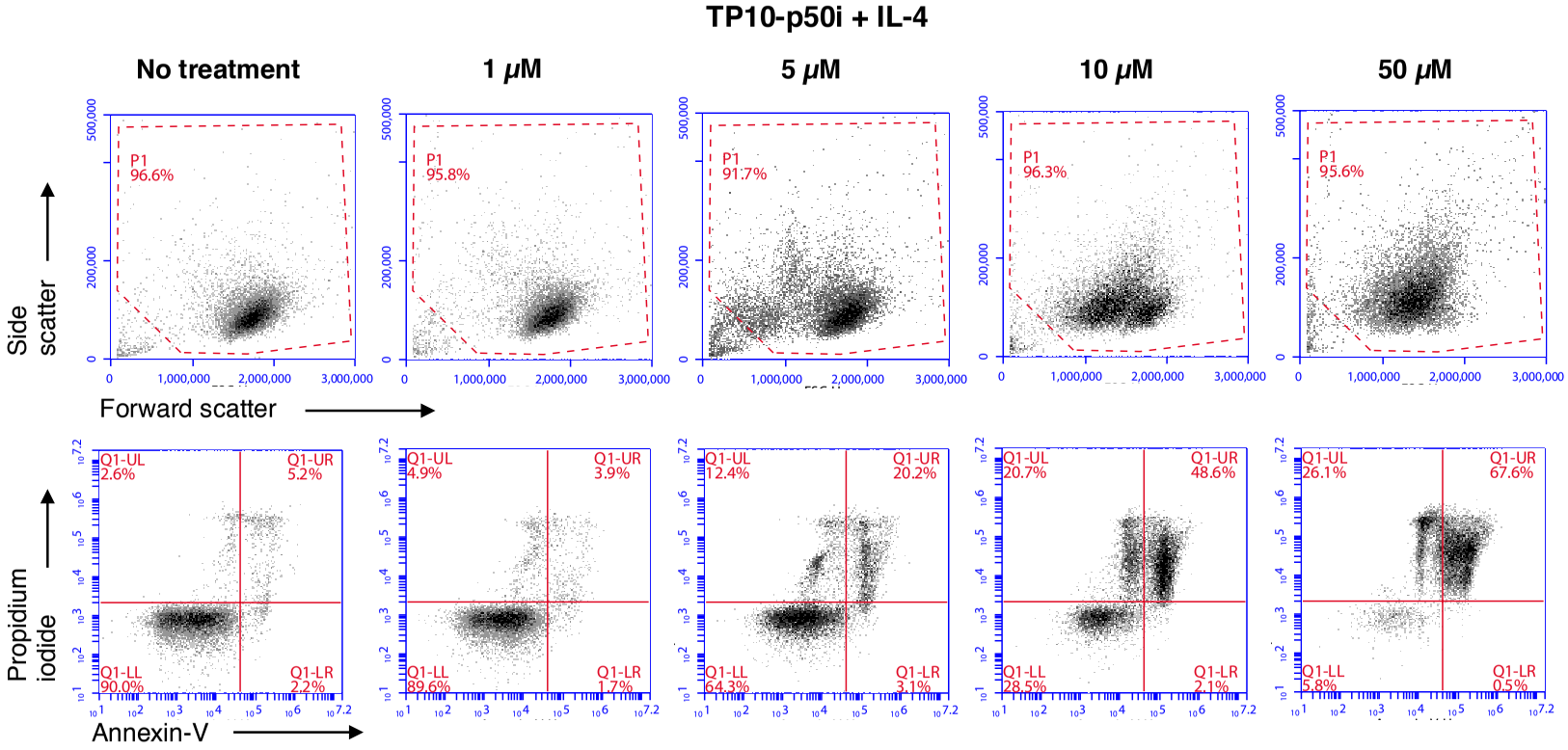

Figure 4.11 – Flow cytometry data of primary CLL cells incubated for 24 hours with TP10-p50i with 5ng/ml of IL-4.
Primary CLL cells were incubated with 0, 1, 2.5, 5, 10, 25 and 50 μM of TP10-p50i with 5ng/ml of IL-4 for a period of 24 hours. Cells were collected and washed with PBS. Cells were stained for Annexin-V and PI. Viable lymphocytes were gated in the forward and side scatter plot within P1. Cells gated in P1 were plotted according to their fluorescence in FL2 (propidium iodide) and FL4 (Annexin-V). Cells in the lower left quadrant (Q1-LL) are viable cells. Cells in the lower right quadrant (Q1-LR) are in an early apoptosis state. Cells in the upper right quadrant (Q1-UR) are in a late apoptosis state.

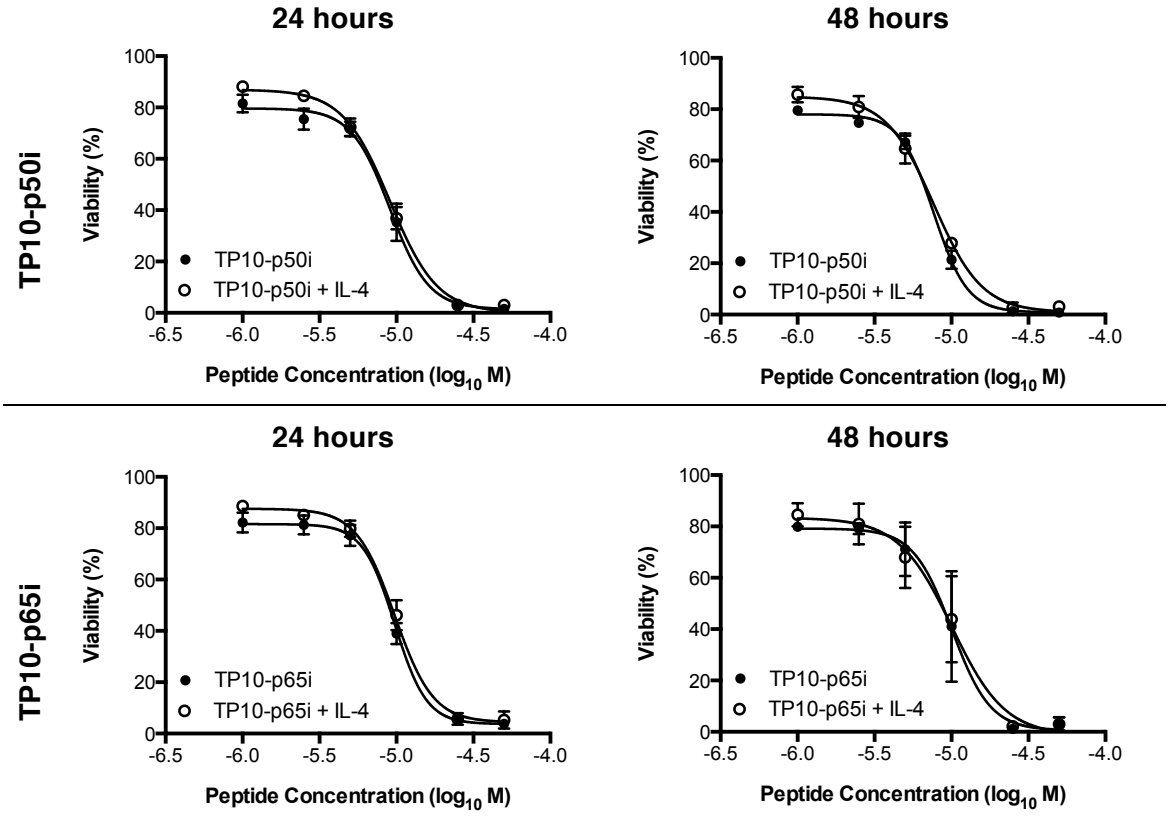

Figure 4.12 - Viability of primary CLL cells incubated with TP10-p50i and TP10- p65i with and without 5ng/ml of IL-4 for a period of 24 and 48 hours.
Primary CLL cells were incubated with 0, 1, 2.5, 5, 10, 25 and 50 µM of TP10-p50i and TP10-p65i with an without 5ng/ml of IL-4 for a period of 24 and 48 hours. Viability measured by Annexin-V and PI. Percentage of viable cells corresponds to cells Annexin-V and PI negative. The viability curves were generated using Prism 6 software. Data are presented as the mean (+/- SD) for four patient samples.

Table 4.6 - NF-κB inhibiting CPPs LC_{50} with and without IL-4.

NF-κB inhibiting CPP	24 hours		48 hours	
	LC_{50}	95% Confidence Interval	LC_{50}	95% Confidence Interval
TP10-p50i TP10-p50i +IL-4	7.85 μM 8.14 μM	7.01 – 8.51 7.46 – 8.77	6.66 μM 6.79 μM	6.15 – 7.14 6.30 – 7.24
TP10-p65i TP10-p65i +IL-4	8.89 μM 9.20 μM	7.87 – 9.48 8.53 – 9.81	8.62 μM 8.45 μM	5.78 – 11.22 5.90 – 10.51

Note: The LC_{50} values were interpolated using Prism 6 software from the viability curves shown in Figure 4.12.

4.5. The cytotoxic effects of the TP10 NF-κB inhibiting CPPs were apparent in less than one hour

In order to determine if the kinetics of the cytotoxic effects of TP10-p50i and TP10-p65i occurred under 24 hours, cells were cultured for a period of 48 hours and viability was measured at 1, 24 and 48 hours. Primary CLL cells were incubated with 0,1, 2.5, 5 and 10 μM of TP10-p50i and TP10-p65i. At the time points, cells were harvested and labelled with PI and Annexin-V and analysed by flow cytometry. Figure 4.13 shows the flow cytometry profile of primary CLL cells of one patient incubated with TP10-p50i for a period of one hour and Figure 4.14 shows the same patient sample after 24 hours of incubation. Figure 4.15 shows the average viability of 4 CLL patient samples. The cytotoxic effects of both TP10-p50i and TP10-p65i occurred under one hour. The LC_{50} of TP10-p50i increased by 22% from 1 to 48 hours. The LC_{50} of TP10-p65i at 1 hour could not be calculated as the average viability did not decrease below 60%, and therefore it was determined to be higher than 10 μM.

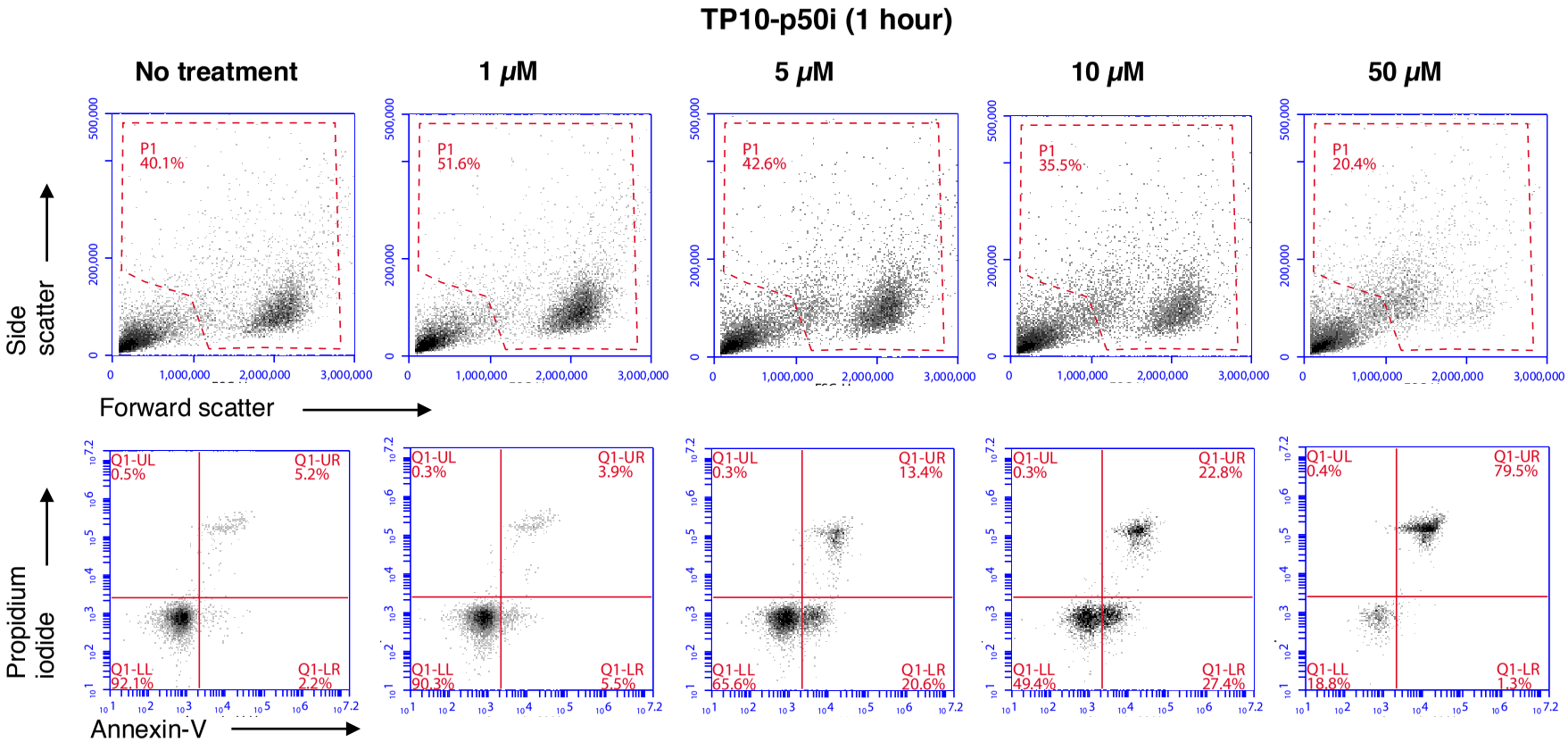

Figure 4.13 – Flow cytometry data of primary CLL cells incubated for 1 hour with TP10-p50i.
Primary CLL cells were incubated with 0, 1, 2.5, 5 and 10 μM of TP10-p50i a period of 1 hour. Cells were collected and washed with PBS. Cells were stained for Annexin-V and PI. Viable lymphocytes were gated in the forward and side scatter plot within P1. Cells gated in P1 were plotted according to their fluorescence in FL2 (propidium iodide) and FL4 (Annexin-V). Cells in the lower left quadrant (Q1-LL) are viable cells. Cells in the lower right quadrant (Q1-LR) are in an early apoptosis state. Cells in the upper right quadrant (Q1-UR) are in a late apoptosis state.

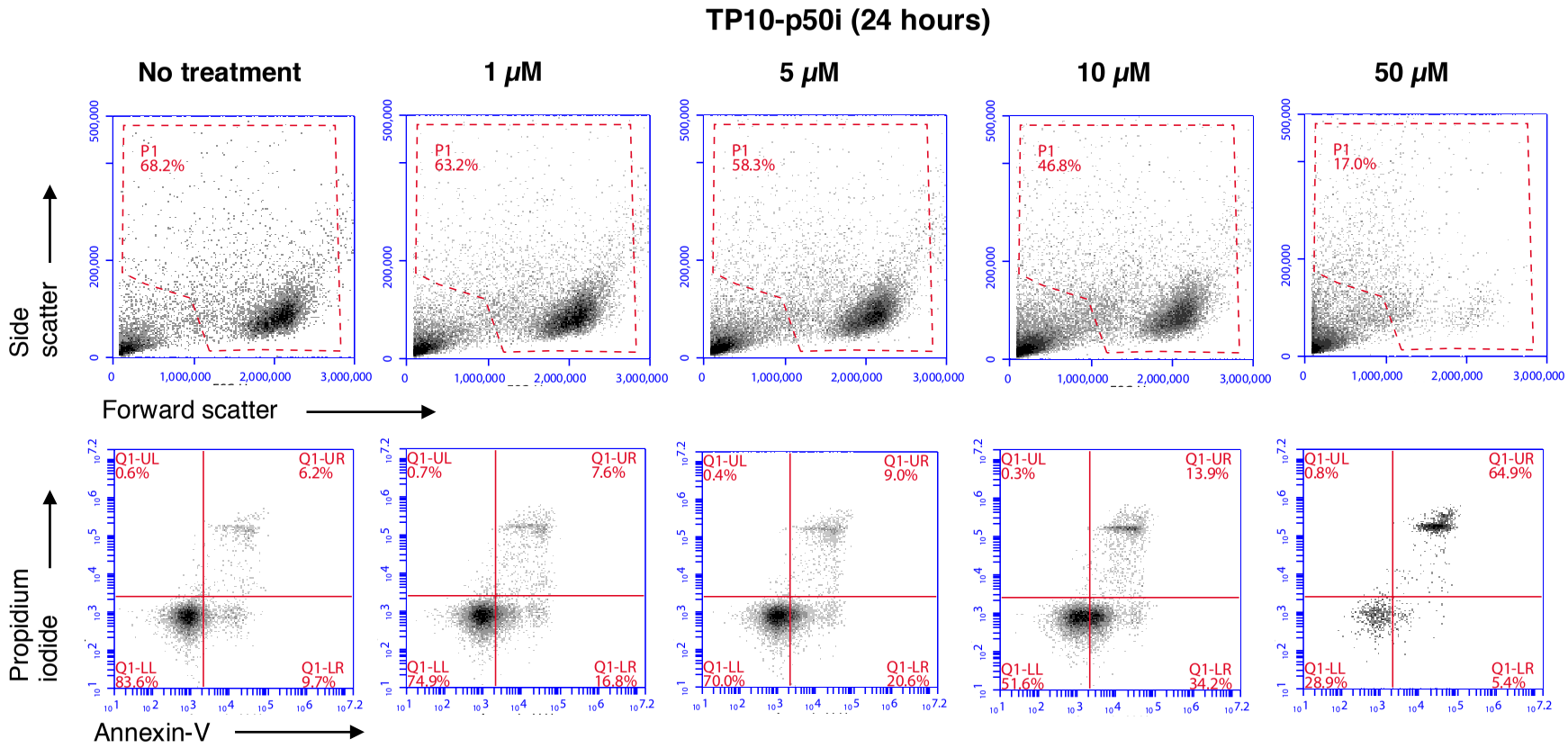

Figure 4.14 – Flow cytometry data of primary CLL cells incubated for 24 hours with TP10-p50i.
Primary CLL cells were incubated with 0,1, 2.5, 5 and 10 μM of TP10-p50i for a period of 24 hours. Cells were collected and washed with PBS. Cells were stained for Annexin-V and PI. Viable lymphocytes were gated in the forward and side scatter plot within P1. Cells gated in P1 were plotted according to their fluorescence in FL2 (propidium iodide) and FL4 (Annexin-V). Cells in the lower left quadrant (Q1-LL) are viable cells. Cells in the lower right quadrant (Q1-LR) are in an early apoptosis state. Cells in the upper right quadrant (Q1-UR) are in a late apoptosis state.

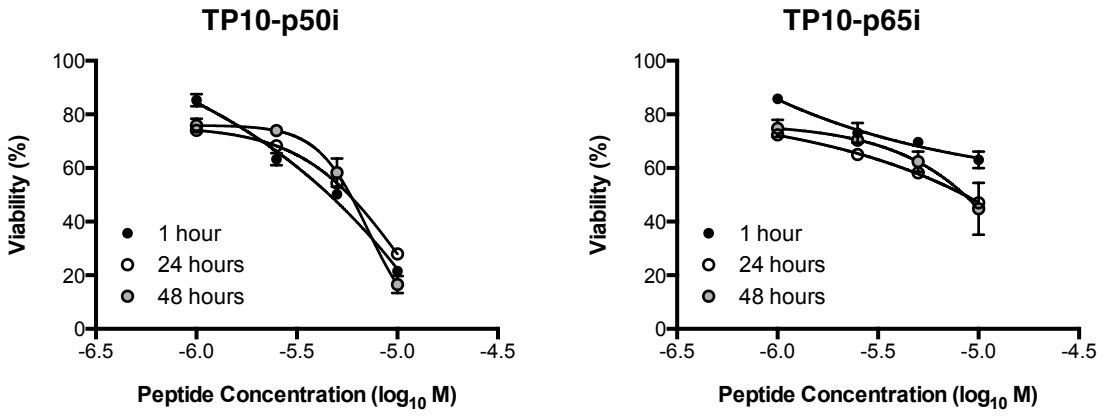

Figure 4.15 - Viability of primary CLL cells incubated with TP10-p50i and TP10- p65i for a period of 1, 24 and 48 hours.
Primary CLL cells were incubated with 0, 1, 2.5, 5, 10, 25 and 50 µM of TP10-p50i and TP10-p65i with an without 5ng/ml of IL-4 for a period of 1, 24 and 48 hours. Viability measured by Annexin-V and PI. Percentage of viable cells corresponds to cells Annexin-V and PI negative. The viability curves were generated using Prism 6 software. Data are presented as the mean (+/- SD) for four patient samples.

Table 4.7 - NF-κB inhibiting CPPs LC_{50} at 1, 24 and 48 hours.

NF-κB inhibiting CPP	1 hour		24 hours		48 hours	
	LC_{50}	95% Confidence Interval	LC_{50}	95% Confidence Interval	LC_{50}	95% Confidence Interval
TP10-p50i	4.59 μM	Und.	5.74 μM	5.32 – 6.30	5.83 μM	5.05 – 8.57
TP10-p65i	> 10 μM	Und.	8.47 μM	Und.	8.51 μM	Und.

Note: The LC_{50} values were interpolated using Prism 6 software from the viability curves shown in Figure 4.15.

4.6. TP10-p50i induced Caspase-3 activation

Apoptosis can be induced by a variety of stimuli (Kurokawa & Kornbluth, 2009). These stimuli activate initiator caspases (caspase-2, -8, -9 and 10) and effector caspases (caspase-3, -6 and -7) that culminate in the packaging of the dying cell and subsequent engulfment by neighbouring cells or professional phagocytes (Kurokawa & Kornbluth, 2009). Measuring the activity of caspases can therefore be used as evidence of apoptosis induction (Martin & Lenardo, 2001; Muppidi et al., 2004; Rodriguez & Schaper, 2005). For the purpose of this project, caspase-3 activity was measured using the PhiPhiLux® G_1D_2 (235430, Calbiochem) substrate that is cleaved by caspase-3 and that emits fluorescence when in the cleaved form. Primary CLL cells were incubated with TP10-p50i and TP10-p65i for 24 hours at the following concentrations: 0, 1, 2.5, 5 and 10 μM. Cells were collected at 1 and 24 hours, washed and incubated for 1 hour with the PhiPhiLux® G_1D_2 substrate at 37˚C. Cells were then analysed by flow cytometry. Figure 4.15 shows the flow cytometry profile of one patient sample incubated with TP10-p50i for one hour. Figure 4.16 shows the caspase-3 activity data for 3 patients incubated with TP10-p50i and TP10-p65i for 1 and 24 hours.

Of the two NF-κB inhibiting CPPs, only TP10-p50i induced caspase-3 activity in the first hour of incubation at 5 and 10 μM. The levels of caspase-3 activity induced were proportional to the dose administrated and they were also maintained after 24 hours of incubation. Primary CLL cells undergo apoptosis when cultured in liquid culture as demonstrated by the increase in caspase-3 activity in untreated samples, concentrations up to 2.5 μM of TP10-p50i and all concentrations of TP10-p65i.

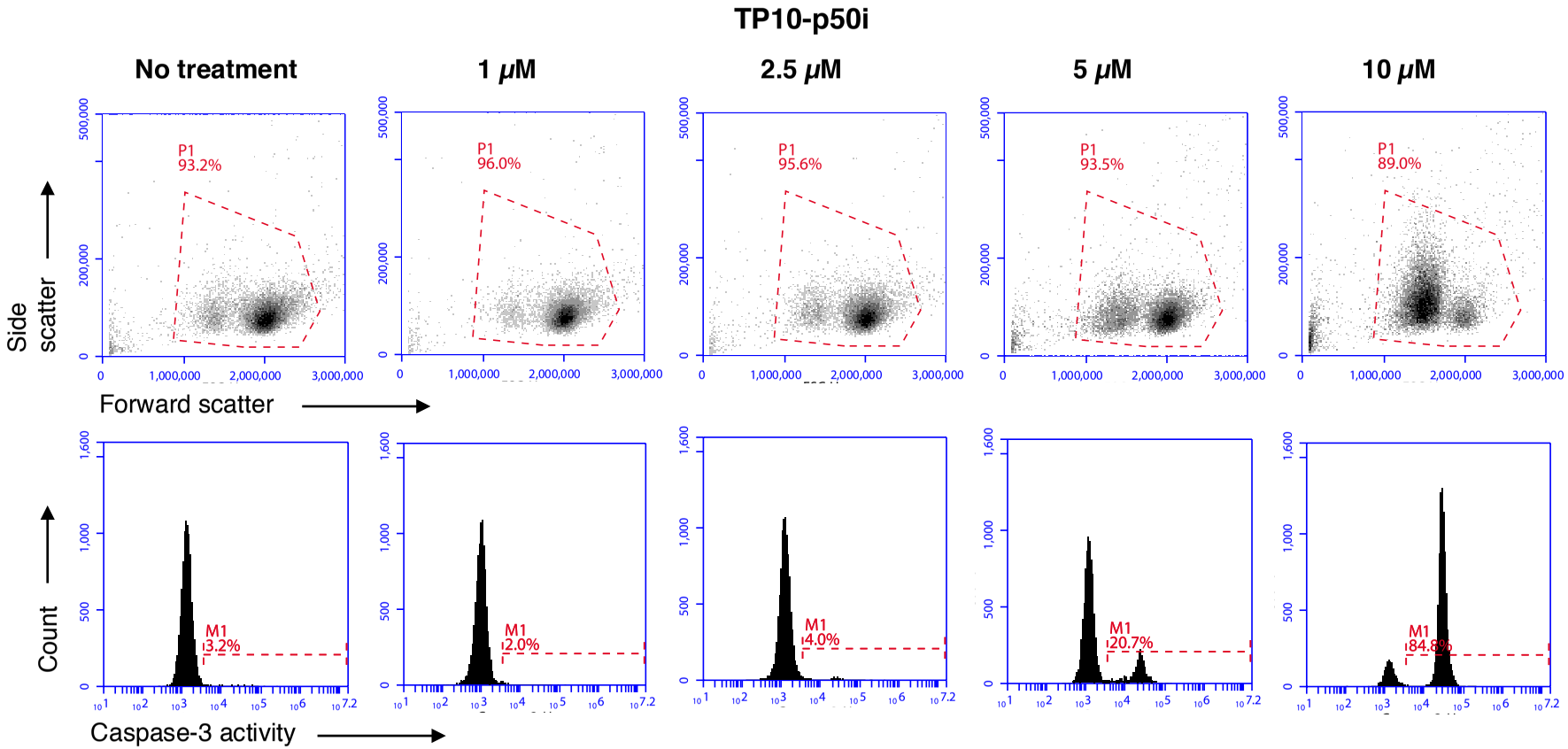

Figure 4.16 – Flow cytometry data of caspase-3 activity of primary CLL cells incubated for 1 hour with TP10-p50i.
Primary CLL cells were incubated with 0,1, 2.5, 5 and 10 μM of FFR8-p50i for a period of 1 hour. Cells were collected and washed with PBS. Cells were incubated with PhiPhiLux G_1D_2 substrate for one hour. The fluorescence of the cleaved substrate was measured by flow cytometry Viable lymphocytes were gated in the forward and side scatter plot within P1. FL1 fluorescence (caspase-3 activity) of cells gated in P1 is plotted in the lower graphs.

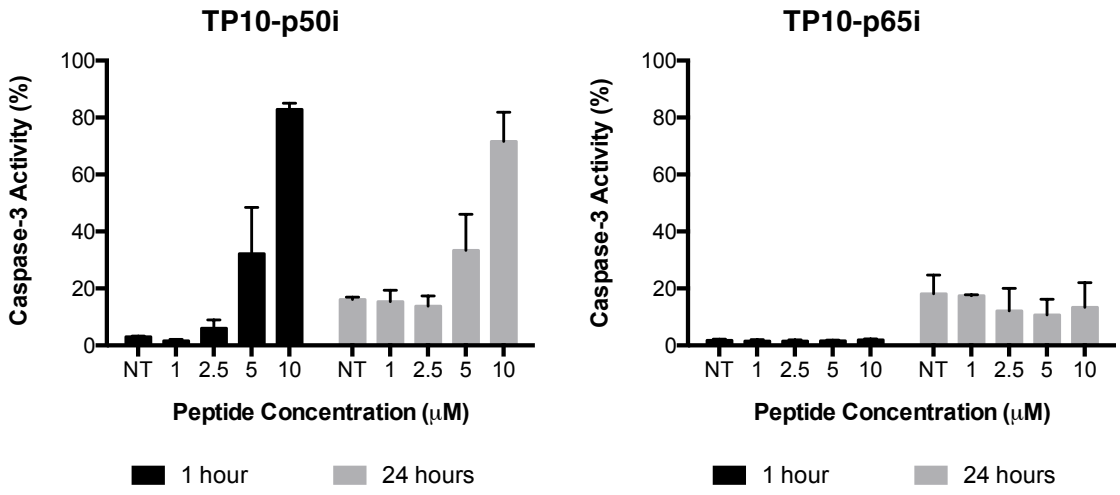

Figure 4.17 – Caspase-3 activity of primary CLL cells incubated with TP10-p50i and TP10-p65i for 1 and 24 hours.

Primary CLL cells were incubated with 0, 1, 2.5, 5 and 10 μM of TP10-p50i and TP10-p65i for a period of 1 and 24 hours. Cells were washed and incubated with the PhiPhiLux G_1D_2 substrate for one hour. The fluorescence of the cleaved substrate was measured by flow cytometry. Data are presented as the mean (+/- SD) for three patient samples.

4.7. TP10 NF-κB inhibitory CPPs were more cytotoxic than commercially available NF-κB inhibitory peptides

To compare the novel TP10 NF-κB inhibiting CPPs to the commercially available peptides, primary CLL cells from the same patient were incubated with a range of doses (0, 1, 2.5, 5, 10, 25 and 50 μM) of the following CPPs:

Table 4.8 - NF-κB inhibiting CPPs sequences used.

CPP	Catalogue Number	Sequences
TP10-p50i		AGYLLGKINLKALAALAKKIL**VQRKRQKLM**
TP10-p65i		AGYLLGKINLKALAALAKKIL**QLRRPSDRELSE**
Imgenex-Ctrl	IMG-2009	DRQIKIWFQNRRMKWKK
Imgenex-p50	IMG-2004	DRQIKIWFQNRRMKWKK**VQRKRQKLM**
Imgenex-p65	IMG-2001	DRQIKIWFQNRRMKWKK**QLRRPSDRELSE**

Note: The highlighted amino acids correspond to the p50/p65 inhibiting sequences.

Cells were incubated for a period of 24 hours and harvested at 1 and 24 hours. Cells were washed and stained with PI and Annexin-V and analysed by flow cytometry. Figure 4.17 shows the flow cytometry profile of one patient's CLL cells incubated with Imgenex-p50 for 1 hour. Figure 4.18 shows the flow cytometry profile of the same patient's CLL cells incubated with TP10-p50i for 1 hour. Figure 4.19 shows the viability data of 3 CLL samples incubated under the same conditions for 1 and 24 hours.

Following one hour of incubation, TP10-p50i and TP10-p65i induced cell death of the samples tested, with LC_{50} of 6.13 μM (4.37 – 7.99) and 14.4 μM (6.39 – 30.61), respectively. The Imgenex CPPs did not alter cell viability following one or 24 hours of incubation at concentrations lower than 50 μM, therefore LC_{50} could not be calculated.

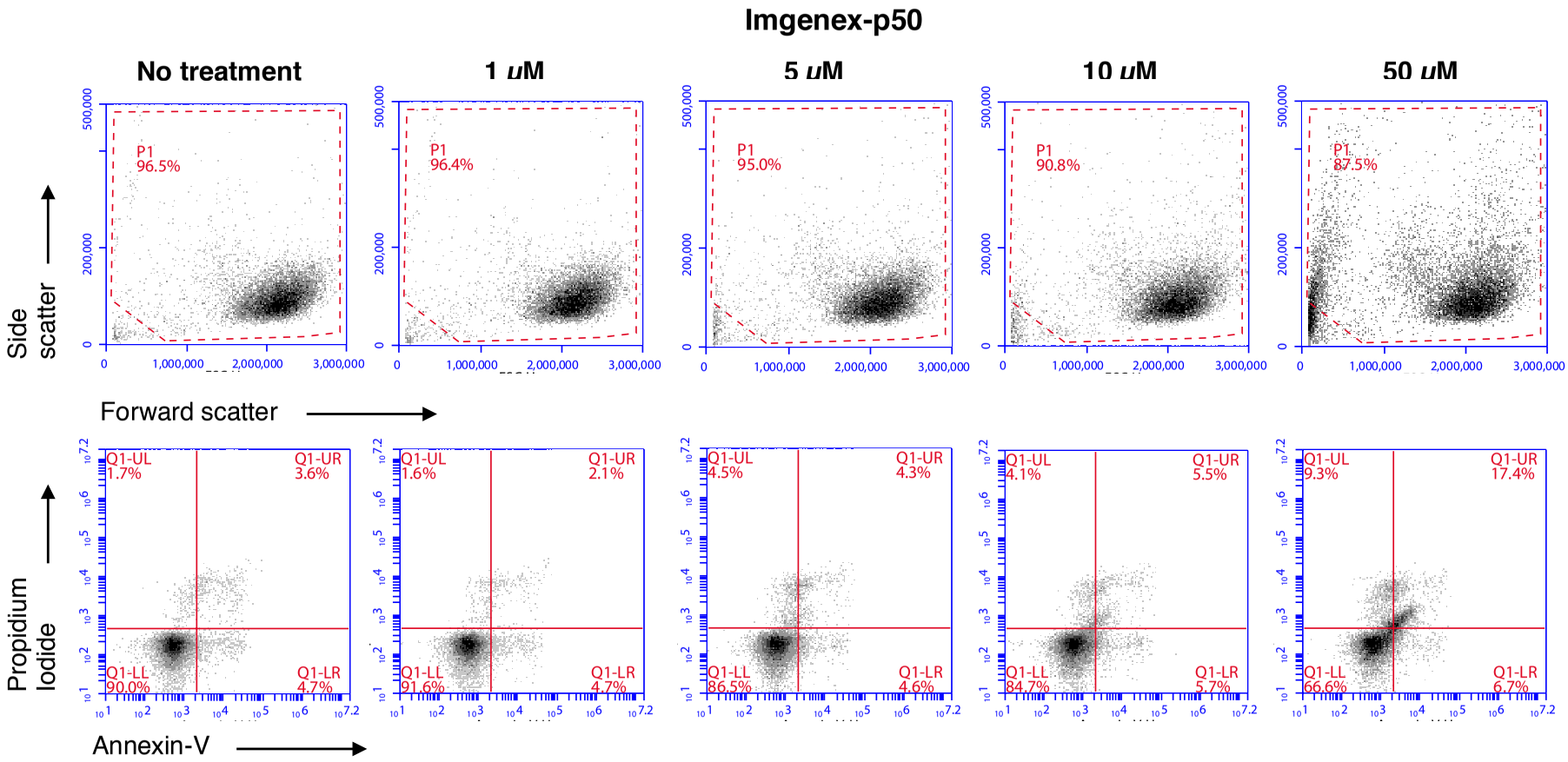

Figure 4.18 – Flow cytometry data of primary CLL cells incubated for 1 hour with Imgenex-p50
Primary CLL cells were incubated with 0,1, 2.5, 5 and 10 μM of Imgenex-p50 for a period of 1 hour. Cells were collected and washed with PBS. Cells were stained for Annexin-V and PI. Viable lymphocytes were gated in the forward and side scatter plot within P1. Cells gated in P1 were plotted according to their fluorescence in FL2 (propidium iodide) and FL4 (Annexin-V). Cells in the lower left quadrant (Q1-LL) are viable cells. Cells in the lower right quadrant (Q1-LR) are in an early apoptosis state. Cells in the upper right quadrant (Q1-UR) are in a late apoptosis state.

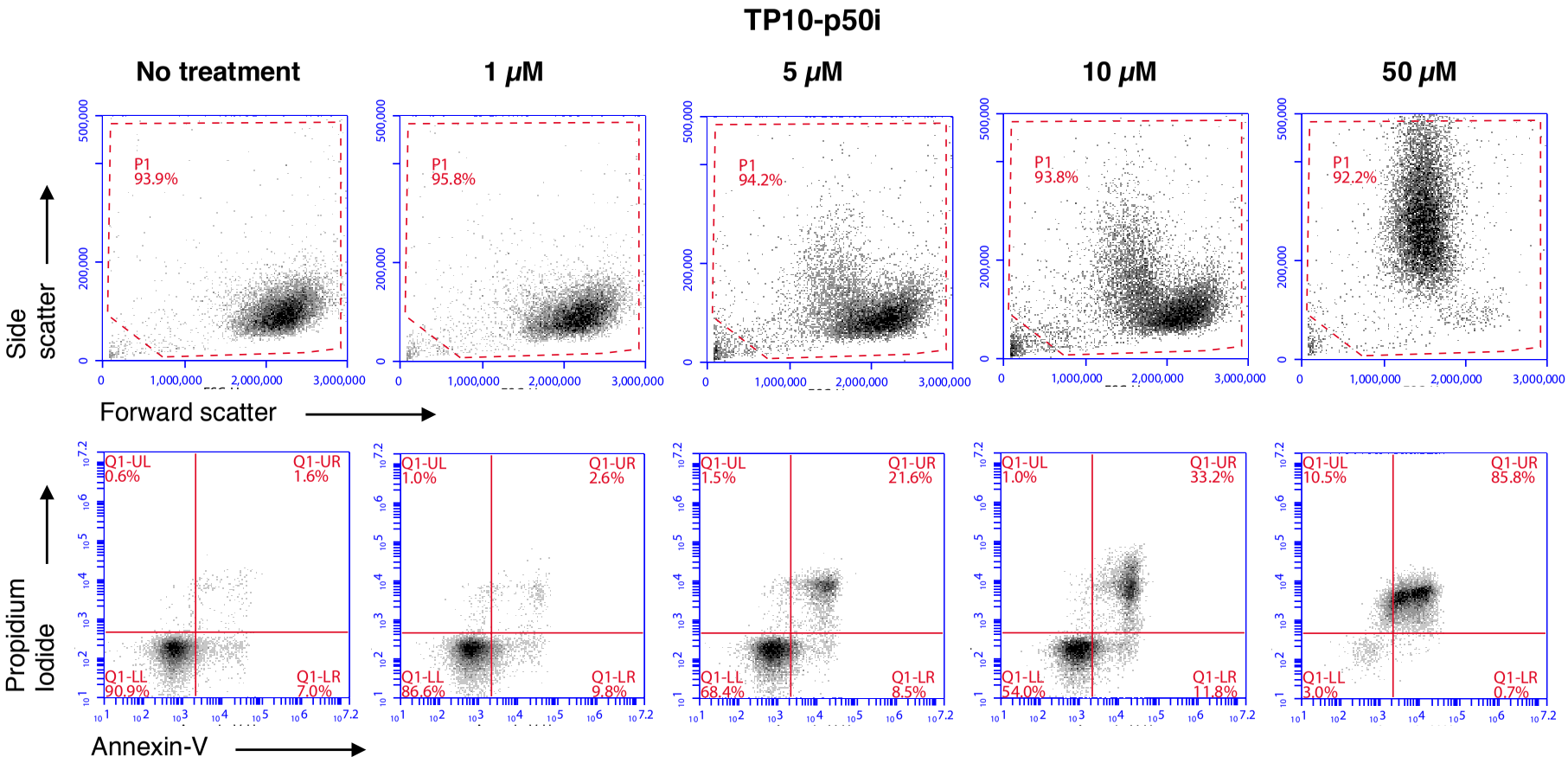

Figure 4.19 – Flow cytometry data of primary CLL cells incubated for 1 hour with TP10-p50i.
Primary CLL cells were incubated with 0,1, 2.5, 5 and 10 μM of TP10-p50i for a period of 1 hour. Cells were collected and washed with PBS. Cells were stained for Annexin-V and PI. Viable lymphocytes were gated in the forward and side scatter plot within P1. Cells gated in P1 were plotted according to their fluorescence in FL2 (propidium iodide) and FL4 (Annexin-V). Cells in the lower left quadrant (Q1-LL) are viable cells. Cells in the lower right quadrant (Q1-LR) are in an early apoptosis state. Cells in the upper right quadrant (Q1-UR) are in a late apoptosis state.

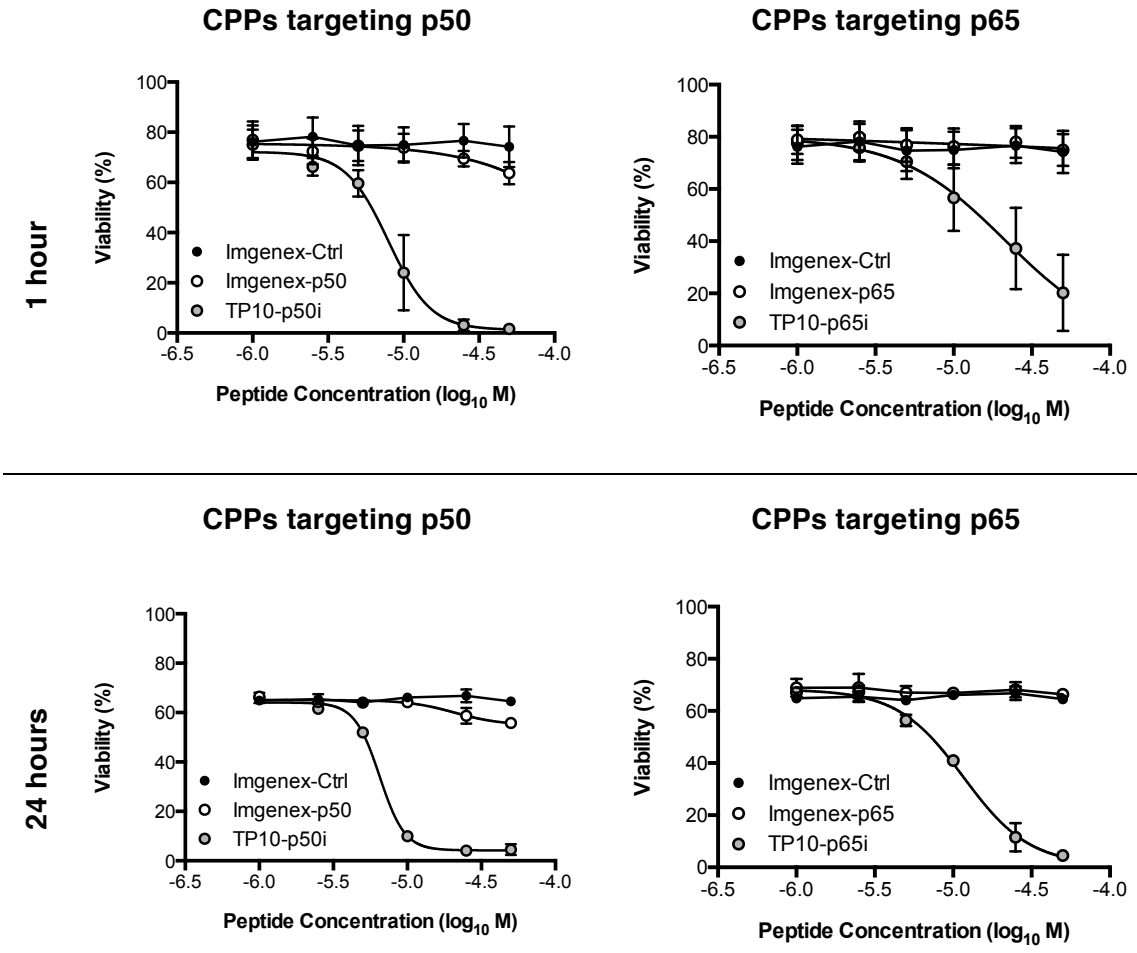

Figure 4.20 - Viability of primary CLL cells incubated with Imgenex-Ctrl, Imgenex-p50, Imgenex-p65, TP10-p50i and TP10- p65i for a period of 1 and 24 hours.
Primary CLL cells were incubated with 0, 1, 2.5, 5 and 10 μM of Imgenex-Ctrl, Imgenex-p50, Imgenex-p65, TP10-p50i and TP10- p65i for a period of 1 and 24 hours. Viability measured by Annexin-V and PI. Percentage of viable cells corresponds to cells Annexin-V and PI negative. The viability curves were generated using Prism 6 software. Data are presented as the mean (+/- SD) for three patient samples.

Table 4.9 - NF-κB inhibiting CPPs LC_{50}.

NF-κB inhibiting CPP	1 hour		24 hours	
	LC_{50}	95% Confidence Interval	LC_{50}	95% Confidence Interval
Imgenex-Ctrl	> 50 μM	Und.	> 50 μM	Und.
Imgenex-p50	> 50 μM	Und.	> 50 μM	Und.
Imgenex-p65	> 50 μM	Und.	> 50 μM	Und.
TP10-p50i	6.13 μM	4.37 – 7.99	5.16 μM	4.81 – 5.55
TP10-p65i	14.4 μM	6.39 – 30.61	7.20 μM	5.97 – 8.47

Note: The LC_{50} values were interpolated using the Prism 6 software from the viability curves shown in Figure 4.19.

4.8. TP10 NF-κB inhibitory CPPs induced cell death in normal B- and T-cells

To assess the effects of the TP10 NF-κB inhibitory CPPs, PBMCs from healthy donors were obtained and cultured with 0, 1, 2.5, 5, 10, 25 and 50 μM of TP10-p50i and TP10-p65i for a period of 1 hour. Cells were harvested and labelled with anti-CD3 to identify T-cells, anti-CD19 to identify B-cells and PI to identify apoptotic cells. The analysis was performed by flow cytometry. Figure 4.20 and 4.21 show the flow cytometry data of one sample cultured with TP10-p50i for one hour. Following the analysis of the flow cytometry data it was clear that measuring viability of B- and T-cells separately was not possible using this strategy, as apoptotic cells did not stain for either CD19 or CD3. A second attempt of determining the percentage of viable lymphocytes gated in the forward and side scatter also proved not ideal as it did not take into account the absolute number of cells present in the gate. Therefore, the strategy chosen to present the data in Figure 4.22 was to show the number of cells within the viable lymphocytes gate (P3) shown in Figure 4.21. Figure 4.22 shows that TP10-p50i induced a decrease in the total numbers from the concentration of 1 μM. This increase was gradual up to 10 μM, where a sudden drop in numbers was observed. These continued to decrease till they reached 0 at 50 μM. TP10-p65i had a similar effect as TP10-p50i with the difference being that the gradual decrease starts at 2.5 μM and goes down with concentrations up to 25 μM, point at which the numbers drop suddenly and reach 0 at 50 μM. This data shows that both TP10-p50i and TP10-p65i do not have specificity for a type of cell; they affected CLL cells, B-cells and T-cells .

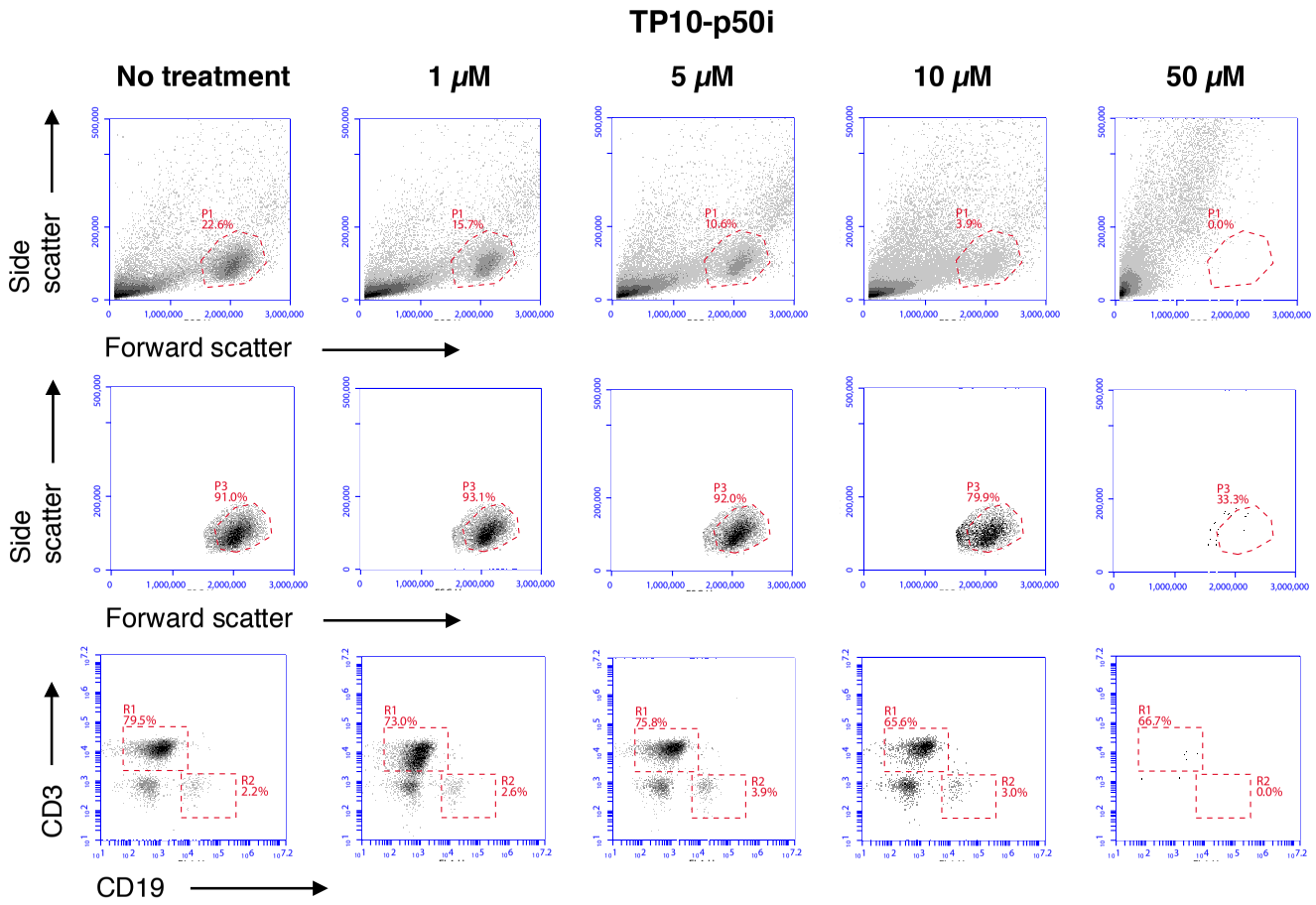

Figure 4.21 - Flow cytometry data of primary PBMCs from healthy donor incubated for 1 hour with TP10-p50i.
PBMCs were incubated with 0,1, 2.5, 5 and 10 μM of TP10-p50i for a period of 1 hour. Cells were collected and washed with PBS. Cells were stained with anti-CD19, anti-CD3 and Annexin-V FITC. Viable lymphocytes were gated in the forward and side scatter plot within P1. Cells gated in P1 were plotted again and viable lymphocytes were gated in P3. Fluorescence in FL3 (CD3) and FL4 (CD19) was plotted and T-cells gated in R1 and B-cells gated in R2. Fluorescence in FL1 (Annexin-V FITC) was measured and the histograms can be found in Figure 4.21. Data from one sample (healthy donor).

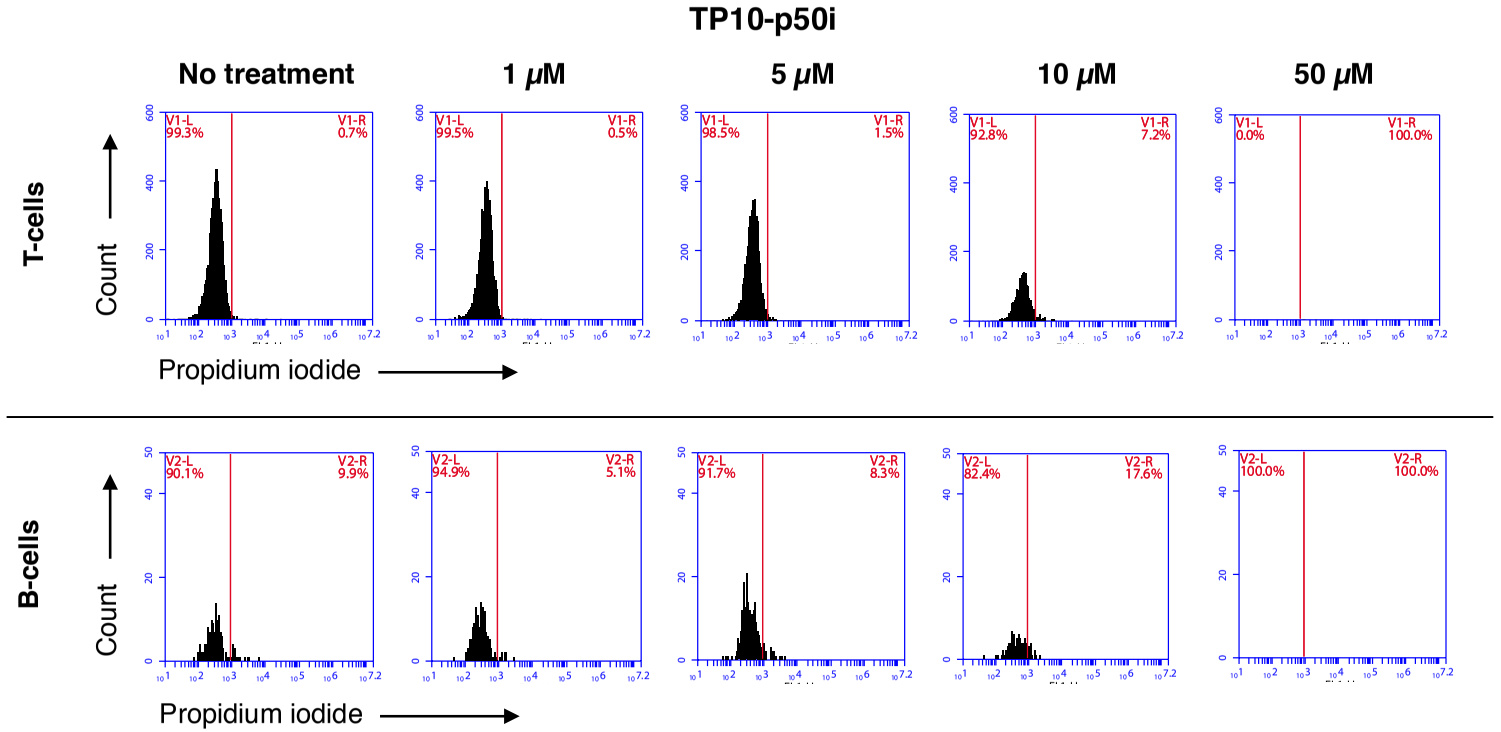

Figure 4.22 - Flow cytometry data of primary PBMCs from healthy donor incubated for 1 hour with TP10-p50i.
PBMCs were incubated with 0,1, 2.5, 5 and 10 μM of TP10-p50i for a period of 1 hour. Cells were collected and washed with PBS. Cells were stained with anti-CD19, anti-CD3 and Annexin-V FITC. Viable lymphocytes were gated in the forward and side scatter plot within P1 (data can be found in Figure 4.20). Cells gated in P1 were plotted again and viable lymphocytes were gated in P3 (data can be found in Figure 4.20). Fluorescence in FL3 (CD3) and FL4 (CD19) was plotted and T-cells gated in R1 and B-cells gated in R2 (data can be found in Figure 4.20). Fluorescence in FL1 (Annexin-V FITC) was measured in R1 (T-cells) and R2 (B-cells). Data from one sample (healthy donor).

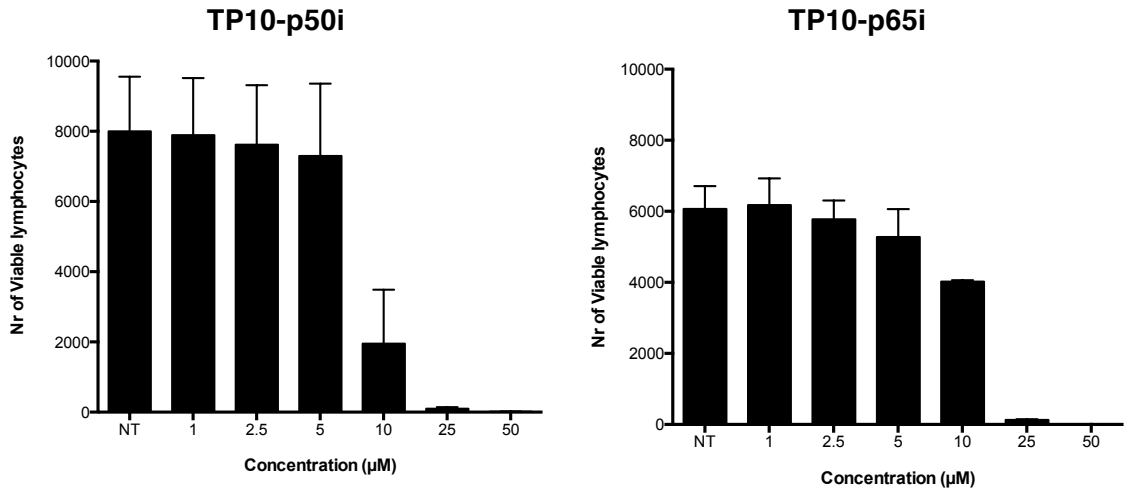

Figure 4.23 – Number of viable normal lymphocytes following 1 hour of incubation with TP10-p50i and TP10-p65i.
Primary PBMCs from healthy donors were incubated with 0, 1, 2.5, 5 and 10 µM of TP10-p50i and TP10-p65i for a period of 1 hour. Cells were stained with anti-CD3, anti-CD19 and Annexin-V FITC. The number of viable lymphocytes within gate P3 from Figure 4.20 were plotted and presented here. Data are presented as the mean (+/- SD) for two samples.

4.9. Jurkat cells were more sensitive than CLL cells to TP10-p50i and TP10-p65i

To assess the effect of the NF-κB inhibiting CPPs in other cell types, Jurkat cells (i.e. a leukaemic T-cell line) were incubated with a range of concentrations (0,1, 2.5, 5, 10, 25 and 50 μM) of TP10-p50i and TP10-p65i for a period of 24 hours. Cells were harvested at 1 and 24 hours, washed and labelled with Annexin-V and PI. The cells were then analysed by flow cytometry. Figure 4.20 shows the flow cytometry profile of Jurkat cells incubated with TP10-p50i for 1 hour. Figure 4.21 shows the flow cytometry profile of primary CLL cells incubated with TP10-p50i. Figure 4.22 shows the data from 3 primary CLL patient cells and 3 Jurkat cell replicates.

Following one hour of incubation, Jurkat cells were more sensitive to both TP10-p50i and TP10-p65i, as the LC_{50} were lower for Jurkat cells than CLL cells (See Table 4.9). However, only LC50 of TP10-p50i were significantly different between CLL and Jurkat cells ($p<0.05$). As with CLL cells, the LC_{50} for TP10-p50i was lower than the LC_{50} of TP10-p65i. Following 24 hours of incubation, the LC_{50} doses were higher in Jurkat cells for both TP10-p50i and TP10-p65i and lower for CLL cells. Regarding the flow cytometry profile, there were two distinct populations of Jurkat cells. One presented the characteristic lymphocyte profile (i.e. high forward scatter and low side scatter) and the other population presented the characteristic apoptotic profile (i.e. low forward scatter and high side scatter). Of all the events recorded within P1, 21% were Annexin-V and PI positive, in concordance with the apoptotic population found in the forward and side scatter. As the concentrations increase, so does the percentage of Annexin-V and PI positive cells.

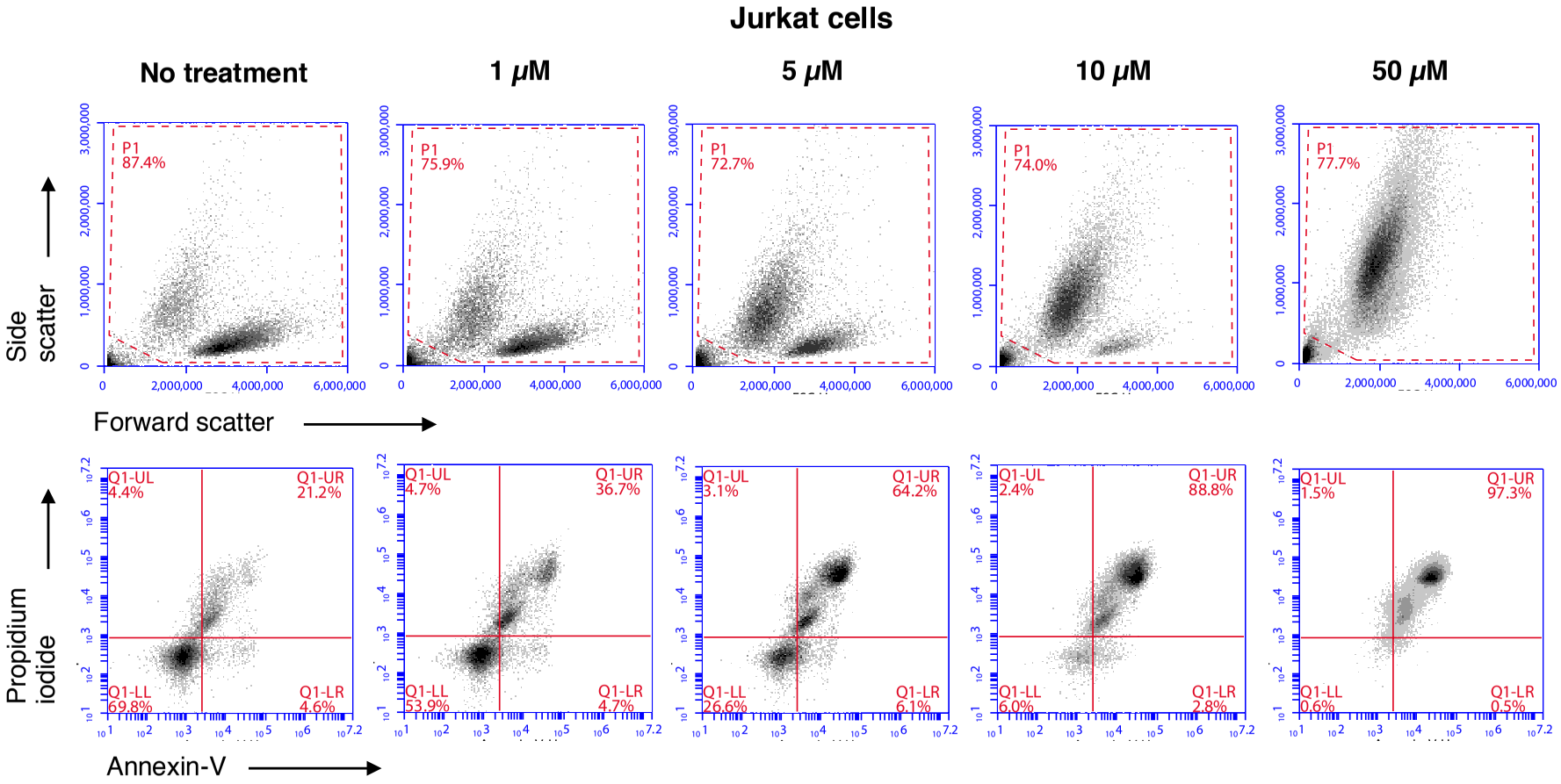

Figure 4.24 – Representative flow cytometry data of Jurkat cells incubated for 1 hour with TP10-p50i.
Jurkat cells were incubated with 0,1, 2.5, 5 and 10 μM of TP10-p50i for a period of 1 hour. Cells were collected and washed with PBS. Cells were stained for Annexin-V and PI. Viable lymphocytes were gated in the forward and side scatter plot within P1. Cells gated in P1 were plotted according to their fluorescence in FL2 (propidium iodide) and FL4 (Annexin-V). Cells in the lower left quadrant (Q1-LL) are viable cells. Cells in the lower right quadrant (Q1-LR) are in an early apoptosis state. Cells in the upper right quadrant (Q1-UR) are in a late apoptosis state.

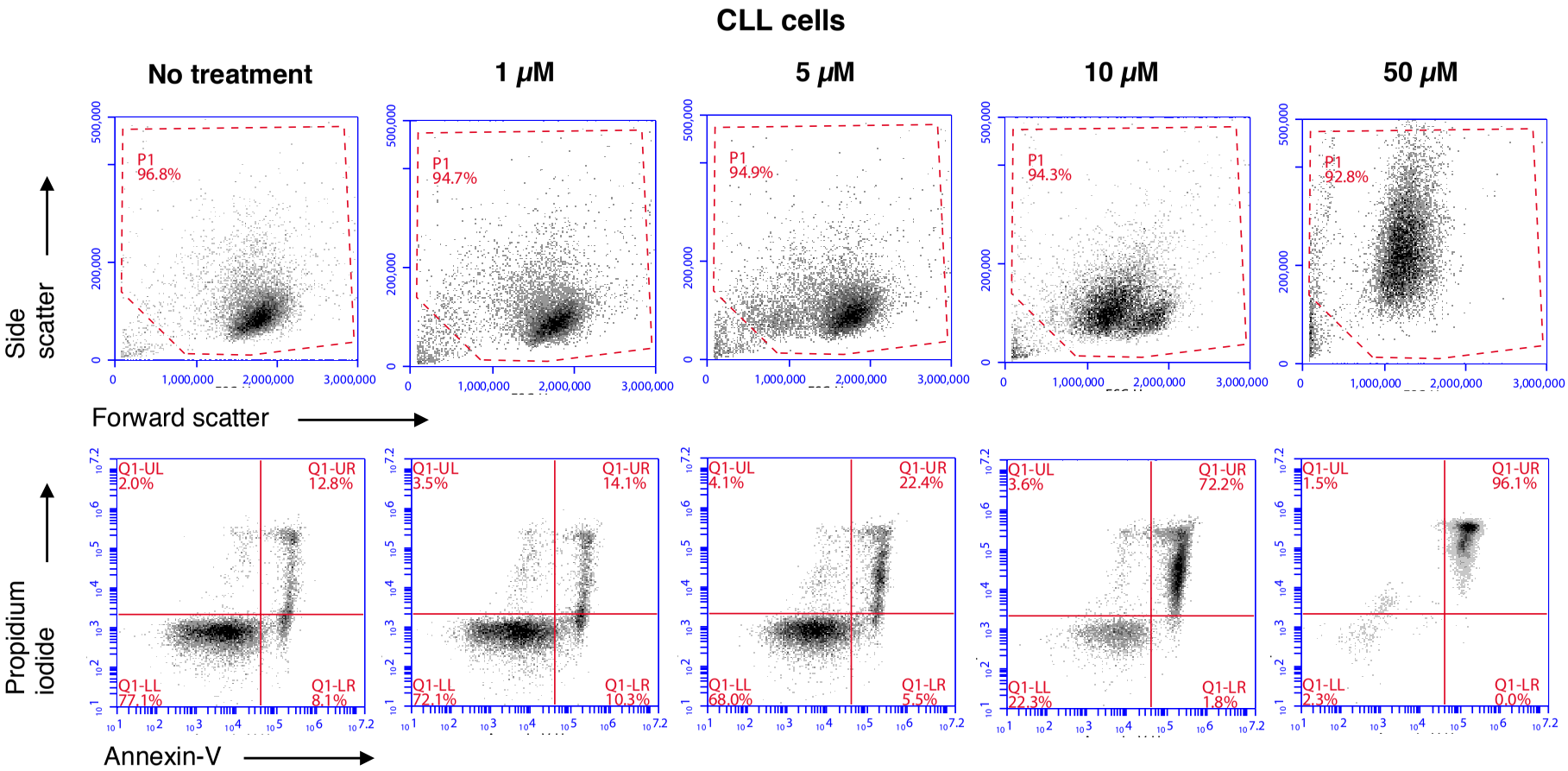

Figure 4.25 – Flow cytometry data of primary CLL cells incubated for 1 hour with TP10-p50.
Primary CLL cells were incubated with 0,1, 2.5, 5 and 10 μM of TP10-p50i for a period of 1 hour. Cells were collected and washed with PBS. Cells were stained for Annexin-V and PI. Viable lymphocytes were gated in the forward and side scatter plot within P1. Cells gated in P1 were plotted according to their fluorescence in FL2 (propidium iodide) and FL4 (Annexin-V). Cells in the lower left quadrant (Q1-LL) are viable cells. Cells in the lower right quadrant (Q1-LR) are in an early apoptosis state. Cells in the upper right quadrant (Q1-UR) are in a late apoptosis state.

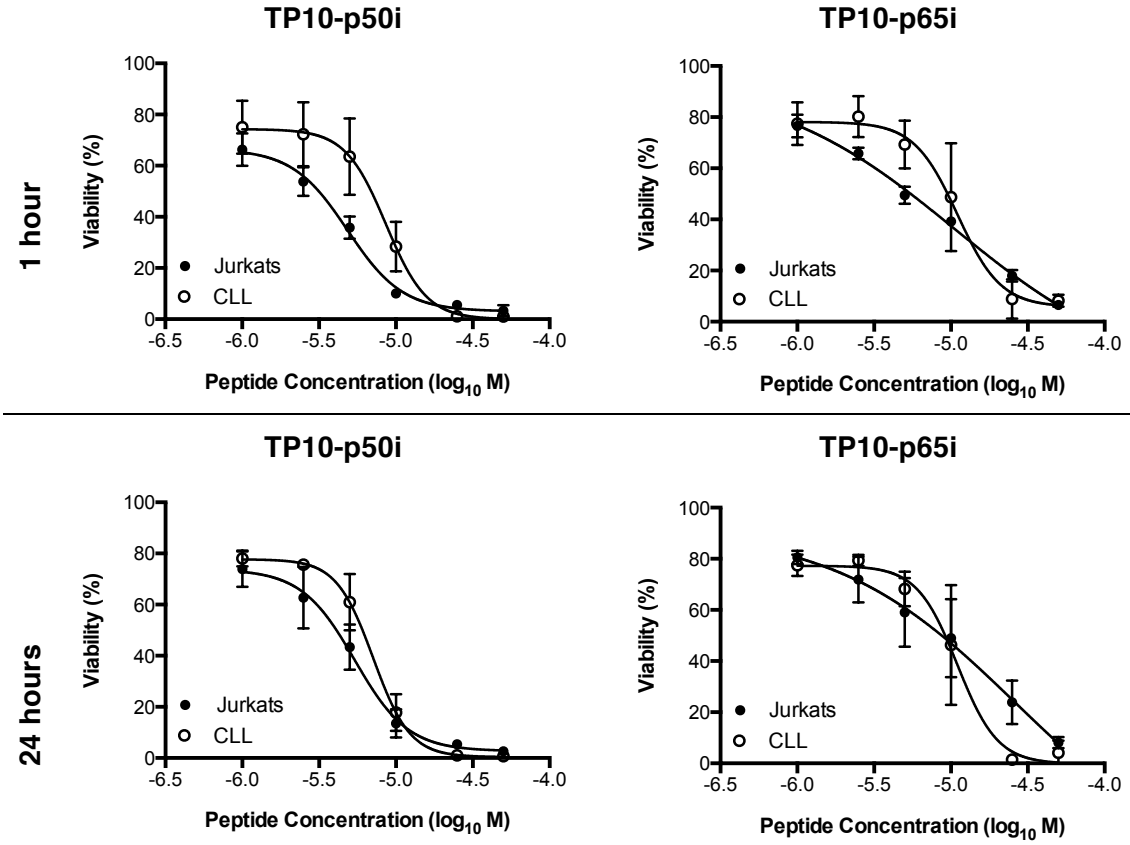

Figure 4.26 - Viability of primary CLL cells and Jurkat cells incubated with TP10-p50i and TP10-p65i for a period of 1 and 24 hours.
Primary CLL cells were incubated with 0, 1, 2.5, 5, 10, 25 and 50 µM of TP10-p50i and TP10- p65i for a period of 1 and 24 hours. Viability measured by Annexin-V and PI. Percentage of viable cells corresponds to cells Annexin-V and PI negative. The viability curves were generated using Prism 6 software. Data are the mean (+/- SD) for three individual CLL patients. Apoptosis in the Jurkat cells was measured in triplicate.

Table 4.10 - NF-κB inhibiting CPPs LC_{50} in Jurkat and CLL cells.

Cell type	NF-κB inhibiting CPP	1 hour		24 hours	
		LC_{50} (μM)	95% Confidence Interval	LC_{50} (μM)	95% Confidence Interval
Jurkat	TP10-p50i TP10-p65i	3.15 5.47	1.08 – 4.36 3.72 – 7.55	4.10 8.70	3.31 – 4.87 5.91 – 12.70
CLL	TP10-p50i TP10-p65i	6.91 9.50	6.15 – 7.60 6.56 – 14.48	6.05 9.16	5.43 – 6.71 6.83 – 11.96

Note: The LC_{50} values were interpolated using Prism 6 software from the viability curves shown in Figure 4.22.

4.10. Discussion & Conclusion

In the previous chapter TP10 and FFR8 were selected to be the delivery vehicles of two NF-κB inhibiting cargos. The aim of this chapter was to determine if the four novel NF-κB inhibiting CPPs were capable of inducing cell death. In all the samples tested, only two of the four CPPs were capable of inducing cell death at doses lower than 50 μM; TP10-p50i and TP10-p65i. The LC_{50} for TP10-p50i was 5.28 μM (4.03 – 6.50) at 24 hours, making it the CPP with the lowest LC_{50}, and TP10-p65i had a LC_{50} of 9.95 μM (7.44 – 13.45) at 24 hours. The LC_{50} values for FFR8-p50i and FFR8-p65i were greater than 50 μM.

Both TP10-p50i and TP10-p65i were capable of inducing cell toxicity under 1 hour. However, the cytotoxic effects did not increase following 24 or 48 hours of incubation indicating a rapid mechanism of action. Of the NF-κB inhibitors previously reported in the CLL literature only two target translocation into the nucleus, DHMEQ (Horie et al., 2006) and IMG-2004 (Hewamana et al., 2008b). Studies with CLL cells showed that the cytotoxic effects of these two inhibitors were induced in the first 24 hours of incubation (Hewamana et al., 2008b; Horie et al., 2006), indicating that TP10-p50i and TP10-p65i act faster than DHMEQ and IMG-2004.

In the previous chapter the flow cytometry and confocal microscopy data showed the superior penetrating capabilities of FFR8 compared to all other CPPs tested. However, in this chapter, despite carrying the same cargo, FFR8 peptides were incapable of affecting CLL viability, while both TP10 peptides presented LC_{50} values less than 10 μM. In an attempt to determine if the cause of cell toxicity exhibited by the TP10 peptides was due to the CPPs and not the cargo (i.e. the only difference between the TP10 and FFR8 NF-κB inhibiting CPPs), FFR8-Alexa488 and TP10-Alexa488 were incubated under the same conditions as the four novel CPPs. Unexpectedly, FFR8-Alexa488 caused more cell toxicity than FFR8-p50i and FFR8-p65i, while TP10-Alexa488 did not cause cell toxicity of CLL cells at doses lower than 50μM. As previously mentioned, the fluorescent tag can alter dramatically either positively or negatively the penetrating abilities of CPPs (Jones & Sayers, 2012). What was initially an attempt to determine if the delivery vehicle was causing cell toxicity became an interesting observation on the effects a cargo can have on cell viability and how complex the appropriate choice of control can become. In a way, TP10-Alexa488, FFR8-p50i and FFR8-p65i proved to be good negative controls for the TP10 peptides as they showed that TP10 with a fluorescent tag does not cause cell toxicity and that

the p50 and p65 inhibiting sequences when attached to another CPP also did not cause cell toxicity. This indicates that the toxicity induced by TP10-p50i and TP10-p65i is caused by the combination of TP10 and the inhibiting sequences.

CLL cell survival *in vivo* has been shown to be dependant on stimuli from the microenvironment (Caligaris-Cappio, 2003; Ramsay & Rodriguez-Justo, 2013). IL-4 is one of the reported stimuli that confers protection to CLL cells *in vitro* (Banchereau & Rousset, 1991; Banchereau et al., 1991; Thieu et al., 2007). In order to determine if the cytotoxic effects produced by TP10-p50i and TP10-p65i would be inhibited by IL-4, this cytokine was added to cultures. Although IL-4 was capable of increasing the number of viable cells in the untreated samples even at concentrations lower than 2.5 μM, it did not effectively abrogate the cytotoxic effects of TP10-p50i and TP10-p65i. Hewamana et al. (2008b) showed a similar effect, where IL-4 did not protect primary CLL cells from the cytotoxic effect of LC-1, an IKK inhibitor. This data indicates that NF-κB inhibition can potentially overcome the *in vivo* pro-survival signals induced by IL-4 and possibly other molecules.

In order to determine if the cytotoxic effects of TP10-p50i and TP10-p65i measured by Annexin-V and PI staining were indeed a result of apoptosis induction, caspase-3 activity was measured using a fluorescence producing substrate. Unexpectedly, only TP10-p50i induced activation of caspase-3 at 1 and 24 hours. Studies on caspase-3 activation by SN50 (a CPP linked to the same p50 inhibiting sequence as TP10-p50i) show contrasting results. Kolenko and colleagues measured caspase-3 activity in primary T-cells, following incubation with SN50 for 6 and 24 hours, using fluorometric tetrapetide substrates and detected no activity (Kolenko et al., 1999). Poulaki and colleagues measured caspase-3 activity in Y79 and WERI-Rb1 cells (two retinoblastoma cell lines), following incubation with SN50 for 8 and 16 hours, using the PhiPhiLux substrate and also detected no caspase-3 activity (Poulaki et al., 2002). Mitsiades and colleagues measured caspase-3 activity in MM.1S cells (multiple myeloma cell line), following incubation with SN50 for 4, 8 and 16 hours, performing immunoblot analysis of caspase-3 cleaved products and detected caspase-3 activity (Mitsiades et al., 2002). It is difficult to ascertain the cause of the conflicting results in the studies presented and those observed between TP10-p50i and TP10-p65. Although the inhibiting sequences are different the putative mechanism of action is similar and the presumed result is the same i.e. inhibition of NF-κB nuclear translocation that culminating in the induction of apoptosis. Perhaps TP10-p65i is not

truly inhibiting NF-κB nuclear translocation and/or cell death is caused by the other means that do not require caspase-3 activation.

Comparison studies using the Imgenex peptide and the two novel TP10 CPPs, demonstrated the ability of TP10-p50i and TP10-p65i to induce cell death at doses lower than 10 μM. The commercially available peptides Imgenex-p50 (IMG-2004, Imgenex) and Imgenex-p65 (IMG-2001, Imgenex) have demonstrated to inhibit translocation of NF-κB subunits p50 and p65 in a variety of cell types (Poylin et al., 2008; Takada et al., 2004; Zou & Crews, 2005), including primary CLL cells (Buggins et al., 2010; Hewamana et al., 2008b). The doses required to achieve NF-κB inhibition or cell death vary between 50 μM and 100 μM (Buggins et al., 2010; Hewamana et al., 2008b; Poylin et al., 2008; Takada et al., 2004; Zou & Crews, 2005). Considering that both TP10 peptides and the Imgenex peptides possess the same inhibiting sequences, the reduction in LC_{50} can be attributed to the combination of TP10 and p50i or p65i. These novel CPPs represent a potential new tool to target NF-κB as they induced cytotoxicity at significantly lower concentrations than the commercially available NF-κB inhibitory peptides.

TP10 peptides have been shown to penetrate a wide range of cell types, with or without cargo, which shows their lack of specificity. However, CPPs tend to behave differently with different cell types (Fretz et al., 2007). To assess the effects of the TP10 NF-κB inhibiting peptides in T-cells, Jurkat cells were used. The LC_{50} of the peptides with Jurkat cells revealed an increased sensitivity to TP10-p50i and TP10-p65i. The causes for this increased sensitivity were not tested in this study, however it is possible that these differences were due to the different collection of membrane lipids, proteins and carbohydrates found on these cell types (Fretz et al., 2007).

In summary, out of the four novel NF-κB inhibiting CPPs, TP10-p50i and TP10-p65i were capable of inducing apoptosis in primary CLL cells at doses lower than 10 μM under 1 hour. The LC_{50} of the TP10 peptides was 10 times lower than the LC_{50} of commercially available peptides that carry the same inhibiting sequence. The cytotoxic effects induced by the TP10 peptides were not abolished by the cytoprotective cytokine IL-4, and at least one of the peptides was capable of inducing caspase-3 activity. The cytotoxic effects of the peptides were not exclusive to primary CLL cells, in fact they induced cell death in Jurkat cells at doses lower than in CLL cells. The next step of this study was to investigate if the mechanism by which the peptides induced apoptosis was a result of NF-κB nuclear translocation inhibition.

Chapter 5 - Characterising the effects of TP10-p50i and TP10-p65i on NF-κB expression in primary CLL cells

5.1. Introduction

In the previous chapter, four novel NF-κB inhibiting CPPs were developed and their cytotoxic effects were studied in primary CLL cells. The CPPs carried amino acid sequences that mimicked the NLS of p50 or a phosphorylation sites of p65; sequences required for the translocation of these subunits into the nucleus. The hypothesis was that the inhibitory sequences function as decoys for the nuclear translocation of p50 and p65; as such they should target the *de novo* translocation of NF-κB subunits and may not inhibit NF-κB that is already in the nucleus. NF-κB is a transcription factor known to regulate a variety of genes involved in apoptosis, survival, cell proliferation and immune and inflammatory responses (Hayden & Ghosh, 2008). NF-κB has been shown to be constitutively active in CLL and therefore represents a very attractive target (Furman et al., 2000; Hewamana et al., 2008a). Furthermore, the *in vitro* use of NF-κB inhibitors resulted in CLL cell apoptosis validating the importance of this pathway in CLL survival (Hewamana et al., 2009; Lopez-Guerra & Colomer, 2010). Of the four novel CPPs evaluated in the previous chapter, only TP10-p50i and TP10-p65i were capable of inducing cell toxicity. Therefore the aim of this chapter was to investigate whether this cytotoxicity was associated with the inhibition of NF-κB in primary CLL cells.

Previous studies using identical NF-κB inhibiting sequences (but not tagged to the current CPPs) showed a significant reduction in the amount of NF-κB subunits found in the nucleus following stimulation (Lin et al., 1995; Takada et al., 2004). Lin et al. (1995), induced NF-κB activation with LPS in endothelial LE-II cells, and showed that SN50 (a different CPP attached to the same p50 inhibiting sequence used in this study) could partially inhibit the translocation of NF-κB into the nucleus. Takada et al. (2004) stimulated NF-κB activation using TNF and showed that the same p65 inhibitory peptide decreased NF-κB DNA binding in KBM-5 chronic myelogenous leukaemia cells.

To study the effects of TP10-p50i and TP10-p65i, three aspects of the NF-κB pathway were assessed: translocation of the subunits into the nucleus, which was assessed by

SDS-PAGE and western blotting; NF-κB DNA binding activity, assessed by EMSA; and the expression of proteins regulated by NF-κB, assessed by flow cytometric quantification in CLL cells.

The constitutive NF-κB activation observed in CLL seems to be closely linked to the interaction of CLL cells with their *in vivo* microenvironment (Lopez-Guerra & Colomer, 2010). Several mechanisms have been reported to induce NF-κB activation in CLL cells, including interaction with stromal cells (Edelmann et al., 2008), activation of the tumour necrosis factor receptor (TNFR) family members (Endo et al., 2007; Munzert et al., 2002), activation of the cell surface receptor CD40 by its ligand CD154 (Furman et al., 2000), activation of the BCR (Caligaris-Cappio et al., 2009) and activation of TLRs (Arvaniti et al., 2011; Caligaris-Cappio et al., 2009). In this chapter, two NF-κB activation mechanisms were employed: incubation with CD40L-expressing fibroblasts and incubation with CpG ODN2006 oligonucleotides. Co-culture of CLL cells with CD40L-expressing fibroblasts mimics the interactions of CLL cells with activated T-cells in the bone marrow and neoplastic follicles (Kaileh & Sen, 2012; Lopez-Guerra & Colomer, 2010). CpG ODN2006 oligonucleotides, are short single-stranded unmethylated DNA molecules designed to mimic pathogenic DNA, which are recognised by TLR9, which is highly expressed in CLL cells (Caligaris-Cappio et al., 2009; Rozková et al., 2010). CpGs enter B-cells by endocytosis and activate TLR9 located in the cytoplasm (Efremov et al., 2013). Both CD40/CD40L interaction and TLR9 activation culminate in the induction of the NF-κB canonical pathway (Furman et al., 2000; Kaileh & Sen, 2012; Ozato et al., 2002).

In addition to measuring nuclear NF-κB binding, the effect of the NF-κB inhibiting CPPs was also assessed by measuring the surface expression of four cellular activation markers. The activation markers were CD38, CD69, CD49d and CD25; all of which have been shown to be transcriptionally regulated by NF-κB (Ballard et al., 1988; Buggins et al., 2010; Fu et al., 2013; Hideshima et al., 2001; Kang et al., 2006; Lopez-Cabrera et al., 1995; Tirumurugaan et al., 2008). CD38 is a cell surface enzyme/receptor found on a variety of cells, including CLL cells (Deaglio et al., 2008). It has been linked to CLL pathogenesis and its expression is associated with the aggressive form of the disease (Deaglio et al., 2008). CD69 is a type II integral membrane protein, that is overexpressed in CLL cells (Del Poeta et al., 2012a). It is an activation marker that is rapidly expressed upon cell stimulation and it has been shown to have prognostic value in CLL (Del Poeta et al., 2012a). CD49d is variably expressed in CLL and it has been shown to act as an adhesion structure for extracellular matrix

components or to mediate cell to cell interactions by binding to fibronectin or VCAM-1 (Gattei et al., 2008). It has been shown to be an independent predictor of OS in CLL (Bulian et al., 2014; Gattei et al., 2008; Shanafelt et al., 2008). CD25 is the alpha chain of the IL-2 receptor and it is a classical activation marker (Chiorazzi et al., 2002; Fu et al., 2013). It is variably expressed in CLL patients and it has been shown to hold a prognostic value in CLL, although this is still controversial (Shvidel et al., 2012; Sulda et al., 2012).

5.2. Effects of TP10-p50i and TP10-p65i on the translocation of NF-κB into the nucleus

5.2.1. Assessment of NF-κB in the nuclear and cytosolic fractions of untreated primary CLL cells

To assess the levels of NF-κB in the different compartments of untreated *ex vivo* primary CLL cells, nuclear and cytosolic fractions were prepared as previously described (Section 2.6.1). The fractions were analysed by SDS-PAGE, followed by western blot analysis using antibodies against p105/p50, p65 and HSP90. Figure 5.1 shows the levels of the different proteins in eight CLL patient samples. To permit some analysis of patient-to-patient variation, densitometry was used to assess the intensity of individual bands. Values were normalised to HSP90 to allow comparison between patients. p105, the precursor of p50, was only found in the cytosolic fractions, with the exception of two samples (i.e. 3340 and 4130). p65 was also predominantly found in the cytosolic fractions, while p50 was evident in both compartments and appeared to be more readily detected than p65. Although levels of p50 in the cytosol were similar between samples, there was variation in the p50 expression found in the nuclear fractions.

A common nuclear extraction control is tubulin, which is confined to the cytosolic fraction. However, its molecular weight is approximately 50 kDa, which is the same molecular weight as the NF-κB subunit p50. Therefore, HSP90 was proposed as a control for the nuclear extraction as it is considered to be a cytosolic protein (UniProt Consortium, 2014). Expression of HSP90 was relatively constant in the cytosolic fractions, however it was also present in varying amounts in the nuclear fraction of all samples tested. Equivalent numbers of cells from each patient were extracted and the same sample volume was loaded into the gel for each sample. However, the variable

detection of HSP90 indicated that the amount of protein in each sample was not equivalent. Variable expression could be caused by biological or technical factors, such as a naturally occurring variable expression of HSP90 in the nucleus, or inconsistent loss of protein during the extraction protocol. It is likely that the variation was caused by a combination of both technical and biological causes, therefore another protein was chosen as a control. In addition, the amount of total protein in the nuclear/cytosolic fractions was quantified and 2 μg of each sample was loaded into the gels.

Figure 5.2 shows the nuclear fraction of another eight CLL patient samples. Poly-ADP ribose polymerase (PARP), which is restricted to the nuclear fraction, was used as a control and a total of 2 μg of protein were loaded into the gel. p50 expression in the nuclear fraction of the untreated samples was variable, as seen in Figure 5.1. However, the levels of PARP were also variable despite an attempt to ensure equivalent loading by assaying total protein. It appears that variation in PARP is not sufficient to explain the variation in p50 levels, as differences in p50 were still observable in samples where PARP expression was very similar. Examples of this are the fourth and eight lanes of Figure 5.2. Densitometry where the levels of p50 are compared to the levels of PARP makes this variation more obvious. In contrast to p50, basal levels of p65 were almost undetectable in all samples tested making interpretation of the levels of p65 very challenging.

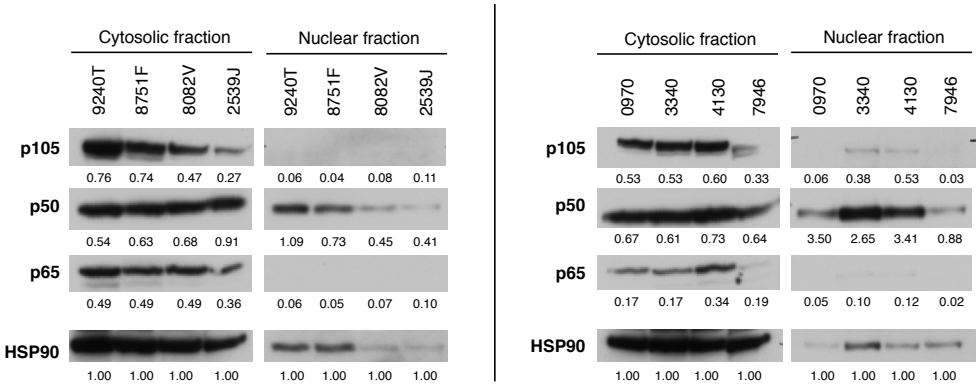

Figure 5.1 – p105/p50 and p65 in the nuclear and cytosolic fractions of primary CLL cells of 8 patients' samples.
Nuclear extracts from $5x10^6$ primary CLL cells were prepared as previously described in section 2.6.1. 20μl of each fraction was analysed by SDS-PAGE and western blotting analysis. Blots were incubated with the following antibodies: NF-κB p105/p50 (3035S, Cell Signaling), NF-κB p65 (D14E12) XP (8242S, Cell Signaling), HSP90 (4877S, Cell Signaling). Detection was performed by chemiluminescence. Densitometry was performed using ImageJ software. Values are presented as a ratio, normalised to HSP90.

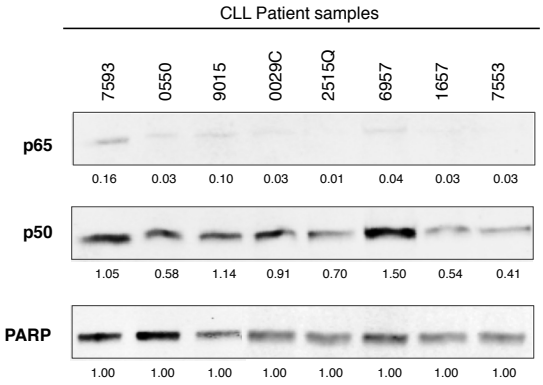

Figure 5.2 – p50 and p65 in the nuclear fraction of primary CLL cells of 8 patients' samples.
Nuclear extracts from $5x10^6$ primary CLL cells were prepared as previously described in section 2.6.1. The volume equivalent to 2μg of total protein was analysed by SDS-PAGE and western blotting. Blots were incubated with the following antibodies: NF-κB p105/p50 (3035S, Cell Signaling), NF-κB p65 (D14E12) XP (8242S, Cell Signaling), PARP (9532S, Cell Signaling). Densitometry was performed using ImageJ software. Values are presented as a ratio, normalised to PARP. Molecular weight of proteins of interest: p50 – 50 kDa, p65 – 65 kDa, PARP – 116 kDa.

5.2.2. Assessment of NF-κB in the nuclear fraction of primary CLL cells treated with TP10-p65i and TP10-p50i

Despite the challenges associated with analysing the levels of p50 and p65, one further set of experiments was performed with TP10-p50i and TP10-p65i on NF-κB in CLL cells. The goal was to determine if clear changes in p50 expression in the nuclear fraction of treated CLL cells could be observed. $5x10^6$ primary cells were cultured with 0, 1, 2.5 or 5 μM of TP10-p50i or TP10-p65i for a period of one hour, at 37˚C with 5% CO_2. Cells were then harvested and cytosolic and nuclear extracts were prepared. Nuclear extracts were analysed by SDS-PAGE and western blotting.

The TP10-p50i peptide caused a reduction in the levels of p50 detectable in cells treated with the TP10-p50i peptide (Figure 5.3). Densitometry was performed to allow comparison between the different peptide treatment conditions, with untreated cells used as a reference. In all three cases, the highest concentration of peptide (5 μM) showed a reduction in the amount of p50 detected in the nuclear fraction of CLL cells.

As previously observed in Figures 5.1 and 5.2, levels of p65 were undetectable in the nuclear fraction of all the samples tested (Figures 5.3 and 5.4). This prevented a meaningful analysis of effect of TP10-p65i on the levels of nuclear p65. However, TP10-p65i did not cause any significant change in the p50 levels (Figure 5.4). For these two reasons, a decision was made not to study TP10-p65i further but rather to focus on TP10-p50i. This decision was further justified by the previous results showing that TP10-p50i was more cytotoxic than TP10-p65i (Section 4.2).

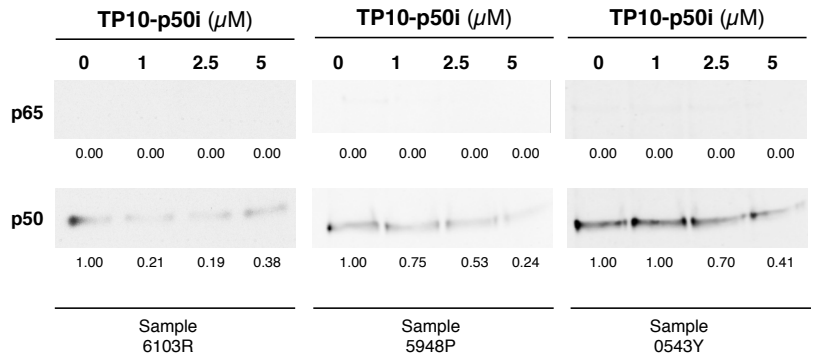

Figure 5.3 – p50 and p65 of primary CLL cells incubated with TP10-p50i.
$5x10^6$ primary CLL cells were incubated with 0, 1, 2.5 and 5 μM of TP10-p50i for a period of 1 hour. Cells were harvested and nuclear extracts were prepared as previously described. Samples were analysed by SDS-PAGE and western blotting. Blots were incubated with the following antibodies: NF-κB p105/p50 (3035S, Cell Signaling), NF-κB p65 (D14E12) XP (8242S, Cell Signaling). Densitometry was performed using ImageJ software. Bands were normalised to the untreated sample (0 μM of TP10-p50i).

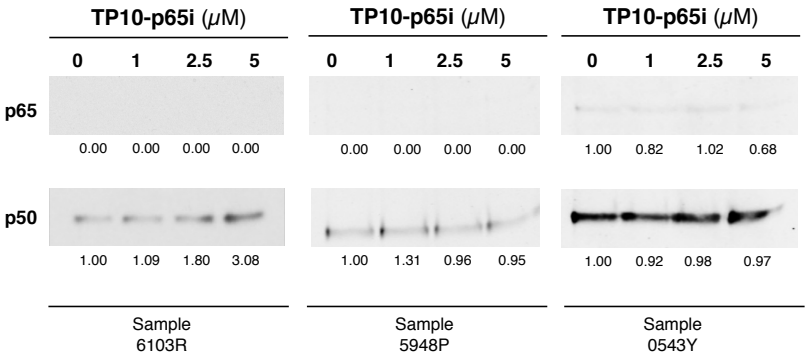

Figure 5.4 - p50 and p65 of primary CLL cells incubated with TP10-p65i.
$5x10^6$ primary CLL cells were incubated with 0, 1, 2.5 and 5 μM of TP10-p65i for a period of 1 hour. Cells were harvested and nuclear extracts were prepared as previously described. Samples were analysed by SDS-PAGE and western blotting. Blots were incubated with the following antibodies: NF-κB p105/p50 (3035S, Cell Signaling), NF-κB p65 (D14E12) XP (8242S, Cell Signaling). Bands were normalised to the untreated sample (0 μM of TP10-p50i).

5.3. Effects of TP10-p50i on DNA binding of NF-κB

5.3.1. Assessment of NF-κB binding activity in untreated primary CLL cells

The analysis of p50 protein levels in the nuclear fraction of CLL cells treated with TP10-p50i led to the decision to investigate the effects of this peptide on NF-κB activity, as determined by electrophoretic mobility shift assay (EMSA). To assess the basal DNA binding activity of NF-κB, nuclear fractions of primary untreated CLL cells were prepared. The amount of protein was measured in each sample, and 2 μg of protein from the nuclear extract was incubated with a radioactive-labelled oligonucleotide consisting of the NF-κB consensus sequence. Samples were run in a non-denaturing acrylamide gel, under conditions previously described (Section 2.6.4). Figure 5.5 shows a positive control, Jurkat cells stimulated with the pro-inflammatory cytokine TNF-α for one hour, and samples from ten CLL patient samples. Levels of NF-κB DNA binding in the nuclear fraction of CLL cells varied between patient samples; densitometry was performed to quantify the variation. NF-κB in CLL cell samples seemed to run as two bands. These could represent two different homo/heterodimers. The variation in the levels of NF-κB was in agreement with previously published data (Hewamana et al, 2008).

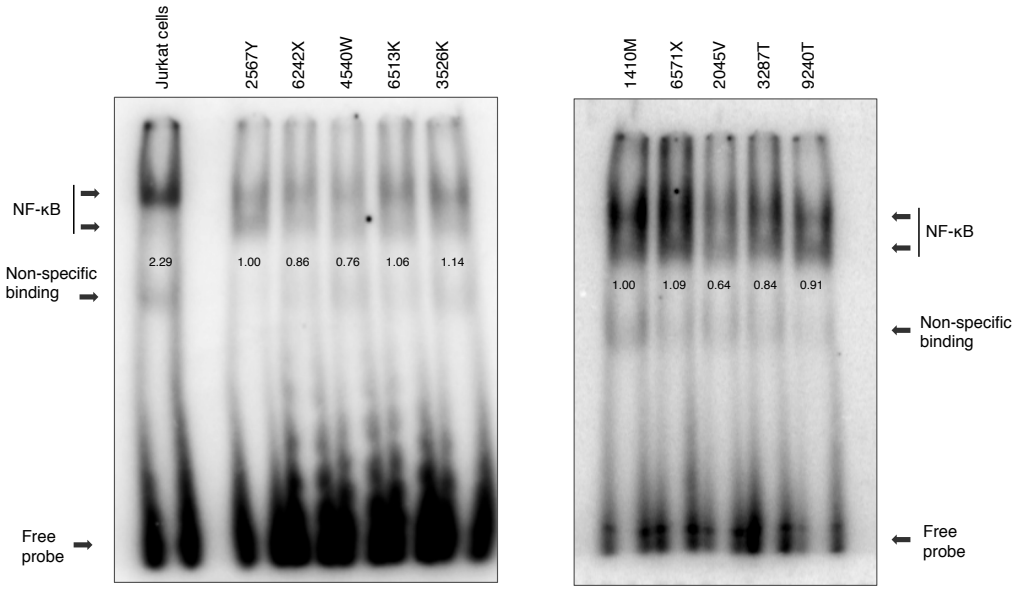

Figure 5.5 - NF-κB in the nuclear fraction of primary CLL cells.
Nuclear extracts of $5x10^6$ untreated and unstimulated primary CLL cells were prepared for EMSA to assess the levels of NF-κB binding in the nucleus. 2 μg of protein were loaded into each well. Positive control consists of Jurkat cells stimulated with 100 μg/μl of TNF. Densitometry was performed using ImageJ software, and bands were normalised to the first sample in the gel (i.e. 2567Y and 1410M).

5.3.2. Assessment of NF-κB binding activity in primary CLL cells treated with TP10-p50i

To further assess the effects of TP10-p50i on NF-κB, primary CLL cells were cultured with 0, 1, 2.5 and 5 μM of TP10-p50i for a period of one hour. Cells were then harvested and nuclear fractions were extracted. An EMSA was performed and Figure 5.6 shows the level of NF-κB binding activity in six CLL patient samples following incubation with TP10-p50i.

Different patient samples showed a different effect on NF-κB binding activity following treatment with the TP1-p50i peptide. A reduction in nuclear NF-κB binding following treatment with TP10-p50i was evident in three of the six samples tested (i.e. 9687, 1272 and 5948). The three other samples, showed relatively little change in the amount of NF-κB capable of binding to the consensus oligonucleotide. Densitometry was performed to inform the analysis. This showed that only two patient samples demonstrated a concentration-dependent inhibition of NF-κB. This was observable in sample 9687, but most obviously in sample 5948. Sample 1272 seemed to be more sensitive to low concentrations of TP10-p50i than the other samples, while 9687 showed higher sensitivity at 5 μM. Although the decrease in NF-κB binding activity was not as pronounced for sample 1228 than other samples, a small reduction was still visible. The lack of a reproducible inhibition of NF-κB contrasts with the data obtained in section 4.2, where all samples were equally susceptible to the cytotoxic effects of the peptide. This suggests the peptide-induced apoptosis may not relate to NF-κB inhibition.

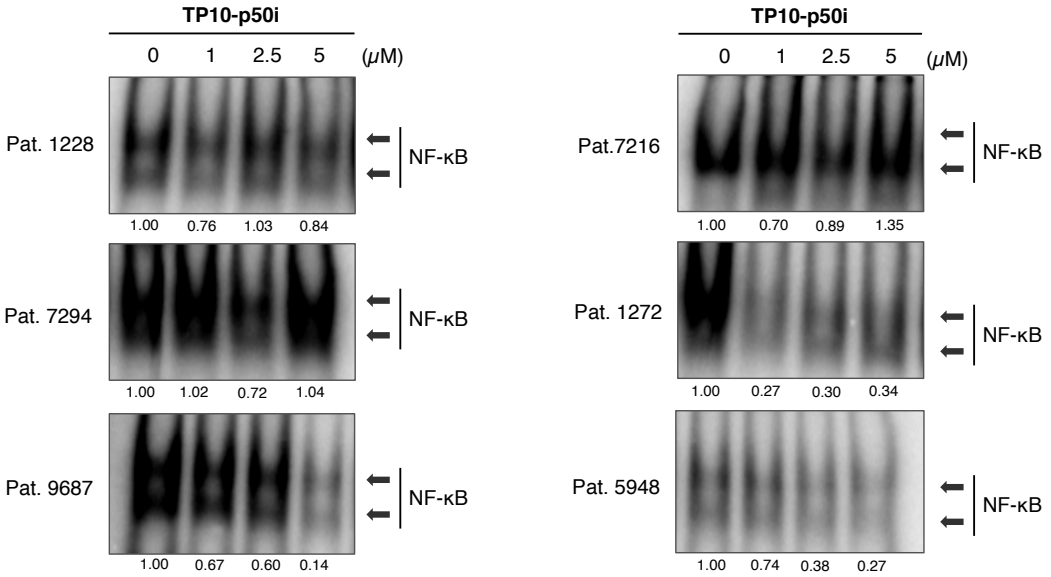

Figure 5.6 - NF-κB in the nuclear fraction of primary CLL cells treated with TP10-p50i for 1 hour. $5x10^6$ primary CLL cells were incubated with 0, 1, 2.5 and 5 μM of TP10-p50i for a period of 1 hour. Cells were harvested and nuclear extracts were prepared. Samples were analysed by EMSA. 2 μg of protein were loaded into each well. Densitometry was performed using ImageJ software, and bands were normalised to the respective untreated sample (i.e. first lane).

5.3.3. Assessment of NF-κB binding activity in primary CLL cells following co-culture with CD40L

The variable effect of TP10-p50i on NF-κB DNA binding could be due to the lack of NF-κB activation by external stimuli during the course of peptide treatment. To understand whether TP10-p50i could inhibit NF-κB activation in primary CLL cells, cells were co-cultured with CD40L-expressing fibroblasts, which has been shown to induce activation of NF-κB (Furman et al., 2000). An initial assessment of this activation was performed, by culturing primary CLL cells with CD40L-expressing fibroblasts or non-transfected cells (NTL) as a control, for a period of 1, 24 or 48 hours. Cells were harvested, washed and cytosolic and nuclear extracts were prepared. Figure 5.7 shows an EMSA of nuclear extracts derived from a CLL sample following co-culture with NTL and CD40L. CD40L-expressing co-culture induced NF-κB activation within one hour and levels of NF-κB continued to increase after 24 and 48 hours of co-culture. Based on this assessment, the incubation period with CD40L-expressing fibroblasts was set at one hour.

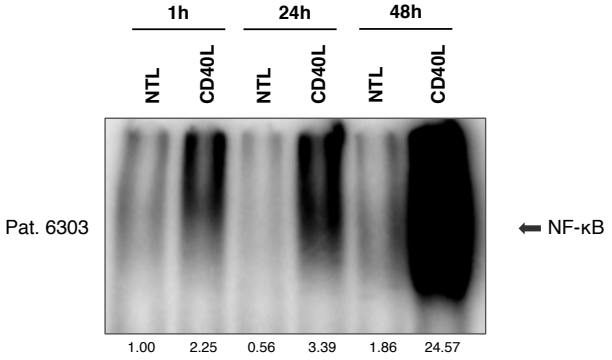

Figure 5.7 - NF-κB in the nuclear extracts of CD40L stimulated and unstimulated primary CLL cells. $5x10^6$ primary CLL cells were incubated with $1x10^6$ CD40L-expressing fibroblasts or non-transfected fibroblasts (NTL) for a period of 1, 24 or 48 hours. Cells were washed and the nuclear and cytosolic extracts prepared for analysis by EMSA. 2 μg of protein were loaded into each well. Densitometry was performed using ImageJ software, and bands were normalised to the sample incubated with NTL cells for one hour.

5.3.4. Assessment of NF-κB binding activity in primary CLL cells following co-culture with CD40L and pre-treatment with TP10-p50i

Primary CLL cells were then pre-incubated with 0, 1, 2.5 and 5 μM of TP10-p50i for one hour, and then transferred onto co-culture with CD40L cells. The aim was to assess if TP10-p50i was capable of preventing NF-κB activation via CD40 ligation. BAY 11-7082, an established NF-κB inhibitor (Pickering et al., 2007), was used as a positive control for NF-κB inhibition. Cells were cultured under the same conditions as described for treatment with TP10-p50i, with BAY 11-7082 used at concentrations of 2.5 μM and/or 5 μM. Figure 5.8 and 5.9 show five CLL patient samples treated under the conditions described.

Co-culture for one hour with CD40L cells induced an increase in NF-κB binding activity in all the samples tested. In CLL cells treated with BAY 11-7082, the levels of NF-κB binding activity were reduced to the levels found in unstimulated cells (i.e. NTL), at both concentrations tested. In contrast to BAY 11-7082, the data with TP10-p50i was more variable. Four of the five patient samples showed a reduction in NF-κB DNA binding at the highest concentration of peptide (5 μM). However, the reduction was relatively modest, particularly in comparison with that observed following incubation with BAY 11-7082. Even when an effect of TP10-p50i was observed, the samples did not show a concentration-dependent inhibition. Samples 275T and 838X show lower NF-κB binding activity following treatment with 2.5 μM when compared with 5 μM, implying less inhibition at higher doses of the peptide. As for samples 2450 and 9284, higher levels of NF-κB bound to the consensus oligonucleotide were found in samples treated with 2.5 μM. This variability may be due to technical issues, such as uneven loading of samples into the gel, even though the total amount of protein was quantified in a previous step and a set amount of 2 μg was then loaded into the gel, to specifically avoid this problem. It is also conceivable that it may be caused by differential uptake and/or processing of the peptide by specific CLL samples.

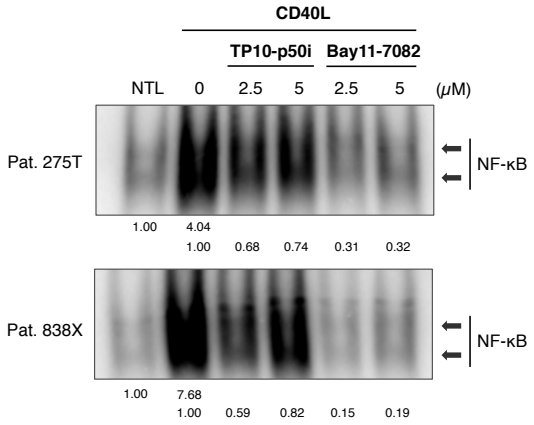

Figure 5.8 - NF-κB in the nuclear fraction of CD40L stimulated primary CLL cells pre-treated with TP10-p50i and BAY 11-7082.
$5x10^6$ primary CLL cells were pre-treated with 0, 2.5, and 5 μM TP10-p50i or 2.5 and 5 μM of BAY 11-7082 for 1 hour. Cells were harvested and incubated with $1x10^6$ CD40L-expressing fibroblasts or non-transfected fibroblasts (NTL) for one hour. Cells were harvested and the nuclear extracts prepared for analysis by EMSA. 2 μg of protein were loaded into each well. Densitometry was performed using ImageJ software, and bands normalised to cells cultured with NTL cells.

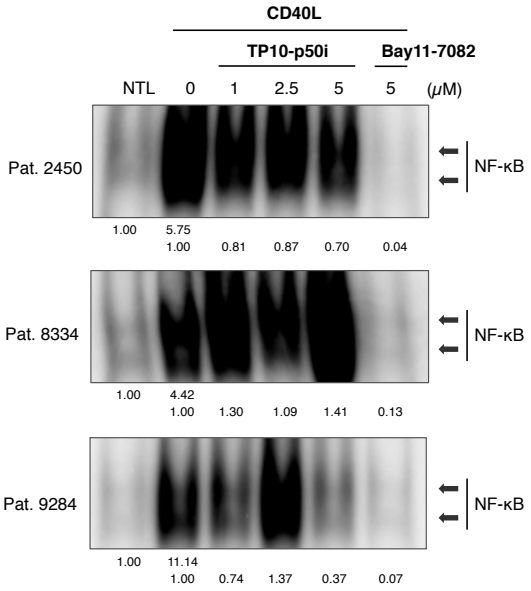

Figure 5.9 - NF-κB in the nuclear fraction of CD40L-stimulated primary CLL cells pre-treated with TP10-p50i and BAY 11-7082.
$5x10^6$ primary CLL cells were pre-treated with 0, 1, 2.5, and 5 μM TP10-p50i and 5 μM of BAY 11-7082 for 1 hour. Cells were harvested and incubated with $1x10^6$ CD40L-expressing fibroblasts or non-transfected fibroblasts (NTL) for one hour. Cells were harvested and the nuclear extracts prepared for analysis by EMSA. 2 μg of protein were loaded into each well. Densitometry was performed using ImageJ software, and bands normalised to cells cultured with NTL cells.

5.3.5. Assessment of NF-κB binding activity in primary CLL cells pre-treated with TP10-p50i and stimulated with CpG

In parallel to the assessment previously described in section 5.3.4, the effects of pre-treatment with TP10-p50i followed by stimulation with another NF-κB activator, CpG oligonucleotides, was measured by EMSA. Primary CLL cells were treated with 0, 1, 2.5 and 5 μM of TP10-p50i for a period of one hour, and then treated for a further hour with 500 nM of CpG ODN2006. BAY 11-7082 was again used as a control for NF-κB inhibition, at the concentration of 5 μM. Cells were harvested, nuclear extracts were prepared and the nuclear fractions were analysed by EMSA.

Figure 5.10 shows data from four CLL patient samples. Stimulation with CpG ODN2006 was capable of inducing an increase in NF-κB binding. TP10-p50i showed a convincing inhibition of CpG-induced NF-κB binding activity in two of the four samples tested (i.e. 4665F and 9284). However, NF-κB inhibition was concentration-dependent in only one of the samples tested (i.e. 4665F). Sample 9284 showed a reduction of NF-κB at all the TP10-p50i concentrations used, with an unusual reduced sensitivity at 2.5 μM, perhaps suggesting a technical failure related to the processing of this sample for EMSA. In contrast, cells treated with BAY 11-7082 showed a consistent repression of CpG-induced NF-κB binding activity to similar or lower levels than unstimulated cells. Comparing the results of TP10-p50i on both CD40L stimulation and CpG stimulation, the data show that the inhibition of NF-κB was variable and was patient sample dependent. Furthermore, the inhibition was modest relative to pharmacological inhibition with BAY 11-7082. The next step was to investigate cell surface markers following CD40L stimulation, to assess whether the variable effects of TP10-p50i on NF-κB would alter expression of cell proteins.

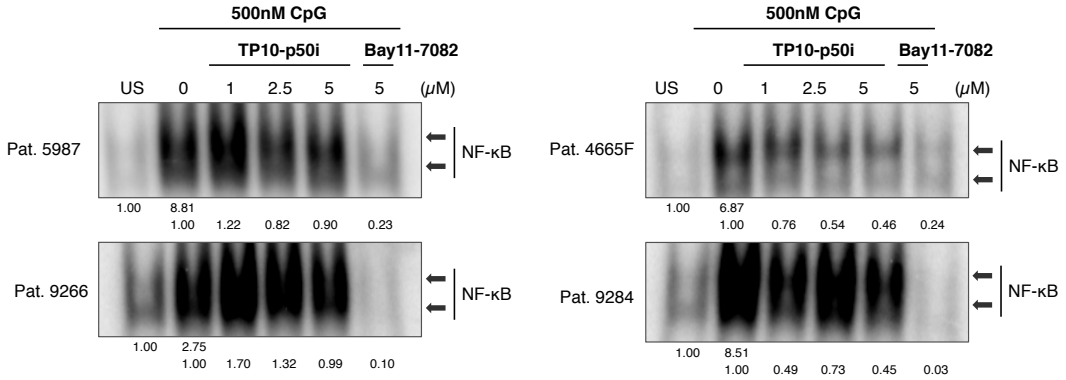

Figure 5.10 - NF-κB in the nuclear extracts of CpG-stimulated primary CLL cells pre-treated with TP10-p50i and BAY 11-7082.
$5x10^6$ primary CLL cells were pre-treated with 1, 2.5, and 5 μM TP10-p50i, 5 μM of BAY 11-7082 or untreated for 1 hour. Cells were harvested and incubated in liquid culture with 500nM of CpG ODN2006 for one hour. Cells were harvested and the nuclear extracts prepared for analysis by EMSA. 2 μg of protein were loaded into each well. Densitometry was performed using ImageJ software, and bands normalised to the unstimulated (US) sample.

5.4. Effects of TP10-p50i on cell surface markers regulated by NF-κB

5.4.1. Assessment of viability of primary CLL cells pre-treated with TP10-p50i and Bay 11-7082, followed by stimulation with CD40L

Although the TP10-p50i peptide was uniformly capable of inducing apoptosis in primary CLL samples, its ability to inhibit NF-κB appeared variable. To assess if the reduction in NF-κB activity in the nucleus translated into altered expression of proteins that are transcriptionally regulated by NF-κB, cell surface markers were quantified by flow cytometry in cells treated and untreated with TP10-p50i followed by co-culture with CD40L.

Flow cytometry requires a careful gating strategy. The strategy used for the following experiments is shown in Figure 5.11 and consisted of four steps. The initial step involved drawing a gate that excluded cell debris from the analysis (box i). The second step used the forward and side scatter to identify viable cells (box ii). Dead cells become smaller and more granular, meaning they move to the left of the plot. A population of dead cells was visible in box ii (see arrow). Viable cells were then forward gated into a doublet discrimination gate (box iii), which excluded clumps of cells (box iii). The fourth step specifically identified CLL cells based on the co-expression of CD19 and CD5 antigens. This final gate (v) allowed the analysis of the surface markers of interest in viable, discreet CLL cells.

Figure 5.12 shows the “Live Lymphocyte” gates for one patient sample and the percentage of cells within the “Live Lymphocyte” gate for the 17 patient samples tested was plotted in Figure 5.13. Cells cultured with CD40L had a higher percentage of viable cells (76.1%) when compared to cell cultured with NTL (67.5%), indicating that CD40L stimulation confers cytoprotection to CLL cells in culture. Cells cultured with 2.5 (75%) and 5 μM (74.9%) of TP10-p50i showed no significant change in viability, while cells cultured with 10 μM (66.6%) showed a small but significant decrease in viability. Cells cultured with 5 μM of BAY 11-7082 (used as positive control for NF-κB inhibition) reduced the average percentage of viable cells to 14%, showing that BAY 11-7082 is a more potent cytotoxic agent (mol for mol) than TP10-p50i.

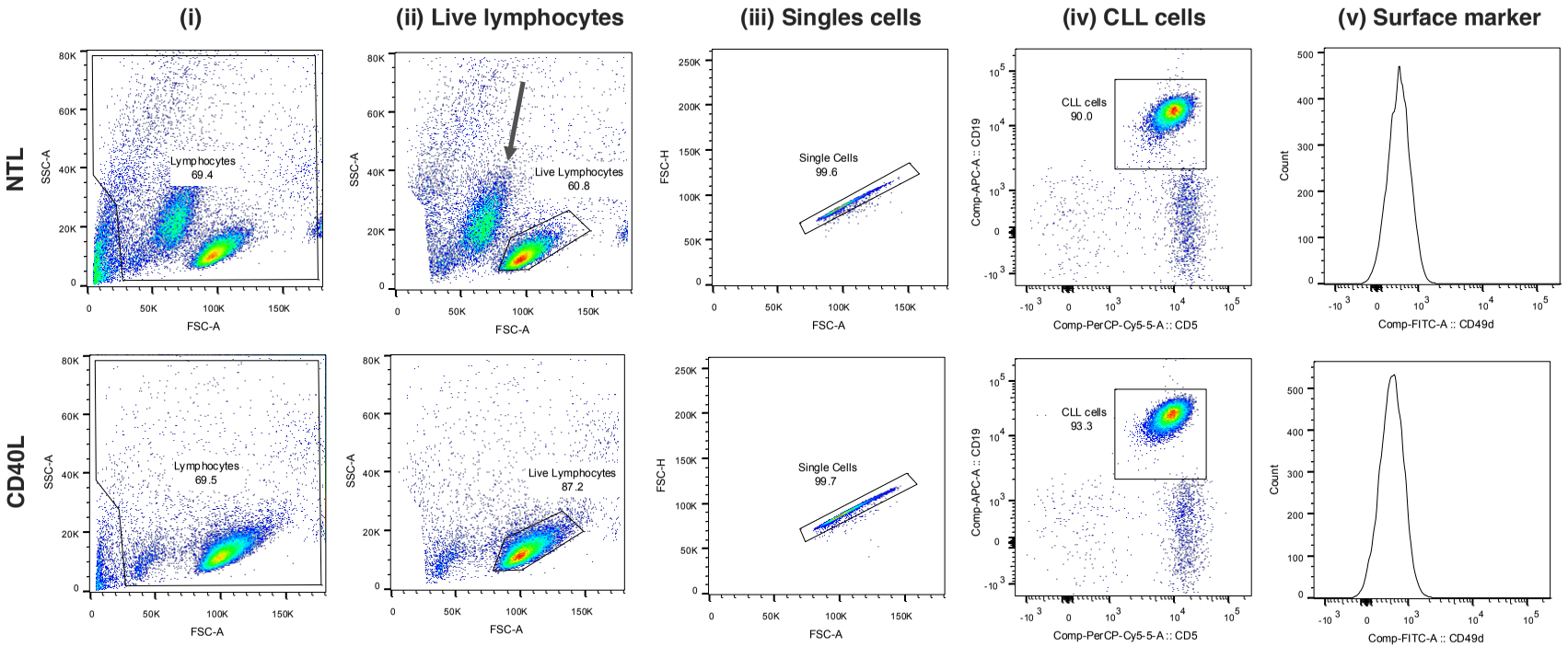

Figure 5.11 – Gating strategy used to measure CD49d, CD38, CD69 and CD25 of primary CLL cells following co-culture with NTL and CD40L cells and pre-treatment with TP10-p50i and Bay 11-7082.

This example shows primary CLL cells cultured for 1 hour in liquid culture without any treatment that were posteriorly transferred onto co-culture with NTL and CD40L cells for a period of 24 hours. In the first instance, a broad gate was drawn with the intention to exclude the debris found on the left-bottom corner of the FSC v SSC graph. Within this gate, a tight gate surrounding the live lymphocyte population was drawn, using as reference primary CLL cells untreated and co-cultured with CD40L cells. The percentage of cells within this gate was used to measure viability. Within the live lymphocyte gate, a gate to exclude duplets was used. Within the single cells gate, another gate was used to determine the CLL cells population that expresses CD19 and CD5. Cells within this gate were used to measure the activation markers CD49d, CD38, CD69 and CD25.

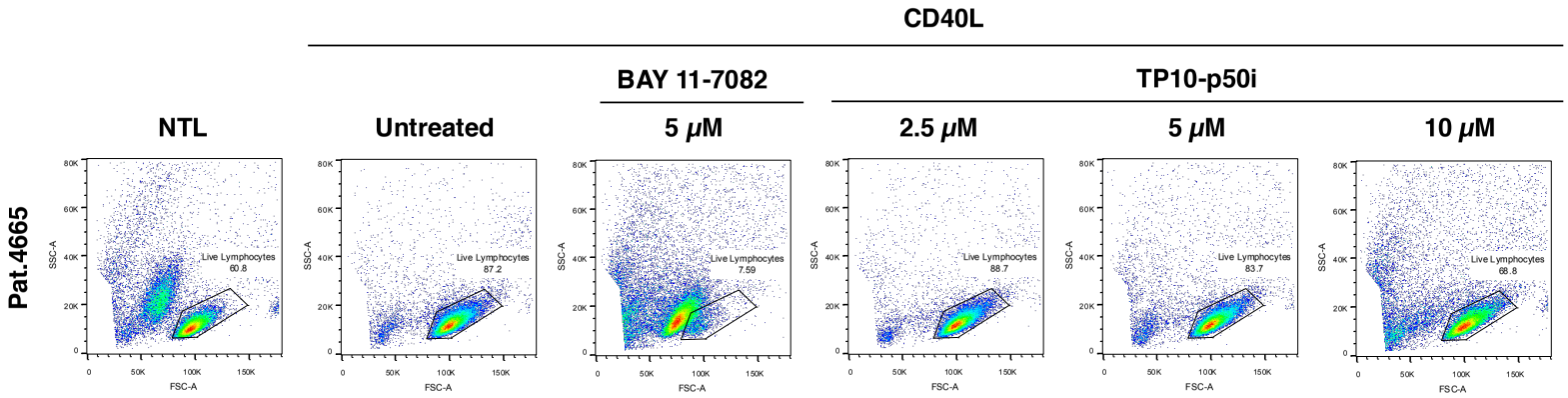

Figure 5.12 – "Live Lymphocytes" gate of sample 4665, pre-treated with TP10-p50i or Bay 11-7082 followed by 24 hours of co-culture with CD40L expressing fibroblasts.
Primary CLL cells were cultured with BAY 11-7082 (5 μM), TP10-p50i (2.5, 5 or 10 μM) or untreated for a period of one hour. Following incubation, cells were transferred to either NTL (previously untreated) or CD40L-expressing fibroblasts for a period of 24 hours. Cells were posteriorly washed and incubated with antibodies targeting cell surface markers. The gating strategy is described in Figure 5.11. Viability of cells were quantified within the "Live Lymphocyte" gate, as seen in this Figure. A summary of 17 patient samples can be found in Figure 5.13.

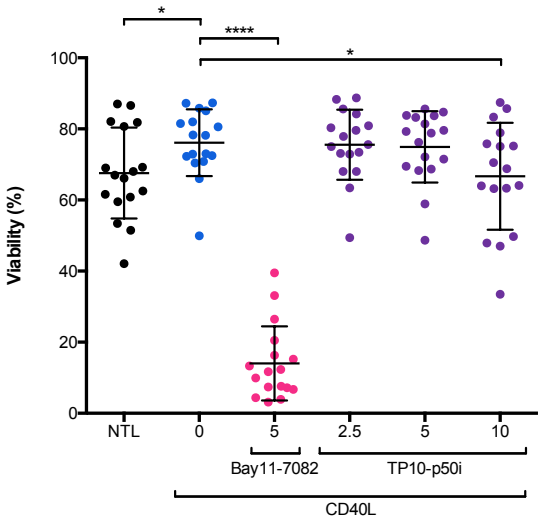

Figure 5.13 - Viability of primary CLL cells following co-culture with NTL and CD40L cells and pre-treatment with 2.5, 5 and 10 μM of TP10-p50i and 5 μM of BAY 11-7082.
Primary CLL cells were treated with 0, 2.5, 5 and 10 μM of TP10-p50i or 5 μM of BAY 11-7082 for one hour in liquid culture. Cells were then transferred onto co-culture with NTL or CD40L cells for a period of 24 hours. Cell viability was measured using the gating strategy presented in Figure 5.11. Data from 17 patient samples, presented as individual percentage values, plus mean +/- SD. Statistical analysis was performed using the software GraphPad Prism 6. Repeated-measures one-way ANOVA was applied followed by a multiple-comparisons test. * - represents the level of statistical significance.

5.4.2. Assessment of cell surface markers regulated by NF-κB in primary CLL cells

The effects of CD40L stimulation and treatment with BAY 11-7082 (i.e. positive control for NF-κB inhibition), on cell surface markers CD25, CD49d, CD38 and CD69 were analysed. Primary CLL cells were cultured with 5 μM BAY 11-7082 for one hour. Cells were then harvested and cultured for 24 hours with CD40L or NTL cells. Samples were analysed by flow cytometry. Cell surface markers CD25, CD49d, CD38 and CD69 were measured within the "CLL cell" gate. The effects of CD40L and BAY 11-7082 are shown for two samples (Figure 5.14 to 5.17). Using FlowJo software, the MFI of this population was obtained from 17 patient samples and is shown in the summary graphs (Figure 5.18 to 5.21).

Of the four markers tested, CD25 and CD69 were up regulated by CD40L within 24 hours. BAY 11-7082 was capable of inducing changes in three of the four markers tested: CD25, CD49d and CD69. However, only CD69 was down regulated. Figure 5.18 shows that pre-treatment with BAY 11-7082 and co-culture with CD40L induced a significant increase in CD25 expression when compared with untreated co-culture with CD40L. This event was unexpected as CD25 is a cell surface marker regulated by NF-κB (Fu et al., 2013). To further understand this increase, dot plots for the expression of CD25 and CD19 in two patient samples are presented in Figure 5.14. This Figure illustrates that untreated cells, when co-cultured with CD40L, show an increase in CD25 expression. However, cells pre-treated with BAY 11-7082 do not uniformly present an increased CD25 expression, as suggested by the summary MFI data presented in Figure 5.18. In fact two cell populations can be seen, one that expresses CD25 at the same level as cells cultured with NTL, indicating that BAY 11-7082 was capable of inhibiting the up-regulating effects of CD40L co-culture, and a smaller sub-population of cells (i.e. 12.4% and 4.08%) in which pre-treatment with BAY 11-7082 induced an up-regulation of CD25. A similar effect can be seen in Figure 5.19 and 5.15, for the expression of CD49d. The cause of increased expression of both CD25 and CD49d following treatment with BAY 11-7082 requires further investigation but may represent an escape mechanism from BAY 11-7082 induced apoptosis.

CD69 was the only marker up-regulated by CD40L and down-regulated by BAY 11-7082, within the timeframe of this study indicating that it was a good candidate for a directly regulated NF-κB protein. And for this reason, CD69 was selected for assessment in the context of TP10-p50i treatment (section 5.4.3).

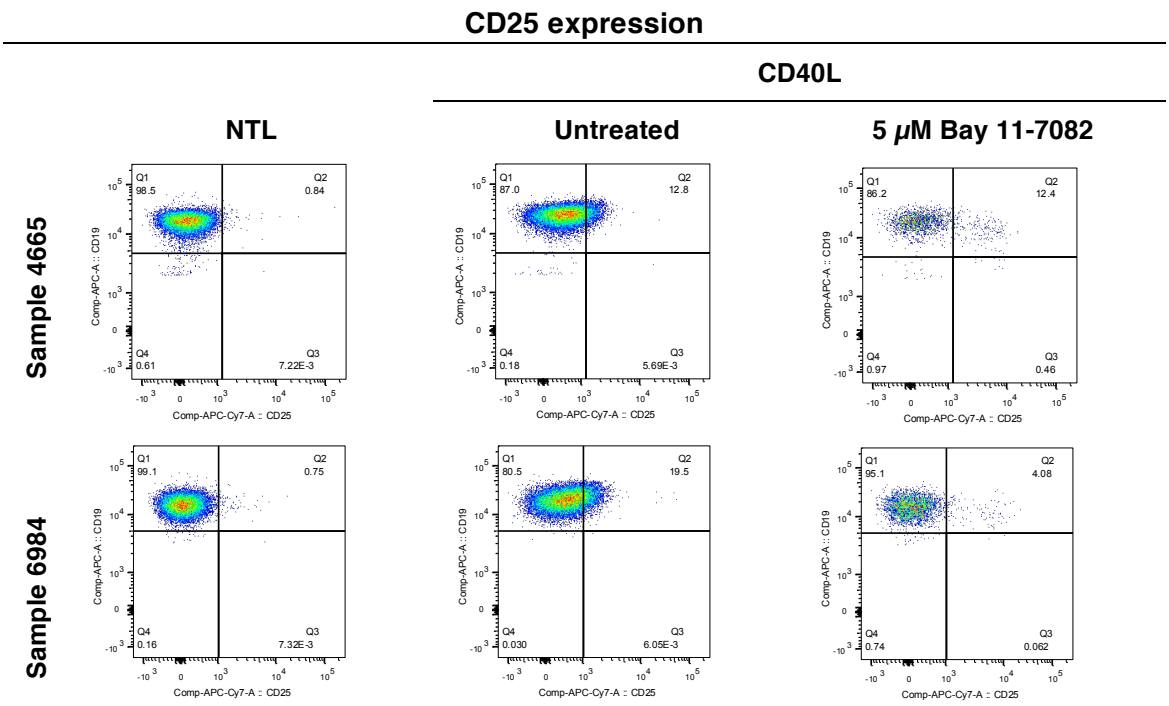

Figure 5.14 – Expression of CD25 and CD19 of cell within the CLL cell gate.
CD19 and CD25 dot plot of patient samples 4665 and 6984, incubated under the conditions described in Figure 5.11. Cells present in these dot plots were gated previously in the "CLL cell" gate as described in Figure 5.11. Dot plots obtained using the software FlowJo X.

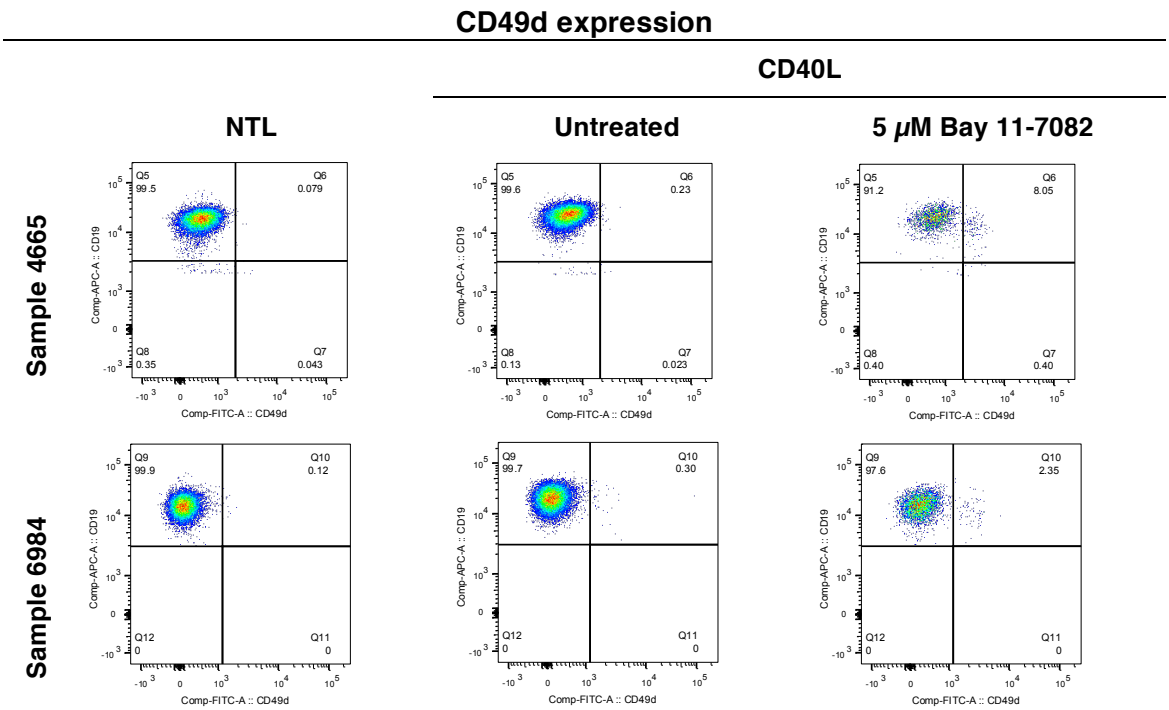

Figure 5.15 – Expression of CD49d and CD19 of cell within the CLL cell gate.
CD19 and CD49d dot plot of patient samples 4665 and 6984, incubated under the conditions described in Figure 5.11. Cells present in these dot plots were gated previously in the "CLL cell" gate as described in Figure 5.11. Dot plots obtained using the software FlowJo X.

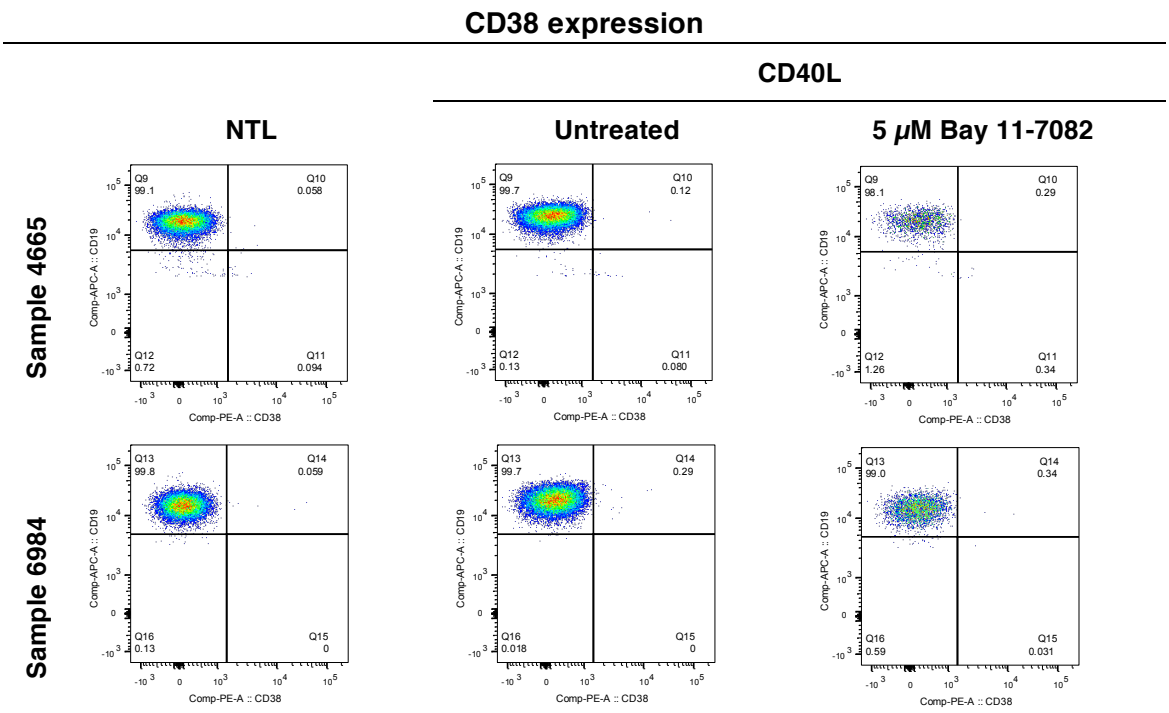

Figure 5.16 – Expression of CD38 and CD19 of cell within the CLL cell gate.
CD19 and CD38 dot plot of patient samples 4665 and 6984, incubated under the conditions described in Figure 5.11. Cells present in these dot plots were gated previously in the "CLL cell" gate as described in Figure 5.11. Dot plots obtained using the software FlowJo X.

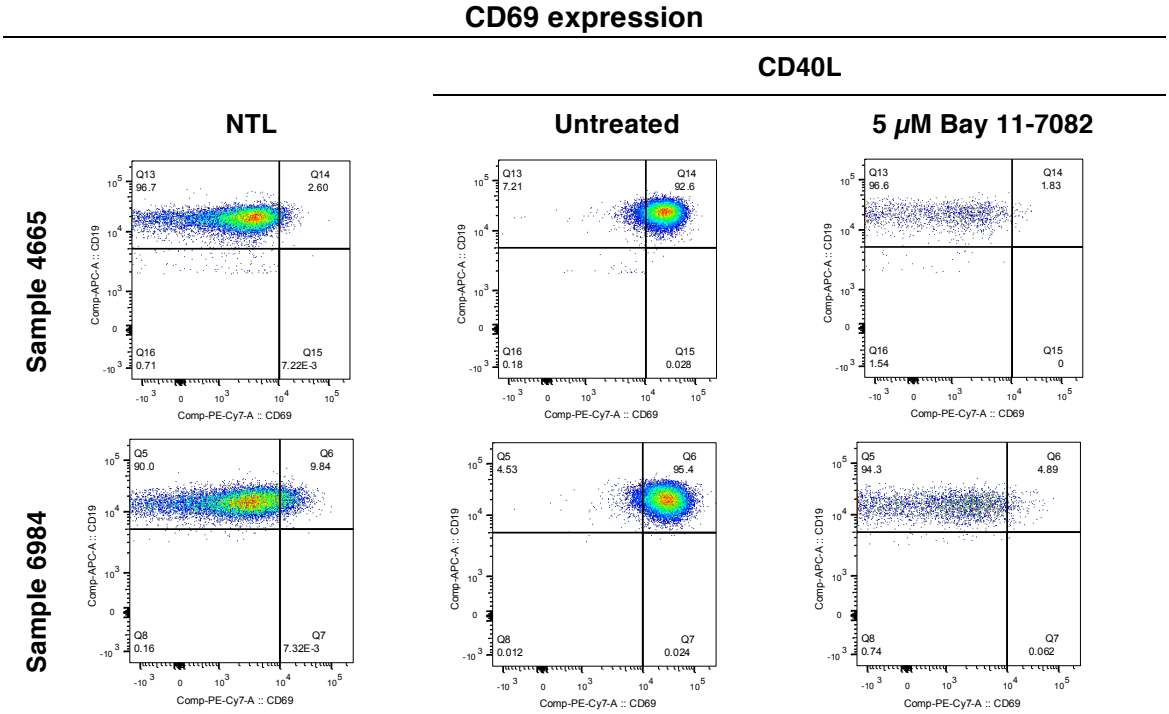

Figure 5.17 – Expression of CD69 and CD19 of cell within the CLL cell gate.
CD19 and CD69 dot plot of patient samples 4665 and 6984, incubated under the conditions described in Figure 5.11. Cells present in these dot plots were gated previously in the "CLL cell" gate as described in Figure 5.11. Dot plots obtained using the software FlowJo X.

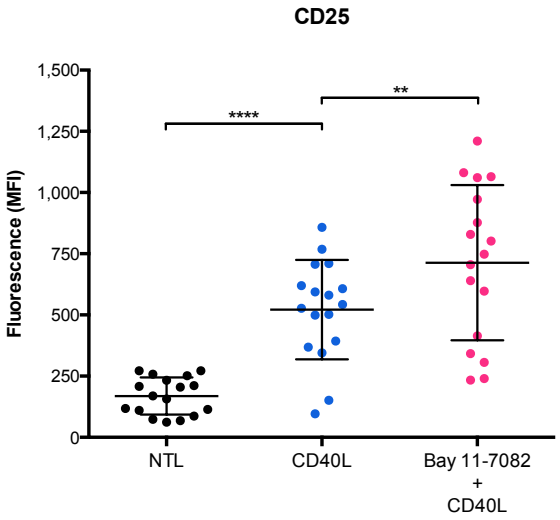

Figure 5.18 - Expression of CD25 on primary CLL cells pre-treated with BAY 11-7082, followed by co-culture with NTL and CD40L cells.
Primary CLL were incubated in liquid culture without any treatment or with 5 μM of BAY 11-7082 for a period of 1 hour. Cells were harvested and transferred onto co-culture with NTL or CD40L for a period of 24 hours. Cells were then harvested, washed and incubated with anti-CD25 antibody (560225, BD Pharmingen). The gating strategy used is presented in Figure 5.11. Data from 17 patient samples, presented as MFI values for each individual sample, plus mean and +/- SD. Statistical analysis was performed using GraphPad Prism 6 software. Repeated-measures one-way ANOVA was applied followed by a multiple-comparisons test. * - represents the level of statistical significance.

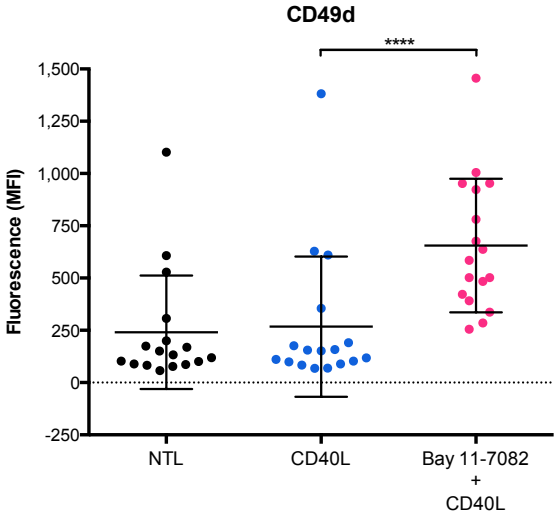

Figure 5.19 - Expression of CD49d on primary CLL cells pre-treated with BAY 11-7082, followed by co-culture with NTL and CD40L cells.
Primary CLL were cultured under the conditions described in Figure 5.12. Prior to flow cytometry, cells were incubated with anti-CD49d antibody (MCA2503F, AbD Serotec). The gating strategy used is presented in Figure 5.11. Data from 17 patient samples, presented as MFI values for each individual sample, plus mean and +/- SD. Statistical analysis was performed using GraphPad Prism 6 software. Repeated-measures one-way ANOVA was applied followed by a multiple-comparisons test. * - represents the level of statistical significance.

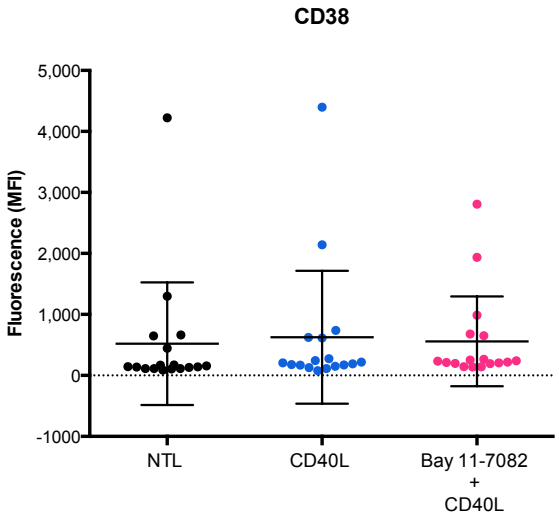

Figure 5.20 - Expression of CD38 on primary CLL cells pre-treated with BAY 11-7082, followed by co-culture with NTL and CD40L cells.
Primary CLL were cultured under the conditions described in Figure 5.12. Prior to flow cytometry, cells were incubated with anti-CD38 antibody (MHCD3804, Invitrogen). The gating strategy used is presented in Figure 5.11. Data from 17 patient samples, presented as MFI values for each individual sample, plus mean and +/- SD. Statistical analysis was performed using GraphPad Prism 6 software. Repeated-measures one-way ANOVA was applied followed by a multiple-comparisons test. No statistically significant differences were found between the different conditions tested.

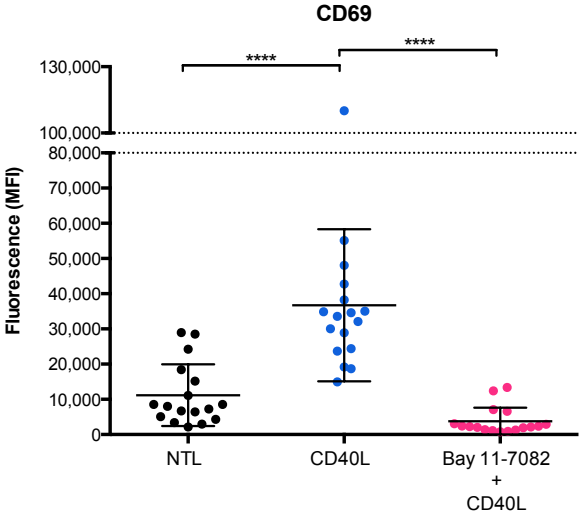

Figure 5.21 - Expression of CD69 on primary CLL cells pre-treated with BAY 11-7082, followed by co-culture with NTL and CD40L cells.
Primary CLL were cultured under the conditions described in Figure 5.12. Prior to flow cytometry, cells were incubated with anti-CD69 antibody (310912, Biolegend). The gating strategy used is presented in Figure 5.11. Data from 17 patient samples, presented as MFI values for each individual sample, plus mean and +/- SD. Statistical analysis was performed using GraphPad Prism 6 software. Repeated-measures one-way ANOVA was applied followed by a multiple-comparisons test. * - represents the level of statistical significance.

5.4.3. Assessment of CD69, a cell surface markers regulated by NF-κB in primary CLL cells pre-treated with TP10-p50i

To assess the effects of TP10-p50i on CD69 expression, primary CLL cells were treated with 0, 2.5, 5 and 10 μM of TP10-p50i for 1 hour. Cells were harvested and cultured with CD40L cells for a period of 24 hours. Cells were collected and incubated with the multi-colour flow cytometry antibody panel described previously (section 5.4.2). Data from two patients is shown in Figure 5.22. A summary of the expression of CD69 on CLL cells of 17 patient samples can be found in Figure 5.23. The expression of CD25, CD49d and CD38 was also measured in these experiments and the results of this analysis can be found in Appendix III. Figure 5.23 shows that MFI levels were not altered following treatment with 2.5, 5 or 10 μM of the TP10-p50i peptide.

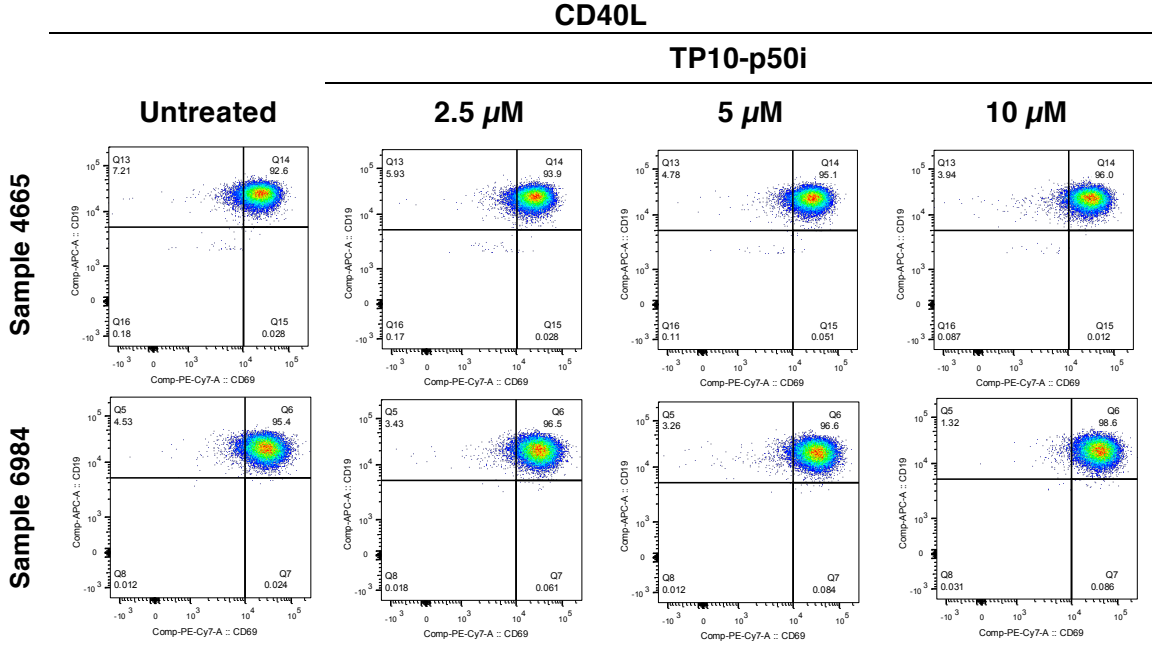

Figure 5.22 - Expression of CD69 and CD19 of cell within the CLL cell gate for cells treated with TP10-p50i and untreated.
CD19 and CD69 dot plot of patient samples 4665 and 6984, incubated under the conditions described in Figure 5.11. Cells present in these dot plots were gated previously in the "CLL cell" gate as described in Figure 5.11. Dot plots obtained using the software FlowJo X.

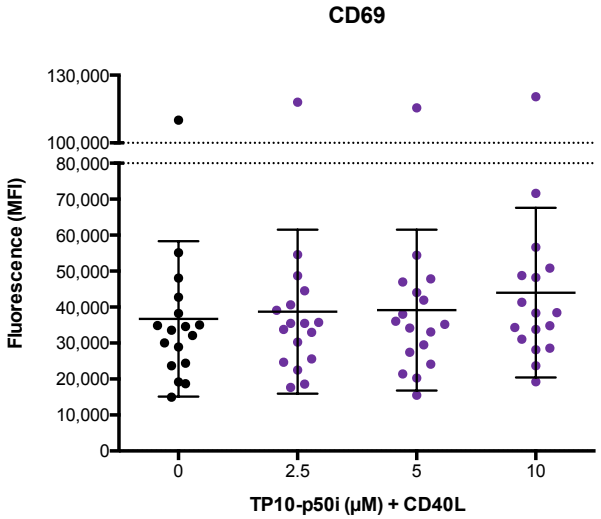

Figure 5.23 - Expression of CD69 on primary CLL cells pre-treated with TP10-p50i, followed by co-culture with NTL and CD40L cells.
Primary CLL were incubated in liquid culture without any treatment or with 2.5, 5 or 10 μM of TP10-p50i for a period of 1 hour. Cells were harvested and transferred onto co-culture with CD40L for a period of 24 hours. Cells were then harvested, washed and incubated with anti-CD69 antibody (310912, Biolegend). The gating strategy used is presented in Figure 5.11. Data from 17 patient samples, presented as MFI values for each individual sample, plus mean and +/- SD. Statistical analysis was performed using GraphPad Prism 6 software. Repeated-measures one-way ANOVA was applied followed by a multiple-comparisons test. No statistically significant differences were found between the different conditions tested.

5.5. Discussion & Conclusion

In the previous Chapter, it was demonstrated that TP10-p50i and TP10-p65i induced apoptotic cell death of primary CLL cells *in vitro*. The aim of this chapter was to investigate the effect of these peptides on NF-κB. NF-κB expression and activation were assessed in three different ways: nuclear translocation of NF-κB subunits p50 and p65; DNA binding activity of NF-κB; and the expression of cell surface markers regulated by NF-κB.

The first key finding from this chapter was that TP10-p50i did not inhibit the translocation of NF-κB in all CLL patient samples. This conclusion reflects the variable effects of the peptide on NF-κB. TP10-p50i was capable of reducing translocation of p50 into the nucleus and inhibiting NF-κB DNA binding activity in some of the patient samples tested but other samples showed little or no sensitivity to the peptide. This differential responsiveness was not dependent on basal or inducible levels of NF-κB. Considering that no variation was observed on viability in Chapter 4, these data suggest that apoptosis caused by TP10-p50i may not be directly connected to NF-κB inhibition. This was supported by the lack of effect on the expression of CD69, a cell surface marker with a rapid turnover that is susceptible to BAY 11-7082, a well-studied NF-κB inhibitor. Therefore, even if TP10-p50i has an effect on NF-κB in some samples, it is not sufficient to alter the expression of proteins transcriptionally regulated by NF-κB.

A second key finding of this chapter, was the restoring effects of CD40L co-culture on viability of cells treated with TP10-p50i. As seen in the previous Chapter (section 4.2), culture with a concentration of approximately 5 μM of TP10-p50i was sufficient to induce apoptosis in 50% of primary CLL cells. However, if primary CLL cells were transferred onto co-culture for a period of 24 hours, the percentage of viable cells was restored to levels similar to untreated cultures. CD40-CD40L engagement has been previously shown to protect cells from apoptotic stimuli (Hayden et al., 2009; 2010; Kater et al., 2004; Vogler et al., 2009). In fact, it is clear when comparing viability between cells untreated co-cultured with NTL cells (67.5%) and cells untreated co-cultured with CD40L cells (76.1%), that CD40-CD40L engagement provides an environment that decreases apoptosis of primary CLL cells. A few studies have also shown that CLL cells are protected from drug-induced apoptosis by co-culture with CD40L (Hayden et al., 2009; 2010; Kater et al., 2004; Kitada et al., 1999; Vogler et al., 2009). The viability data presented in this Chapter suggests that CD40L co-culture

alters the effects caused by TP10-p50i. It is possible that TP10-p50i disturbs the cellular membrane in a way that is further aggravated by the processing of the sample for Annexin-V/PI measurement (i.e. centrifugation), leading to apoptosis induction and the reduced levels of viability presented in Chapter 4. In section 5.4.3, an extra step was introduced that included 24 hours of CD40L-expressing co-culture. It is possible that during this 24-hour period the cells are capable of reversing the effects of TP10-p50i on the cellular membrane. This process may or may not be directly related to CD40L stimulation.

Another key finding was the potential of using cell surface markers, as an indirect measure of NF-κB inhibition. As part of this Chapter, an analysis of the expression of CD25, CD49d, CD38 and CD69 in 17 CLL patient samples was performed. By treating primary CLL cells with 5 μM of BAY 11-7082, and then co-culturing them for a period of 24 hours with CD40L-expressing fibroblasts, it was possible to determine the relative importance of NF-κB activation and inhibition on the expression of the four proteins.

Of the four cell surface markers investigated, only CD69 showed increased expression following co-culture with CD40L and down-regulation when pre-treated with BAY 11-7082 within 24 hours. In keeping with these findings, previous studies have shown increased expression of CD69 following co-culture with CD40L-expressing fibroblasts (Hamilton et al., 2012; Kitada et al., 1999). CLL cells pre-treated with BAY 11-7082 showed the down regulation of CD69 expression to levels lower than unstimulated untreated cells. A rapid down regulation of CD69 expression has also been showed in invariant natural killer T-cells (iNKT) treated with 1 μM of BAY 11-7082 for a period of 30 minutes, followed by culture with an activation stimuli for 24 hours (Lin et al., 2013). In fact, transcriptional down regulation of CD69 by treatment with BAY 11-7082 for one hour, has been shown previously in other cell types (Mori et al., 2011; Ottosson-Wadlund et al., 2014). This demonstrates that CD69 can be used as a readout to study NF-κB inhibition, due to its rapid expression and dependence on NF-κB activity. Furthermore, expression of CD69 proved to be valuable in showing that apoptosis caused by TP10-p50i was not linked to NF-κB inhibition, as it did not alter CD69 expression.

Similarly to CD69, CD25 also showed increased expression following co-culture with CD40L. The use of anti-CD40 antibodies has been previously described to up-regulate expression of CD25 in human tonsillar B-cells in a 24-hour culture system (Burlinson et al., 1996; 1995). A similar increase in CD25 expression has also been reported in CLL cells cultured with soluble CD40 for a period of 4 days (Ghamlouch et al., 2014).

However, both culture systems included soluble cytokines such as IL-4, which has been shown to up-regulate CD25 on its own (Burlinson et al., 1995; Butcher et al., 1990; Ghamlouch et al., 2014). Data found in section 5.4.2 refers to cells cultured solely with CD40L-expressing fibroblasts, demonstrating that CD40 engagement is sufficient to induce an increased CD25 expression. DNA-binding studies showed that the CD25 gene possesses a κB site that acts as a promoter for transcription, so it is probable that NF-κB activation by CD40 engagement is responsible for the up-regulation of this cell surface marker (Ballard et al., 1988; Lowenthal et al., 1989). However, BAY 11-7082, an NF-κB inhibitor, had no effect on the expression of this marker in the majority of the CLL samples analysed. A study performed by Lee and colleagues, showed that down-regulation of CD25 in iNKT by treatment with 10 μM BAY 11-7082 occurred within 3 hours (Lee et al., 2009). This indicates that a longer exposure to this compound, and possibly higher concentrations, would have been required to see an effect on this cell marker. It is very likely that no effects would be seen on CD25 expression in CLL cells treated with TP10-p50i, as BAY 11-7082 is a stronger and more consistent inhibitor of NF-κB.

The other two cell surface markers tested were CD38 and CD49d. However, expression of these markers was not altered upon stimulation with CD40L for a period of 24 hours. Although their expression has been shown to be altered by co-culture with CD40L-expressing fibroblasts (Hamilton et al., 2012), in the study presented in section 5.4.2, up-regulation seems to require longer exposure to CD40L stimulation than 24 hours. A direct measure of gene expression, for example qPCR (quantitative polymerase chain reaction) could be used to determine transcriptional regulation of the cell surface markers with longer turnover periods, such as CD25, CD49d and CD38 (Buggins et al., 2010).

In conclusion, the work described in this Chapter has investigated the effects of TP10-p50i on three distinct measures of NF-κB activity. The results generated and discussed here, do not support the hypothesis that CLL cell apoptosis caused by TP10-p50i is a direct consequence of NF-κB inhibition.

Chapter 6 - General discussion and conclusion

Key Findings

The following key findings were demonstrated in this thesis:

1) All of the five CPPs studied entered primary CLL cells. Cationic peptides, in particular FFR8, showed the highest level of cell entry. Based on confocal microscopic evidence of intracellular distribution, the mechanisms of entry of the CPPs were distinct. For example, TP10 appeared to be taken up via the endocytic pathway but over time it demonstrated the ability to escape vesicles and allowed release of fluorescence within the cytosol.
2) The NF-κB targeting peptides TP10-p50i and TP10-p65i induced the death of primary CLL cells, primary non-malignant lymphocytes and the Jurkat T-cell line at concentrations lower than 10 μM.
3) Mechanistically, TP10-p50i and TP10-p65i were capable of inhibiting NF-κB in some CLL samples but not others. This appeared to be independent of basal or inducible NF-κB expression levels.
4) The apoptotic cell death induced by TP10-p50i and TP10-p65i appeared to be independent of NF-κB inhibition.
5) The reduced NF-κB binding activity did not translate into a decrease in expression of CD69, a protein induced by CD40L stimulation and inhibited by a pharmacological inhibitor of NF-κB (BAY 11-7082).

Uptake comparison studies

The initial step of this project was a comparative study of five CPPs, focusing on their uptake and intracellular distribution in primary CLL cells. To achieve this, the five CPPs were tagged with the fluorochrome Alexa488, and analysed by flow cytometry and confocal microscopy. The use of two techniques to assess CPP uptake provided two layers of information: quantitative evaluation of the uptake of each of the CPPs and an assessment of their intracellular localisation. The combined used of these two techniques overcame the fact that flow cytometry does not allow distinction between membrane-bound and internalised peptide. Whilst confocal microscopy provided

valuable information regarding the cellular localisation of the peptide, it did not allow discrimination between intact or degraded peptide. However, since the fluorescent cargo was successfully delivered to cells, the unknown condition of the peptide within the cell was not detrimental to the study and did not receive further attention.

The most interesting finding of the comparison studies was the large difference in uptake when small changes in the CPP sequence were made. As is now widely known, altering the amino acid sequence of the peptide can have either a positive or negative impact on uptake. As seen by the data presented in Chapter 3, the addition of phenylalanine residues to the N-terminal of R8 increased the ability of the peptide to be taken up by cells. The use of a fluorochrome or other cargo can therefore also have a great impact, not only on the uptake pattern but also on entry route, as seen in other studies (Fischer et al., 2002). Performing comparative studies to aid the choice of CPP to carry a different a cargo may therefore not seem useful as the inhibiting CPPs have the potential to behave in a different manner. However, it is not possible to predict with certainty how they will behave under specific conditions and this is where comparison studies can provide an insight. The obvious choice of CPP to link with an NF-κB inhibitory peptide cargo after the flow cytometry analysis of fluorescence was FFR8. This CPP was able to deliver the highest amounts of fluorescence into the cells and so appeared to be taken up most readily by CLL cells. However, confocal microscopy revealed TP10's most interesting characteristic: the capacity to overcome vesicle entrapment over time. This offered the potential for a slower, but more sustained, release of NF-κB inhibitory peptide, which may have therapeutic benefits. With the two best CPPs chosen, the next step was to determine if the novel CPPs were capable of inducing apoptosis (Chapter 4). Surprisingly, the most effective CPP to deliver fluorescence to CLL cells was not the most effective at inducing a pro-apoptotic response. This, however, does not invalidate the results obtained in the comparative studies. Instead, it highlighted the effects produced by the cargo on the uptake of a peptide.

The effects of TP10-p50 on primary CLL cells

Two novel CPPs were developed, TP10-p50i and TP10-p65i, which were capable of inducing the death of CLL cells at concentrations lower than 10 μM. The hypothesis was that these would cause CLL cell death by targeting the NF-κB pathway. Putting the

work of this thesis together suggests that TP10-p50i causes cell death without targeting NF-κB. This conclusion is based on the following results:

a. The cytotoxic effects were observed following one hour of peptide treatment.
b. TP10-p50i caused the death of primary B and T-cells which lack detectable NF-κB activity
c. Variability in the effects of TP10p50i on NF-κB DNA binding was observed, while variation in susceptibility to cell death was not.
d. The expression of CD69 was not altered, suggesting that TP10-p50i could not effectively to modulate NF-κB.

It seems likely that cell death caused by TP10-p50i, and possibly by TP10-p65i, was caused by peptide-mediated membrane disruption. An indication of this was the ability of CLL cells to recover from the exposure to TP10-p50i when cultured with CD40L-expressing fibroblasts (section 5.4.2). Although co-culture with CD40L has been shown to protect CLL cells from apoptosis when cultured *in vitro*, it was not capable of rescuing dead cells or cells in an advanced apoptotic state. It is known that as a result of membrane interactions between the CPP and the cellular membrane, non-specific cytotoxicity can be observed (Saar et al., 2005). It is possible that culture with TP10-p50i induces conformation changes in the membrane as the amino acids of the peptide interact with the phospholipid bilayer. These changes might not be enough to induce non-specific cell death, but enough to destabilise the membrane. If cells are removed from culture and processed for apoptotic assays, such as Annexin-V that includes a centrifugation step, the membrane changes caused by TP10-p50i plus the stress caused by high speed centrifugation can possibly induce apoptosis. The nurturing environment provided by co-culture with CD40L-expressing fibroblasts could reverse the membrane disturbing effects of TP10-p50i and allow CLL cells to recover, an effect that may or may not be dependent on CD40 signalling.

The combination of TP10 and p50i seemed to cause cell death by membrane disruption, an effect that was not evident with TP10-Alex488. A similar effect has previously been shown with the use of R8 and the pro-apoptotic domain (PAD) peptide, where the combination of the two sequences generated a peptide with non-specific cytotoxicity (Watkins et al., 2009a). As additional experiments, it would be interesting to measure apoptosis levels during the course of co-culture with NTL and CD40L-expressing fibroblasts. This would help to understand if the cause of reduced viability was due to co-culture specifically with CD40L, and it would provide insight into how

long CLL cells require to overcome the membrane destabilisation induced by TP10-p50i.

NF-κB activation by CD40L and CpG

An interesting finding of this project was the response of CLL cells, regarding NF-κB activation, to stimuli such as CD40L and CpG. Regardless of basal levels of NF-κB activity, culture with CpG or co-culture with CD40L-expressing fibroblasts, invariably resulted in increased NF-κB activity. Previous work has shown that NF-κB activation is closely linked to the microenvironment stimuli. Included in these stimuli are interactions with stromal cells (Edelmann et al., 2008), activation of the TNF receptor family members (Endo et al., 2007; Munzert et al., 2002), activation of the BCR (Caligaris-Cappio et al., 2009), activation of the CD40 receptor (Furman et al., 2000) and activation of TLRs (Arvaniti et al., 2011; Caligaris-Cappio et al., 2009). The work presented here demonstrated that stimulation with CpG or CD40L for a period of one hour was sufficient to induce a clear increase in NF-κB binding activity. This demonstrated that although heterogeneous basal NF-κB expression was commonly observed, stimulation with CD40L or CpG can consistently increase NF-κB activity in CLL cells.

Choosing adequate CPP controls

The use of appropriate controls is a vital part of every experiment, as these are designed to minimise the effects of variables other then the test variable. Although in the majority of experiments choosing a control is a straight forward task, in the case of CPPs this requires careful thought and possibly a few extra experiments until the right control can be determined. As this work has shown in Chapter 3, altering the sequence of a CPP can have a strong impact on uptake. Ideally, the control peptide would have the same sequence as the parent peptide, with the exception of a functional residue or segment that would be mutated or inexistent. In the case of TP10-p50i, the p50i portion contained the NLS and therefore was the functional segment of the CPP. Using TP10 on its own would then be the ideal control. Due to availability of TP10-Alexa488, this CPP was used as a control as seen in section 4.3. This peptide proved to be a good control, as it did not cause cell death up to a concentration of 50 μM. In the case of the FFR8 peptides, the FFR8-Alexa488 proved to be more toxic to CLL cells than FFR8-

p50i and FFR8-p65i. This showed that one type of control might be perfect to validate the results of one CPP but it might not be suitable for others. Considering the knowledge obtained in the studies presented in Chapter 5, cell death induced by TP10-p50i was non-specific, indicating that the combination of TP10 with the p50i sequence was lethal to CLL cells. It would be interesting to test a variety of CPPs with the same sequence as TP10-p50i, each with a mutation in a different residue of the p50i sequence. This would validate the data presented in Chapter 5, as the most likely outcome of this experiment would be that all control CPPs would cause non-specific cell death. However, such results are not possible to predict. In fact, it could potentially result in the discovery of a new CPP with better properties than the parent peptide, as seen in other studies (El-Andaloussi et al., 2007).

The future of NF-κB targeting

Constitutive activation of the NF-κB pathway continues to be a characteristic of CLL. And as a regulator of survival and proliferation pathways, it remains an attractive target for anti-tumoural therapy. Even though NF-κB expression in CLL is heterogeneous, this work confirmed that CLL cells respond well to environment stimuli such as CD40L and CpG, inducing increased NF-κB activity. This reinforced the importance of this pathway in the survival of CLL cells.

However, the landscape in CLL treatment has recently changed as Gazyva, a third generation anti-CD20 monoclonal antibodies (also known as GA101 or Obinutuzumab), has been approved by the FDA to be used as therapy in previously untreated CLL (F. Hoffmann-La Roche Ltd, 2013). Other agents, such as Ibrutinib (Btk inhibitor) and Idelalisib (PI3Kδ inhibitor), have also entered clinical trials and shown promising results in the treatment of CLL (Byrd et al., 2013; Furman et al., 2014). Therefore, it is unlikely that a new NF-κB inhibitor will be used to target CLL. Nevertheless, NF-κB plays an important role in other B-cell malignancies, such as multiple myeloma (Demchenko & Kuehl, 2010). In such malignancies, a NF-κB inhibitor could be an efficient therapeutic approach.

The potential of using CPPs as delivery vectors of a cargo targeting NF-κB should not be overlooked, as it remains a very attractive tool for targeted therapy. Although the CPPs developed in this work did not directly inhibited NF-κB, there are others that have succeeded (Lin et al., 1995; Takada et al., 2004; Wang et al., 2011). However, few of

these inhibitors present NF-κB specificity. Therefore, future work should focus on the development of NF-κB inhibiting CPPs with improved efficacy and specificity. In the context of CLL and other B-cell malignancies, it would be important to determine what stimuli contribute to the increased activity of NF-κB. Further understanding could lead to the development of NF-κB inhibitors with increased specificity and improve the therapeutic options. As NF-κB activation contributes to resistance to chemotherapy in some malignancies, the combination of CPPs targeting the NF-κB pathway with other agents presents as a promising therapeutic tool.

As for CPP therapeutics beyond CLL and NF-κB, the BMI BH3 peptide that targets the anti-apoptotic protein Bcl-2 in acute myeloid leukaemia, has shown promising results (LaBelle et al., 2012). Beyond cancer treatment, a few CPPs have entered clinical trials. AZX100, a smooth muscle relaxer (Flynn et al., 2010); RT001 and RT002, a topical and injectable formulation of Botulinum Toxin (Revance Therapeutics, n.d.); KAI-9803, a protein kinase C inhibitor (Miyaji et al., 2011); and XG-102, a c-Jun N-terminal kinase (JNK) inhibitor (Reinecke et al., 2012) are a few examples. These demonstrate the potential of CPPs as vectors of therapeutic agents.

References

Abes, S., Moulton, H.M., Clair, P., Prevot, P., Youngblood, D.S., Wu, R.P., Iversen, P.L. & Lebleu, B. (2006). Vectorization of morpholino oligomers by the (R-Ahx-R)4peptide allows efficient splicing correction in the absence of endosomolytic agents. *Journal of controlled release : official journal of the Controlled Release Society*. 116 (3). pp. 304–313.

Advani, R.H., Buggy, J.J., Sharman, J.P., Smith, S.M., Boyd, T.E., Grant, B., Kolibaba, K.S., Furman, R.R., Rodriguez, S., Chang, B.Y., Sukbuntherng, J., Izumi, R., Hamdy, A., Hedrick, E. & Fowler, N.H. (2013). Bruton Tyrosine Kinase Inhibitor Ibrutinib (PCI-32765) Has Significant Activity in Patients With Relapsed/Refractory B-Cell Malignancies. *Journal of Clinical Oncology*. 31 (1). pp. 88–94.

Aggarwal, S., Takada, Y., Ichikawa, H., Sandur, S.K., Shishodia, S. & Aggarwal, B.B. (2006). Curcumin (diferuloylmethane) down-regulates expression of cell proliferation and antiapoptotic and metastatic gene products through suppression of IkappaBalpha kinase and Akt activation. *Molecular Pharmacology*. 69 (1). pp. 195–206.

Agou, F., Courtois, G., Chiaravalli, J., Baleux, F., Coïc, Y.-M., Traincard, F., Israël, A. & Véron, M. (2004). Inhibition of NF-kappa B activation by peptides targeting NF-kappa B essential modulator (nemo) oligomerization. *The Journal of biological chemistry*. 279 (52). pp. 54248–54257.

Al-Taei, S., Penning, N.A., Simpson, J.C., Futaki, S., Takeuchi, T., Nakase, I. & Jones, A.T. (2006). Intracellular traffic and fate of protein transduction domains HIV-1 TAT peptide and octaarginine. Implications for their utilization as drug delivery vectors. *Bioconjugate Chemistry*. 17 (1). pp. 90–100.

Amantana, A., Moulton, H.M., Cate, M.L., Reddy, M.T., Whitehead, T., Hassinger, J.N., Youngblood, D.S. & Iversen, P.L. (2007). Pharmacokinetics, biodistribution, stability and toxicity of a cell-penetrating peptide-morpholino oligomer conjugate. *Bioconjugate Chemistry*. 18 (4). pp. 1325–1331.

Arakawa, T., Nakamura, M., Yoshimoto, T. & Yamamoto, S. (1995). The transcriptional regulation of human arachidonate 12-lipoxygenase gene by NFκB/Rel. *FEBS Letters*. 363 (1). pp. 105–110.

Araki, D., Takayama, K., Inoue, M., Watanabe, T., Kumon, H., Futaki, S., Matsui, H. & Tomizawa, K. (2010). Cell-penetrating d-Isomer Peptides of p53 C-terminus: Long-term Inhibitory Effect on the Growth of Bladder Cancer. *URL*. 75 (4). pp. 813–819.

Arenzana-Seisdedos, F., Thompson, J., Rodriguez, M.S., Bachelerie, F., Thomas, D. & Hay, R.T. (1995). Inducible Nuclear Expression of Newly Synthesized I-Kappa-B-Alpha Negatively Regulates Dna-Binding and Transcriptional Activities of Nf-Kappa-B. *Molecular and Cellular Biology*. 15 (5). pp. 2689–2696.

Arenzana-Seisdedos, F., Turpin, P., Rodriguez, M., Thomas, D., Hay, R.T., Virelizier, J.L. & Dargemont, C. (1997). Nuclear localization of I kappa B alpha promotes active transport of NF-kappa B from the nucleus to the cytoplasm. *Journal of Cell Science*. 110 (3). pp. 369–378.

Arrighi, R.B.G., Langel, Ü., Ebikeme, C., Jiang, Y., Ranford-Cartwright, L., Barrett, M.P. & Faye, I. (2008). Cell-penetrating peptide TP10 shows broad-spectrum activity against both Plasmodium falciparum and Trypanosoma brucei brucei. *Antimicrobial Agents and*

Chemotherapy. 52 (9). pp. 3414–3417.

Arvaniti, E., Caligaris-Cappio, F.F., Ntoufa, S., Papakonstantinou, N., Touloumenidou, T., Laoutaris, N., Anagnostopoulos, A., Lamnissou, K., Stamatopoulos, K., Ghia, P., Muzio, M. & Belessi, C. (2011). Toll-like receptor signaling pathway in chronic lymphocytic leukemia: distinct gene expression profiles of potential pathogenic significance in specific subsets of patients. *Haematologica*. 96 (11). pp. 1644–1652.

Baeuerle, P.A. & Baltimore, D. (1988). Activation of DNA-binding activity in an apparently cytoplasmic precursor of the NF-κB transcription factor. *Cell*. 53 (2). pp. 211–217.

Bagnara, D., Kaufman, M.S., Calissano, C., Marsilio, S., Patten, P.E.M., Simone, R., Chum, P., Yan, X.-J., Allen, S.L., Kolitz, J.E., Baskar, S., Rader, C., Mellstedt, H., Rabbani, H., Lee, A., Gregersen, P.K., Rai, K.R. & Chiorazzi, N. (2011). A novel adoptive transfer model of chronic lymphocytic leukemia suggests a key role for T lymphocytes in the disease. *Blood*. 117 (20). pp. 5463–5472.

Bakalkin, G., Yakovleva, T. & Terenius, L. (1994). Prodynorphin gene expression relates to NF-κB factors. *Molecular Brain Research*. 24 (1-4). pp. 301–312.

Balatti, V., Bottoni, A., Palamarchuk, A., Alder, H., Rassenti, L.Z., Kipps, T.J., Pekarsky, Y. & Croce, C.M. (2012). NOTCH1 mutations in CLL associated with trisomy 12. *Blood*. 119 (2). pp. 329–331.

Balistreri, C.R., Candore, G., Accardi, G., Colonna-Romano, G. & Lio, D. (2013). NF-κB pathway activators as potential ageing biomarkers: targets for new therapeutic strategies. *Immunity and Ageing*. 10 (1). pp. 24–24.

Ballard, D.W., Böhnlein, E., Lowenthal, J.W., Wano, Y., Franza, B.R. & Greene, W.C. (1988). HTLV-I tax induces cellular proteins that activate the kappa B element in the IL-2 receptor alpha gene. *Science*. 241 (4873). pp. 1652–1655.

Baltimore, D. & Beg, A.A. (1995). DNA-binding proteins. A butterfly flutters by. *Nature*. 373 (6512). pp. 287–288.

Banchereau, J. & Rousset, F. (1991). Growing human B lymphocytes in the CD40 system. *Nature*. 353 (6345). pp. 678–679.

Banchereau, J., De Paoli, P., Valle, A., Garcia, E. & Rousset, F. (1991). Long-Term Human B-Cell Lines Dependent on Interleukin-4 and Antibody to Cd40. *Science*. 251 (4989). pp. 70–72.

Banno, T., Gazel, A. & Blumenberg, M. (2005). Pathway-specific profiling identifies the NF-kappa B-dependent tumor necrosis factor alpha-regulated genes in epidermal keratinocytes. *The Journal of biological chemistry*. 280 (19). pp. 18973–18980.

Baudot, A.D., Jeandel, P.Y., Mouska, X., Maurer, U., Tartare-Deckert, S., Raynaud, S.D., Cassuto, J.P., Ticchioni, M. & Deckert, M. (2009). The tyrosine kinase Syk regulates the survival of chronic lymphocytic leukemia B cells through PKC delta and proteasome-dependent regulation of Mcl-1 expression. *Oncogene*. 28 (37). pp. 3261–3273.

Bánóczi, Z., Gorka-Kereskényi, A. & Reményi, J. (2010). Synthesis and in Vitro Antitumor Effect of Vinblastine Derivative– Oligoarginine Conjugates. *Bioconjugate ….*

Beinke, S. & Ley, S. (2004). *Functions of NF-kappaB1 and NF-kappaB2 in immune cell biology*. 382 (2). p. 393. Available from: http://www.biochemj.org/bj/382/bj3820393.htm.

Berberich, I., Shu, G.L. & Clark, E.A. (1994). Cross-linking CD40 on B cells rapidly activates nuclear factor-kappa B. *Journal of immunology (Baltimore, Md. : 1950)*. 153 (10). pp. 4357–4366.

Bergwelt-Baildon, von, M., Maecker, B., Schultze, J. & Gribben, J.G. (2004). CD40 activation: Potential for specific immunotherapy in B-CLL. *Annals of Oncology*. 15 (6). pp. 853–857.

Berlose, J.P., Convert, O., Derossi, D., Brunissen, A. & Chassaing, G. (1996). Conformational and associative behaviours of the third helix of antennapedia homeodomain in membrane-mimetic environments. *European Journal of Biochemistry*. 242 (2). pp. 372–386.

Bernal, A., Pastore, R.D., Asgary, Z., Keller, S.A., Cesarman, E., Liou, H.C. & Schattner, E.J. (2001). Survival of leukemic B cells promoted by engagement of the antigen receptor. *Blood*. 98 (10). pp. 3050–3057.

Binet, J.L., Auquier, A., Dighiero, G., Chastang, C., Piguet, H., Goasguen, J., Vaugier, G., Potron, G., Colona, P., Oberling, F., Thomas, M., Tchernia, G., Jacquillat, C., Boivin, P., Lesty, C., Duault, M.T., Monconduit, M., Belabbes, S. & Gremy, F. (1981). A new prognostic classification of chronic lymphocytic leukemia derived from a multivariate survival analysis. *Cancer*. 48 (1). pp. 198–206.

Boersma, H.H., Kietselaer, B.L.J.H., Stolk, L.M.L., Bennaghmouch, A., Hofstra, L., Narula, J., Heidendal, G.A.K. & Reutelingsperger, C.P.M. (2005). Past, Present, and Future of Annexin A5: From Protein Discovery to Clinical Applications*. *Journal of nuclear medicine*. 46 (12). pp. 2035–2050.

Boisguerin, P., Redt-Clouet, C., Franck-Miclo, A., Licheheb, S., Nargeot, J., Barrère-Lemaire, S. & Lebleu, B. (2011). Systemic delivery of BH4 anti-apoptotic peptide using CPPs prevents cardiac ischemia–reperfusion injuriesin vivo. *Journal of controlled release : official journal of the Controlled Release Society*. 156 (2). pp. 146–153.

Bonizzi, G. & Karin, M. (2004). The two NF-kappaB activation pathways and their role in innate and adaptive immunity. *Trends in immunology*. 25 (6). pp. 280–288.

Bradford, M.M. (1976). A rapid and sensitive method for the quantitation of microgram quantities of protein utilizing the principle of protein-dye binding. *Analytical Biochemistry*. 72 (1-2). pp. 248–254.

Braggio, E., Kay, N.E., VanWier, S., Tschumper, R.C., Smoley, S., Eckel-Passow, J.E., Sassoon, T., Barrett, M., Van Dyke, D.L., Byrd, J.C., Jelinek, D.F., Shanafelt, T.D. & Fonseca, R. (2012). *Longitudinal genome-wide analysis of patients with chronic lymphocytic leukemia reveals complex evolution of clonal architecture at disease progression and at the time of relapse*. 26 (7). pp. 1698–1701.

Brennan, P. & O'Neill, L.A. (1995). Effects of oxidants and antioxidants on nuclear factor kappa B activation in three different cell lines: evidence against a universal hypothesis involving oxygen radicals. *Biochimica et biophysica acta*. 1260 (2). pp. 167–175.

Brocke-Heidrich, K., Ge, B., Cvijic, H., Pfeifer, G., Löffler, D., Henze, C., McKeithan, T.W. & Horn, F. (2006). BCL3 is induced by IL-6 via Stat3 binding to intronic enhancer

HS4 and represses its own transcription. *Oncogene*. 25 (55). pp. 7297–7304.

Brodsky, F.M., Chen, C.Y. & Knuehl, C. (2001). Biological basket weaving: formation and function of clathrin-coated vesicles. *Annual review of cell …*.

Brugnano, J.L., Chan, B.K., Seal, B.L. & Panitch, A. (2011). Cell-penetrating peptides can confer biological function: Regulation of inflammatory cytokines in human monocytes by MK2 inhibitor peptides. *Journal of controlled release : official journal of the Controlled Release Society*. 155 (2). pp. 128–133.

Buggins, A.G.S., Levi, A., Gohil, S., Fishlock, K., Patten, P.E.M., Calle, Y., Yallop, D. & Devereux, S. (2011). Evidence for a macromolecular complex in poor prognosis CLL that contains CD38, CD49d, CD44 and MMP-9. *British Journal of Haematology*. 154 (2). pp. 216–222.

Buggins, A.G.S., Patten, P.E.M., Richards, J., Wotherspoon, A., Salisbury, J., Mufti, G.J., Hamblin, T.J. & Devereux, S. (2008). CD38 expression in chronic lymphocytic leukemia is regulated by the tumor microenvironment. *Blood*. 111 (10). pp. 5173–5181.

Buggins, A.G.S., Pepper, C.C., Patten, P.E.M.P., Hewamana, S., Gohil, S.S., Moorhead, J.J., Folarin, N.N., Yallop, D.D., Thomas, N.S.B.N., Mufti, G.J.G., Fegan, C.C. & Devereux, S.S. (2010). Interaction with vascular endothelium enhances survival in primary chronic lymphocytic leukemia cells via NF-kappaB activation and de novo gene transcription. *Audio, Transactions of the IRE Professional Group on*. 70 (19). pp. 7523–7533.

Bulian, P., Shanafelt, T.D., Fegan, C., Zucchetto, A., Cro, L., Nückel, H., Baldini, L., Kurtova, A.V., Ferrajoli, A., Burger, J.A., Gaidano, G., Del Poeta, G., Pepper, C.J., Rossi, D. & Gattei, V. (2014). CD49d is the strongest flow cytometry-based predictor of overall survival in chronic lymphocytic leukemia. *Journal of Clinical Oncology*. 32 (9). pp. 897–904.

Burger, J.A. (2011). Nurture versus nature: the microenvironment in chronic lymphocytic leukemia. *Hematology / the Education Program of the American Society of Hematology. American Society of Hematology. Education Program*. 2011. pp. 96–103.

Burger, J.A., Quiroga, M.P., Hartmann, E., Bürkle, A., Wierda, W.G., Keating, M.J. & Rosenwald, A. (2009). High-level expression of the T-cell chemokines CCL3 and CCL4 by chronic lymphocytic leukemia B cells in nurselike cell cocultures and after BCR stimulation. *Blood*. 113 (13). pp. 3050–3058.

Burger, J.A.J. & Kipps, T.J.T. (2006). CXCR4: a key receptor in the crosstalk between tumor cells and their microenvironment. *Blood*. 107 (5). pp. 1761–1767.

Burger, J.A.J., Burger, M.M. & Kipps, T.J.T. (1999). Chronic lymphocytic leukemia B cells express functional CXCR4 chemokine receptors that mediate spontaneous migration beneath bone marrow stromal cells. *Blood*. 94 (11). pp. 3658–3667.

Burke, J.R., Pattoli, M.A., Gregor, K.R., Brassil, P.J., MacMaster, J.F., McIntyre, K.W., Yang, X., Iotzova, V.S., Clarke, W., Strnad, J., Qiu, Y. & Zusi, F.C. (2003). BMS-345541 is a highly selective inhibitor of I kappa B kinase that binds at an allosteric site of the enzyme and blocks NF-kappa B-dependent transcription in mice. *The Journal of biological chemistry*. 278 (3). pp. 1450–1456.

Burlinson, E.L., Graber, P., Bonnefoy, J.Y., Ozanne, B.W. & Cushley, W. (1996). Soluble CD40 ligand induces expression of CD25 and CD23 in resting human tonsillar

B lymphocytes. *European Journal of Immunology*. 26 (5). pp. 1069–1073.

Burlinson, E.L., Pringle, H.M., Ozanne, B.W. & Cushley, W. (1995). Anti-immunoglobulin and anti-CD40 stimulation induces CD25 expression by resting human tonsillar B lymphocytes. *Immunology Letters*. 45 (1). pp. 93–98.

Burns, K., Janssens, S., Brissoni, B., Olivos, N., Beyaert, R. & Tschopp, J. (2003). Inhibition of interleukin 1 receptor/toll-like receptor signaling through the alternatively spliced, short form of MyD88 is due to its failure to recruit IRAK-4. *Journal of Experimental Medicine*. 197 (2). pp. 263–268.

Burrer, R., Neuman, B.W., Ting, J.P.C., Stein, D.A., Moulton, H.M., Iversen, P.L., Kuhn, P. & Buchmeier, M.J. (2007). Antiviral effects of antisense morpholino oligomers in murine coronavirus infection models. *Journal of Virology*. 81 (11). pp. 5637–5648.

Butcher, R.D.J., McGarvie, G.M. & Cushley, W. (1990). Recombinant interleukin-4 promotes expression of the CD25 (Tac) antigen at the plasma membrane of high-density human tonsillar B lymphocytes. *Immunology*. 69 (1). pp. 57–64.

Bürkle, A., Niedermeier, M., Schmitt-Gräff, A., Wierda, W.G., Keating, M.J. & Burger, J.A. (2007). Overexpression of the CXCR5 chemokine receptor, and its ligand, CXCL13 in B-cell chronic lymphocytic leukemia. *Blood*. 110 (9). pp. 3316–3325.

Byrd, J.C., Furman, R.R., Coutre, S.E., Flinn, I.W., Burger, J.A., Blum, K.A., Grant, B., Sharman, J.P., Coleman, M., Wierda, W.G., Jones, J.A., Zhao, W., Heerema, N.A., Johnson, A.J., Sukbuntherng, J., Chang, B.Y., Clow, F., Hedrick, E., Buggy, J.J., James, D.F. & O'Brien, S.M. (2013). Targeting BTK with ibrutinib in relapsed chronic lymphocytic leukemia. *New England Journal of Medicine*. 369 (1). pp. 32–42.

Caligaris-Cappio, F.F. (2003). Role of the microenvironment in chronic lymphocytic leukaemia. *British Journal of Haematology*. 123 (3). pp. 380–388.

Caligaris-Cappio, F.F., Scielzo, C., Muzio, M., Bertilaccio, M.T.S., Frenquelli, M. & Ghia, P. (2009). Expression and function of toll like receptors in chronic lymphocytic leukaemia cells. *British Journal of Haematology*. 144 (4). pp. 507–516.

Calin, G.A., Dumitru, C.D., Shimizu, M., Bichi, R., Zupo, S., Noch, E., Aldler, H., Rattan, S., Keating, M., Rai, K., Rassenti, L., Kipps, T., Negrini, M., Bullrich, F. & Croce, C.M. (2002). Frequent deletions and down-regulation of micro- RNA genes miR15 and miR16 at 13q14 in chronic lymphocytic leukemia. *Proceedings of the National Academy of Sciences*. 99 (24). pp. 15524–15529.

Calpe, E., Codony, C., Baptista, M.J., Abrisqueta, P., Carpio, C., Purroy, N., Bosch, F. & Crespo, M. (2011). ZAP-70 enhances migration of malignant B lymphocytes toward CCL21 by inducing CCR7 expression via IgM-ERK1/2 activation. *Blood*. 118 (16). pp. 4401–4410.

Cao, S., Zhang, X., Edwards, J.P. & Mosser, D.M. (2006). NF-kappaB1 (p50) homodimers differentially regulate pro- and anti-inflammatory cytokines in macrophages. *The Journal of biological chemistry*. 281 (36). pp. 26041–26050.

Capobianco, A.J., Chang, D., Mosialos, G. & Gilmore, T.D. (1992). p105, the NF-kappa B p50 precursor protein, is one of the cellular proteins complexed with the v-Rel oncoprotein in transformed chicken spleen cells. *Journal of Virology*. 66 (6). pp. 3758–3767.

Carminati, P., Gallo, G., Fantò, N., Ruggiero, V., Sassano, M. & Mastroianni, D. (2006). *MYD88 HOMODIMERIZATION INHIBITORS*.

Caruso, A., Licenziati, S., Corulli, M., Canaris, A.D., De Francesco, M.A., Fiorentini, S., Peroni, L., Fallacara, F., Dima, F., Balsari, A. & Turano, A. (1997). Flow cytometric analysis of activation markers on stimulated T cells and their correlation with cell proliferation. *Cytometry*. 27 (1). pp. 71–76.

Carvalho, G., Fabre, C., Braun, T., Grosjean, J., Ades, L., Agou, F., Tasdemir, E., Boehrer, S., Israel, A., Véron, M., Fenaux, P. & Kroemer, G. (2007). Inhibition of NEMO, the regulatory subunit of the IKK complex, induces apoptosis in high-risk myelodysplastic syndrome and acute myeloid leukemia. *Oncogene*. 26 (16). pp. 2299–2307.

Catz, S.D. & Johnson, J.L. (2001). Transcriptional regulation of bcl-2 by nuclear factor κB and its significance in prostate cancer. *Oncogene*.

Chen, F.E., Huang, D.B., Chen, Y.Q. & Ghosh, G. (1998). Crystal structure of p50/p65 heterodimer of transcription factor NF-kappaB bound to DNA. *Nature*. 391 (6665). pp. 410–413.

Chen, H.J., Treweeke, A.T., West, D.C., Till, K.J., Cawley, J.C., Zuzel, M. & Toh, C.H. (2000). In vitro and in vivo production of vascular endothelial growth factor by chronic lymphocytic leukemia cells. *Blood*. 96 (9). pp. 3181–3187.

Chen, J.X., Xu, X.D. & Chen, W.H. (2013). Multi-Functional Envelope-Type Nanoparticles Assembled from Amphiphilic Peptidic Prodrug with Improved Anti-Tumor Activity. *ACS applied materials & ….*

Chen, L., Huynh, L., Apgar, J., Tang, L., Rassenti, L., Weiss, A. & Kipps, T.J. (2008). ZAP-70 enhances IgM signaling independent of its kinase activity in chronic lymphocytic leukemia. *Blood*. 111 (5). pp. 2685–2692.

Chen, L., Widhopf, G., Huynh, L., Rassenti, L., Rai, K.R., Weiss, A. & Kipps, T.J. (2002). Expression of ZAP-70 is associated with increased B-cell receptor signaling in chronic lymphocytic leukemia. *Blood*. 100 (13). pp. 4609–4614.

Chiorazzi, N. (2012). Implications of new prognostic markers in chronic lymphocytic leukemia. *Hematology / the Education Program of the American Society of Hematology. American Society of Hematology. Education Program*. 2012. pp. 76–87.

Chiorazzi, N. & Burger, J.A. (2013). B cell receptor signaling in chronic lymphocytic leukemia. *Trends in immunology*.

Chiorazzi, N. & Ferrarini, M. (2011). Cellular origin(s) of chronic lymphocytic leukemia: cautionary notes and additional considerations and possibilities. *Blood*. 117 (6). pp. 1781–1791.

Chiorazzi, N., Damle, R.N., Ghiotto, F., Valetto, A., Albesiano, E., Fais, F., Yan, X.-J., Sison, C.P., Allen, S.L., Kolitz, J., Schulman, P., Vinciguerra, V.P., Budde, P., Frey, J., Rai, K.R. & Ferrarini, M. (2002). B-cell chronic lymphocytic leukemia cells express a surface membrane phenotype of activated, antigen-experienced B lymphocytes. *Blood*. 99 (11). pp. 4087–4093.

Chiorazzi, N., Rai, K.R. & Ferrarini, M. (2005). Chronic Lymphocytic Leukemia. *New England Journal of Medicine*. 352 (8). pp. 804–815.

Choi, M., Rolle, S., Wellner, M., Cardoso, M.C., Scheidereit, C., Luft, F.C. & Kettritz, R. (2003). Inhibition of NF-kappaB by a TAT-NEMO-binding domain peptide accelerates constitutive apoptosis and abrogates LPS-delayed neutrophil apoptosis. *Blood*. 102 (6). pp. 2259–2267.

Chu, Z.L., McKinsey, T.A., Liu, L., Gentry, J.J., Malim, M.H. & Ballard, D.W. (1997). Suppression of tumor necrosis factor-induced cell death by inhibitor of apoptosis c-IAP2 is under NF-kappaB control. *Proceedings of the National Academy of Sciences*. 94 (19). pp. 10057–10062.

Cimmino, A., Calin, G.A., Fabbri, M., Iorio, M.V., Ferracin, M., Shimizu, M., Wojcik, S.E., Aqeilan, R.I., Zupo, S., Dono, M., Rassenti, L., Alder, H., Volinia, S., Liu, C.-G., Kipps, T.J., Negrini, M. & Croce, C.M. (2005). miR-15 and miR-16 induce apoptosis by targeting BCL2. *Proceedings of the National Academy of Sciences*. 102 (39). pp. 13944–13949.

Claudio, E., Brown, K., Park, S., Wang, H. & Siebenlist, U. (2002). BAFF-induced NEMO-independent processing of NF-kappa B2 in maturing B cells. *Nature Immunology*. 3 (10). pp. 958–965.

Contri, A., Brunati, A.M., Trentin, L., Cabrelle, A., Miorin, M., Cesaro, L., Pinna, L.A., Zambello, R., Semenzato, G. & Donella-Deana, A. (2005). Chronic lymphocytic leukemia B cells contain anomalous Lyn tyrosine kinase, a putative contribution to defective apoptosis. *Journal of Clinical Investigation*. 115 (2). pp. 369–378.

Copolovici, D.-M., Langel, K., Eriste, E. & Langel, Ü. (2014). Cell-penetrating peptides: design, synthesis, and applications. *ACS Nano*. 8 (3). pp. 1972–1994.

Cuní, S., Pérez-Aciego, P., Pérez-Chacón, G., Vargas, J.A., Sánchez, A., Martín-Saavedra, F.M., Ballester, S., García-Marco, J., Jordá, J. & Durántez, A. (2004). *A sustained activation of PI3K/NF-kappaB pathway is critical for the survival of chronic lymphocytic leukemia B cells.* 18 (8). pp. 1391–1400. Available from: http://eutils.ncbi.nlm.nih.gov/entrez/eutils/elink.fcgi?dbfrom=pubmed&id=15175625&retmode=ref&cmd=prlinks.

Da Silva, C.A., Heilbock, C., Kassel, O. & Frossard, N. (2003). Transcription of stem cell factor (SCF) is potentiated by glucocorticoids and interleukin-1beta through concerted regulation of a GRE-like and an NF-kappaB response element. *FASEB journal : official publication of the Federation of American Societies for Experimental Biology*. 17 (15). pp. 2334–2336.

Damle, R.N., Chiorazzi, N., Wasil, T.T., Fais, F.F., Ghiotto, F.F., Valetto, A.A., Allen, S.L.S., Buchbinder, A.A., Budman, D.D., Dittmar, K.K., Kolitz, J.J., Lichtman, S.M.S., Schulman, P.P., Vinciguerra, V.P.V., Rai, K.R.K. & Ferrarini, M.M. (1999). Ig V gene mutation status and CD38 expression as novel prognostic indicators in chronic lymphocytic leukemia. *Blood*. 94 (6). pp. 1840–1847.

Danilov, A.V. (2013). Targeted therapy in chronic lymphocytic leukemia: past, present, and future. *Clinical therapeutics*. 35 (9). pp. 1258–1270.

Dave, S.H., Tilstra, J.S., Matsuoka, K. & Li, F. (2007). Amelioration of chronic murine colitis by peptide-mediated transduction of the IκB kinase inhibitor NEMO binding domain peptide. *The Journal of …*.

Deaglio, S. & Malavasi, F. (2009). Chronic lymphocytic leukemia microenvironment:

shifting the balance from apoptosis to proliferation. *Haematologica*. 94 (6). pp. 752–756.

Deaglio, S., Aydin, S., Vaisitti, T., Bergui, L. & Malavasi, F. (2008). CD38 at the junction between prognostic marker and therapeutic target. *Trends in Molecular Medicine*. 14 (5). pp. 210–218.

Deaglio, S., Mallone, R., Baj, G., Arnulfo, A., Surico, N., Dianzani, U., Mehta, K. & Malavasi, F. (2000). CD38/CD31, a Receptor/Ligand System Ruling Adhesion and Signaling in Human Leukocytes. In: *karger.com*. Chemical Immunology and Allergy. Karger, Basel, pp. 99–120.

Deaglio, S., Vaisitti, T., Zucchetto, A., Gattei, V. & Malavasi, F. (2010). CD38 as a molecular compass guiding topographical decisions of chronic lymphocytic leukemia cells. *Seminars in Cancer Biology*. 20 (6). pp. 416–423.

Del Poeta, G., Bulian, P., Del Principe, M.I., Zucchetto, A., Luciano, F., Buccisano, F., Rossi, F.M., Bruno, A., Biagi, A., Maurillo, L., Neri, B., Bomben, R., Simotti, C., Coletta, A.M., Dal Bo, M., de Fabritiis, P., Venditti, A., Gattei, V. & Amadori, S. (2012a). CD69 is independently prognostic in chronic lymphocytic leukemia: a comprehensive clinical and biological profiling study. *Haematologica*. 97 (2). pp. 279–287.

Del Poeta, G., Zucchetto, A., Gattei, V., Vaisitti, T., Benedetti, D., Tissino, E., Bertagnolo, V., Rossi, D., Bomben, R., Dal Bo, M., Del Principe, M.I., Gorgone, A., Pozzato, G., Gaidano, G., Malavasi, F. & Deaglio, S. (2012b). The CD49d/CD29 complex is physically and functionally associated with CD38 in B-cell chronic lymphocytic leukemia cells. *Leukemia*. 26 (6). pp. 1301–1312.

Demchenko, Y.N. & Kuehl, W.M. (2010). A critical role for the NFkB pathway in multiple myeloma. *Oncotarget*. 1 (1). pp. 59–68.

Derossi, D., Calvet, S., Trembleau, A., Brunissen, A., Chassaing, G. & Prochiantz, A. (1996). Cell internalization of the third helix of the Antennapedia homeodomain is receptor-independent. *The Journal of biological chemistry*. 271 (30). pp. 18188–18193.

Dighiero, G. & Hamblin, T.J. (2008). Chronic lymphocytic leukaemia. *The Lancet*.

Dive, C.C., Gregory, C.D.C., Phipps, D.J.D., Evans, D.L.D., Milner, A.E.A. & Wyllie, A.H.A. (1992). Analysis and discrimination of necrosis and apoptosis (programmed cell death) by multiparameter flow cytometry. *Biochimica et Biophysica Acta (BBA) - Bioenergetics*. 1133 (3). pp. 275–285.

Do Carmo, S., Levros, L.-C. & Rassart, E. (2007). Modulation of apolipoprotein D expression and translocation under specific stress conditions. *Biochimica et Biophysica Acta (BBA) - Molecular Cell Research*. 1773 (6). pp. 954–969.

Dobrzanski, P., Ryseck, R.P. & Bravo, R. (1994). Differential interactions of Rel-NF-kappaB complexes with IkappaBalpha determine pools of constitutive and inducible NF-kappaB activity. *The EMBO journal*. 13 (19). pp. 4608–4616.

Dobrzanski, P., Ryseck, R.P. & Bravo, R. (1993). Both N- and C-terminal domains of RelB are required for full transactivation: role of the N-terminal leucine zipper-like motif. *Molecular and Cellular Biology*. 13 (3). pp. 1572–1582.

Dobrzanski, P., Ryseck, R.P. & Bravo, R. (1995). Specific inhibition of RelB/p52 transcriptional activity by the C-terminal domain of p100. *Oncogene*. 10 (5). pp. 1003–

1007.

Doherty, G.J. & McMahon, H.T. (2009). Mechanisms of endocytosis. *Annual review of biochemistry*. 78 (1). pp. 857–902.

Döhner, H., Stilgenbauer, S., Benner, A., Leupolt, E., Kröber, A., Bullinger, L., Döhner, K., Bentz, M. & Lichter, P. (2000). Genomic aberrations and survival in chronic lymphocytic leukemia. *New England Journal of Medicine*. 343 (26). pp. 1910–1916.

Duchardt, F., Fotin-Mleczek, M., Schwarz, H., Fischer, R. & Brock, R. (2007). *A comprehensive model for the cellular uptake of cationic cell-penetrating peptides.* 8 (7). pp. 848–866. Available from: http://eutils.ncbi.nlm.nih.gov/entrez/eutils/elink.fcgi?dbfrom=pubmed&id=17587406&retmode=ref&cmd=prlinks.

Dunkin, C.M., Pokorny, A., Almeida, P.F. & Lee, H.-S. (2011). Molecular dynamics studies of transportan 10 (tp10) interacting with a POPC lipid bilayer. *Journal of Physical Chemistry B*. 115 (5). pp. 1188–1198.

Duyao, M.P., Buckler, A.J. & Sonenshein, G.E. (1990). Interaction of an NF-kappa B-like factor with a site upstream of the c-myc promoter. *Proceedings of the National Academy of Sciences*. 87 (12). pp. 4727–4731.

Edelmann, J., Klein-Hitpass, L., Carpinteiro, A., Führer, A., Sellmann, L., Stilgenbauer, S., Dührsen, U. & Dürig, J. (2008). Bone marrow fibroblasts induce expression of PI3K/NF-kappaB pathway genes and a pro-angiogenic phenotype in CLL cells. *Leukemia Research*. 32 (10). pp. 1565–1572.

Efremov, D.G., Bomben, R., Gobessi, S. & Gattei, V. (2013). TLR9 signaling defines distinct prognostic subsets in CLL. *Frontiers in Bioscience*. 18. pp. 371–386.

El-Andaloussi, S., Johansson, H., Magnusdottir, A., Järver, P., Lundberg, P. & Langel, Ü. (2005). TP10, a delivery vector for decoy oligonucleotides targeting the Myc protein. *Journal of controlled release : official journal of the Controlled Release Society*. 110 (1). pp. 189–201.

El-Andaloussi, S., Johansson, H.J., Holm, T. & Langel, Ü. (2007). A novel cell-penetrating peptide, M918, for efficient delivery of proteins and peptide nucleic acids. *Molecular Therapy*. 15 (10). pp. 1820–1826.

Elder, M.E., Lin, D., Clever, J., Chan, A.C., Hope, T.J., Weiss, A. & Parslow, T.G. (1994). Human severe combined immunodeficiency due to a defect in ZAP-70, a T cell tyrosine kinase. *Science*. 264 (5165). pp. 1596–1599.

Elmquist, A., Lindgren, M., Bartfai, T. & Langel, Ü. (2001). VE-Cadherin-Derived Cell-Penetrating Peptide,pVEC, with Carrier Functions. *Experimental Cell Research*. 269 (2). pp. 237–244.

Endo, T., Nishio, M., Enzler, T., Cottam, H.B., Fukuda, T., James, D.F., Karin, M. & Kipps, T.J. (2007). BAFF and APRIL support chronic lymphocytic leukemia B-cell survival through activation of the canonical NF-kappaB pathway. *Blood*. 109 (2). pp. 703–710.

Enesa, K., Zakkar, M., Chaudhury, H., Le A Luong, Rawlinson, L., Mason, J.C., Haskard, D.O., Dean, J.L.E. & Evans, P.C. (2008). NF-kappaB suppression by the deubiquitinating enzyme Cezanne: a novel negative feedback loop in pro-inflammatory

signaling. *The Journal of biological chemistry*. 283 (11). pp. 7036–7045.

Everett, P.C., Meyers, J.A., Makkinje, A., Rabbi, M. & Lerner, A. (2007). Preclinical assessment of curcumin as a potential therapy for B-CLL. *American Journal of Hematology*. 82 (1). pp. 23–30.

F. Hoffmann-La Roche Ltd (2013). *FDA approves Roche's Gazyva (obinutuzumab) for people with previously untreated chronic lymphocytic leukemia (CLL)*. pp. 1–4.

Fabbri, G., Rasi, S., Rossi, D. & Trifonov, V. (2011). Analysis of the chronic lymphocytic leukemia coding genome: role of NOTCH1 mutational activation. *The Journal of …*.

Faderl, S., Rai, K., Gribben, J., Byrd, J.C., Flinn, I.W., O'Brien, S.M., Sheng, S., Esseltine, D.-L. & Keating, M.J. (2006). Phase II study of single-agent bortezomib for the treatment of patients with fludarabine-refractory B-cell chronic lymphocytic leukemia. *Cancer*. 107 (5). pp. 916–924.

Farahani, M., Treweeke, A.T., Toh, C.H., Till, K.J., Harris, R.J., Cawley, J.C., Zuzel, M. & Chen, H. (2005). Autocrine VEGF mediates the antiapoptotic effect of CD154 on CLL cells. *Leukemia*. 19 (4). pp. 524–530.

Fei, L., Ren, L., Zaro, J.L. & Shen, W.-C. (2011). The influence of net charge and charge distribution on cellular uptake and cytosolic localization of arginine-rich peptides. *Journal of drug targeting*. 19 (8). pp. 675–680.

Fenyo, D., Wang, Q., DeGrasse, J.A., Padovan, J.C., Cadene, M. & Chait, B.T. (2007). MALDI Sample Preparation: the Ultra Thin Layer Method. *Journal of Visualized Experiments*. (3). Available from: http://www.jove.com/index/Details.stp?ID=192.

Ferrajoli, A., Lee, B.-N., Schlette, E.J., O'Brien, S.M., Gao, H., Wen, S., Wierda, W.G., Estrov, Z., Faderl, S., Cohen, E.N., Li, C., Reuben, J.M. & Keating, M.J. (2008). Lenalidomide induces complete and partial remissions in patients with relapsed and refractory chronic lymphocytic leukemia. *Blood*. 111 (11). pp. 5291–5297.

Ferrari, A., Pellegrini, V., Arcangeli, C. & Fittipaldi, A. (2003). Caveolae-mediated internalization of extracellular HIV-1 tat fusion proteins visualized in real time. *Molecular …*.

Fischer, R., Waizenegger, T., Kohler, K. & Brock, R. (2002). A quantitative validation of fluorophore-labelled cell-permeable peptide conjugates: fluorophore and cargo dependence of import. *BBA - Biomembranes*. 1564 (2). pp. 365–374.

Fisher, L., Langel, Ü., Soomets, U., Cortés Toro, V., Chilton, L., Jiang, Y. & Iverfeldt, K. (2004). Cellular delivery of a double-stranded oligonucleotide NFkappaB decoy by hybridization to complementary PNA linked to a cell-penetrating peptide. *Gene therapy*. 11 (16). pp. 1264–1272.

Fittipaldi, A., Ferrari, A., Zoppé, M., Arcangeli, C., Pellegrini, V., Beltram, F. & Giacca, M. (2003). Cell membrane lipid rafts mediate caveolar endocytosis of HIV-1 Tat fusion proteins. *The Journal of biological chemistry*. 278 (36). pp. 34141–34149.

Fletcher, S., Honeyman, K., Fall, A.M., Harding, P.L., Johnsen, R.D., Steinhaus, J.P., Moulton, H.M., Iversen, P.L. & Wilton, S.D. (2007). Morpholino oligomer-mediated exon skipping averts the onset of dystrophic pathology in the mdx mouse. *Molecular Therapy*. 15 (9). pp. 1587–1592.

Flynn, C.R., Cheung-Flynn, J., Smoke, C.C., Lowry, D., Roberson, R., Sheller, M.R. & Brophy, C.M. (2010). Internalization and intracellular trafficking of a PTD-conjugated anti-fibrotic peptide, AZX100, in human dermal keloid fibroblasts. *Journal of Pharmaceutical Sciences*. 99 (7). pp. 3100–3121.

Frankel, A.D. & Pabo, C.O. (1988). Cellular uptake of the tat protein from human immunodeficiency virus. *Cell*.

Franzoso, G., Bours, V., Azarenko, V., Park, S., Tomita-Yamaguchi, M., Kanno, T., Brown, K. & Siebenlist, U. (1993). The oncoprotein Bcl-3 can facilitate NF-kappa B-mediated transactivation by removing inhibiting p50 homodimers from select kappa B sites. *The EMBO journal*. 12 (10). pp. 3893–3901.

Fretz, M.M., Penning, N.A., Al-Taei, S., Futaki, S., Takeuchi, T., Nakase, I., Storm, G. & Jones, A.T. (2007). Temperature-, concentration- and cholesterol-dependent translocation of L- and D-octa-arginine across the plasma and nuclear membrane of CD34+ leukaemia cells. *Biochemical Journal*. 403 (2). pp. 335–342.

Friedrichsen, S., Harper, C.V., Semprini, S., Wilding, M., Adamson, A.D., Spiller, D.G., Nelson, G., Mullins, J.J., White, M.R.H. & Davis, J.R.E. (2006). Tumor necrosis factor-alpha activates the human prolactin gene promoter via nuclear factor-kappaB signaling. *Endocrinology*. 147 (2). pp. 773–781.

Fu, K., Sun, X., Zheng, W., Wier, E.M., Hodgson, A., Tran, D.Q., Richard, S. & Wan, F. (2013). Sam68 modulates the promoter specificity of NF-κB and mediates expression of CD25 in activated T cells. *Nature Communications*. 4. pp. 1909–1909.

Fuchs, O. (2010). Transcription factor NF-κB inhibitors as single therapeutic agents or in combination with classical chemotherapeutic agents for the treatment of hematologic malignancies. *Current molecular pharmacology*. 3 (3). pp. 98–122.

Fujihara, S.M., Cleaveland, J.S., Grosmaire, L.S., Berry, K.K., Kennedy, K.A., Blake, J.J., Loy, J., Rankin, B.M., Ledbetter, J.A. & Nadler, S.G. (2000). A D-amino acid peptide inhibitor of NF-kappa B nuclear localization is efficacious in models of inflammatory disease. *Journal of Immunology*. 165 (2). pp. 1004–1012.

Fujita, T., Nolan, G.P., Liou, H.C. & Scott, M.L. (1993). The candidate proto-oncogene bcl-3 encodes a transcriptional coactivator that activates through NF-kappa B p50 homodimers. *Genes & …*.

Funaro, A., Spagnoli, G.C., Ausiello, C.M., Alessio, M., Roggero, S., Delia, D., Zaccolo, M. & Malavasi, F. (1990). Involvement of the multilineage CD38 molecule in a unique pathway of cell activation and proliferation. *Journal of immunology (Baltimore, Md. : 1950)*. 145 (8). pp. 2390–2396.

Furman, R.R., Asgary, Z., Mascarenhas, J.O., Liou, H.C. & Schattner, E.J. (2000). Modulation of NF-kappa B activity and apoptosis in chronic lymphocytic leukemia B cells. *Journal of immunology (Baltimore, Md. : 1950)*. 164 (4). pp. 2200–2206.

Furman, R.R., Sharman, J.P., Coutre, S.E., Cheson, B.D., Pagel, J.M., Hillmen, P., Barrientos, J.C., Zelenetz, A.D., Kipps, T.J., Flinn, I., Ghia, P., Eradat, H., Ervin, T., Lamanna, N., Coiffier, B., Pettitt, A.R., Ma, S., Stilgenbauer, S., Cramer, P., Aiello, M., Johnson, D.M., Miller, L.L., Li, D., Jahn, T.M., Dansey, R.D., Hallek, M. & O'Brien, S.M. (2014). Idelalisib and rituximab in relapsed chronic lymphocytic leukemia. *New England Journal of Medicine*. 370 (11). pp. 997–1007.

Futaki, S., Nakase, I., Tadokoro, A., Takeuchi, T. & Jones, A.T. (2007). Arginine-rich peptides and their internalization mechanisms. *Biochemical Society transactions*. 35 (Pt 4). pp. 784–787.

Futaki, S., Suzuki, T., Ohashi, W., Yagami, T., Tanaka, S., Ueda, K. & Sugiura, Y. (2001). Arginine-rich peptides. An abundant source of membrane-permeable peptides having potential as carriers for intracellular protein delivery. *The Journal of biological chemistry*. 276 (8). pp. 5836–5840.

Gao, C., Mao, S., Ditzel, H.J., Farnaes, L., Wirsching, P., Lerner, R.A. & Janda, K.D. (2002). A cell-penetrating peptide from a novel pVII-pIX phage-displayed random peptide library. *Bioorganic & Medicinal Chemistry*. 10 (12). pp. 4057–4065.

Gattei, V., Bulian, P., Del Principe, M.I., Zucchetto, A., Maurillo, L., Buccisano, F., Bomben, R., Dal Bo, M., Luciano, F., Rossi, F.M., Degan, M., Amadori, S. & Del Poeta, G. (2008). Relevance of CD49d protein expression as overall survival and progressive disease prognosticator in chronic lymphocytic leukemia. *Blood*. 111 (2). pp. 865–873.

Geeraerts, B., Vanhoecke, B., Berghe, W.V., Philippé, J., Offner, F. & Deforce, D. (2007). Deguelin inhibits expression of IkappaBalpha protein and induces apoptosis of B-CLL cells in vitro. *Leukemia*. 21 (8). pp. 1610–1618.

Ghamlouch, H., Ouled-Haddou, H., Guyart, A., Regnier, A., Trudel, S., Claisse, J.F., Fuentes, V., Royer, B., Marolleau, J.P. & Gubler, B. (2014). Phorbol myristate acetate, but not CD40L, induces the differentiation of CLL B cells into Ab-secreting cells. *Immunology and Cell Biology*.

Ghia, P., Guida, G., Stella, S., Gottardi, D., Geuna, M., Strola, G., Scielzo, C. & Caligaris-Cappio, F.F. (2003). The pattern of CD38 expression defines a distinct subset of chronic lymphocytic leukemia (CLL) patients at risk of disease progression. *Blood*. 101 (4). pp. 1262–1269.

Ghosh, A.K., Kay, N.E., Secreto, C.R. & Shanafelt, T.D. (2009). Curcumin inhibits prosurvival pathways in chronic lymphocytic leukemia B cells and may overcome their stromal protection in combination with EGCG. *Clinical cancer research : an official journal of the American Association for Cancer Research*. 15 (4). pp. 1250–1258.

Ghosh, G., Duyne, G.V., Ghosh, S. & Sigler, P.B. (1995). Structure of NF-kB p50 homodimer bound to a kB site. *Nature*.

Ghosh, G., Malek, S., Chen, Y. & Huxford, T. (2001). IκBβ, but Not IκBα, Functions as a Classical Cytoplasmic Inhibitor of NF-κB Dimers by Masking Both NF-κB Nuclear Localization Sequences in Resting Cells. *Journal of Biological Chemistry*. 276 (48). pp. 45225–45235.

Gilmore, T.D. (2008). *NF-kB Transcription Factors*. Available from: http://www.bu.edu/nf-kb/ (Accessed: 13 February 2014).

Gobessi, S., Laurenti, L., Longo, P.G., Sica, S., Leone, G. & Efremov, D.G. (2007). ZAP-70 enhances B-cell-receptor signaling despite absent or inefficient tyrosine kinase activation in chronic lymphocytic leukemia and lymphoma B cells. *Blood*. 109 (5). pp. 2032–2039.

Gourzi, P.P., Leonova, T.T. & Papavasiliou, F.N.F. (2007). Viral induction of AID is independent of the interferon and the Toll-like receptor signaling pathways but requires NF-kappaB. *The Journal of experimental medicine*. 204 (2). pp. 259–265.

Green, M., Ishino, M. & Loewenstein, P.M. (1989). Mutational analysis of HIV-1 Tat minimal domain peptides: Identification oftrans-dominant mutants that suppress HIV-LTR-driven gene expression. *Cell*. 58 (1). pp. 215–223.

Grimm, T., Schneider, S., Naschberger, E., Huber, J., Guenzi, E., Kieser, A., Reitmeir, P., Schulz, T.F., Morris, C.A. & Stürzl, M. (2005). EBV latent membrane protein-1 protects B cells from apoptosis by inhibition of BAX. *Blood*. 105 (8). pp. 3263–3269.

Grossmann, M., O'Reilly, L.A., Gugasyan, R., Strasser, A., Adams, J.M. & Gerondakis, S. (2000). The anti-apoptotic activities of Rel and RelA required during B-cell maturation involve the regulation of Bcl-2 expression. *The EMBO journal*. 19 (23). pp. 6351–6360.

Gump, J.M., June, R.K. & Dowdy, S.F. (2010). Revised role of glycosaminoglycans in TAT protein transduction domain-mediated cellular transduction. *The Journal of biological chemistry*. 285 (2). pp. 1500–1507.

Gunnarsson, R., Mansouri, L., Isaksson, A., Göransson, H., Cahill, N., Jansson, M., Rasmussen, M., Lundin, J., Norin, S., Buhl, A.M., Smedby, K.E., Hjalgrim, H., Karlsson, K., Jurlander, J., Geisler, C., Juliusson, G. & Rosenquist, R. (2011). Array-based genomic screening at diagnosis and during follow-up in chronic lymphocytic leukemia. *Haematologica*. 96 (8). pp. 1161–1169.

Gupta, N., Delrow, J., Drawid, A., Sengupta, A.M., Fan, G. & Gélinas, C. (2008). Repression of B-cell linker (BLNK) and B-cell adaptor for phosphoinositide 3-kinase (BCAP) is important for lymphocyte transformation by rel proteins. *Cancer Research*. 68 (3). pp. 808–814.

Guttridge, D.C., Albanese, C., Reuther, J.Y., Pestell, R.G. & Baldwin, A.S. (1999). NF-kappa B controls cell growth and differentiation through transcriptional regulation of cyclin D1. *Molecular and Cellular Biology*. 19 (8). pp. 5785–5799.

Guy, C.S. & Vignali, D.A.A. (2009). Organization of proximal signal initiation at the TCR:CD3 complex. *Immunological reviews*. 232 (1). pp. 7–21.

Guzman, M.L., Neering, S.J., Upchurch, D., Grimes, B., Howard, D.S., Rizzieri, D.A., Luger, S.M. & Jordan, C.T. (2001). Nuclear factor-kappaB is constitutively activated in primitive human acute myelogenous leukemia cells. *Blood*. 98 (8). pp. 2301–2307.

Hacker, U., Albrecht, R. & Maniak, M. (1997). Fluid-phase uptake by macropinocytosis in Dictyostelium. *Journal of Cell Science*. 110. pp. 105–112.

Hallek, M. (2013). Chronic lymphocytic leukemia: 2013 update on diagnosis, risk stratification and treatment. *American Journal of Hematology*. 88 (9). pp. 803–816.

Hamblin, T.J., Orchard, J.A., Ibbotson, R.E., Davis, Z., Thomas, P.W., Stevenson, F.K. & Oscier, D.G. (2002). CD38 expression and immunoglobulin variable region mutations are independent prognostic variables in chronic lymphocytic leukemia, but CD38 expression may vary during the course of the disease. *Blood*. 99 (3). pp. 1023–1029.

Hamblin, T.J.T., Davis, Z.Z., Gardiner, A.A., Oscier, D.G.D. & Stevenson, F.K.F. (1999). Unmutated Ig V(H) genes are associated with a more aggressive form of chronic lymphocytic leukemia. *Blood*. 94 (6). pp. 1848–1854.

Hamilton, E.E., Pearce, L.L., Morgan, L.L., Robinson, S.S., Ware, V.V., Brennan, P.P., Thomas, N.S.B.N., Yallop, D.D., Devereux, S.S., Fegan, C.C., Buggins, A.G.S. &

Pepper, C.C. (2012). Mimicking the tumour microenvironment: three different co-culture systems induce a similar phenotype but distinct proliferative signals in primary chronic lymphocytic leukaemia cells. *British Journal of Haematology*. 158 (5). pp. 589–599.

Harhaj, E.W. & Sun, S.C. (1999). Regulation of RelA subcellular localization by a putative nuclear export signal and p50. *Molecular and Cellular Biology*. 19 (10). pp. 7088–7095.

Hayden, M.S. & Ghosh, S. (2008). Shared Principles in NF-κB Signaling. *Cell*. 132 (3). pp. 344–362.

Hayden, M.S. & Ghosh, S. (2012). NF-κB, the first quarter-century: remarkable progress and outstanding questions. *Genes & Development*. 26 (3). pp. 203–234.

Hayden, R.E., Pratt, G., Davies, N.J., Khanim, F.L., Birtwistle, J., Delgado, J., Pearce, C., Sant, T., Drayson, M.T. & Bunce, C.M. (2009). Treatment of primary CLL cells with bezafibrate and medroxyprogesterone acetate induces apoptosis and represses the pro-proliferative signal of CD40-ligand, in part through increased 15dDelta12,14,PGJ2. *Leukemia*. 23 (2). pp. 292–304.

Hayden, R.E., Pratt, G., Drayson, M.T. & Bunce, C.M. (2010). Lycorine sensitizes CD40 ligand-protected chronic lymphocytic leukemia cells to bezafibrate- and medroxyprogesterone acetate-induced apoptosis but dasatanib does not overcome reported CD40-mediated drug resistance. *Haematologica*. 95 (11). pp. 1889–1896.

Heissmeyer, V., Krappmann, D., Hatada, E.N. & Scheidereit, C. (2001). Shared pathways of IkappaB kinase-induced SCF(betaTrCP)-mediated ubiquitination and degradation for the NF-kappaB precursor p105 and IkappaBalpha. *Molecular and Cellular Biology*. 21 (4). pp. 1024–1035.

Heitz, F., Morris, M.C. & Divita, G. (2009). Twenty years of cell-penetrating peptides: from molecular mechanisms to therapeutics. *British Journal of Pharmacology*. 157 (2). pp. 195–206.

Hellman, L.M. & Fried, M.G. (2007). Electrophoretic mobility shift assay (EMSA) for detecting protein–nucleic acid interactions. *Nature Protocols*. 2 (8). pp. 1849–1861.

Herishanu, Y., Pérez-Galán, P., Liu, D., Biancotto, A., Pittaluga, S., Vire, B., Gibellini, F., Njuguna, N., Lee, E., Stennett, L., Raghavachari, N., Liu, P., McCoy, J.P., Raffeld, M., Stetler-Stevenson, M., Yuan, C., Sherry, R., Arthur, D.C., Maric, I., White, T., Marti, G.E., Munson, P., Wilson, W.H. & Wiestner, A. (2011). The lymph node microenvironment promotes B-cell receptor signaling, NF-kappaB activation, and tumor proliferation in chronic lymphocytic leukemia. *Blood*. 117 (2). pp. 563–574.

Herman, S.E.M., Gordon, A.L., Hertlein, E., Ramanunni, A., Zhang, X., Jaglowski, S., Flynn, J., Jones, J., Blum, K.A., Buggy, J.J., Hamdy, A., Johnson, A.J. & Byrd, J.C. (2011). Bruton tyrosine kinase represents a promising therapeutic target for treatment of chronic lymphocytic leukemia and is effectively targeted by PCI-32765. *Blood*. 117 (23). pp. 6287–6296.

Hewamana, S., Alghazal, S., Lin, T.T., Clement, M., Jenkins, C., Guzman, M.L., Jordan, C.T., Neelakantan, S., Crooks, P.A., Burnett, A.K., Pratt, G., Fegan, C., Rowntree, C., Brennan, P. & Pepper, C.J. (2008a). The NF-kappaB subunit Rel A is associated with in vitro survival and clinical disease progression in chronic lymphocytic leukemia and represents a promising therapeutic target. *Blood*. 111 (9). pp. 4681–

4689.

Hewamana, S., Lin, T.T., Jenkins, C., Burnett, A.K., Jordan, C.T., Fegan, C., Brennan, P., Rowntree, C. & Pepper, C.J. (2008b). The novel nuclear factor-kappaB inhibitor LC-1 is equipotent in poor prognostic subsets of chronic lymphocytic leukemia and shows strong synergy with fludarabine. *Clinical cancer research : an official journal of the American Association for Cancer Research*. 14 (24). pp. 8102–8111.

Hewamana, S., Lin, T.T., Rowntree, C., Karunanithi, K., Pratt, G., Hills, R., Fegan, C., Brennan, P. & Pepper, C.J. (2009). Rel a is an independent biomarker of clinical outcome in chronic lymphocytic leukemia. *Journal of Clinical Oncology*. 27 (5). pp. 763–769.

Hideshima, T., Chauhan, D., Schlossman, R., Richardson, P. & Anderson, K.C. (2001). The role of tumor necrosis factor alpha in the pathophysiology of human multiple myeloma: therapeutic applications. *Oncogene*. 20 (33). pp. 4519–4527.

Hinz, M., Lemke, P., Anagnostopoulos, I., Hacker, C., Krappmann, D., Mathas, S., Dörken, B., Zenke, M., Stein, H. & Scheidereit, C. (2002). Nuclear factor κb-dependent gene expression profiling of Hodgkin's disease tumor cells, pathogenetic significance, and link to constitutive signal transducer and activator of transcription 5a activity. *Journal of Experimental Medicine*. 196 (5). pp. 605–617.

Hiscott, J., Alper, D., Cohen, L., LeBlanc, J.F., Sportza, L., Wong, A. & Xanthoudakis, S. (1989). Induction of Human Interferon Gene-Expression Is Associated with a Nuclear Factor That Interacts with the Nf-Kappa-B Site of the Human Immunodeficiency Virus Enhancer. *Journal of Virology*. 63 (6). pp. 2557–2566.

Hoffmann, A.A., Natoli, G.G. & Ghosh, G. (2006). Transcriptional regulation via the NF-kappaB signaling module. *Oncogene*. 25 (51). pp. 6706–6716.

Horie, R., Watanabe, M., Okamura, T., Taira, M., Shoda, M., Motoji, T., Utsunomiya, A., Watanabe, T., Higashihara, M. & Umezawa, K. (2006). DHMEQ, a new NF-kappaB inhibitor, induces apoptosis and enhances fludarabine effects on chronic lymphocytic leukemia cells. *Leukemia*. 20 (5). pp. 800–806.

Horng, T., Barton, G.M. & Medzhitov, R. (2001). TIRAP: an adapter molecule in the Toll signaling pathway. *Nature Immunology*. 2 (9). pp. 835–841.

Howard, M., Grimaldi, J.C., Bazan, J.F., Lund, F.E., Santos-Argumedo, L., Parkhouse, R.M., Walseth, T.F. & Lee, H.C. (1993). Formation and hydrolysis of cyclic ADP-ribose catalyzed by lymphocyte antigen CD38. *Science*. 262 (5136). pp. 1056–1059.

Howl, J., Jones, S. & Farquhar, M. (2003). Intracellular Delivery of Bioactive Peptides to RBL-2H3 Cells Induces β-Hexosaminidase Secretion and Phospholipase D Activation. *ChemBioChem*. 4 (12). pp. 1312–1316.

Huang, Y., Krein, P.M., Muruve, D.A. & Winston, B.W. (2002). Complement factor B gene regulation: Synergistic effects of TNF-alpha and IFN-gamma in macrophages. *Journal of immunology (Baltimore, Md. : 1950)*. 169 (5). pp. 2627–2635.

Huxford, T. & Ghosh, G. (2009). A Structural Guide to Proteins of the NF-κB Signaling Module. *Cold Spring Harbor Perspectives in Biology*. 1 (3). pp. a000075–a000075.

Hymowitz, S.G. & Wertz, I.E. (2010). A20: from ubiquitin editing to tumour suppression. *Nature Reviews Cancer*. 10 (5). pp. 332–341.

Iademarco, M.F., McQuillan, J.J., Rosen, G.D. & Dean, D.C. (1992). Characterization of the Promoter for Vascular Cell-Adhesion Molecule-1 (Vcam-1). *The Journal of biological chemistry*. 267 (23). pp. 16323–16329.

Inoue, J., Kerr, L.D., Kakizuka, A. & Verma, I.M. (1992). IκBγ, a 70 kd protein identical to the C-terminal half of p110 NF-κB: a new member of the IκB family. *Cell*. 68 (6). pp. 1109–1120.

International Workshop on Chronic Lymphocytic Leukemia (1989). Chronic Lymphocytic Leukemia: Recommendations for Diagnosis, Staging, and Response Criteria. *Annals of Internal Medicine*. 110 (3). pp. 236–238.

Israel, A., Yano, O., Logeat, F., Kieran, M. & Kourilsky, P. (1989). Two purified factors bind to the same sequence in the enhancer of mouse MHC class I genes: one of them is a positive regulator induced upon differentiation of teratocarcinoma cells. *Nucleic Acids Research*. 17 (13). pp. 5245–5257.

Iwanaga, R., Ozono, E., Fujisawa, J., Ikeda, M.A., Okamura, N., Huang, Y. & Ohtani, K. (2008). Activation of the cyclin D2 and cdk6 genes through NF-kappaB is critical for cell-cycle progression induced by HTLV-I Tax. *Oncogene*. 27 (42). pp. 5635–5642.

Iwashima, M., Irving, B.A., van Oers, N.S., Chan, A.C. & Weiss, A. (1994). Sequential interactions of the TCR with two distinct cytoplasmic tyrosine kinases. *Science*. 263 (5150). pp. 1136–1139.

Jasmin, J.-F., Frank, P. & Lisanti, M.P. (2012). *Caveolins and Caveolae*. J.-F. Jasmin, P. G. Frank, & M. P. Lisanti (eds.). Springer, New York, NY.

Jearawiriyapaisarn, N., Moulton, H.M., Buckley, B., Roberts, J., Sazani, P., Fucharoen, S., Iversen, P.L. & Kole, R. (2008). Sustained dystrophin expression induced by peptide-conjugated morpholino oligomers in the muscles of mdx mice. *Molecular Therapy*. 16 (9). pp. 1624–1629.

Johansson, H.J., El-Andaloussi, S., Holm, T., Mäe, M., Jänes, J., Maimets, T. & Langel, Ü. (2008). Characterization of a novel cytotoxic cell-penetrating peptide derived from p14ARF protein. *Molecular Therapy*. 16 (1). pp. 115–123.

Johnson, D.R. & Pober, J.S. (1994). HLA class I heavy-chain gene promoter elements mediating synergy between tumor necrosis factor and interferons. *Molecular and Cellular Biology*.

Joliot, A.A., Pernelle, C.C., Deagostini-Bazin, H.H. & Prochiantz, A.A. (1991). Antennapedia homeobox peptide regulates neural morphogenesis. *Proceedings of the National Academy of Sciences*. 88 (5). pp. 1864–1868.

Jones, A.T. (2007). Macropinocytosis: searching for an endocytic identity and role in the uptake of cell penetrating peptides. *Journal of cellular and molecular medicine*. 11 (4). pp. 670–684.

Jones, A.T. & Sayers, E.J. (2012). Cell entry of cell penetrating peptides: tales of tails wagging dogs. *Journal of controlled release : official journal of the Controlled Release Society*. 161 (2). pp. 582–591.

Jones, A.T., Gumbleton, M. & Duncan, R. (2003). Understanding endocytic pathways and intracellular trafficking: a prerequisite for effective design of advanced drug delivery systems. *Advanced Drug Delivery Reviews*. 55 (11). pp. 1353–1357.

Jones, S., Holm, T., Mäger, I., Langel, Ü. & Howl, J. (2010). Characterization of Bioactive Cell Penetrating Peptides from Human Cytochromec: Protein Mimicry and the Development of a Novel Apoptogenic Agent. *Chemistry & biology*. 17 (7). pp. 735–744.

Kaileh, M. & Sen, R. (2012). NF-κB function in B lymphocytes. *Immunological reviews*. 246 (1). pp. 254–271.

Kang, B.N., Tirumurugaan, K.G., Deshpande, D.A., Amrani, Y., Panettieri, R.A., Walseth, T.F. & Kannan, M.S. (2006). Transcriptional regulation of CD38 expression by tumor necrosis factor-alpha in human airway smooth muscle cells: role of NF-kappaB and sensitivity to glucocorticoids. *FASEB journal : official publication of the Federation of American Societies for Experimental Biology*. 20 (7). pp. 1000–1002.

Kaplan, I.M., Wadia, J.S. & Dowdy, S.F. (2005). Cationic TAT peptide transduction domain enters cells by macropinocytosis. *Journal of controlled release : official journal of the Controlled Release Society*. 102 (1). pp. 247–253.

Karin, M. & Ben-Neriah, Y. (2011). Inflammation meets cancer, with NF-κB as the matchmaker. *Nature Publishing Group*. 12 (8). pp. 715–723.

Karin, M. & Ben-Neriah, Y. (2000). Phosphorylation meets ubiquitination: the control of NF-[kappa]B activity. *Annual Review of Immunology*. 18. pp. 621–663.

Karin, M. & Lin, A. (2002). NF-kappaB at the crossroads of life and death. *Nature Immunology*. 3 (3). pp. 221–227.

Kater, A.P., Evers, L.M., Remmerswaal, E.B.M., Jaspers, A., Oosterwijk, M.F., van Lier, R.A.W., van Oers, M.H.J. & Eldering, E. (2004). CD40 stimulation of B-cell chronic lymphocytic leukaemia cells enhances the anti-apoptotic profile, but also Bid expression and cells remain susceptible to autologous cytotoxic T-lymphocyte attack. *British Journal of Haematology*. 127 (4). pp. 404–415.

Kearns, J.D., Basak, S., Werner, S.L., Huang, C.S. & Hoffmann, A. (2006). IkappaBepsilon provides negative feedback to control NF-kappaB oscillations, signaling dynamics, and inflammatory gene expression. *Journal of Cell Biology*. 173 (5). pp. 659–664.

Kern, C., Cornuel, J.-F., Billard, C., Tang, R., Rouillard, D., Stenou, V., Defrance, T., Ajchenbaum-Cymbalista, F., Simonin, P.-Y., Feldblum, S. & Kolb, J.-P. (2004). Involvement of BAFF and APRIL in the resistance to apoptosis of B-CLL through an autocrine pathway. *Blood*. 103 (2). pp. 679–688.

Kirchner, D., Duyster, J., Ottmann, O. & Schmid, R.M. (2003). Mechanisms of BCR-ABL-mediated NF-κB/Rel activation. *Experimental ….*

Kitada, S., Zapata, J.M. & Andreeff, M. (1999). Bryostatin and CD40-ligand enhance apoptosis resistance and induce expression of cell survival genes in B-cell chronic lymphocytic leukaemia. *British journal of ….*

Klein, U. & Dalla-Favera, R.R. (2008). Germinal centres: role in B-cell physiology and malignancy. *Nature reviews. Immunology*. 8 (1). pp. 22–33.

Klein, U., Lia, M.M., Crespo, M., Siegel, R., Shen, Q., Mo, T., Ambesi-Impiombato, A., Califano, A., Migliazza, A., Bhagat, G. & Dalla-Favera, R.R. (2010). TheDLEU2/miR-15a/16-1Cluster Controls B Cell Proliferation and Its Deletion Leads to Chronic Lymphocytic Leukemia. *Cancer Cell*. 17 (1). pp. 28–40.

Klein, U., Tu, Y., Stolovitzky, G.A., Mattioli, M., Cattoretti, G., Husson, H., Freedman, A., Inghirami, G., Cro, L., Baldini, L., Neri, A., Califano, A. & Dalla-Favera, R.R. (2001). Gene expression profiling of B cell chronic lymphocytic leukemia reveals a homogeneous phenotype related to memory B cells. *The Journal of experimental medicine*. 194 (11). pp. 1625–1638.

Knight, S.J.L., Yau, C., Clifford, R., Timbs, A.T., Akha, E.S., au, H.M.D.E., Burns, A., Ciria, C., Oscier, D.G., Pettitt, A.R., Dutton, S., Holmes, C.C., Taylor, J., Cazier, J.-B. & Schuh, A. (2012). Quantification of subclonal distributions of recurrent genomic aberrations in paired pre-treatment and relapse samples from patients with B-cell chronic lymphocytic leukemia. *Leukemia*. pp. 1–12.

Kolenko, V.V., Bloom, T.T., Rayman, P.P., Bukowski, R.R., Hsi, E.E. & Finke, J.J. (1999). Inhibition of NF-kappa B activity in human T lymphocytes induces caspase-dependent apoptosis without detectable activation of caspase-1 and -3. *Journal of immunology (Baltimore, Md. : 1950)*. 163 (2). pp. 590–598.

Kolluri, S.K., Zhu, X., Zhou, X., Lin, B., Chen, Y., Sun, K., Tian, X., Town, J., Cao, X., Lin, F., Zhai, D., Kitada, S., Luciano, F., O'Donnell, E., Cao, Y., He, F., Lin, J., Reed, J.C., Satterthwait, A.C. & Zhang, X.-K. (2008). A Short Nur77-Derived Peptide Converts Bcl-2 from a Protector to a Killer. *Cancer Cell*. 14 (4). pp. 285–298.

Kovalenko, A., Chable-Bessia, C., Cantarella, G., Israël, A., Wallach, D. & Courtois, G. (2003). The tumour suppressor CYLD negatively regulates NF-kappaB signalling by deubiquitination. *Nature*. 424 (6950). pp. 801–805.

Krieg, A.M. (2000). Immune effects and mechanisms of action of CpG motifs. *Vaccine*. 19 (6). pp. 618–622.

Kurokawa, M. & Kornbluth, S. (2009). Caspases and Kinases in a Death Grip. *Cell*. 138 (5). pp. 838–854.

Kwok, B.H., Koh, B., Ndubuisi, M.I., Elofsson, M. & Crews, C.M. (2001). The anti-inflammatory natural product parthenolide from the medicinal herb Feverfew directly binds to and inhibits IkappaB kinase. *Chemistry & biology*. 8 (8). pp. 759–766.

LaBelle, J.L., Katz, S.G., Bird, G.H., Gavathiotis, E., Stewart, M.L., Lawrence, C., Fisher, J.K., Godes, M., Pitter, K., Kung, A.L. & Walensky, L.D. (2012). A stapled BIM peptide overcomes apoptotic resistance in hematologic cancers. *Journal of Clinical Investigation*. 122 (122(6)). pp. 2018–2031.

Lagneaux, L.L., Delforge, A.A., Bron, D.D., De Bruyn, C.C. & Stryckmans, P.P. (1998). Chronic lymphocytic leukemic B cells but not normal B cells are rescued from apoptosis by contact with normal bone marrow stromal cells. *Blood*. 91 (7). pp. 2387–2396.

Lai, S.-H., Stein, D.A., Guerrero-Plata, A., Liao, S.-L., Ivanciuc, T., Hong, C., Iversen, P.L., Casola, A. & Garofalo, R.P. (2008). Inhibition of respiratory syncytial virus infections with morpholino oligomers in cell cultures and in mice. *Molecular Therapy*. 16 (6). pp. 1120–1128.

Lang, V., Janzen, J., Fischer, G.Z., Soneji, Y., Beinke, S., Salmeron, A., Allen, H., Hay, R.T., Ben-Neriah, Y. & Ley, S.C. (2003). TrCP-Mediated Proteolysis of NF- B1 p105 Requires Phosphorylation of p105 Serines 927 and 932. *Molecular and Cellular Biology*. 23 (1). pp. 402–413.

Le Bail, O., Schmidt-Ullrich, R. & Israel, A. (1993). Promoter analysis of the gene encoding the I kappa B-alpha/MAD3 inhibitor of NF-kappa B: positive regulation by members of the rel/NF-kappa B family. *The EMBO journal*. 12 (13). pp. 5043–5049.

Lee, B.-H., Park, S.-Y., Kang, K.-B., Park, R.-W. & Kim, I.-S. (2002). NF-kappaB activates fibronectin gene expression in rat hepatocytes. *Biochemical and Biophysical Research Communications*. 297 (5). pp. 1218–1224.

Lee, S.J., Long, M., Adler, A.J., Mittler, R.S. & Vella, A.T. (2009). The IKK-neutralizing compound Bay11 kills supereffector CD8 T cells by altering caspase-dependent activation-induced cell death. *Journal of Leukocyte Biology*. 85 (1). pp. 175–185.

Letoha, T., Somlai, C., Takacs, T., Szabolcs, A., Jarmay, K., Rakonczay, Z., Hegyi, P., Varga, I., Kaszaki, J., Krizbai, I., Boros, I., Duda, E., Kusz, E. & Penke, B. (2005). A nuclear import inhibitory peptide ameliorates the severity of cholecystokinin-induced acute pancreatitis. *World Journal of Gastroenterology*. 11 (7). pp. 990–999.

Lf, C., Fischle, W.W., Verdin, E.E. & Greene, W.C.W. (2001). Duration of nuclear NF-kappaB action regulated by reversible acetylation. *Science*. 293 (5535). pp. 1653–1657.

Li, S., Song, K.S. & Lisanti, M.P. (1996). Expression and Characterization of Recombinant Caveolin PURIFICATION BY POLYHISTIDINE TAGGING AND CHOLESTEROL-DEPENDENT INCORPORATION …. *Journal of Biological Chemistry*.

Li, Z. & Nabel, G.J. (1997). A new member of the I kappaB protein family, I kappaB epsilon, inhibits RelA (p65)-mediated NF-kappaB transcription. *Molecular and Cellular Biology*. 17 (10). pp. 6184–6190.

Lia, M.M., Carette, A.A., Tang, H.H., Shen, Q.Q., Mo, T.T., Bhagat, G.G., Dalla-Favera, R.R. & Klein, U.U. (2012). Functional dissection of the chromosome 13q14 tumor-suppressor locus using transgenic mouse lines. *Blood*. 119 (13). pp. 2981–2990.

Liao, R.X., Sun, J.G., Zhong, X.L. & Zhou, J.X. (2006). [Experimental study on transcription regulation of mouse hepcidin gene by NF-kB]. *Zhonghua gan zang …*.

Lin, G., Field, J.J., Yu, J.C., Ken, R., Neuberg, D., Nathan, D.G. & Linden, J. (2013). NF-κB is activated in CD4+ iNKT cells by sickle cell disease and mediates rapid induction of adenosine A2A receptors. *PLoS ONE*. 8 (10). pp. e74664–e74664.

Lin, Y.Z., Yao, S., Veach, R.A., Torgerson, T.R. & Hawiger, J. (1995). Inhibition of nuclear translocation of transcription factor NF-κB by a synthetic peptide containing a cell membrane-permeable motif and nuclear localization sequence. *Journal of Biological Chemistry*. 270 (24). pp. 14255–14258.

Lindgren, M. & Langel, Ü. (2011). Classes and prediction of cell-penetrating peptides. *Methods in molecular biology (Clifton, N.J.)*. 683. pp. 3–19.

Lindhagen, E., Nissle, S., Leoni, L., Elliott, G., Chao, Q., Larsson, R. & Åleskog, A. (2007). R-etodolac (SDX-101) and the related indole-pyran analogues SDX-308 and SDX-309 potentiate the antileukemic activity of standard cytotoxic agents in primary chronic lymphocytic leukaemia cells. *Cancer Chemotherapy and Pharmacology*. 60 (4). pp. 545–553.

Liou, H.-C., Nolan, G.P., Ghosh, S., Fujita, T. & Baltimore, D. (1992). The NF-kappa B p50 precursor, p105, contains an internal I kappa B-like inhibitor that preferentially

inhibits p50. *The EMBO journal*. 11 (8). p. 3003.

Liu, R., Zhao, X. & Gurney, T.A. (1998). Functional analysis of the proximal CCR5 promoter. *AIDS research and …*.

Lobetti-Bodoni, C., Bertoni, F., Stussi, G., Cavalli, F. & Zucca, E. (2013). The changing paradigm of chronic lymphocytic leukemia management. *European journal of internal medicine*. 24 (5). pp. 401–410.

Loiarro, M., Capolunghi, F., Fantò, N., Gallo, G., Campo, S., Arseni, B., Carsetti, R., Carminati, P., De Santis, R., Ruggiero, V. & Sette, C. (2007). Pivotal Advance: Inhibition of MyD88 dimerization and recruitment of IRAK1 and IRAK4 by a novel peptidomimetic compound. *Journal of Leukocyte Biology*. 82 (4). pp. 801–810.

Loiarro, M., Sette, C., Gallo, G., Ciacci, A., Fantò, N., Mastroianni, D., Carminati, P. & Ruggiero, V. (2005). Peptide-mediated interference of TIR domain dimerization in MyD88 inhibits interleukin-1-dependent activation of NF-{kappa}B. *The Journal of biological chemistry*. 280 (16). pp. 15809–15814.

Looi, C.Y., Imanishi, M., Takaki, S., Sato, M. & Chiba, N. (2011). Octa-arginine mediated delivery of wild-type Lnk protein inhibits TPO-induced M-MOK megakaryoblastic leukemic cell growth by promoting apoptosis C. Schulz (ed.). *PLoS ONE*.

Lopez-Cabrera, M., Munoz, E., Blazquez, M.V., Ursa, M.A., Santis, A.G. & Sanchez-Madrid, F. (1995). Transcriptional regulation of the gene encoding the human C-type lectin leukocyte receptor AIM/CD69 and functional characterization of its tumor necrosis factor-α-responsive elements. *Journal of Biological Chemistry*. 270 (37). pp. 21545–21551.

Lopez-Guerra, M. & Colomer, D. (2010). NF-kappaB as a therapeutic target in chronic lymphocytic leukemia. *Expert opinion on therapeutic targets*. 14 (3). pp. 275–288.

Lopez-Guerra, M., Puente, X.S., Pinyol, M., Quesada, V., Conde, L., Ordóñez, G.R., Villamor, N., Escaramis, G., Jares, P., Beà, S., González-Díaz, M., Bassaganyas, L., Baumann, T., Juan, M., Colomer, D., Tubío, J.M.C., López, C., Navarro, A., Tornador, C., Aymerich, M., Rozman, M., Hernández, J.M., Puente, D.A., Freije, J.M.P., Velasco, G., Gutiérrez-Fernández, A., Costa, D., Carrió, A., Guijarro, S., Enjuanes, A., Hernández, L., Yagüe, J., Nicolás, P., Romeo-Casabona, C.M., Himmelbauer, H., Castillo, E., Dohm, J.C., de Sanjosé, S., Piris, M.Á., de Alava, E., Miguel, J.S., Royo, R., Gelpí, J.L., Torrents, D., Orozco, M., Pisano, D.G., Valencia, A., Guigó, R., Bayés, M., Heath, S., Gut, M., Klatt, P., Marshall, J., Raine, K., Stebbings, L.A., Futreal, P.A., Stratton, M.R., Campbell, P.J., Gut, I., López-Guillermo, A., Estivill, X., Montserrat, E., López-Otín, C. & Campo, E. (2012). Whole-genome sequencing identifies recurrent mutations in chronic lymphocytic

leukaemia. *Nature*. 475 (7354). pp. 101–105.

Lopez-Guerra, M., Roue, G., Perez-Galan, P., Alonso, R., Villamor, N., Montserrat, E., Campo, E. & Colomer, D. (2009). *p65 activity and ZAP-70 status predict the sensitivity of chronic lymphocytic leukemia cells to the selective IkappaB kinase inhibitor BMS-345541*. 15 (8). pp. 2767–2776. Available from: http://clincancerres.aacrjournals.org/cgi/doi/10.1158/1078-0432.CCR-08-2382.

Lowenthal, J.W., Ballard, D.W., Böhnlein, E. & Greene, W.C. (1989). Tumor necrosis

factor alpha induces proteins that bind specifically to kappa B-like enhancer elements and regulate interleukin 2 receptor alpha-chain gene expression in primary human T lymphocytes. *Proceedings of the National Academy of Sciences*. 86 (7). pp. 2331–2335.

Lozanski, G., Heerema, N.A., Flinn, I.W., Smith, L., Harbison, J., Webb, J., Moran, M., Lucas, M., Lin, T., Hackbarth, M.L., Proffitt, J.H., Lucas, D., Grever, M.R. & Byrd, J.C. (2004). Alemtuzumab is an effective therapy for chronic lymphocytic leukemia with p53 mutations and deletions. *Blood*. 103 (9). pp. 3278–3281.

Lundberg, M. & Johansson, M. (2002). Positively Charged DNA-Binding Proteins Cause Apparent Cell Membrane Translocation. *Biochemical and Biophysical Research Communications*. 291 (2). pp. 367–371.

Lupfer, C., Stein, D.A., Mourich, D.V., Tepper, S.E., Iversen, P.L. & Pastey, M. (2008). Inhibition of influenza A H3N8 virus infections in mice by morpholino oligomers. *Archives of Virology*. 153 (5). pp. 929–937.

Madani, F., Lindberg, S., Langel, Ü., Futaki, S. & Gräslund, A. (2011). Mechanisms of cellular uptake of cell-penetrating peptides. *Journal of biophysics (Hindawi Publishing Corporation : Online)*. 2011. p. 414729.

Majid, A., Lin, T.T., Best, G., Fishlock, K., Hewamana, S., Pratt, G., Yallop, D., Buggins, A.G.S., Wagner, S., Ben J Kennedy, Miall, F., Hills, R., Devereux, S., Oscier, D.G., Dyer, M.J.S., Fegan, C. & Pepper, C.J. (2011). CD49d is an independent prognostic marker that is associated with CXCR4 expression in CLL. *Leukemia Research*. 35 (6). pp. 750–756.

Malavasi, F., Deaglio, S., Damle, R., Cutrona, G., Ferrarini, M. & Chiorazzi, N. (2011). CD38 and chronic lymphocytic leukemia: a decade later. *Blood*. 118 (13). pp. 3470–3478.

Malavasi, F., Funaro, A., Roggero, S., Horenstein, A., Calosso, L. & Mehta, K. (1994). Human CD38: a glycoprotein in search of a function. *Immunology today*. 15 (3). pp. 95–97.

Marshall, N.B., Oda, S.K., London, C.A., Moulton, H.M., Iversen, P.L., Kerkvliet, N.I. & Mourich, D.V. (2007). Arginine-rich cell-penetrating peptides facilitate delivery of antisense oligomers into murine leukocytes and alter pre-mRNA splicing. *Journal of Immunological Methods*. 325 (1-2). pp. 114–126.

Martin, D. & Lenardo, M. (2001). Morphological, biochemical, and flow cytometric assays of apoptosis. *Current protocols in molecular biology / edited by Frederick M. Ausubel ... [et al.]*. Chapter 14. p. Unit 14.13.

Mason, A.J., Moussaoui, W., Abdelrahman, T., Boukhari, A., Bertani, P., Marquette, A., Shooshtarizaheh, P., Moulay, G., Boehm, N., Guerold, B., Sawers, R.J.H., Kichler, A., Metz-Boutigue, M.-H., Candolfi, E., Prévost, G. & Bechinger, B. (2009). Structural determinants of antimicrobial and antiplasmodial activity and selectivity in histidine-rich amphipathic cationic peptides. *The Journal of biological chemistry*. 284 (1). pp. 119–133.

Matsumoto, N., Ariga, A., To-e, S., Nakamura, H., Agata, N., Hirano, S., Inoue, J. & Umezawa, K. (2000). Synthesis of NF-kappaB activation inhibitors derived from epoxyquinomicin C. *Bioorganic & medicinal chemistry letters*. 10 (9). pp. 865–869.

Matsuzaki, K., Sugishita, K. & Miyajima, K. (1999). Interactions of an antimicrobial peptide, magainin 2, with lipopolysaccharide-containing liposomes as a model for outer membranes of gram-negative bacteria. *FEBS Letters*. 449 (2-3). pp. 221–224.

Matsuzaki, K., Yoneyama, S., Murase, O. & Miyajima, K. (1996). Transbilayer transport of ions and lipids coupled with mastoparan X translocation. *Biochemistry*. 35 (25). pp. 8450–8456.

May, M.J., D'Acquisto, F., Madge, L.A., Glockner, J., Pober, J.S. & Ghosh, S. (2000). Selective inhibition of NF-κB activation by a peptide that blocks the interaction of NEMO with the IκB kinase complex. *Science*. 289 (5484). pp. 1550–1554.

May, M.J., Mariendfeld, R.B. & Ghosh, S. (2002). Characterization of the Ikappa B-kinase NEMO binding domain. *The Journal of biological chemistry*. 277 (48). pp. 45992–46000.

Mayor, S. & Pagano, R.E. (2007). Pathways of clathrin-independent endocytosis. *Nature Reviews Molecular Cell Biology*. 8 (8). pp. 603–612.

McMahon, H.T. & Boucrot, E. (2011). Molecular mechanism and physiological functions of clathrin-mediated endocytosis. *Nature Reviews Molecular Cell Biology*. 12 (8). pp. 517–533.

Mercurio, F., DiDonato, J.A., Rosette, C. & Karin, M. (1993). p105 and p98 precursor proteins play an active role in NF-kappa B-mediated signal transduction. *Genes & Development*. 7 (4). pp. 705–718.

Milletti, F. (2012). Cell-penetrating peptides: classes, origin, and current landscape. *Drug Discovery Today*. 17 (15-16). pp. 850–860.

Mitsiades, N., Mitsiades, C.S., Poulaki, V., Chauhan, D., Richardson, P.G., Hideshima, T., Munshi, N., Treon, S.P. & Anderson, K.C. (2002). Biologic sequelae of nuclear factor–κB blockade in multiple myeloma: therapeutic applications. *Blood*. 99 (11). pp. 4079–4086.

Miyaji, Y.Y., Walter, S.S., Chen, L.L., Kurihara, A.A., Ishizuka, T.T., Saito, M.M., Kawai, K.K. & Okazaki, O.O. (2011). Distribution of KAI-9803, a novel δ-protein kinase C inhibitor, after intravenous administration to rats. *Drug Metabolism and Disposition*. 39 (10). pp. 1946–1953.

Moghimi, S.M. & Rajabi-Siahboomi, A.R. (2000). Recent advances in cellular, sub-cellular and molecular targeting. *Advanced Drug Delivery Reviews*. 41 (2). pp. 129–133.

Mogi, M., Kondo, T., Mizuno, Y. & Nagatsu, T. (2007). p53 protein, interferon-γ, and NF-κB levels are elevated in the parkinsonian brain. *Neuroscience Letters*. 414 (1). pp. 94–97.

Monier, S., Dietzen, D.J., Hastings, W., Lublin, D.M. & Kurzchalia, T.V. (1996). Oligomerization of VIP21-caveolin in vitro is stabilized by long chain fatty acylation or cholesterol. *FEBS Letters*. 388 (2). pp. 143–149.

Moon, E.Y. & Park, H. (2007). B cell activating factor (BAFF) gene promoter activity depends upon co-activator, p300. *Immunobiology*. 212 (8). pp. 637–645.

Mori, N., Ishikawa, C. & Senba, M. (2011). Induction of CD69 expression by cagPAI-

positive Helicobacter pylori infection. *World journal of gastroenterology : WJG*. 17 (32). pp. 3691–3699.

Morris, M.C., Depollier, J., Mery, J., Heitz, F. & Divita, G. (2001). A peptide carrier for the delivery of biologically active proteins into mammalian cells. *Nature Biotechnology*. 19 (12). pp. 1173–1176.

Morris, M.C., Vidal, P., Chaloin, L., Heitz, F. & Divita, G. (1997). A new peptide vector for efficient delivery of oligonucleotides into mammalian cells. *Nucleic Acids Research*. 25 (14). pp. 2730–2736.

Moulton, H.M., Nelson, M.H., Hatlevig, S.A., Reddy, M.T. & Iversen, P.L. (2004). Cellular uptake of antisense morpholino oligomers conjugated to arginine-rich peptides. *Bioconjugate Chemistry*. 15 (2). pp. 290–299.

Mueller, J., Kretzschmar, I., Volkmer, R. & Boisguerin, P. (2008). Comparison of cellular uptake using 22 CPPs in 4 different cell lines. *Bioconjugate Chemistry*. 19 (12). pp. 2363–2374.

Mukundan, L., Bishop, G.A., Head, K.Z., Zhang, L.H., Wahl, L.M. & Suttles, J. (2005). TNF receptor-associated factor 6 is an essential mediator of CD40-activated proinflammatory pathways in monocytes and macrophages. *Journal of Immunology*. 174 (2). pp. 1081–1090.

Munzert, G., Kirchner, D., Stobbe, H., Bergmann, L., Schmid, R.M., Döhner, H. & Heimpel, H. (2002). Tumor necrosis factor receptor-associated factor 1 gene overexpression in B-cell chronic lymphocytic leukemia: analysis of NF-kappa B/Rel-regulated inhibitors of apoptosis. *Blood*. 100 (10). pp. 3749–3756.

Muppidi, J., Porter, M. & Siegel, R.M. (2004). Measurement of apoptosis and other forms of cell death. *Current protocols in immunology / edited by John E. Coligan ... [et al.]*. Chapter 3. p. Unit 3.17.

Murata, M., Peränen, J., Schreiner, R., Wieland, F., Kurzchalia, T.V. & Simons, K. (1995). VIP21/caveolin is a cholesterol-binding protein. *Proceedings of the National Academy of Sciences*. 92 (22). pp. 10339–10343.

Müller, C.W., Rey, F.A. & Harrison, S.C. (1996). Comparison of two different DNA-binding modes of the NF-kappa B p50 homodimer. *Nature Structural Biology*. 3 (3). pp. 224–227.

Müller, C.W., Rey, F.A. & Sodeoka, M. (1995). Structure of the NF-κB p50 homodimer bound to DNA. *Nature*.

Nair, A.S., Shishodia, S., Ahn, K.S., Kunnumakkara, A.B., Sethi, G. & Aggarwal, B.B. (2006). Deguelin, an Akt inhibitor, suppresses IkappaBalpha kinase activation leading to suppression of NF-kappaB-regulated gene expression, potentiation of apoptosis, and inhibition of cellular invasion. *Journal of immunology (Baltimore, Md. : 1950)*. 177 (8). pp. 5612–5622.

Nakamura, T., Yamazaki, D., Yamauchi, J. & Harashima, H. (2013). *The nanoparticulation by octaarginine-modified liposome improves α-galactosylceramide-mediated antitumor therapy via systemic administration*. 171 (2). pp. 216–224.

Nakanishi, C. & Toi, M. (2005). Nuclear factor-kappaB inhibitors as sensitizers to anticancer drugs. *Nature Reviews Cancer*. 5 (4). pp. 297–309.

Nakase, I., NIWA, M., Takeuchi, T., Sonomura, K., Kawabata, N., Koike, Y., Takehashi, M., Tanaka, S., Ueda, K., Simpson, J.C., Jones, A.T., Sugiura, Y. & Futaki, S. (2004). *Cellular uptake of arginine-rich peptides: Roles for macropinocytosis and actin rearrangement*. 10 (6). pp. 1011–1022. Available from: http://www.nature.com/mt/journal/v10/n6/abs/mt20041311a.html.

Nakase, I., Takeuchi, T., Tanaka, G. & Futaki, S. (2008). Methodological and cellular aspects that govern the internalization mechanisms of arginine-rich cell-penetrating peptides. *Advanced Drug Delivery Reviews*. 60 (4-5). pp. 598–607.

Nakase, I., Tanaka, G. & Futaki, S. (2013). Cell-penetrating peptides (CPPs) as a vector for the delivery of siRNAs into cells. *Molecular bioSystems*. 9 (5). pp. 855–861.

Ni, H., Ergin, M., Huang, Q. & Qin, J.Z. (2001). Analysis of expression of nuclear factor κB (NF-κB) in multiple myeloma: downregulation of NF-κB induces apoptosis. *British journal of …*.

Nückel, H., Switala, M., Collins, C.H., Sellmann, L., Grosse-Wilde, H., Dührsen, U. & Rebmann, V. (2009). High CD49d protein and mRNA expression predicts poor outcome in chronic lymphocytic leukemia. *Clinical Immunology*. 131 (3). pp. 472–480.

Oeckinghaus, A. & Ghosh, S. (2009). The NF-κB Family of Transcription Factors and Its Regulation. *Cold Spring Harbor Perspectives in Biology*. 1 (4). pp. a000034–a000034.

Oehlke, J., Krause, E., Wiesner, B. & Beyermann, M. (1997). Extensive cellular uptake into endothelial cells of an amphipathic β-sheet forming peptide. *FEBS Letters*.

Oehlke, J., Scheller, A., Wiesner, B., Krause, E., Beyermann, M., Klauschenz, E., Melzig, M. & Bienert, M. (1998). Cellular uptake of an alpha-helical amphipathic model peptide with the potential to deliver polar compounds into the cell interior non-endocytically. *Biochimica et biophysica acta*. 1414 (1-2). pp. 127–139.

Orange, J.S. & May, M.J. (2008). Cell penetrating peptide inhibitors of nuclear factor-kappa B. *Cellular and molecular life sciences : CMLS*. 65 (22). pp. 3564–3591.

Osborn, L., Kunkel, S. & Nabel, G.J. (1989). *Tumor necrosis factor α and interleukin 1 stimulate the human immunodeficiency virus enhancer by activation of the nuclear factor κB*. In: 1989, pp. 2336–2340.

Otero, D.C., Anzelon, A.N. & Rickert, R.C. (2003). CD19 function in early and late B cell development: I. Maintenance of follicular and marginal zone B cells requires CD19-dependent survival signals. *The Journal of Immunology*.

Ottosson-Wadlund, A., Jitkaew, S., Johansson, I., Fucharoen, S., Hedenfalk, I. & Fadeel, B. (2014). *Overcoming chemoresistance in B lymphoma cells: elucidating the role of NF-kB in caspase-independent apoptosis by transcriptomic assessment* GSE31258. NCBI,

Ozato, K., Tsujimura, H. & Tamura, T. (2002). Toll-like receptor signaling and regulation of cytokine gene expression in the immune system. *BioTechniques*. Suppl. pp. 66–passim.

Palm-Apergi, C., Lönn, P. & Dowdy, S.F. (2012). Do cell-penetrating peptides actually ‘penetrate’ cellular membranes? *Molecular Therapy*. 20 (4). pp. 695–697.

Palombella, V.J., Rando, O.J., Goldberg, A.L. & Maniatis, T. (1994). The ubiquitinproteasome pathway is required for processing the NF-κB1 precursor protein and the activation of NF-κB. *Cell*. 78 (5). pp. 773–785.

Pepper, C.J., Hewamana, S., Brennan, P. & Fegan, C. (2009). NF-kappaB as a prognostic marker and therapeutic target in chronic lymphocytic leukemia. *Future oncology (London, England)*. 5 (7). pp. 1027–1037.

Pepper, C.J., Mahdi, J.G., Buggins, A.G.S., Hewamana, S., Walsby, E., Mahdi, E., Al-Haza'a, A., Mahdi, A.J., Lin, T.T., Pearce, L., Morgan, L., Bowen, I.D., Brennan, P. & Fegan, C. (2011). Two novel aspirin analogues show selective cytotoxicity in primary chronic lymphocytic leukaemia cells that is associated with dual inhibition of Rel A and COX-2. *Cell Proliferation*. 44 (4). pp. 380–390.

Pepper, C.J., Majid, A., Lin, T.T., Hewamana, S., Pratt, G., Walewska, R., Gesk, S., Siebert, R., Wagner, S., Ben Kennedy, Miall, F., Davis, Z.A., Tracy, I., Gardiner, A.C., Brennan, P., Hills, R.K., Dyer, M.J.S., Oscier, D. & Fegan, C. (2012). Defining the prognosis of early stage chronic lymphocytic leukaemia patients. *British Journal of Haematology*. 156 (4). pp. 499–507.

Perez-Galan, P., Roue, G., Lopez-Guerra, M., Nguyen, M., Villamor, N., Montserrat, E., Shore, G.C., Campo, E. & Colomer, D. (2008). BCL-2 phosphorylation modulates sensitivity to the BH3 mimetic GX15-070 (Obatoclax) and reduces its synergistic interaction with bortezomib in chronic lymphocytic leukemia cells. *Leukemia*. 22 (9). pp. 1712–1720.

Pérez-Galán, P., Roué, G., Villamor, N., Montserrat, E., Campo, E. & Colomer, D. (2006). The proteasome inhibitor bortezomib induces apoptosis in mantle-cell lymphoma through generation of ROS and Noxa activation independent of p53 status. *Blood*. 107 (1). pp. 257–264.

Pickering, B.M., de Mel, S.S., Lee, M.M., Howell, M.M., Habens, F.F., Dallman, C.L.C., Neville, L.A.L., Potter, K.N.K., Mann, J.J., Mann, D.A.D., Johnson, P.W.M.P., Stevenson, F.K.F. & Packham, G.G. (2007). Pharmacological inhibitors of NF-kappaB accelerate apoptosis in chronic lymphocytic leukaemia cells. *Oncogene*. 26 (8). pp. 1166–1177.

Pierce, J.W., Schoenleber, R., Jesmok, G., Best, J., Moore, S.A., Collins, T. & Gerritsen, M.E. (1997). Novel inhibitors of cytokine-induced IkappaBalpha phosphorylation and endothelial cell adhesion molecule expression show anti-inflammatory effects in vivo. *The Journal of biological chemistry*. 272 (34). pp. 21096–21103.

Pittner, B.T., Shanafelt, T.D., Kay, N.E. & Jelinek, D.F. (2005). CD38 expression levels in chronic lymphocytic leukemia B cells are associated with activation marker expression and differential responses to interferon stimulation. *Leukemia*. 19 (12). pp. 2264–2272.

Plaksin, D., Baeuerle, P.A. & Eisenbach, L. (1993). KBF1 (p50 NF-kappa B homodimer) acts as a repressor of H-2Kb gene expression in metastatic tumor cells. *The Journal of experimental medicine*. 177 (6). pp. 1651–1662.

Pooga, M., Langel, Ü., Hällbrink, M. & ZORKO, M. (1998a). Cell penetration by transportan. *FASEB journal : official publication of the Federation of American Societies for Experimental Biology*. 12 (1). pp. 67–77.

Pooga, M.M., Langel, Ü., Soomets, U.U., Hällbrink, M.M., Valkna, A.A., Saar, K.K., Rezaei, K.K., Kahl, U.U., Hao, J.X.J., Xu, X.J.X., Wiesenfeld-Hallin, Z.Z., Hökfelt, T.T. & Bartfai, T.T. (1998b). Cell penetrating PNA constructs regulate galanin receptor levels and modify pain transmission in vivo. *Nature Biotechnology*. 16 (9). pp. 857–861.

Poulaki, V., Mitsiades, C.S., Joussen, A.M. & Lappas, A. (2002). Constitutive nuclear factor-κB activity is crucial for human retinoblastoma cell viability. *The American journal of …*.

Pouny, Y., Rapaport, D., Mor, A., Nicolas, P. & Shai, Y. (1992). Interaction of antimicrobial dermaseptin and its fluorescently labeled analogues with phospholipid membranes. *Biochemistry*. 31 (49). pp. 12416–12423.

Poylin, V., Fareed, M.U., O'Neal, P. & Alamdari, N. (2008). The NF-κ B Inhibitor Curcumin Blocks Sepsis-Induced Muscle Proteolysis. *Mediators of …*.

Quiroga, M.P., Balakrishnan, K., Kurtova, A.V., Sivina, M., Keating, M.J., Wierda, W.G., Gandhi, V. & Burger, J.A. (2009). B-cell antigen receptor signaling enhances chronic lymphocytic leukemia cell migration and survival: specific targeting with a novel spleen tyrosine kinase inhibitor, R406. *Blood*. 114 (5). pp. 1029–1037.

Rai, K.R., Sawitsky, A., Cronkite, E.P., Chanana, A.D., Levy, R.N. & Pasternack, B.S. (1975). Clinical Staging of Chronic Lymphocytic Leukemia. *Blood*. 46 (2). pp. 219–234.

Ramsay, A.G. & Rodriguez-Justo, M. (2013). Chronic lymphocytic leukaemia--the role of the microenvironment pathogenesis and therapy. *British Journal of Haematology*. 162 (1). pp. 15–24.

Ramsay, A.G., Johnson, A.J., Lee, A.M., Gorgün, G., Le Dieu, R., Blum, W., Byrd, J.C. & Gribben, J.G. (2008). Chronic lymphocytic leukemia T cells show impaired immunological synapse formation that can be reversed with an immunomodulating drug. *Journal of Clinical Investigation*. 118 (118(7)). pp. 2427–2437.

Rao, P., Hayden, M.S., Long, M., Scott, M.L., West, A.P., Zhang, D., Oeckinghaus, A., Lynch, C., Hoffmann, A., Baltimore, D. & Ghosh, S. (2010). IkappaBbeta acts to inhibit and activate gene expression during the inflammatory response. *Nature*. 466 (7310). pp. 1115–1119.

Rassenti, L.Z., Huynh, L., Toy, T.L., Chen, L., Keating, M.J., Gribben, J.G., Neuberg, D.S., Flinn, I.W., Rai, K.R., Byrd, J.C., Kay, N.E., Greaves, A., Weiss, A. & Kipps, T.J. (2004). ZAP-70 compared with immunoglobulin heavy-chain gene mutation status as a predictor of disease progression in chronic lymphocytic leukemia. *New England Journal of Medicine*. 351 (9). pp. 893–901.

Rehman, K.K., Bertera, S., Bottino, R., Balamurugan, A.N., Mai, J.C., Mi, Z., Trucco, M. & Robbins, P.D. (2003). Protection of islets by in situ peptide-mediated transduction of the Ikappa B kinase inhibitor Nemo-binding domain peptide. *The Journal of biological chemistry*. 278 (11). pp. 9862–9868.

Reinecke, K., Eminel, S., Dierck, F., Roessner, W., Kersting, S., Chromik, A.M., Gavrilova, O., Laukevicience, A., Leuschner, I., Waetzig, V., Rosenstiel, P., Herdegen, T. & Sina, C. (2012). The JNK inhibitor XG-102 protects against TNBS-induced colitis. *PLoS ONE*. 7 (3). pp. e30985–e30985.

Revance Therapeutics (n.d.). *RT001 - Lateral canthal lines*. Available from: http://www.revance.com/rt001-lateral-canthal-lines/ (Accessed: 10 June 2014).

Rhee, M. & Davis, P. (2006). Mechanism of uptake of C105Y, a novel cell-penetrating peptide. *The Journal of biological chemistry*. 281 (2). pp. 1233–1240.

Richard, J.P., Melikov, K., Brooks, H., Prevot, P., Lebleu, B. & Chernomordik, L.V. (2005). Cellular uptake of unconjugated TAT peptide involves clathrin-dependent endocytosis and heparan sulfate receptors. *The Journal of biological chemistry*. 280 (15). pp. 15300–15306.

Richard, J.P., Melikov, K., Vives, E., Ramos, C., Verbeure, B., Gait, M.J., Chernomordik, L.V. & Lebleu, B. (2002). Cell-penetrating peptides. A reevaluation of the mechanism of cellular uptake. *The Journal of biological chemistry*. 278 (1). pp. 585–590.

Richardson, S.J., Matthews, C., Catherwood, M.A., Alexander, H.D., Carey, B.S., Farrugia, J., Gardiner, A., Mould, S., Oscier, D., Copplestone, J.A. & Prentice, A.G. (2006). ZAP-70 expression is associated with enhanced ability to respond to migratory and survival signals in B-cell chronic lymphocytic leukemia (B-CLL). *Blood*. 107 (9). pp. 3584–3592.

Ridley, A.J. (1994). Membrane ruffling and signal transduction. *Bioessays*. 16 (5). pp. 321–327.

Ringshausen, I., Schneller, F., Bogner, C., Hipp, S., Duyster, J., Peschel, C. & Decker, T. (2002). Constitutively activated phosphatidylinositol-3 kinase (PI-3K) is involved in the defect of apoptosis in B-CLL: association with protein kinase Cdelta. *Blood*. 100 (10). pp. 3741–3748.

Rodriguez, M. & Schaper, J. (2005). Apoptosis: measurement and technical issues. *Journal of molecular and cellular cardiology*. 38 (1). pp. 15–20.

Rodriguez, M.S., Thompson, J., Hay, R.T. & Dargemont, C. (1999). Nuclear retention of IκBα protects it from signal-induced degradation and inhibits nuclear factor κB transcriptional activation. *Journal of Biological Chemistry*. 274 (13). pp. 9108–9115.

Roman-Blas, J.A. & Jimenez, S.A. (2006). NF-κB as a potential therapeutic target in osteoarthritis and rheumatoid arthritis. *Osteoarthritis and Cartilage*. 14 (9). pp. 839–848.

Romano, M.F., Lamberti, A., Tassone, P., Alfinito, F., Costantini, S., Chiurazzi, F., Defrance, T., Bonelli, P., Tuccillo, F., Turco, M.C. & Venuta, S. (1998). Triggering of CD40 antigen inhibits fludarabine-induced apoptosis in B chronic lymphocytic leukemia cells. *Blood*. 92 (3). pp. 990–995.

Rose, D.M., Han, J. & Ginsberg, M.H. (2002). Alpha4 integrins and the immune response. *Immunological reviews*. 186 (1). pp. 118–124.

Rosenquist, R., Cortese, D., Bhoi, S., Mansouri, L. & Gunnarsson, R. (2013). Prognostic markers and their clinical applicability in chronic lymphocytic leukemia: where do we stand? *Leukemia & Lymphoma*. 54 (11). pp. 2351–2364.

Rosenwald, A., Alizadeh, A.A., Widhopf, G., Simon, R., Davis, R.E., Yu, X., Yang, L., Pickeral, O.K., Rassenti, L.Z., Powell, J., Botstein, D., Byrd, J.C., Grever, M.R., Cheson, B.D., Chiorazzi, N., Wilson, W.H., Kipps, T.J., Brown, P.O. & Staudt, L.M. (2001). Relation of gene expression phenotype to immunoglobulin mutation genotype in B cell chronic lymphocytic leukemia. *The Journal of experimental medicine*. 194 (11). pp. 1639–1647.

Rossi, D., Zucchetto, A., Rossi, F.M., Capello, D., Cerri, M., Deambrogi, C., Cresta, S., Rasi, S., De Paoli, L., Bodoni, C.L., Bulian, P., Del Poeta, G., Ladetto, M., Gattei, V. & Gaidano, G. (2008). CD49d expression is an independent risk factor of progressive disease in early stage chronic lymphocytic leukemia. *Haematologica*. 93 (10). pp. 1575–1579.

Rothbard, J.B., Jessop, T.C., Lewis, R.S., Murray, B.A. & Wender, P.A. (2004). Role of membrane potential and hydrogen bonding in the mechanism of translocation of guanidinium-rich peptides into cells. *Journal of the American Chemical Society*. 126 (31). pp. 9506–9507.

Rothbard, J.B., Kreider, E., VanDeusen, C.L., Wright, L., Wylie, B.L. & Wender, P.A. (2002). Arginine-rich molecular transporters for drug delivery: Role of backbone spacing in cellular uptake. *Journal of Medicinal Chemistry*. 45 (17). pp. 3612–3618.

Rozková, D., Novotná, L., Pytlík, R., Hochová, I., Kozák, T., Bartůnková, J. & Spísek, R. (2010). Toll-like receptors on B-CLL cells: expression and functional consequences of their stimulation. *International Journal of Cancer*. 126 (5). pp. 1132–1143.

Ruland, J. & Mak, T.W. (2003). Transducing signals from antigen receptors to nuclear factor kappaB. *Immunological reviews*. 193. pp. 93–100.

Ryseck, R.P., Bull, P., Takamiya, M., Bours, V., Siebenlist, U., Dobrzanski, P. & Bravo, R. (1992). RelB, a new Rel family transcription activator that can interact with p50-NF-kappa B. *Molecular and Cellular Biology*. 12 (2). pp. 674–684.

Saar, K., Lindgren, M., Hansen, M., Eiríksdóttir, E., Jiang, Y., Rosenthal-Aizman, K., Sassian, M. & Langel, Ü. (2005). Cell-penetrating peptides: a comparative membrane toxicity study. *Analytical Biochemistry*. 345 (1). pp. 55–65.

Sadler, K., Eom, K.D., Yang, J.L., Dimitrova, Y. & Tam, J.P. (2002). Translocating proline-rich peptides from the antimicrobial peptide bactenecin 7. *Biochemistry*. 41 (48). pp. 14150–14157.

Scheibel, M., Klein, B., Merkle, H., Schulz, M., Fritsch, R., Greten, F.R., Arkan, M.C., Schneider, G. & Schmid, R.M. (2010). IkappaBbeta is an essential co-activator for LPS-induced IL-1beta transcription in vivo. *Journal of Experimental Medicine*. 207 (12). pp. 2621–2630.

Scheidereit, C.C. (2006). IkappaB kinase complexes: gateways to NF-kappaB activation and transcription. *Oncogene*. 25 (51). pp. 6685–6705.

Schmid, S.L. (1997). Clathrin-coated vesicle formation and protein sorting: an integrated process. *Annual review of biochemistry*.

Schmidt, N., Mishra, A., Lai, G.H. & Wong, G.C. (2010). Arginine-rich cell-penetrating peptides. *FEBS Letters*. 584 (9). pp. 1806–1813.

Schmitz, M.L.M., Henkel, T.T. & Baeuerle, P.A.P. (1991). Proteins controlling the nuclear uptake of NF-kappa B, Rel and dorsal. *Trends in Cell Biology*. 1 (5). pp. 130–137.

Schwarze, S.R.S., Ho, A.A., Vocero-Akbani, A.A. & Dowdy, S.F.S. (1999). In vivo protein transduction: delivery of a biologically active protein into the mouse. *Science*. 285 (5433). pp. 1569–1572.

Sebbage, V. (2009). Cell-penetrating peptides and their therapeutic applications. *Bioscience Horizons*. 2 (1). pp. 64–72.

Seifert, M., Sellmann, L., Bloehdorn, J., Wein, F., Stilgenbauer, S., Dürig, J. & Küppers, R. (2012). Cellular origin and pathophysiology of chronic lymphocytic leukemia. *The Journal of experimental medicine*. 209 (12). pp. 2183–2198.

Sen, R. & Baltimore, D. (1986a). Multiple nuclear factors interact with the immunoglobulin enhancer sequences. *Cell*. 46 (5). pp. 705–716.

Sen, R. & Baltimore, D. (1986b). *Inducibility of κ immunoglobulin enhancer-binding protein NF-κB by a posttranslational mechanism*. 47 (6). pp. 921–928. Available from: http://eutils.ncbi.nlm.nih.gov/entrez/eutils/elink.fcgi?dbfrom=pubmed&id=3096580&retmode=ref&cmd=prlinks.

Shai, Y. (1999). Mechanism of the binding, insertion and destabilization of phospholipid bilayer membranes by alpha-helical antimicrobial and cell non-selective membrane-lytic peptides. *Biochimica et biophysica acta*. 1462 (1-2). pp. 55–70.

Shakhov, A.N.A., Collart, M.A.M., Vassalli, P.P., Nedospasov, S.A.S. & Jongeneel, C.V.C. (1990). Kappa B-type enhancers are involved in lipopolysaccharide-mediated transcriptional activation of the tumor necrosis factor alpha gene in primary macrophages. *The Journal of experimental medicine*. 171 (1). pp. 35–47.

Shanafelt, T.D., Geyer, S.M., Bone, N.D., Tschumper, R.C., Witzig, T.E., Nowakowski, G.S., Zent, C.S., Call, T.G., LaPlant, B., Dewald, G.W., Jelinek, D.F. & Kay, N.E. (2008). CD49d expression is an independent predictor of overall survival in patients with chronic lymphocytic leukaemia: a prognostic parameter with therapeutic potential. *British Journal of Haematology*. 140 (5). pp. 537–546.

Shin, M.C., Zhang, J., Min, K.A., Lee, K., Byun, Y., David, A.E., He, H. & Yang, V.C. (2014). Cell-penetrating peptides: achievements and challenges in application for cancer treatment. *Journal of Biomedical Materials Research, Part A*. 102 (2). pp. 575–587.

Shvidel, L.L., Braester, A.A., Bairey, O.O., Rahimi-Levene, N.N., Herishanu, Y.Y., Tadmor, T.T., Klepfish, A.A., Ruchlemer, R.R., Shtalrid, M.M., Berrebi, A.A. & Polliack, A.A. (2012). Cell surface expression of CD25 antigen (surface IL-2 receptor α-chain) is not a prognostic marker in chronic lymphocytic leukemia: results of a retrospective study of 281 patients. *Annals of Hematology*. 91 (10). pp. 1597–1602.

Smale, S.T. (2011). Hierarchies of NF-κB target-gene regulation. *Nature Immunology*. 12 (8). pp. 689–694.

Smolej, L., Vroblova, V. & Novosad, J. (2008). Expression of ZAP-70 in patients with chronic lymphocytic leukemia may change significantly during the course of the disease. *International Journal of Laboratory Hematology*. 30 (3). pp. 259–260.

Song, J., Kai, M., Zhang, W., Zhang, J., Liu, L., Zhang, B., Liu, X. & Wang, R. (2011). Cellular uptake of transportan 10 and its analogs in live cells: Selectivity and structure–activity relationship studies. *Peptides*. 32 (9). pp. 1934–1941.

Soomets, U., Langel, Ü., Lindgren, M., Gallet, X., Hällbrink, M., Elmquist, A., Balaspiri, L., ZORKO, M., Pooga, M. & Brasseur, R. (2000). Deletion analogues of transportan. *Biochimica et biophysica acta*. 1467 (1). pp. 165–176.

Sparr, C., Purkayastha, N., Kolesinska, B., Gengenbacher, M., Amulic, B., Matuschewski, K., Seebach, D. & Kamena, F. (2013). Improved efficacy of fosmidomycin against Plasmodium and Mycobacterium species by combination with the cell-penetrating peptide octaarginine. *Antimicrobial Agents and Chemotherapy*. 57 (10). pp. 4689–4698.

Srahna, M., Remacle, J.E., Annamalai, K., Pype, S., Huylebroeck, D., Boogaerts, M.A. & Vandenberghe, P. (2001). NF-κB is involved in the regulation of CD154 (CD40 ligand) expression in primary human T cells. *Clinical & Experimental Immunology*. 125 (2). pp. 229–236.

Stalmans, S., Wynendaele, E., Bracke, N., Gevaert, B., D'Hondt, M., Peremans, K., Burvenich, C. & De Spiegeleer, B. (2013). Chemical-functional diversity in cell-penetrating peptides. *PLoS ONE*. 8 (8). pp. e71752–e71752.

Staudt, L.M. (2010). Oncogenic activation of NF-κB. *Cold Spring Harbor Perspectives in Biology*.

Steele, A.J., Jones, D.T., Ganeshaguru, K., Duke, V.M., Yogashangary, B.C., North, J.M., Lowdell, M.W., Kottaridis, P.D., Mehta, A.B., Prentice, A.G., Hoffbrand, A.V. & Wickremasinghe, R.G. (2006). The sesquiterpene lactone parthenolide induces selective apoptosis of B-chronic lymphocytic leukemia cells in vitro. *Leukemia*. 20 (6). pp. 1073–1079.

Stilgenbauer, S., Bullinger, L., Lichter, P. & Döhner, H. (2002). Genetics of chronic lymphocytic leukemia: genomic aberrations and V(H) gene mutation status in pathogenesis and clinical course. *Leukemia*. 16 (6). pp. 993–1007.

Sulda, M.L., Kuss, B.J., Hall, R.K., Bailey, S. & Macardle, P.J. (2012). Clinical utility of molecular and flow cytometric markers in chronic lymphocytic leukaemia. *Internal Medicine Journal*. 42 (2). pp. 137–146.

Sun, S.C., Ganchi, P.A., Ballard, D.W. & Greene, W.C. (1993). NF-kappa B controls expression of inhibitor I kappa B alpha: evidence for an inducible autoregulatory pathway. *Science*.

Suyang, H., Phillips, R., Douglas, I. & Ghosh, S. (1996). Role of unphosphorylated, newly synthesized I kappa B beta in persistent activation of NF-kappa B. *Molecular and Cellular Biology*. 16 (10). pp. 5444–5449.

Szabó, R., Bánóczi, Z., Mező, G., Láng, O., Kőhidai, L. & Hudecz, F. (2010). Daunomycin-polypeptide conjugates with antitumor activity. *BBA - Biomembranes*. 1798 (12). pp. 2209–2216.

Takada, Y., Singh, S. & Aggarwal, B.B. (2004). Identification of a p65 peptide that selectively inhibits NF-kappa B activation induced by various inflammatory stimuli and its role in down-regulation of NF-kappaB-mediated gene expression and up-regulation of apoptosis. *The Journal of biological chemistry*. 279 (15). pp. 15096–15104.

Takayama, K., Nakase, I., Michiue, H., Takeuchi, T., Tomizawa, K., Matsui, H. & Futaki, S. (2009). Enhanced intracellular delivery using arginine-rich peptides by the addition of penetration accelerating sequences (Pas). *Journal of controlled release : official journal of the Controlled Release Society*. 138 (2). pp. 128–133.

Tergaonkar, V., Correa, R.G., Ikawa, M. & Verma, I.M. (2005). Distinct roles of IkappaB proteins in regulating constitutive NF-kappaB activity. *Nature Cell Biology*. 7 (9). pp.

921–923.

Terzidou, V., Lee, Y., Lindström, T., Johnson, M., Thornton, S. & Bennett, P.R. (2006). Regulation of the human oxytocin receptor by nuclear factor-kappaB and CCAAT/enhancer-binding protein-beta. *Journal of Clinical Endocrinology & Metabolism*. 91 (6). pp. 2317–2326.

Thieu, V.T., Nguyen, E.T., McCarthy, B.P., Bruns, H.A., Kapur, R., Chang, C.-H. & Kaplan, M.H. (2007). IL-4-stimulated NF-kappaB activity is required for Stat6 DNA binding. *Journal of Leukocyte Biology*. 82 (2). pp. 370–379.

Thompson, J.E., Phillips, R.J., Erdjument-Bromage, H., Tempst, P. & Ghosh, S. (1995). IκB-β regulates the persistent response in a biphasic activation of NF-κB. *Cell*. 80 (4). pp. 573–582.

Thorén, P., Persson, D., Isakson, P. & Goksör, M. (2003). Uptake of analogs of penetratin, Tat (48–60) and oligoarginine in live cells. *Biochemical and …*.

Till, K.J., Lin, K., Zuzel, M. & Cawley, J.C. (2002). The chemokine receptor CCR7 and alpha4 integrin are important for migration of chronic lymphocytic leukemia cells into lymph nodes. *Blood*. 99 (8). pp. 2977–2984.

Tirumurugaan, K.G., Kang, B.N., Panettieri, R.A., Foster, D.N., Walseth, T.F. & Kannan, M.S. (2008). Regulation of the cd38 promoter in human airway smooth muscle cells by TNF-alpha and dexamethasone. *Respiratory Research*. 9. pp. 26–26.

Tolnay, M., Vereshchagina, L.A. & Tsokos, G.C. (2002). NF-kappaB regulates the expression of the human complement receptor 2 gene. *Journal of immunology (Baltimore, Md. : 1950)*. 169 (11). pp. 6236–6243.

Trabulo, S., Cardoso, A.L., Mano, M. & de Lima, M.C.P. (2010). Cell-penetrating peptides-mechanisms of cellular uptake and generation of delivery systems. *Pharmaceuticals*. 3 (4). pp. 961–993.

Tsai, C.-W., Hsu, N.-Y., Wang, C.-H., Lu, C.-Y., Chang, Y., Tsai, H.-H.G. & Ruaan, R.-C. (2009). Coupling Molecular Dynamics Simulations with Experiments for the Rational Design of Indolicidin-Analogous Antimicrobial Peptides. *Journal of Molecular Biology*. 392 (3). pp. 837–854.

Tsukada, N., Burger, J.A., Zvaifler, N.J. & Kipps, T.J. (2002). Distinctive features of ‘nurselike’ cells that differentiate in the context of chronic lymphocytic leukemia. *Blood*. 99 (3). pp. 1030–1037.

Tünnemann, G., Ter-Avetisyan, G., Martin, R.M., Stöckl, M., Herrmann, A. & Cardoso, M.C. (2008). Live-cell analysis of cell penetration ability and toxicity of oligo-arginines. M. A. R. B. Castanho & M. Dathe (eds.). *Journal of Peptide Science*. 14 (4). pp. 469–476.

Udalova, I.A., Richardson, A., Denys, A., Smith, C., Ackerman, H., Foxwell, B. & Kwiatkowski, D. (2000). Functional consequences of a polymorphism affecting NF-kappaB p50-p50 binding to the TNF promoter region. *Molecular and Cellular Biology*. 20 (24). pp. 9113–9119.

UniProt Consortium (2014). *Heat shock protein HSP 90-alpha - P07900*. Available from: http://www.uniprot.org/uniprot/P07900 (Accessed: 12 May 2014).

Valen, G., Yan, Z.Q. & Hansson, G.K. (2001). Nuclear factor kappa-B and the heart. *Journal of the American College of Cardiology*. 38 (2). pp. 307–314.

Valero, J.G., Sancey, L., Kucharczak, J., Guillemin, Y., Gimenez, D., Prudent, J., Gillet, G., Salgado, J., Coll, J.-L. & Aouacheria, A. (2011). Bax-derived membrane-active peptides act as potent and direct inducers of apoptosis in cancer cells. *Journal of Cell Science*. 124 (Pt 4). pp. 556–564.

Vallabhapurapu, S. & Karin, M. (2009). Regulation and function of NF-kappaB transcription factors in the immune system. *Annual Review of Immunology*. 27. pp. 693–733.

Vaslin, A., Naegele-Tollardo, S., Puyal, J. & Clarke, P.G.H. (2011). Excitotoxicity-induced endocytosis mediates neuroprotection by TAT-peptide-linked JNK inhibitor. *Journal of Neurochemistry*. 119 (6). pp. 1243–1252.

Verstrepen, L., Adib-Conquy, M., Kreike, M., Carpentier, I., Adrie, C., Cavaillon, J.-M. & Beyaert, R. (2008). Expression of the NF-kappaB inhibitor ABIN-3 in response to TNF and toll-like receptor 4 stimulation is itself regulated by NF-kappaB. *Journal of cellular and molecular medicine*. 12 (1). pp. 316–329.

Vives, E., Brodin, P. & Lebleu, B. (1997). A truncated HIV-1 Tat protein basic domain rapidly translocates through the plasma membrane and accumulates in the cell nucleus. *The Journal of biological chemistry*. 272 (25). pp. 16010–16017.

Vogler, M., Butterworth, M., Majid, A., Walewska, R.J., Sun, X.-M., Dyer, M.J.S. & Cohen, G.M. (2009). Concurrent up-regulation of BCL-XL and BCL2A1 induces approximately 1000-fold resistance to ABT-737 in chronic lymphocytic leukemia. *Blood*. 113 (18). pp. 4403–4413.

Vroblova, V., Vrbacky, F., Hrudkova, M., Jankovicova, K., Schmitzova, D., Maly, J., Krejsek, J. & Smolej, L. (2010). Significant change in ZAP-70 expression during the course of chronic lymphocytic leukemia. *European journal of haematology*. 84 (6). pp. 513–517.

Vuillier, F., Dumas, G., Magnac, C., Prevost, M.-C., Lalanne, A.I., Oppezzo, P., Melanitou, E., Dighiero, G. & Payelle-Brogard, B. (2005). Lower levels of surface B-cell-receptor expression in chronic lymphocytic leukemia are associated with glycosylation and folding defects of the mu and CD79a chains. *Blood*. 105 (7). pp. 2933–2940.

Wadia, J.S., Stan, R.V. & Dowdy, S.F. (2004). Transducible TAT-HA fusogenic peptide enhances escape of TAT-fusion proteins after lipid raft macropinocytosis. *Nature Medicine*. 10 (3). pp. 310–315.

Wang, C.Y., Mayo, M.W., Korneluk, R.G., Goeddel, D.V. & Baldwin, A.S., Jr (1998). **NF-κB** antiapoptosis: Induction of TRAF1 and TRAF2 and c-IAP1 and c- IAP2 to suppress caspase-8 activation. *Science*. 281 (5383). pp. 1680–1683.

Wang, H., Guo, Q., Jiang, Y., Liu, E., Zhao, Y., Li, Y. & Huang, Y. (2013). Co-delivery of cell-permeable chimeric apoptosis AVPIR8 peptide/p53 DNA for cocktail therapy. *Advanced Functional Materials*. 23 (48). pp. 6068–6075.

Wang, T., Lafuse, W.P. & Zwilling, B.S. (2001). NFkappaB and Sp1 elements are necessary for maximal transcription of toll-like receptor 2 induced by Mycobacterium avium. *Journal of immunology (Baltimore, Md. : 1950)*. 167 (12). pp. 6924–6932.

Wang, Y., Xiao, H., Wu, N., Shi, H., Xu, H., Zhou, L., Xi, X.-G., Wang, T. & Wang, X. (2010). Characterization of the Antiviral Activity for Influenza Viruses M1 Zinc Finger Peptides. *Current Microbiology*. 62 (1). pp. 126–132.

Wang, Y.F., Xu, X., Fan, X., Zhang, C., Wei, Q., Wang, X., Guo, W., Xing, W., Yu, J., Yan, J.-L. & Liang, H.-P. (2011). A cell-penetrating peptide suppresses inflammation by inhibiting NF-κB signaling. *Molecular Therapy*. 19 (10). pp. 1849–1857.

Warton, K., Foster, N.C., Gold, W.A. & Stanley, K.K. (2004). A novel gene family induced by acute inflammation in endothelial cells. *Gene*. 342 (1). pp. 85–95.

Watkins, C.L., Brennan, P., Fegan, C., Takayama, K., Nakase, I., Futaki, S. & Jones, A.T. (2009a). Cellular uptake, distribution and cytotoxicity of the hydrophobic cell penetrating peptide sequence PFVYLI linked to the proapoptotic domain peptide PAD. *Journal of controlled release : official journal of the Controlled Release Society*. 140 (3). pp. 237–244.

Watkins, C.L., Sayers, E.J., Allender, C., Barrow, D., Fegan, C., Brennan, P. & Jones, A.T. (2011). Co-operative membrane disruption between cell-penetrating peptide and cargo: implications for the therapeutic use of the Bcl-2 converter peptide D-NuBCP-9-r8. *Molecular Therapy*. 19 (12). pp. 2124–2132.

Watkins, C.L., Schmaljohann, D., Futaki, S. & Jones, A.T. (2009b). Low concentration thresholds of plasma membranes for rapid energy-independent translocation of a cell-penetrating peptide. *Biochemical Journal*. 420 (2). pp. 179–189.

Wender, P.A., Mitchell, D.J., Pattabiraman, K., Pelkey, E.T., Steinman, L. & Rothbard, J.B. (2000). The design, synthesis, and evaluation of molecules that enable or enhance cellular uptake: Peptoid molecular transporters. *Proceedings of the National Academy of Sciences*. 97 (24). pp. 13003–13008.

Whiteside, S.T. & Israël, A. (1997). IκB proteins: structure, function and regulation. *Seminars in Cancer Biology*. 8 (2). pp. 75–82.

Willimott, S., Baou, M., Huf, S., Deaglio, S. & Wagner, S.D. (2007a). Regulation of CD38 in proliferating chronic lymphocytic leukemia cells stimulated with CD154 and interleukin-4. *Haematologica*. 92 (10). pp. 1359–1366.

Willimott, S., Baou, M., Naresh, K. & Wagner, S.D. (2007b). CD154 induces a switch in pro-survival Bcl-2 family members in chronic lymphocytic leukaemia. *British Journal of Haematology*. 138 (6). pp. 721–732.

Woyach, J.A., Johnson, A.J. & Byrd, J.C. (2012). The B-cell receptor signaling pathway as a therapeutic target in CLL. *Blood*. 120 (6). pp. 1175–1184.

Wu, K., Jiang, S.W., Thangaraju, M., Wu, G. & Couch, F.J. (2000). Induction of the BRCA2 promoter by nuclear factor-κB. *Journal of Biological Chemistry*. 275 (45). pp. 35548–35556.

Wu, M., Akinleye, A. & Zhu, X. (2013). Novel agents for chronic lymphocytic leukemia. *Journal of hematology & oncology*. 6. p. 36.

Xu, L.G. & Shu, H.B. (2002). TNFR-associated factor-3 is associated with BAFF-R and negatively regulates BAFF-R-mediated NF-κB activation and IL-10 production. *Journal of Immunology*. 169 (12). pp. 6883–6889.

Yamamoto, K., Arakawa, T. & Ueda, N. (1995). Transcriptional roles of nuclear factor B and nuclear factor-interleukin-6 in the tumor necrosis factor-dependent induction of cyclooxygenase-2 in MC3T3-E1 cells. *Journal of Biological …*.

Yamaoka, S., Courtois, G., Bessia, C. & Whiteside, S.T. (1998). Complementation cloning of NEMO, a component of the IκB kinase complex essential for NF-κB activation. *Cell*.

Yandek, L.E., Pokorny, A., Florén, A., Knoelke, K., Langel, Ü. & Almeida, P.F. (2007). Mechanism of the Cell-Penetrating Peptide Transportan 10 Permeation of Lipid Bilayers. *Biophysical Journal*. 92 (7). pp. 2434–2444.

Yang, J., Tsutsumi, H., Furuta, T., Sakurai, M. & Mihara, H. (2014). Interaction of amphiphilic α-helical cell-penetrating peptides with heparan sulfate. *Organic and Biomolecular Chemistry*. 12 (26). pp. 4673–4681.

Yang, N., Huang, J., Greshock, J., Liang, S., Barchetti, A., Hasegawa, K., Kim, S., Giannakakis, A., Li, C., O'Brien-Jenkins, A., Katsaros, D., Bützow, R., Coukos, G. & Zhang, L. (2008). Transcriptional regulation of PIK3CA oncogene by NF-kappaB in ovarian cancer microenvironment. E. Abraham (ed.). *PLoS ONE*. 3 (3). pp. e1758–e1758.

Ye, H., Arron, J.R., Lamothe, B., Cirilli, M., Kobayashi, T., Shevde, N.K., Segal, D., Dzivenu, O.K., Vologodskaia, M., Yim, M., Du, K., Singh, S., Pike, J.W., Darnay, B.G., Choi, Y. & Wu, H. (2002). Distinct molecular mechanism for initiating TRAF6 signalling. *Nature*. 418 (6896). pp. 443–447.

Yin, H., Moulton, H.M., Betts, C., Merritt, T., Seow, Y., Ashraf, S., Wang, Q., Boutilier, J. & Wood, M.J. (2010). Functional rescue of dystrophin-deficient mdx mice by a chimeric peptide-PMO. *Molecular Therapy*. 18 (10). pp. 1822–1829.

Yin, Y., Wu, X., Yang, Z., Zhao, J., Wang, X., Zhang, Q., Yuan, M., Xie, L., Liu, H. & He, Q. (2013). The potential efficacy of R8-modified paclitaxel-loaded liposomes on pulmonary arterial hypertension. *Pharmaceutical Research*. 30 (8). pp. 2050–2062.

You, M.J., Ku, P.T., Hrdlickova, R. & Bose, H.R. (1997). ch-IAP1, a member of the inhibitor-of-apoptosis protein family, is a mediator of the antiapoptotic activity of the v-Rel oncoprotein. *Molecular and Cellular Biology*. 17 (12). pp. 7328–7341.

Zamorano, J., Mora, A.L., Boothby, M. & Keegan, A.D. (2001). NF-kappa B activation plays an important role in the IL-4-induced protection from apoptosis. *International immunology*. 13 (12). pp. 1479–1487.

Zenz, T., Mertens, D., Küppers, R., Döhner, H. & Stilgenbauer, S. (2010). From pathogenesis to treatment of chronic lymphocytic leukaemia. *Nature Reviews Cancer*. 10 (1). pp. 37–50.

Zenz, T., Mohr, J., Eldering, E., Kater, A.P., Bühler, A., Kienle, D., Winkler, D., Dürig, J., van Oers, M.H.J., Mertens, D., Döhner, H. & Stilgenbauer, S. (2009). miR-34a as part of the resistance network in chronic lymphocytic leukemia. *Blood*. 113 (16). pp. 3801–3808.

Zhang, D.X., Jiang, S.L., Rzewinicki, D., Samols, D. & Kushner, I. (1995). The Effect of Interleukin-1 on C-Reactive Protein Expression in Hep3b Cells Is Exerted at the Transcriptional Level. *Biochemical Journal*. 310 (1). pp. 143–148.

Zielinski, J., Kilk, K., Peritz, T., Kannanayakal, T., Miyashiro, K.Y., Eiríksdóttir, E., Jochems, J., Langel, Ü. & Eberwine, J. (2006). In vivo identification of ribonucleoprotein-RNA interactions. *Proceedings of the National Academy of Sciences*. 103 (5). pp. 1557–1562.

Zou, J.Y. & Crews, F.T. (2005). TNFα potentiates glutamate neurotoxicity by inhibiting glutamate uptake in organotypic brain slice cultures: neuroprotection by NFκB inhibition. *Brain Research*. 1034 (1). pp. 11–24.

Zucchetto, A., Benedetti, D., Tripodo, C., Bomben, R., Bo, M.D., Marconi, D., Bossi, F., Lorenzon, D., Degan, M., Rossi, F.M., Rossi, D., Bulian, P., Franco, V., Del Poeta, G., Deaglio, S., Gaidano, G., Tedesco, F., Malavasi, F. & Gattei, V. (2009). CD38/CD31, the CCL3 and CCL4 chemokines, and CD49d/vascular cell adhesion molecule-1 are interchained by sequential events sustaining chronic lymphocytic leukemia cell survival. *Cancer Research*. 69 (9). pp. 4001–4009.

Appendix I

A primary study was performed were conditions applied in Section 4.2 were reproduced. An extra step was added that included co-culture of CLL cells pre-treated with TP10-p50i for one hour. CLL cells were kept in co-culture for one hour, and cell surface markers CD25, CD49d, CD38 and CD69 were measured by flow cytometry. Figures I to IV show the data collected for six patient samples. Based on the data presented here, it was determined that expression of the majority of the cell surface markers wasn't significantly altered after one hour of co-culture. In subsequent experiments the co-culture period was extended to 24 hours.

CD25

CD40L

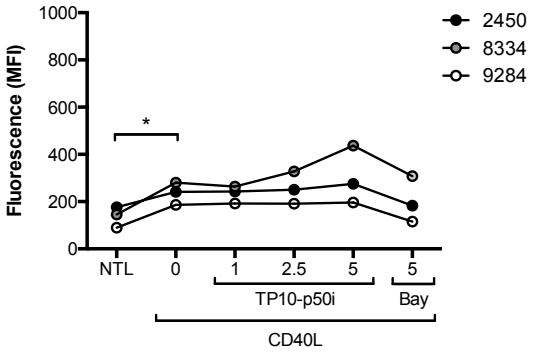

CpG

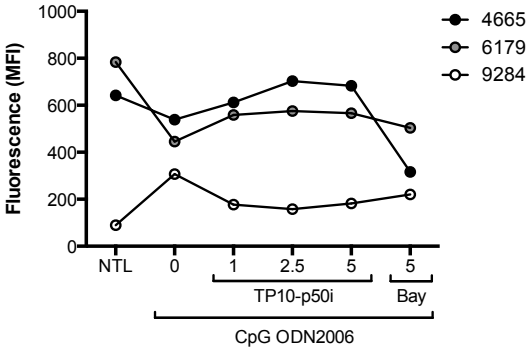

Figure XXIV – CD25 MFI of primary CLL cells pre-treated with TP10-p50i and Bay, and subsequently stimulated with CD40L and CpG.
Primary CLL cells were pre-treated with 0, 1, 2.5, 5 μM of TP10-p50i and 5 μM of Bay for one hour. Cells were harvested and one set of cells was co-cultured with CD40L-expressing fibroblasts or NTL cells, the other was cultured with 500 nM of CpG for one hour. Cells were harvested and analysed by flow cytometry. Data is presented separately for each sample tested. Total of 3 patient samples.

CD49d

CD40L

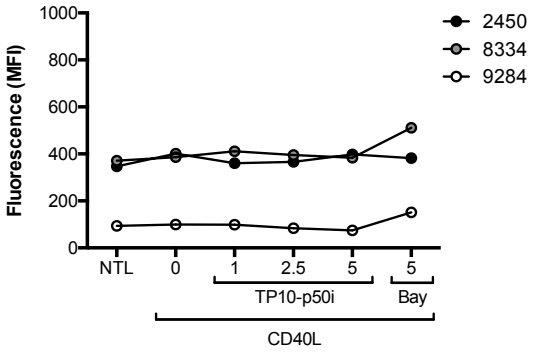

CpG

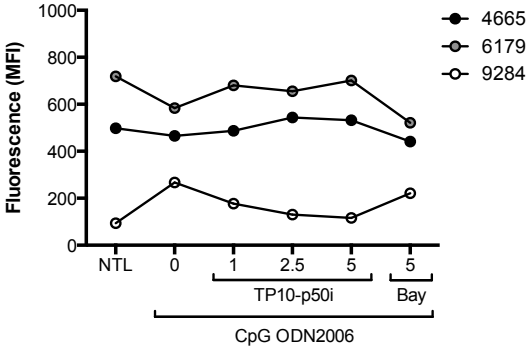

Figure XXV – CD49d MFI of primary CLL cells pre-treated with TP10-p50i and Bay, and subsequently stimulated with CD40L and CpG.
Primary CLL cells were pre-treated with 0, 1, 2.5, 5 μM of TP10-p50i and 5 μM of Bay for one hour. Cells were harvested and one set of cells was co-cultured with CD40L-expressing fibroblasts or NTL cells, the other was cultured with 500 nM of CpG for one hour. Cells were harvested and analysed by flow cytometry. Data is presented separately for each sample tested. Total of 3 patient samples.

CD38

CD40L

CpG

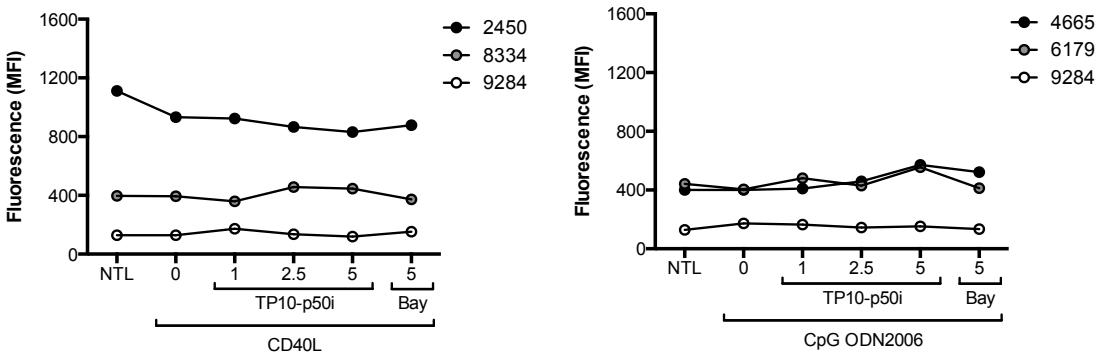

Figure XXVI - CD38 MFI of primary CLL cells pre-treated with TP10-p50i and Bay, and subsequently stimulated with CD40L and CpG.

Primary CLL cells were pre-treated with 0, 1, 2.5, 5 μM of TP10-p50i and 5 μM of Bay for one hour. Cells were harvested and one set of cells was co-cultured with CD40L-expressing fibroblasts or NTL cells, the other was cultured with 500 nM of CpG for one hour. Cells were harvested and analysed by flow cytometry. Data is presented separately for each sample tested. Total of 5 patient samples tested, where one was used in duplicate and stimulated with CD40L and CpG, separately.

CD69

CD40L

CpG

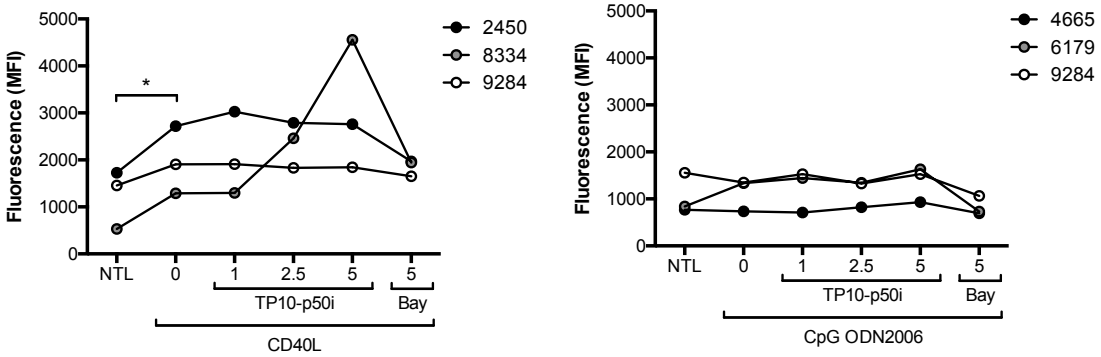

Figure XXVII – CD69 MFI of primary CLL cells pre-treated with TP10-p50i and Bay, and subsequently stimulated with CD40L and CpG.

Primary CLL cells were pre-treated with 0, 1, 2.5, 5 μM of TP10-p50i and 5 μM of Bay for one hour. Cells were harvested and one set of cells was co-cultured with CD40L-expressing fibroblasts or NTL cells, the other was cultured with 500 nM of CpG for one hour. Cells were harvested and analysed by flow cytometry. Data is presented separately for each sample tested. Total of 3 patient samples.

Appendix II

To further understand the increase in CD25 expression caused by pre-treatment with 5 μM of Bay 11-7082, dot plots of CD25 and CD19 expression are presented in the following Figures. Four patient samples were selected, that would represent all the variations found in CD25 expression (i.e. increased, decreased or maintained expression of CD25 following pre-treatment with Bay 11-7082).

In the four samples shown, cells pre-treated with Bay 11-7082 can be divided into two populations, whilst cells incubated in other conditions only present one population. The largest population in the plot of cell pre-treated with Bay 11-7082, corresponds to CD25 levels similar to the population found in the plot of untreated and co-cultured with NTL cells. However, the smallest population expresses CD25 at levels higher that the population found in untreated and co-cultured with CD40L cells. This indicates that Bay 11-7082 actually induces upregulation of CD25 in a small number of cells. Determining the cause for this upregulation is unfortunately beyond the scope of this project.

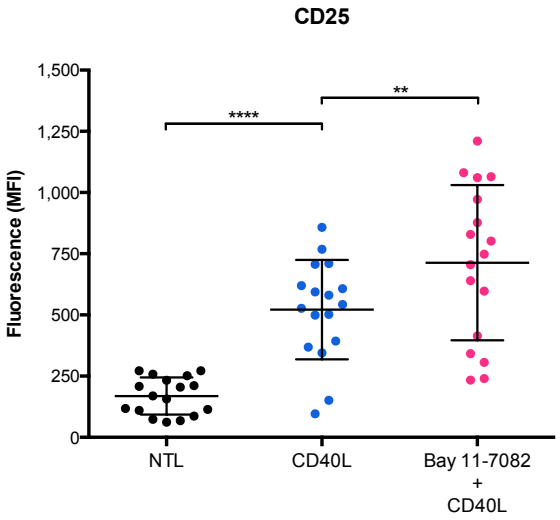

Figure XXVIII - Expression of CD25 on primary CLL cells pre-treated with Bay 11-7082, followed by co-culture with NTL and CD40L cells.

Primary CLL were incubated in liquid culture without any treatment or with 5 μM of Bay 11-7082 for a period of 1 hour. Cells were harvested and transferred onto co-culture with NTL or CD40L for a period of 24 hours. Cells were then harvested, washed and incubated with anti-CD25 antibody (560225, BD Pharmogen). The gating strategy used is presented in Figure 5.11. Data from 17 patient samples, presented as MFI values for each individual sample, plus mean and +/- SD. Statistical analysis was performed using the software GraphPad Prism 6. Repeated-measures one-way ANOVA was applied followed by a multiple-comparisons test. * - represents the level of statistical significance.

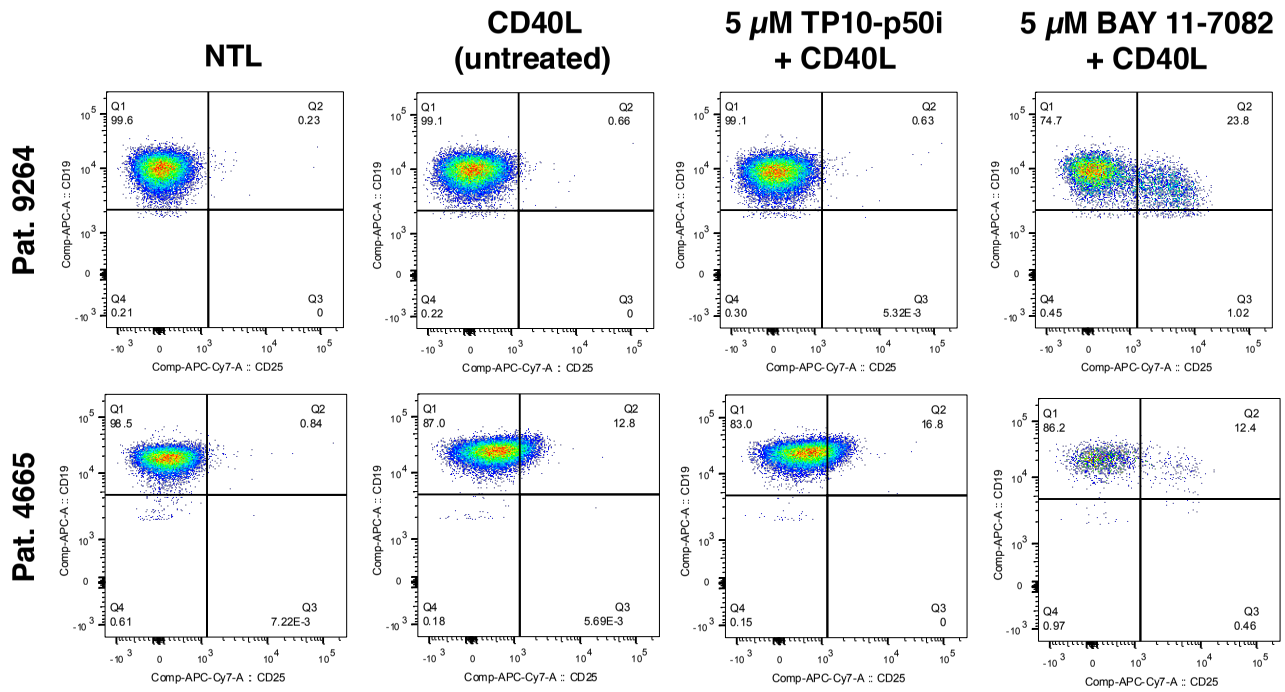

Figure XXIX – CD25 and CD19 expression of primary CLL cells pre-treated with TP10-p50i and Bay 11-7082 and co-cultured with NTL and CD40L cells of samples 9264 and 4665.

CD19 and CD25 dot plot of patient samples 9264 and 4665, incubated under the conditions described in Figure I. Cells present in these dot plots were gated previously in the “CLL cell” gate as described in Figure 5.17. Dot plots obtained using the software FlowJo X.

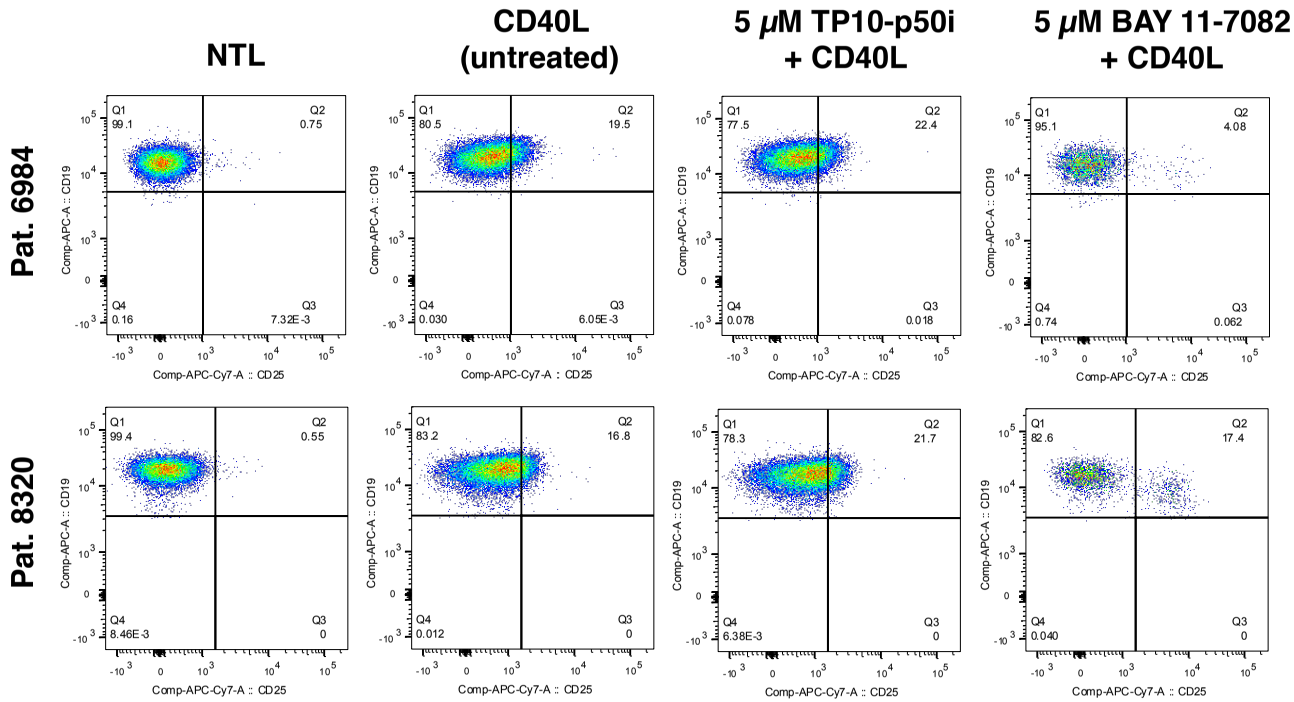

Figure XXX – CD25 and CD19 expression of primary CLL cells pre-treated with TP10-p50i and Bay 11-7082 and co-cultured with NTL and CD40L cells of samples 6984 and 8320.

CD19 and CD25 dot plot of patient samples 6984 and 8320, incubated under the conditions described in Figure I. Cells present in these dot plots were gated previously in the “CLL cell” gate as described in Figure 5.17. Dot plots obtained using the software FlowJo X

Appendix III

Expression of CD25, CD49d and CD38, following co-culture with CD40L and pre-treatment with TP10-p50i

To assess the effects of TP10-p50i in cell surface markers regulated by NF-κB, primary CLL cells were treated with 0, 2.5, 5 and 10 μM of TP10-p50i for 1 hour. Cells were harvested and cultured with CD40L cells for a period of 24 hours. Cells were harvested and incubated with anti-CD19, -CD5, -CD25, -CD49d, -CD38 and -CD69 antibodies. Cells were analysed by flow cytometry and a summary of the expression of CD69 on CLL cells of 17 patient samples can be found in Figure 5.16 (Chapter 5). Data for the other three cell surface markers analysed is presented here in Figures I to III. Two additional incubation conditions were tested, pre-treatment with BAY 11-7082 followed by CD40L co-culture and liquid culture of CLL cells without any treatment followed by co-culture with NTL cells.

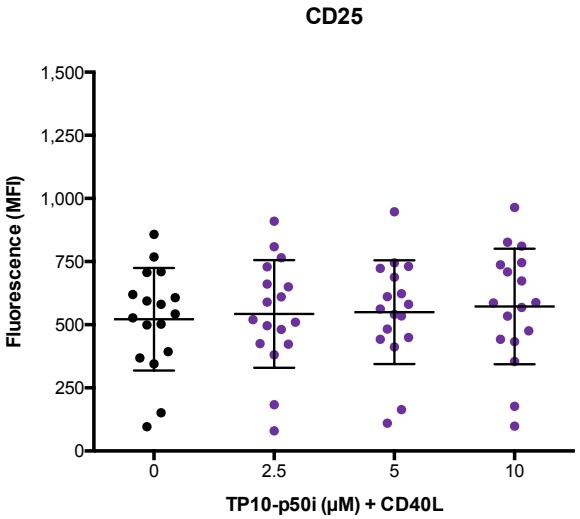

Figure XXXI - Expression of CD25 on primary CLL cells pre-treated with BAY 11-7082, followed by co-culture with NTL and CD40L cells.
Primary CLL were cultured under the conditions described in Figure 5.16. Prior to flow cytometry, cells were incubated with anti-CD25 antibody (560225, BD Pharmogen). The gating strategy used is presented in Figure 5.11. Data from 17 patient samples, presented as MFI values for each individual sample, plus mean and +/- SD. Statistical analysis was performed using the software GraphPad Prism 6. Repeated-measures one-way ANOVA was applied followed by a multiple-comparisons test. No statistically significant differences were found between the different conditions tested.

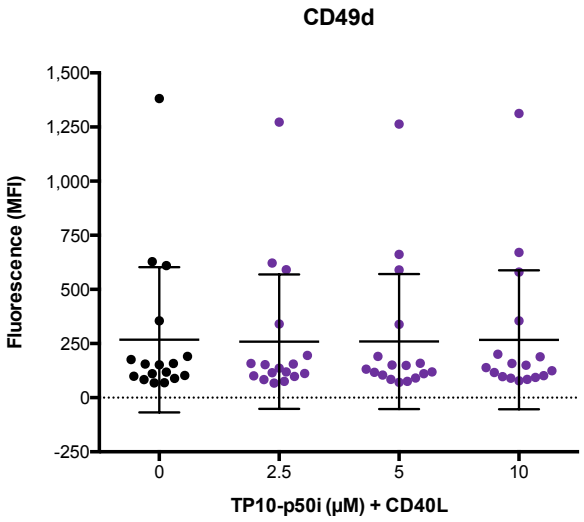

Figure XXXII - Expression of CD49d on primary CLL cells pre-treated with BAY 11-7082, followed by co-culture with NTL and CD40L cells.
Primary CLL were cultured under the conditions described in Figure 5.16. Prior to flow cytometry, cells were incubated with anti-CD49d antibody (MCA2503F, AbD Serotec). The gating strategy used is presented in Figure 5.11. Data from 17 patient samples, presented as MFI values for each individual sample, plus mean and +/- SD. Statistical analysis was performed using the software GraphPad Prism 6. Repeated-measures one-way ANOVA was applied followed by a multiple-comparisons test. No statistically significant differences were found between the different conditions tested.

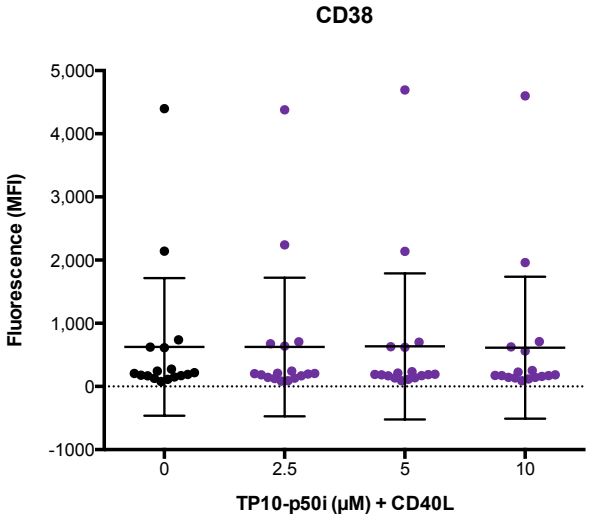

Figure XXXIII - Expression of CD38 on primary CLL cells pre-treated with BAY 11-7082, followed by co-culture with NTL and CD40L cells.
Primary CLL were cultured under the conditions described in Figure 5.16. Prior to flow cytometry, cells were incubated with anti-CD38 antibody (MHCD3804, Invitrogen). The gating strategy used is presented in Figure 5.11. Data from 17 patient samples, presented as MFI values for each individual sample, plus mean and +/- SD. Statistical analysis was performed using the software GraphPad Prism 6. Repeated-measures one-way ANOVA was applied followed by a multiple-comparisons test. No statistically significant differences were found between the different conditions tested.